

Smart Material-Cell Interaction for Guided Proliferation and Differentiation of Stem Cells

Lead Guest Editor: Adam Ye

Guest Editors: Fernando Guastaldi, Jing Yan, and Tzu-Cheng Sung





Smart Material-Cell Interaction for Guided Proliferation and Differentiation of Stem Cells

Stem Cells International

**Smart Material-Cell Interaction
for Guided Proliferation and
Differentiation of Stem Cells**

Lead Guest Editor: Adam Ye

Guest Editors: Fernando Guastaldi, Jing Yan, and
Tzu-Cheng Sung



Copyright © 2021 Hindawi Limited. All rights reserved.

This is a special issue published in “Stem Cells International.” All articles are open access articles distributed under the Creative Commons Attribution License, which permits unrestricted use, distribution, and reproduction in any medium, provided the original work is properly cited.

Chief Editor

Renke Li , Canada

Associate Editors

James Adjaye , Germany
Andrzej Lange, Poland
Tao-Sheng Li , Japan
Heinrich Sauer , Germany
Holm Zaehres , Germany

Academic Editors

Cinzia Allegrucci , United Kingdom
Eckhard U Alt, USA
Francesco Angelini , Italy
James A. Ankrum , USA
Stefan Arnhold , Germany
Marta Baiocchi, Italy
Julie Bejoy , USA
Philippe Bourin , France
Benedetta Bussolati, Italy
Leonora Buzanska , Poland
Stefania Cantore , Italy
Simona Ceccarelli , Italy
Alain Chapel , France
Sumanta Chatterjee, USA
Isotta Chimenti , Italy
Mahmood S. Choudhery , Pakistan
Pier Paolo Claudio , USA
Gerald A. Colvin , USA
Joery De Kock, Belgium
Valdo Jose Dias Da Silva , Brazil
Leonard M. Eisenberg , USA
Alessandro Faroni , United Kingdom
Ji-Dong Fu , USA
Marialucia Gallorini , Italy
Jacob H. Hanna , Israel
David A. Hart , Canada
Zhao Huang , China
Elena A. Jones , United Kingdom
Oswaldo Keith Okamoto , Brazil
Alexander Kleger , Germany
Laura Lasagni , Italy
Shinn-Zong Lin , Taiwan
Zhao-Jun Liu , USA
Valeria Lucchino, Italy
Risheng Ma, USA
Giuseppe Mandraffino , Italy

Katia Mareschi , Italy
Pasquale Marrazzo , Italy
Francesca Megiorni , Italy
Susanna Miettinen , Finland
Claudia Montero-Menei, France
Christian Morszeck, Germany
Patricia Murray , United Kingdom
Federico Mussano , Italy
Mustapha Najimi , Belgium
Norimasa Nakamura , Japan
Karim Nayernia, United Kingdom
Toru Ogasawara , Japan
Paulo J Palma Palma, Portugal
Zhaoji Pan , China
Gianpaolo Papaccio, Italy
Kishore B. S. Pasumarthi , Canada
Manash Paul , USA
Yuriy Petrenko , Czech Republic
Phuc Van Pham, Vietnam
Alessandra Pisciotta , Italy
Bruno P#ault, USA
Liren Qian , China
Md Shaifur Rahman, Bangladesh
Pranela Rameshwar , USA
Syed Shadab Raza Raza , India
Alessandro Rosa , Italy
Subhadeep Roy , India
Antonio Salgado , Portugal
Fermin Sanchez-Guijo , Spain
Arif Siddiqui , Saudi Arabia
Shimon Slavin, Israel
Sieghart Sopper , Austria
Valeria Sorrenti , Italy
Ann Steele, USA
Alexander Storch , Germany
Hirotaka Suga , Japan
Gareth Sullivan , Norway
Masatoshi Suzuki , USA
Daniele Torella , Italy
H M Arif Ullah , USA
Aijun Wang , USA
Darius Widera , United Kingdom
Wasco Wruck , Germany
Takao Yasuhara, Japan
Zhaohui Ye , USA



Shuiqiao Yuan , China
Dunfang Zhang , China
Ludovic Zimmerlin, USA
Ewa K. Zuba-Surma , Poland

Contents

Classification and Characteristics of Mesenchymal Stem Cells and Its Potential Therapeutic Mechanisms and Applications against Ischemic Stroke

Pian Gong, Wei Zhang, Yan He, Jianfeng Wang, Song Li, Songyu Chen, Qingsong Ye , and Mingchang Li 

Review Article (13 pages), Article ID 2602871, Volume 2021 (2021)

3D Spheroid Formation Using BMP-Loaded Microparticles Enhances Odontoblastic Differentiation of Human Dental Pulp Stem Cells

Tae-Jun Min, Min Ji Kim, Kyung-Jung Kang, Yeoung Jo Jeoung, Se Heang Oh , and Young-Joo Jang 

Research Article (12 pages), Article ID 9326298, Volume 2021 (2021)

Interleukin-20 Acts as a Promotor of Osteoclastogenesis and Orthodontic Tooth Movement

Yuanbo Liu , Yilong Ai , Xuan Sun , Bowen Meng , Xi Chen , Dongle Wu , Lei Gan , Benyi Yang , Chaoran Fu , Yilin Wu , and Yang Cao 

Research Article (20 pages), Article ID 5539962, Volume 2021 (2021)

Biocompatibility and Angiogenic Effect of Chitosan/Graphene Oxide Hydrogel Scaffolds on EPCs

Lifang Zhang , Xinping Li, Congying Shi , Gaoying Ran, Yuting Peng, Shuguang Zeng , and Yan He

Research Article (17 pages), Article ID 5594370, Volume 2021 (2021)

Mesenchymal Stem Cells: An Overview of Their Potential in Cell-Based Therapy for Diabetic Nephropathy

Yan Wu, Chunlei Zhang, Ran Guo, Dan Wu, Jiayi Shi, Luxin Li, Yanhui Chu, Xiaohuan Yuan , and Jie Gao 

Review Article (12 pages), Article ID 6620811, Volume 2021 (2021)

Semaphorin3B Promotes Proliferation and Osteogenic Differentiation of Bone Marrow Mesenchymal Stem Cells in a High-Glucose Microenvironment

Quan Xing , Jingyi Feng , and Xiaolei Zhang 

Research Article (9 pages), Article ID 6637176, Volume 2021 (2021)

Review Article

Classification and Characteristics of Mesenchymal Stem Cells and Its Potential Therapeutic Mechanisms and Applications against Ischemic Stroke

Pian Gong,¹ Wei Zhang,¹ Yan He,² Jianfeng Wang,¹ Song Li,³ Songyu Chen,³ Qingsong Ye ⁴ and Mingchang Li ¹

¹Department of Neurosurgery, Renmin Hospital of Wuhan University, Wuhan, Hubei 430060, China

²Regenerative Medicine Lab, Tianyou Hospital, Wuhan University of Science and Technology, Wuhan, Hubei 430064, China

³Department of Neurosurgery, Shanghai Tenth People's Hospital, Tongji University, Shanghai, China

⁴Center of Regenerative Medicine, Renmin Hospital of Wuhan University, Wuhan, Hubei 430060, China

Correspondence should be addressed to Qingsong Ye; qingsongye@hotmail.com and Mingchang Li; mingcli@whu.edu.cn

Received 19 July 2021; Accepted 11 October 2021; Published 9 November 2021

Academic Editor: Jing Yan

Copyright © 2021 Pian Gong et al. This is an open access article distributed under the Creative Commons Attribution License, which permits unrestricted use, distribution, and reproduction in any medium, provided the original work is properly cited.

Ischemic stroke is a serious cerebral disease that often induces death and long-term disability. As a currently available therapy for recanalization after ischemic stroke, thrombolysis, including intravenous thrombolysis and endovascular therapy, still cannot be applicable to all patients due to the narrow time window. Mesenchymal stem cell (MSC) transplantation therapy, which can trigger neuronal regeneration and repair, has been considered as a significant advance in treatment of ischemic stroke. MSC transplantation therapy has exhibited its potential to improve the neurological function in ischemic stroke. Our review describes the current progress and future perspective of MSC transplantation therapy in ischemic stroke treatment, including cell types, transplantation approaches, therapeutic mechanisms, and preliminary clinical trials of MSC transplantation, for providing us an update role of MSC transplantation in ischemic stroke treatment.

1. Introduction

Stroke is the third leading cause of death and disability worldwide that brings a huge burden to the healthcare system [1]. One in six people will suffer from stroke in their lifetime, with over 13.7 million occurring strokes every year and causing 5.8 million people deaths [2]. The major type of stroke is the ischemic stroke, which approximately accounts for 70 percent of all strokes [2]. Although advanced methods for ischemic stroke treatment have been dug up in recent years, no therapy can efficiently improve the overall prognosis of patients [3]. Intravenous administration of recombinant tissue plasminogen activator (rt-PA) thrombolysis is the only drug approved by the Food and Drug Administration to treat the acute ischemic stroke within 4.5 hours [4–6]; however, limited by its therapeutic window, less than 5% patients benefited [7]. Mechanical thrombectomy, as the alternative treatment for ischemic stroke, entails an intra-

arterial (IA) catheter or stent to remove the occluding thrombus, has been proven to be effective within 6 hours of the onset [8]. Both treatments are so highly time-dependent; thus, new treatment strategy is imminent. As a new method to treat ischemic stroke, stem cell transplantation was proved to be a hopeful treatment by a growing body of animal experiments and a few successful clinical trials [9, 10]. As the most studied subtype of stem cells, mesenchymal stem cells (MSCs) have been regarded as a promising therapeutic option for ischemic stroke [11]. Therefore, this review is aimed at summarizing the current progress as well as the future perspective of MSC transplantation in ischemic stroke treatment.

2. Classification and Characteristics of MSCs

MSCs, also known as mesenchymal stromal cells with properties of self-renewal and multipotential for differentiation,

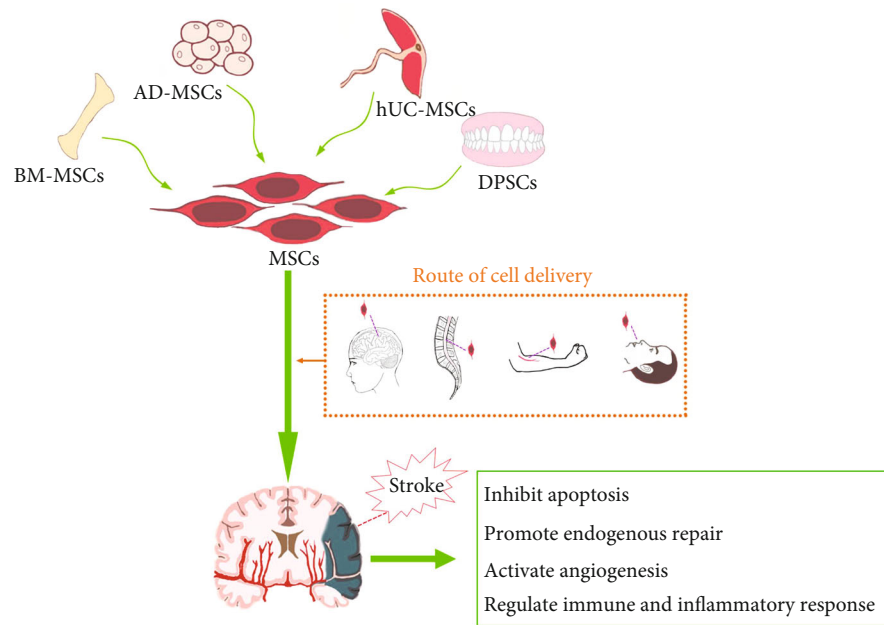


FIGURE 1: Application of MSCs for ischemic stroke. MSCs can be isolated from the bone marrow, adipose tissue, placenta, and teeth and transplanted to the ischemic brain via intracerebral transplantation, intrathecal administration, intravascular administration, and intranasal administration. MSCs can provide neuroprotection and clinical benefits by inhibiting apoptosis, promoting endogenous repair and angiogenesis, and regulating immune and inflammatory response.

can be isolated from various tissues. As shown in Figure 1, varying from cell sources, MSCs can be obtained from the bone marrow, umbilical cord, adipose tissue, placenta, and tissues that originated from the neural crest and others. Furthermore, they can be differed from other stem cells like the hematopoietic stem cells according to the surface molecules expressed by themselves. MSCs express surface molecules such as CD73, CD90, and CD105, and they do not express the surface molecules like CD34, CD45, HLA-antigen D related, CD14 or CD11b, CD79a, or CD19 [12]. MSCs possess multipotential differentiation ability that they can be differentiated into cells like osteoblasts, chondrocytes, and adipocytes. Moreover, they are easy to be isolated and amplified with low immunogenicity and trophic properties [13, 14]. Unlike embryonic stem cells, the collection, research, and usage of MSCs seldomly raise ethical concerns. Therefore, it is possible to transplanting MSCs to repair multiple injuries.

In the past, researchers obtained MSCs mainly from the bone marrow. MSCs were first found in the bone marrow in 1976 and described as fibroblast-like cells [15]. Later studies revealed that this kind of cells could differentiate into osteogenic, chondrogenic, and adipogenic mesenchymal cell lineages in vitro [16]. Up to date, MSCs in the bone marrow, also known as bone marrow mesenchymal stem cells (BM-MSCs), are the most studied and best characterized MSCs. Currently, the most frequent way to obtain BM-MSCs is bone marrow aspiration accompanied by invasion, pain, and the risk of viral and bacterial contamination [17], of which the quality of the obtained cells is determined by age and physical condition of donors [18]. Despite a very low yield, the amplification ability of BM-MSCs is very

strong. In the exponential growth period, its doubling time is about 30 to 33 hours. It is reported that human BM-MSCs can be propagated in vitro for 40 generations and about 100 million times which can still maintain the stemness [16]. A recent investigation suggested that, in rats underwent acute ischemic stroke, intravenous- (IV-) injected human BM-MSCs can survive and migrate along boundary zones adjacent to the ischemic area and differentiate into the neurons and astrocytes in the microenvironment of the ischemic lesion area, as a result of reduced infarct volume and improved neurological function [19]. Moreover, it is reported that transplanting human BM-MSCs into the infarct area not only stimulates angiogenesis and neurogenesis by secreting multiple cytokines like vascular endothelial growth factor (VEGF), basic fibroblast growth factor (bFGF), and TIMP-3 but also induces differentiation of endogenous stem cells, which results in neuroprotection against ischemic stroke [20, 21]. In addition, transplanted human BM-MSCs were shown to inhibit inflammation and neuronal apoptosis in the ischemic brain of rats [22]. The underlying molecular mechanisms of protective effects induced by BM-MSCs are complex and not entirely clear. Interestingly, a study indicated that, shortly after ischemic stroke in mice, the cell proliferation of BM-MSCs was triggered and promoted, leading to the production of downstream myeloid progenitors and increased presence of inflammatory monocytes and neutrophils, suggesting that BM-MSC could be activated by ischemic injury and that the ischemic injury influenced the primary site of hematopoiesis besides the local inflammation in the ischemic brain [23].

Human umbilical cord mesenchymal stem cells (hUC-MSCs) are isolated from the umbilical cord, which are

featured with the surface molecules of CD29, CD44, CD51, CD105, SH2, and SH3 except CD34 and CD45 [24]. Lots of research explored the effectiveness of hUC-MSCs in ischemic stroke. It was reported that rats underwent middle cerebral artery occlusion (MCAO) for 2 hours and treated with intracerebral hUC-MSC transplantation 1 d after MCAO operation showed enhancement in neurogenesis and angiogenesis, as a consequence of reduced neurological functional deficits and infarct volume; besides, the hUC-MSCs could be detected for at least 5 weeks in the damaged area [25]. The transplanted hUC-MSCs could differentiate into neural progenitors and cells [26], promote the proliferation of neural stem cells and neural differentiation, produce multiple neurotrophic factors, and prevent inflammatory reaction through regulating the activity of the spleen [27], followed by promoted neurological recovery and reduced mortality in animals underwent ischemic stroke. However, hUC-MSC therapy in ischemic stroke is currently limited due to the risk of infection and tumorigenesis [28]. In conclusion, as a kind of MSC that possesses the unique advantage of low immunogenicity without ethical controversy, hUC-MSC is proposed as an excellent candidate in cell therapy for ischemic stroke.

The placenta is thought to be an abundant source that contains two kinds of MSCs: amniotic mesenchymal stromal cells (hA-MSCs) and chorionic mesenchymal stromal cells (hC-MSCs). Both types of cells can be isolated directly from the placenta at the end of gestation through chorionic villus sampling during an invasive prenatal diagnosis. The characteristics of hA-MSCs and hC-MSCs, including low immunogenicity and powerful proliferation [29, 30], enable both of them various promising biological properties and make it possible to culture them under good manufacturing practice grade, as a result of numbers of clinical trials on placenta-derived stem cell therapy for ischemic stroke [31].

Adipose tissue-derived mesenchymal stem cells (AD-MSCs) are abundant, accessible, and easy to obtain using lip aspiration techniques [32]. Efficacy and safety of human AD-MSC in the treatment of stroke has been confirmed in animal models [33]. AD-MSC transplantation was shown to attenuate the neuronal apoptosis and death to exert significant neuroprotective effects through inhibiting the action of KDM6B/BMP2/BMF axis in rats underwent the MCAO [34].

Dental pulp stem cells (DPSCs), originated from the embryonic neural crest and oral-derived epithelial stem cells, are considered as a kind of autologously applicable cells [35]. A report in 2000 first clarified that DPSCs could be isolated and characterized from the third molar [36]. It is currently well known that DPSCs are easily extracted and obtained from human teeth such as deciduous teeth, impacted third molars, and orthodontically extracted premolars. DPSCs have the MSC-like characteristics of high growth capacity and multilineage differentiation potential that they can convert into multiple kinds of cells like neural cells, chondroblasts, and endothelium formative cells. For the advantages of DPSCs, the major one is the easy accessibility without invasive surgical procedures or ethical concerns; another one is that they can maintain their stem cell characteristics

after long-term cryopreservation [37, 38]. Moreover, DPSC culture can also be efficiently established from extracted human molars after cryopreservation for up to one month [39].

In addition, DPSCs showed a superior potential for neurogenic differentiation compared with MSCs from other sources like BM-MSCs and AD-MSCs [40]. Upon induction under neuronal differentiation conditions, DPSCs can differentiate into functionally active neuronal cells like mature neurons, dopaminergic-like cells, Schwann cells, and oligodendrocytes [41, 42]. Even without preinduction of neuronal differentiation, DPSCs can express neural stem cell-like markers like nestin and β -III tubulin [40]. Studies showed that DPSCs can express neurotrophic factors like brain-derived neurotrophic factor (BDNF) and VEGF which have been proven to exert neuroprotection against ischemic stroke in both in vitro and in vivo experiments [40]. DPSC-treated primary cortical neurons and astrocytes underwent the oxygen/glucose deprivation (OGD) exhibited promoted neurite regeneration and angiogenesis, and relieved inflammation [19]. DPSC secretion/exosome-implanted rats with ischemic stroke showed promoted nerve cell proliferation, reduced infarct volume and brain edema, and attenuated neurological dysfunction [43, 44]. Moreover, the culture supernatant of DPSCs that is called dental pulp conditioned medium (DPCM) has been reported to contain cytoprotective factor, revascularization factor, and fibrosis inhibitory factor that contribute to neuronal survival, proliferation, and differentiation [45]; importantly, all of which are well known to be the key mechanisms of neuroprotection against cerebral ischemic stroke. Above evidence shows that both DPSC transplantation and DPCM exert therapeutic effects against ischemic stroke. Furthermore, it was reported that no immune rejection was observed in the brain of mice that had been administered with DPSC implantation derived from rhesus monkeys [46], suggesting that the degree of transplantation rejection of DPSCs was low. When combining with neurotrophic factors, DPSCs can repair both the central nerve and the peripheral nerve once they were attacked by various injuries [47–51]. However, few in-depth studies have examined the effects of DPSCs on the ischemic stroke. Therefore, further research is needed and worthy.

3. Route of Cell Delivery

To date, MSCs are delivered via intracerebral transplantation, intrathecal administration, intravascular administration, and intranasal administration to repair ischemic-damaged brain tissue, as shown in Figure 1. Despite intracerebral transplantation and intravascular administration are the commonly used methods [52], there is no optimal route of delivery as every method possesses its own vantages and limitations.

Intracerebral transplantation, also known as stereotactic transplantation, directly injects the MSCs into brain parenchyma or cerebrospinal fluid by stereotactic apparatus. When injected via parenchyma, in order to provide a good microenvironment for stem cells to promote graft survival,

delivering the MSCs into penumbra or the hemisphere contralateral to the infarct is suggestive [53, 54]. However, intracerebral transplantation may cause mechanical damage and the number of MSCs is limited. Research has showed that not only the endogenous neural stem cells but also exogenous transplanted MSCs are able to migrate to the ischemic region [55, 56]. Yet, other researchers argue that even the stem cells successfully arrived at the center of ischemic area, and some survived the initial ischemic damage, the ideal regenerative niches might only appear several days after the stroke in adult mouse brain [57]. Intracerebroventricular injection delivers the MSCs in cerebrospinal fluid mainly to treat brain functional diseases, especially in cerebral ischemia. It was verified that implanted hUC-MSCs by intracerebroventricular injection migrated into the periventricular tissue, followed by promoted functional recovery in the rat model of hypoxic-ischemic encephalopathy [58]. In terms of the timing of administration, both early (12 hours after stroke) and delayed (7 days after stroke) administrations have been proved effective in improving functional outcomes of rats underwent ischemic stroke [59, 60]. Owing to the importance to control the increased intracranial pressure, multiple administrations of intracerebral transplantation are thought to be impractical, especially for the patients in critical conditions [61]. Intracerebral injection bypasses the blood-brain barrier (BBB) and allows more MSCs into the ischemic lesion. However, as an invasive operation, it is highly technique-sensitive and equipment-dependent [62]. For instance, the positioning accuracy of injection site on MSC transplantation can reach 0.1 mm using a stereo orientation technique [63].

Intrathecal injection delivers MSCs throughout the entire neuraxis without the invasive brain surgery, making it different from the intraparenchymal and intracerebroventricular administrations [64]. Lim et al. found that therapeutic effects of intrathecal injection of hUC-MSCs can be achieved at a lower dosage in treating cerebral ischemic stroke of rats, compared with intravenous administration [65]. A prospective phase II trial has been initiated in 2019 to assess the effectiveness of allogenic BM-MSC transplantation in severe ischemic stroke, in which eligible patients received BM-MSCs intrathecally at the subacute phase (30 to 90 days following onset) and follow-up assessment were conducted at 7, 30, 90, 180, and 360 days after the injection; after all, the project is in progress with no conclusions published so far [66]. This study may provide a good knowledge of intrathecally implanted BM-MSC therapy for severe ischemic stroke.

Intravascular injection is a safe and feasible delivery way of MSCs, including IV and IA administrations. We find an interesting phenomenon that most clinical trials have used IV injection, and studies with smaller case series preferred IA route [67–69]. Compared with intracerebral injection, intravascular injection is less invasive and allows higher dose and bigger volume of MSCs.

Delivered via IV route, cells are expected to pass the BBB to reach the infarct site of brain and function properly to regenerate new nerve tissue. A research was conducted that the neural stem cells were transplanted into mice at 24 h

after ischemic stroke through IA and IV methods; the results of which showed that IV route leaved the cells traveling through the systemic and pulmonary circulations where cells were more likely to be entrapped in other organs like the spleen, liver, and lungs that 94% of cells were detected in the lungs at 1 week after stroke, resulting in only a small part of injected portion can reach the brain, and that IA route leaved 69% of MSCs in the brain several hours after injection and 93% at 7 days [70]. It was reported that, in rats suffering ischemic stroke, at 14 days after BM-MSC transplantation, the implanted cells through IV injection could not be detected in the ischemic brain and most of them were trapped in the lung, and 35% of intracerebrally injected MSCs migrated along the corpus callosum to the ischemic region [21]. In the MCAO model of rats, AD-MSCs were injected via IA and IV routes at 24 h after onset and results showed that at 1-7 days after implantation, the expression level of neurotrophic substance, such as BDNF and VEGF, was increased and level of proapoptotic factors like caspase-3 and TNF- α was decreased via IA route compared with the IV delivery [71]. IA delivery seems to circumvent the systemic circulation [52], via which the cell number entering the brain was 5 times higher than IV [72]. However, IA injection takes the MSCs nearly 24 hours up to 10 days to reach the brain parenchyma [73, 74].

The intranasal route is another less invasive therapeutic option. By passing the BBB, BM-MSCs that were transplanted 24 h after ischemic stroke in mice could reach the ischemic cortex as early as 1.5 hours postnasal administration, which deposit outside the blood vessels [75]. Cell tracking techniques indicated that the cells can enter the olfactory sheath through the extension adjacent to the olfactory filament after passing through the sieve plate or moving along the surface of the cortex into cerebrospinal fluid and then go into the brain parenchyma [76, 77]. This route minimizes, if not eliminates, the cell dispersion in systemic circulation to peripheral organs such as the lung. A study showed that the 9-day-old mice administered with MSCs intranasally at 10 days after hypoxic-ischemic brain damage suggested that both of the somatosensory cortex and hippocampus were dramatically regenerated and glial scar around the ischemic site was eliminated at 18 days after the cell therapy [78]. Another study implied that 10-day-old rats administered with hUC-MSCs intranasally at 24 h posthypoxic-ischemic displayed relieved neuroinflammation and promoted neural regeneration [79].

4. Treatment Mechanisms of MSCs in Ischemic Stroke

4.1. MSCs Regulate Immune and Inflammatory Response. Both of immune and inflammatory responses are proven to be significantly involved in the pathogenesis of ischemic stroke. Once the ischemia attacks, the activated innate immunity quickly triggers and promotes the neuroinflammation (Figure 1), as a result of the migration of immune cells from periphery into the ischemic brain [80]. At early stage of ischemic stroke, inflammation limits and relieves the ischemic stress, which is beneficial for the patients. But

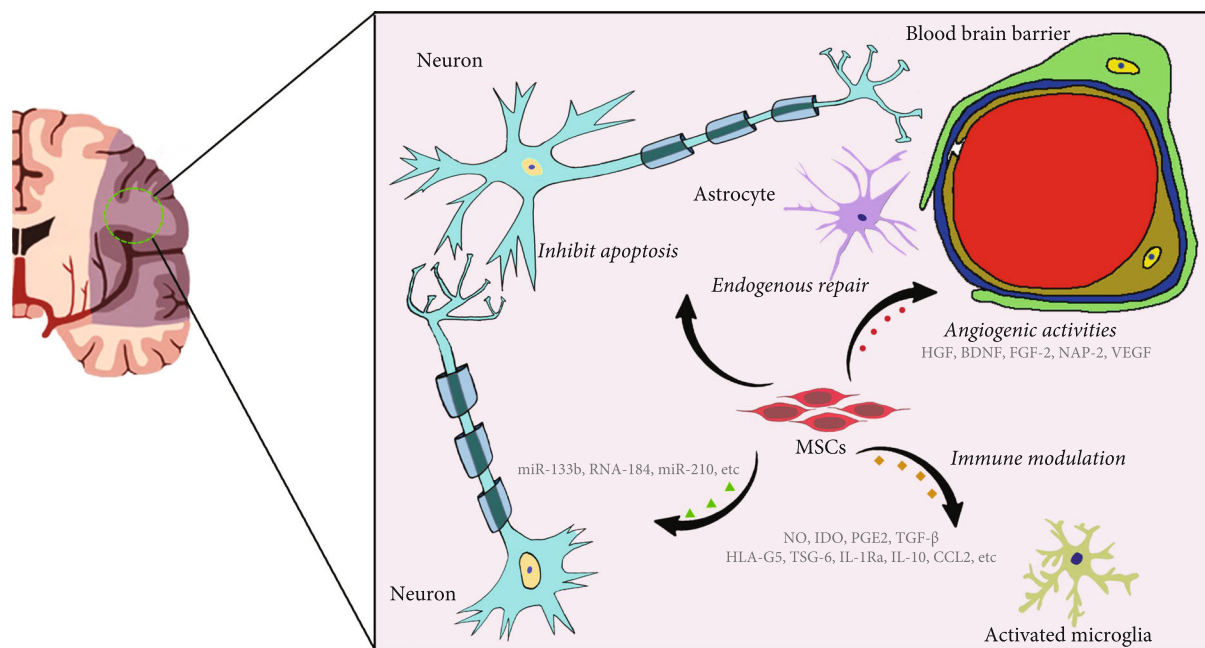


FIGURE 2: Treatment mechanisms of MSCs in ischemic stroke. MSCs produce NO, IDO, PGE2, TGF- β , HLA-G5, TSG-6, IL-1Ra, IL-10, CCL2, etc., to weaken harmful immune and inflammation responses. MSCs induce activation of microglia and persistent reactive astrogliosis. MSCs interact with microRNAs, like miR-133b, RNA-184, and miR-210, to provide neuroprotective functions. MSCs can secrete biologically active cytokines or factors including BDNF, GDNF, NGF, cCSF, SCF, bFGF, PDGFAA, angiotensin-2, NAP2, and VEGF to promote angiogenic activities and attenuate blood-brain barrier disruption.

the following uncontrolled inflammation induced by immune cells, for example, the neutrophils, macrophages, NK cells, and T cells, aggravates the ischemic injury [81, 82]. The ischemic injury is a result of the BBB breakdown, the expression of harmful molecules produced by neural cells, production of glia cell activation-derived proinflammatory factors, and the leukocyte accumulation. MSCs are proven to produce immune regulatory factors such as NO (in mice), IDO (in human), PGE2, TGF- β , HLA-G5, TSG-6, IL-1Ra, IL-10, and antagonistic variants of CCL2 that weaken harmful immune and inflammation responses and promote tissue repair and regeneration (Figure 2) [83, 84]. The soluble factors derived from MSCs are contributed to the suppression of T cell proliferation, and the TGF- β secreted by MSCs prevents the production of PGE2 and HO-1 and also inhibits the autocrine proliferation of IL-2-dependent T cells (Figure 2). In cerebral ischemia, hUC-MSC injection through the tail vein has been shown to modulate TGF- β , leading to the conversion of naïve CD4⁺ T cells into Th17/Treg and regulation of peripheral immune response, followed by inhibited neuroinflammation and attenuated ischemic injury [85]. In addition, MSCs utilize their property on cell cycle arrest to suppress the IFN- γ ⁺/CD8⁺ T cell proliferation through modulating the expression of cyclin D2 and p27kip1, both of which deeply influence the cell cycle of T cells [86]. Moreover, MSC-derived doleamine 2,3-dioxygenase (IDO), PGE2, and TGF- β 1 can downregulate the expression of activated receptors (NKp30, NKp44, and NKG2D), reduce cytotoxicity, inhibit the production of inflammatory cytokines (IFN- γ and TNF- α), and inhibit IL cytotoxic T cell and NK cell pro-

liferation (Figure 2) [87, 88]. Early MSC transplantation significantly drives the IL-10 expression, following the decrease in TNF- α production in the ischemic area. BM-MSC transplantations have important roles in attenuating neutrophil infiltration, astrocyte apoptosis, MMP-9 activation, and aquaporin-4 (AQP4) upregulation through suppressing intracellular adhesion molecule 1 (ICAM-1) and activating the p38 signaling pathway, leading to accelerated and enhanced glial scar formation, and reduced BBB disruption and ischemic lesion volume (Figure 2) [89–91].

Splenic inhibition may be another mechanism of MSCs to lighten the immune inflammation. BM-MSC transplantation allows a potential approach for BBB protection in cerebral ischemia that the cell-based therapy attenuates the adverse effect induced by the spleen which increases the BBB permeability and aggravates the BBB disruption [92, 93]. Besides, BM-MSC therapy modulates the peripheral immune response (Figure 1), which is mainly triggered and promoted by the spleen through releasing lymphocytes and proinflammatory factors into the circulatory system at early stage of ischemia [27, 94, 95].

4.2. MSCs Provide Neurotrophic Functions. At present, the most widely accepted mechanism how MSCs exert the protective effects in ischemic stroke is the neurotrophic factor produced by MSCs through endocrine or paracrine pathway [96]. It has been clarified that the MSCs produce various biologically active cytokines or growth factors like BDNF and bFGF that are crucial for neural regeneration, white matter remodeling, and synaptic plasticity [97–99]. For example, studies have shown that BDNF and bFGF

expressed by MSCs inhibit the neural death and apoptosis partly through interacting with tyrosine kinase receptors in the animal model of ischemic stroke (Figure 2). As a result, MSC transplantation significantly increased the number of multiple nerve cells synaptophysin, as well as synaptic density, number of myelinated axons, and protuberance growth in the ischemic border area [100]. The increased intensities of oligodendrocyte progenitor cells and mature oligodendrocytes are observed in the border zone of lesion due to BM-MSCs transplantation [59]. Moreover, BM-MSCs transplantation enhances white matter remodeling through activation of microglia and persistent reactive astrogliosis (Figure 2), leading to the better long-term neurological outcomes [59, 101].

MicroRNAs are strongly linked to MSCs, which play a neuroprotective role in ischemic stroke. MicroRNA profiling analysis revealed that many microRNAs were significantly changed after ischemic stroke [102, 103]. Xin et al. found that the exosomes from MSCs can modulate the interaction between various microRNAs and neural cells to the structural and functional recovery of neural cells in cerebral ischemia (Figure 2) [104, 105]. It has been proposed that MSCs comodified by targeted peptide and miR-133b can be used as potential therapeutic drugs for cerebral ischemia (Figure 2) [106]. In addition, MSCs act on extracellular vesicles (EVs) in region site to mitigate ischemic injury that the interaction between them promotes neurogenesis and angiogenesis [107]. There is no doubt that MSC treatment has a potential therapeutic value in ischemic stroke with the ability of opening up new avenues and strategies.

4.3. MSCs Induce Angiogenic Activities. Angiogenesis is highly related to the functional recovery of ischemic stroke (Figure 1). In response to the attack of the ischemic stroke, the vascular endothelial cells in the CNS exhibit strong proliferation capability to supply the injured tissue with more oxygen and nutrition. In the next few months after the stroke, as vascular remodeling and vascular density increasing, neuroblasts gradually migrate to the damaged brain area to repair the injured tissue. Existing evidence suggested that MSCs can acquire angiogenic properties through paracrine or autocrine production of appropriate cytokines [108, 109]. Implanted BM-MSCs release many angiogenic growth factors and neurotrophic factors like angiogenin, hepatocyte growth factor, BDNF, and fibroblast growth factor-2 (FGF-2), insulin-like growth factor-1, neutrophil activating protein-2 (NAP-2), and VEGF (Figure 2) [109]. In addition, some researchers have found that, in the area around the infarction, BM-MSCs facilitate the production of various neuroprotective factors, including stromal cell-derived factor-1 (SDF-1), BDNF, platelet-derived growth factor AA (PDGF-AA), basic fibroblast cell growth factor, angiopoietin-2, CXC chemokine ligand 16, NAP-2, and VEGF receptor-3 (Figure 2) [110]. In rats suffering ischemic stroke, BM-MSCs treatment started at 24h after onset markedly increases the microvessel density, as a consequence of enhanced angiogenesis in the boundary zone [101, 111]. Zacharek et al. found that coculture of astrocytes with MSCs increased the expression of VEGF and Ang1/Tie2 and signif-

icantly increased capillary-like formation of mouse brain endothelial cells [112], resulting in the promotion of the angiogenesis to accelerate tissue repair (Figure 1).

5. Clinical Trials

Although preclinical data are promising in terms of both safety and therapeutic efficacy, clinical verification is inevitable for MSCs to treat patients with cerebral ischemia. Up to now, about 1000 clinical trials focused on MSC therapy are currently registered on ClinicalTrials.gov and 20 clinical trials (Table 1) focus on the therapeutic effects of MSCs for cerebral ischemia, among which 4 have been completed and 3 have been withdrawn. A phase II clinical trial from China, in which 10 participants suffering acute ischemic stroke were treated with AD-MSCs via the IV route within 2 weeks after the onset, concluded that AD-MSCs implantation was safe and efficient and could improve the neurological function of patients with severe stroke at two years after ischemic stroke [113]. Another 4-year open trial in China involved 18 participants with acute cerebral ischemic stroke showed that participants in the MSC-treated group had fewer serious adverse events compared with the vehicle group and concluded the long-term safety of MSC treatment for acute cerebral ischemic stroke [114]. In a randomized controlled trial with a 2-year follow-up, 16 patients received the MSC transplantation through the IV route showed improved motor recovery through sensorimotor neuroplasticity, suggesting that MSC treatment was safe and feasible for ischemic stroke [67].

Moreover, clinical trials of 36 patients from Levy et al. [115] showed that the proportion of patients that treated with allogeneic BM-MSCs ($1.6 \times 10^6/\text{kg}$) via IV route with good functional recovery (Barthel score ≥ 95) increased from 11.4% of the baseline to 27.3% at 6 months and 35.5% at 12 months. Levy et al. concluded that allogeneic BM-MSCs injection via IV route was accessible and reasonable in treatment of chronic stroke and suggested behavioral gains in patients with substantial functional defects. In addition, a randomized controlled clinical trial registered as ChiCTR-16008908 focused on intrathecal injection of allogeneic BM-MSCs four infusions (1×10^6 cells/kg body weight) once a week at 1 to 3 months after onset of ischemic stroke is still in progress [66].

6. Conclusions and Prospects

At present, MSCs are notably available from multiple sources. Furthermore, they are immunotolerant and hold unequivocal postnatal multilineage potential. MSC transplantation is indeed an excellent therapeutic technique to treat ischemic stroke; however, of which the optimal therapeutic protocols, in terms of MSC subtype, number, preparation, and timing, need to be further studied. Although preclinical studies have shown that MSC therapy occupies with safety and efficacy in the treatment of ischemic stroke, some investigators concern that MSC transplantation may lead to tumor growth, immunodepression, and adverse events of the respiratory system, particularly the pulmonary

TABLE 1: Summary of clinical trials on mesenchymal stem cells and ischemic stroke.

S. no.	Study title	Status	Phase	Cell type	Patient sample size	Route of therapy	Treatment time	Region	Outcomes
1	Umbilical cord-derived mesenchymal stem cells for ischemic stroke	Recruiting	II	hUC-MSCs	200	IV	Within 6 months after onset	Shenyang, China	No results available
2	Safety of escalating doses of intravenous bone marrow-derived mesenchymal stem cells in patients with a new ischemic stroke	Withdrawn	I/II	BM-MSCs	0	IV	Within 24-72 hours after onset	California, United States	No results available
3	Reparative therapy in acute ischemic stroke with allogenic mesenchymal stem cells from adipose tissue, safety assessment, a randomized, double-blind placebo controlled single-center pilot clinical trial	Completed	II	AD-MSCs	19	IV	Acute cerebral infarction of less than 12 h from stroke onset	Madrid, Spain	Safe, feasible, and has improved neurologic recovery in patients with severe stroke
4	Allogenic adipose tissue-derived mesenchymal stem cells in ischemic stroke	Recruiting	II	AD-MSCs	30	IV	The first 4 days (+/-1) from acute stroke symptoms onset	Madrid, Spain	No results available
5	Combination of conditioned medium and umbilical cord-mesenchymal stem cell therapy for subacute stroke infarct	Not yet recruiting	I/II	hUC-MSCs	15		Acute or subacute phase	Jakarta, Indonesia	No results available
6	Mesenchymal stem cells for the treatment of acute ischemic stroke	Recruiting	I	UMC119-06	9	IV	Within 48 to 168 hours after onset	Taiwan	No results available
7	Mesenchymal stromal cells for ischemic stroke	Withdrawn	I/II	BM-MSCs	0	IV	3-10 days after stroke	Houston	No results available
8	Autologous bone marrow mesenchymal stem cell transplantation for chronic ischemic stroke	Unknown	I	BM-MSCs	40	IV	With stroke history of more than 6 months, less than 60 months	Guangdong, China	No results available
9	Allogenic mesenchymal stem cell-derived exosome in patients with acute ischemic stroke	Recruiting	I/II	MSC-derived exosome	5	IV	Acute phase within 24 h after onset	Tehran, Iran	No results available
10	Evaluate the safety and explore efficacy of umbilical cord mesenchymal stem cells in acute ischemic stroke	Recruiting	I	hUC-MSCs	14	IA and IV	Acute phase	Taiwan	No results available
11	Allogenic mesenchymal stem cells for the survivors of ischemic stroke trial (ASSIST)	Not yet recruiting	I/IIa	it-hMSCs	60	IV	More than 6 months after onset	Beijing, China	No results available

TABLE 1: Continued.

S. no.	Study title	Status	Phase	Cell type	Patient sample size	Route of therapy	Treatment time	Region	Outcomes
12	Perinatal arterial stroke treated with stromal cells intranasally	Recruiting	I/II	BM-MSCs	10	Nasal route	Within the first week after onset	Utrecht, Netherlands	No results available
13	Clinical plan of ischemic stroke	Recruiting	I	it-hMSCs	60	IV	More than 6 months after onset	Beijing, China	No results available
14	Intravenous stem cells after ischemic stroke	Completed	II	BM-MSCs	31	IV	Within 6 weeks after onset	Grenoble, France	Safe, feasible, and improved motor recovery
15	Umbilical cord derived mesenchymal stem cell treatment in ischemic stroke	Unknown	II	hUC-MSCs	2	IV	Within 3 months after onset	Beijing, China	No results available Feasible and safe but not associated with improvements in the 3-month mRS score and 90-day outcomes in patients with chronic stroke
16	The STEM cell Application Researches and Trials In NeuroloGy-2 (STARTING-2)	Unknown	III	Autologous MSCs	60	IV	Within 90 days after onset	Seoul, Korea	No toxicity events or infusional or allergic reactions and may improve recovery after stroke
17	Autologous bone marrow stromal cell and endothelial progenitor cell transplantation in ischemic	Completed	I/II	BM-MSCs	20	IV	Within 7 days after the onset	Guangdong, China	Safe and suggested behavioral gains
18	A study of allogeneic mesenchymal bone marrow cells in subjects with ischemic stroke	Completed	I/II	BM-MSCs	38	IV	More than 6 months after the onset	California, United States	No results available
19	Autologous bone marrow mesenchymal stem cell transplantation for chronic stroke	Unknown	I	BM-MSCs	30	Intracerebral injection	Within 3 to 60 months after the onset	Zhejiang, China	No results available
20	Ex vivo cultured adult allogenic MSCs in ischemic cerebral stroke	Withdrawn	I/II	Allogenic MSCs	0	Intravenous ex vivo cultured	Within 10 days after the onset	Malaysia	No results available

hUC-MSCs: human umbilical cord mesenchymal stem cells; BM-MSCs: bone marrow mesenchymal stem cells; AD-MSCs: adipose tissue-derived mesenchymal stem cells; it-hMSCs: ischemia tolerant human allogeneic bone marrow mesenchymal stem cells; IA: intra-arterial injection; IV: intravenous injection.

embolism [63]. In addition to the encouraging phase I and phase II data, large-scale phase III clinical trials are required to clear the aforementioned doubts. Hence, we should further conduct not only preclinical studies but also clinical researches to illustrate the effectiveness of MSCs in cerebral ischemia treatment.

Abbreviations

MSCs:	Mesenchymal stem cells
BM-MSCs:	Bone marrow mesenchymal stem cells
IV:	Intravenous
VEGF:	Vascular endothelial growth factor
bFGF:	Basic fibroblast growth factor
hUC-MSCs:	Human umbilical cord mesenchymal stem cells
MCAO:	Middle cerebral artery occlusion
hA-MSCs:	Human amniotic mesenchymal stromal cells
hC-MSCs:	Human chorionic mesenchymal stromal cells
AD-MSCs:	Adipose tissue-derived mesenchymal stem cells
DPSCs:	Dental pulp stem cells
BDNF:	Brain-derived neurotrophic factor
DPCM:	Dental pulp conditioned medium
BBB:	Blood-brain barrier
IA:	Intra-arterial
NAP-2:	Neutrophil activating protein-2.

Conflicts of Interest

The authors declare that they have no conflicts of interest.

Authors' Contributions

Pian Gong, Wei Zhang, and Yan He contributed to the conception of this study. Pian Gong, Wei Zhang, Yan He, Jianfeng Wang, Song Li, and Songyu Chen performed the literature research and drafted the manuscript. Qingsong Ye and Mingchang Li participated in revising the paper and finalizing the paper. All authors read and approved the final manuscript. Pian Gong, Wei Zhang, and Yan He contributed equally to this work. Pian Gong, Wei Zhang, and Yan He are co-first authors.

Acknowledgments

This study was supported by grants from the National Natural Science Foundation of China (81971870 to M.C.L.).

References

- [1] G B D C o D Collaborators, "Global, regional, and national age-sex-specific mortality for 282 causes of death in 195 countries and territories, 1980-2017: a systematic analysis for the Global Burden of Disease Study 2017," *The Lancet*, vol. 392, pp. 1736–1788, 2018.
- [2] M. S. Phipps and C. A. Cronin, "Management of acute ischemic stroke," *BMJ*, vol. 368, p. l6983, 2020.
- [3] R. V. Krishnamurthi, V. L. Feigin, M. H. Forouzanfar et al., "Global and regional burden of first-ever ischaemic and haemorrhagic stroke during 1990-2010: findings from the Global Burden of Disease Study 2010," *The Lancet. Global health*, vol. 1, pp. e259–e281, 2013.
- [4] W. Wang, M. Li, Y. Wang et al., "GSK-3beta inhibitor TWS119 attenuates rtPA-induced hemorrhagic transformation and activates the Wnt/beta-catenin signaling pathway after acute ischemic stroke in rats," *Molecular Neurobiology*, vol. 53, pp. 7028–7036, 2016.
- [5] P. Gong, Z. Zhang, C. Zou et al., "Hippo/YAP signaling pathway mitigates blood-brain barrier disruption after cerebral ischemia/reperfusion injury," *Behavioural Brain Research*, vol. 356, pp. 8–17, 2019.
- [6] P. Gong, Z. Zhang, Y. Zou et al., "Tetramethylpyrazine attenuates blood-brain barrier disruption in ischemia/reperfusion injury through the JAK/STAT signaling pathway," *European Journal of Pharmacology*, vol. 854, pp. 289–297, 2019.
- [7] P. A. Lapchak and J. H. Zhang, "The high cost of stroke and stroke cytoprotection research," *Translational Stroke Research*, vol. 8, pp. 307–317, 2017.
- [8] W. J. Powers, "Acute ischemic stroke," *The New England Journal of Medicine*, vol. 383, pp. 252–260, 2020.
- [9] M. Kawabori, H. Shichinohe, S. Kuroda, and K. Houkin, "Clinical trials of stem cell therapy for cerebral ischemic stroke," *International Journal of Molecular Sciences*, vol. 21, 2020.
- [10] G. Zhou, Y. Wang, S. Gao et al., "Potential mechanisms and perspectives in ischemic stroke treatment using stem cell therapies," *Frontiers in Cell and Developmental Biology*, vol. 9, article 646927, 2021.
- [11] J. W. Chung, W. H. Chang, O. Y. Bang et al., "Efficacy and safety of intravenous mesenchymal stem cells for ischemic stroke," *Neurology*, vol. 96, pp. e1012–e1023, 2021.
- [12] M. Dominici, K. Le Blanc, I. Mueller et al., "Minimal criteria for defining multipotent mesenchymal stromal cells. The International Society for Cellular Therapy position statement," *Cytotherapy*, vol. 8, pp. 315–317, 2006.
- [13] E. A. Kimbrel and R. Lanza, "Next-generation stem cells - ushering in a new era of cell-based therapies," *Nature Reviews. Drug Discovery*, vol. 19, pp. 463–479, 2020.
- [14] J. L. Spees, R. H. Lee, and C. A. Gregory, "Mechanisms of mesenchymal stem/stromal cell function," *Stem Cell Research & Therapy*, vol. 7, p. 125, 2016.
- [15] A. J. Friedenstein, J. F. Gorskaja, and N. N. Kulagina, "Fibroblast precursors in normal and irradiated mouse hematopoietic organs," *Experimental Hematology*, vol. 4, pp. 267–274, 1976.
- [16] M. F. Pittenger, A. M. Mackay, S. C. Beck et al., "Multilineage potential of adult human mesenchymal stem cells," *Science*, vol. 284, pp. 143–147, 1999.
- [17] Y. A. Romanov, V. A. Svintsitskaya, and V. N. Smirnov, "Searching for alternative sources of postnatal human mesenchymal stem cells: candidate MSC-like cells from umbilical cord," *Stem Cells*, vol. 21, pp. 105–110, 2003.
- [18] Y. Zhuo, S. H. Li, M. S. Chen et al., "Aging impairs the angiogenic response to ischemic injury and the activity of implanted cells: combined consequences for cell therapy in older recipients," *The Journal of Thoracic and Cardiovascular Surgery*, vol. 139, pp. 1286–1294, 2010.
- [19] M. Song, J. H. Lee, J. Bae, Y. Bu, and E. C. Kim, "Human dental pulp stem cells are more effective than human bone

- marrow-derived mesenchymal stem cells in cerebral ischemic injury," *Cell Transplantation*, vol. 26, pp. 1001–1016, 2017.
- [20] Z. G. Zhang, L. Zhang, Q. Jiang, and M. Chopp, "Bone marrow-derived endothelial progenitor cells participate in cerebral neovascularization after focal cerebral ischemia in the adult mouse," *Circulation Research*, vol. 90, pp. 284–288, 2002.
- [21] Y. Tang, C. Zhang, J. Wang et al., "MRI/SPECT/fluorescent tri-modal probe for evaluating the homing and therapeutic efficacy of transplanted mesenchymal stem cells in a rat ischemic stroke model," *Advanced Functional Materials*, vol. 25, pp. 1024–1034, 2015.
- [22] H. Y. Kim, T. J. Kim, L. Kang et al., "Mesenchymal stem cell-derived magnetic extracellular nanovesicles for targeting and treatment of ischemic stroke," *Biomaterials*, vol. 243, p. 119942, 2020.
- [23] G. Courties, F. Herisson, H. B. Sager et al., "Ischemic stroke activates hematopoietic bone marrow stem cells," *Circulation Research*, vol. 116, pp. 407–417, 2015.
- [24] H. S. Wang, S. C. Hung, S. T. Peng et al., "Mesenchymal stem cells in the Wharton's jelly of the human umbilical cord," *Stem Cells*, vol. 22, pp. 1330–1337, 2004.
- [25] C. P. McGuckin, M. Jurga, A. M. Miller et al., "Ischemic brain injury: a consortium analysis of key factors involved in mesenchymal stem cell-mediated inflammatory reduction," *Archives of Biochemistry and Biophysics*, vol. 534, pp. 88–97, 2013.
- [26] M. Messerli, A. Wagner, R. Sager et al., "Stem cells from umbilical cord Wharton's jelly from preterm birth have neuroglial differentiation potential," *Reproductive Sciences*, vol. 20, pp. 1455–1464, 2013.
- [27] J. H. Seo, I. K. Jang, H. Kim et al., "Early immunomodulation by intravenously transplanted mesenchymal stem cells promotes functional recovery in spinal cord injured rats," *Cell medicine*, vol. 2, pp. 55–67, 2011.
- [28] I. Lua, D. James, J. Wang, K. S. Wang, and K. Asahina, "Mesodermal mesenchymal cells give rise to myofibroblasts, but not epithelial cells, in mouse liver injury," *Hepatology*, vol. 60, pp. 311–322, 2014.
- [29] M. H. Abumaree, M. A. Al Jumah, B. Kalionis et al., "Human placental mesenchymal stem cells (pMSCs) play a role as immune suppressive cells by shifting macrophage differentiation from inflammatory M1 to anti-inflammatory M2 macrophages," *Stem Cell Reviews and Reports*, vol. 9, pp. 620–641, 2013.
- [30] J. M. Lee, J. Jung, H. J. Lee et al., "Comparison of immunomodulatory effects of placenta mesenchymal stem cells with bone marrow and adipose mesenchymal stem cells," *International Immunopharmacology*, vol. 13, pp. 219–224, 2012.
- [31] E. Antoniadou and A. L. David, "Placental stem cells," *Best Practice & Research. Clinical Obstetrics & Gynaecology*, vol. 31, pp. 13–29, 2016.
- [32] L. Casteilla, V. Planat-Benard, B. Cousin et al., "Plasticity of adipose tissue: a promising therapeutic avenue in the treatment of cardiovascular and blood diseases?," *Archives des Maladies du Coeur et des Vaisseaux*, vol. 98, pp. 922–926, 2005.
- [33] M. Gutierrez-Fernandez, L. Otero-Ortega, J. Ramos-Cejudo, B. Rodriguez-Frutos, B. Fuentes, and E. Diez-Tejedor, "Adipose tissue-derived mesenchymal stem cells as a strategy to improve recovery after stroke," *Expert Opinion on Biological Therapy*, vol. 15, pp. 873–881, 2015.
- [34] Y. Zhang, J. Liu, M. Su, X. Wang, and C. Xie, "Exosomal microRNA-22-3p alleviates cerebral ischemic injury by modulating KDM6B/BMP2/BMF axis," *Stem Cell Research & Therapy*, vol. 12, p. 111, 2021.
- [35] W. K. Leong, T. L. Henshall, A. Arthur et al., "Human adult dental pulp stem cells enhance poststroke functional recovery through non-neural replacement mechanisms," *Stem Cells Translational Medicine*, vol. 1, pp. 177–187, 2012.
- [36] S. Gronthos, M. Mankani, J. Brahimi, P. G. Robey, and S. Shi, "Postnatal human dental pulp stem cells (DPSCs) in vitro and in vivo," *Proceedings of the National Academy of Sciences of the United States of America*, vol. 97, pp. 13625–13630, 2000.
- [37] H. Egusa, W. Sonoyama, M. Nishimura, I. Atsuta, and K. Akiyama, "Stem cells in dentistry—part I: stem cell sources," *Journal of Prosthodontic Research*, vol. 56, pp. 151–165, 2012.
- [38] Y. W. Geng, Z. Zhang, M. Y. Liu, and W. P. Hu, "Differentiation of human dental pulp stem cells into neuronal by resveratrol," *Cell Biology International*, vol. 41, pp. 1391–1398, 2017.
- [39] B. C. Perry, D. Zhou, X. Wu et al., "Collection, cryopreservation, and characterization of human dental pulp-derived mesenchymal stem cells for banking and clinical use," *Tissue Engineering. Part C, Methods*, vol. 14, pp. 149–156, 2008.
- [40] K. Sakai, A. Yamamoto, K. Matsubara et al., "Human dental pulp-derived stem cells promote locomotor recovery after complete transection of the rat spinal cord by multiple neuro-regenerative mechanisms," *The Journal of Clinical Investigation*, vol. 122, pp. 80–90, 2012.
- [41] K. Sanen, W. Martens, M. Georgiou, M. Ameloot, I. Lambrichts, and J. Phillips, "Engineered neural tissue with Schwann cell differentiated human dental pulp stem cells: potential for peripheral nerve repair?," *Journal of Tissue Engineering and Regenerative Medicine*, vol. 11, pp. 3362–3372, 2017.
- [42] B. C. Heng, L. W. Lim, W. Wu, and C. Zhang, "An overview of protocols for the neural induction of dental and oral stem cells in vitro," *Tissue Engineering. Part B, Reviews*, vol. 22, pp. 220–250, 2016.
- [43] S. Li, L. Luo, Y. He et al., "Dental pulp stem cell-derived exosomes alleviate cerebral ischaemia-reperfusion injury through suppressing inflammatory response," *Cell Proliferation*, vol. 54, article e13093, 2021.
- [44] T. Inoue, M. Sugiyama, H. Hattori, H. Wakita, T. Wakabayashi, and M. Ueda, "Stem cells from human exfoliated deciduous tooth-derived conditioned medium enhance recovery of focal cerebral ischemia in rats," *Tissue Engineering. Part A*, vol. 19, pp. 24–29, 2013.
- [45] A. Arthur, S. Shi, A. C. Zannettino, N. Fujii, S. Gronthos, and S. A. Koblar, "Implanted adult human dental pulp stem cells induce endogenous axon guidance," *Stem Cells*, vol. 27, pp. 2229–2237, 2009.
- [46] A. H. Huang, B. R. Snyder, P. H. Cheng, and A. W. Chan, "Putative dental pulp-derived stem/stromal cells promote proliferation and differentiation of endogenous neural cells in the hippocampus of mice," *Stem Cells*, vol. 26, pp. 2654–2663, 2008.
- [47] L. Luo, A. A. Albashari, X. Wang et al., "Effects of transplanted heparin-polyoxamer hydrogel combining dental pulp

- stem cells and bFGF on spinal cord injury repair,” *Stem Cells International*, vol. 2018, Article ID 2398521, 2018.
- [48] A. Albashari, Y. He, Y. Zhang et al., “Thermosensitive bFGF-modified hydrogel with dental pulp stem cells on neuroinflammation of spinal cord injury,” *ACS Omega*, vol. 5, pp. 16064–16075, 2020.
- [49] P. Wu, Z. Tong, L. Luo et al., “Comprehensive strategy of conduit guidance combined with VEGF producing Schwann cells accelerates peripheral nerve repair,” *Bioactive Materials*, vol. 6, pp. 3515–3527, 2021.
- [50] S. Zhu, Y. Ying, Y. He et al., “Hypoxia response element-directed expression of bFGF in dental pulp stem cells improve the hypoxic environment by targeting pericytes in SCI rats,” *Bioactive Materials*, vol. 6, pp. 2452–2466, 2021.
- [51] L. Luo, Y. He, L. Jin et al., “Application of bioactive hydrogels combined with dental pulp stem cells for the repair of large gap peripheral nerve injuries,” *Bioactive Materials*, vol. 6, pp. 638–654, 2021.
- [52] L. Wei, Z. Z. Wei, M. Q. Jiang, O. Mohamad, and S. P. Yu, “Stem cell transplantation therapy for multifaceted therapeutic benefits after stroke,” *Progress in Neurobiology*, vol. 157, pp. 49–78, 2017.
- [53] M. H. Theus, L. Wei, L. Cui et al., “In vitro hypoxic preconditioning of embryonic stem cells as a strategy of promoting cell survival and functional benefits after transplantation into the ischemic rat brain,” *Experimental Neurology*, vol. 210, pp. 656–670, 2008.
- [54] M. Modo, R. P. Stroemer, E. Tang, S. Patel, and H. Hodges, “Effects of implantation site of stem cell grafts on behavioral recovery from stroke damage,” *Stroke*, vol. 33, pp. 2270–2278, 2002.
- [55] W. L. Li, S. P. Yu, M. E. Ogle, X. S. Ding, and L. Wei, “Enhanced neurogenesis and cell migration following focal ischemia and peripheral stimulation in mice,” *Developmental Neurobiology*, vol. 68, pp. 1474–1486, 2008.
- [56] M. Modo, K. Mellodew, D. Cash et al., “Mapping transplanted stem cell migration after a stroke: a serial, in vivo magnetic resonance imaging study,” *NeuroImage*, vol. 21, pp. 311–317, 2004.
- [57] M. Q. Jiang, Y. Y. Zhao, W. Cao et al., “Long-term survival and regeneration of neuronal and vasculature cells inside the core region after ischemic stroke in adult mice,” *Brain Pathology*, vol. 27, pp. 480–498, 2017.
- [58] J. Xu, Z. Feng, X. Wang et al., “hUC-MSCs exert a neuroprotective effect via anti-apoptotic mechanisms in a neonatal HIE rat model,” *Cell Transplantation*, vol. 28, pp. 1552–1559, 2019.
- [59] Y. Li, J. Chen, C. L. Zhang et al., “Gliosis and brain remodeling after treatment of stroke in rats with marrow stromal cells,” *Glia*, vol. 49, pp. 407–417, 2005.
- [60] S. M. Hosseini, M. Farahmandnia, Z. Razi, S. Delavarifar, and B. Shakibajahromi, “12 hours after cerebral ischemia is the optimal time for bone marrow mesenchymal stem cell transplantation,” *Neural Regeneration Research*, vol. 10, pp. 904–908, 2015.
- [61] A. Bakshi, A. L. Barshinger, S. A. Swanger et al., “Lumbar puncture delivery of bone marrow stromal cells in spinal cord contusion: a novel method for minimally invasive cell transplantation,” *Journal of Neurotrauma*, vol. 23, pp. 55–65, 2006.
- [62] H. K. Jin, J. E. Carter, G. W. Huntley, and E. H. Schuchman, “Intracerebral transplantation of mesenchymal stem cells into acid sphingomyelinase-deficient mice delays the onset of neurological abnormalities and extends their life span,” *The Journal of Clinical Investigation*, vol. 109, pp. 1183–1191, 2002.
- [63] J. Jiang, Y. Wang, B. Liu, X. Chen, and S. Zhang, “Challenges and research progress of the use of mesenchymal stem cells in the treatment of ischemic stroke,” *Brain & Development*, vol. 40, pp. 612–626, 2018.
- [64] H. Kim, D. L. Na, N. K. Lee, A. R. Kim, S. Lee, and H. Jang, “Intrathecal injection in a rat model: a potential route to deliver human Wharton’s jelly-derived mesenchymal stem cells into the brain,” *International Journal of Molecular Sciences*, vol. 21, 2020.
- [65] J. Y. Lim, C. H. Jeong, J. A. Jun et al., “Therapeutic effects of human umbilical cord blood-derived mesenchymal stem cells after intrathecal administration by lumbar puncture in a rat model of cerebral ischemia,” *Stem Cell Research & Therapy*, vol. 2, p. 38, 2011.
- [66] L. Deng, Q. Peng, H. Wang et al., “Intrathecal injection of allogenic bone marrow-derived mesenchymal stromal cells in treatment of patients with severe ischemic stroke: study protocol for a randomized controlled observer-blinded trial,” *Translational Stroke Research*, vol. 10, pp. 170–177, 2019.
- [67] A. Jaillard, M. Hommel, A. Moisan et al., “Autologous mesenchymal stem cells improve motor recovery in subacute ischemic stroke: a randomized clinical trial,” *Translational Stroke Research*, vol. 11, pp. 910–923, 2020.
- [68] J. S. Lee, J. M. Hong, G. J. Moon, P. H. Lee, Y. H. Ahn, and O. Y. Bang, “A long-term follow-up study of intravenous autologous mesenchymal stem cell transplantation in patients with ischemic stroke,” *Stem Cells*, vol. 28, pp. 1099–1106, 2010.
- [69] O. Y. Bang, J. S. Lee, P. H. Lee, and G. Lee, “Autologous mesenchymal stem cell transplantation in stroke patients,” *Annals of Neurology*, vol. 57, pp. 874–882, 2005.
- [70] A. V. Pendharkar, J. Y. Chua, R. H. Andres et al., “Biodistribution of neural stem cells after intravascular therapy for hypoxic-ischemia,” *Stroke*, vol. 41, pp. 2064–2070, 2010.
- [71] G. Du, Y. Liu, M. Dang et al., “Comparison of administration routes for adipose-derived stem cells in the treatment of middle cerebral artery occlusion in rats,” *Acta Histochemica*, vol. 116, pp. 1075–1084, 2014.
- [72] J. Biernaskie, D. Corbett, J. Peeling, J. Wells, and H. Lei, “A serial MR study of cerebral blood flow changes and lesion development following endothelin-1-induced ischemia in rats,” *Magnetic Resonance in Medicine*, vol. 46, pp. 827–830, 2001.
- [73] J. M. Karp and G. S. Leng Teo, “Mesenchymal stem cell homing: the devil is in the details,” *Cell Stem Cell*, vol. 4, pp. 206–216, 2009.
- [74] M. T. Harting, F. Jimenez, H. Xue et al., “Intravenous mesenchymal stem cell therapy for traumatic brain injury,” *Journal of Neurosurgery*, vol. 110, pp. 1189–1197, 2009.
- [75] N. Wei, S. P. Yu, X. Gu et al., “Delayed intranasal delivery of hypoxic-preconditioned bone marrow mesenchymal stem cells enhanced cell homing and therapeutic benefits after ischemic stroke in mice,” *Cell Transplantation*, vol. 22, pp. 977–991, 2013.
- [76] L. Danielyan, R. Schafer, A. von Ameln-Mayerhofer et al., “Intranasal delivery of cells to the brain,” *European Journal of Cell Biology*, vol. 88, pp. 315–324, 2009.

- [77] C. Galeano, Z. Qiu, A. Mishra et al., "The route by which intranasally delivered stem cells enter the central nervous system," *Cell Transplantation*, vol. 27, pp. 501–514, 2018.
- [78] V. Donega, C. H. Nijboer, G. van Tilborg, R. M. Dijkhuizen, A. Kavelaars, and C. J. Heijnen, "Intranasally administered mesenchymal stem cells promote a regenerative niche for repair of neonatal ischemic brain injury," *Experimental Neurology*, vol. 261, pp. 53–64, 2014.
- [79] C. A. McDonald, Z. Djulianisaa, M. Petraki et al., "Intranasal delivery of mesenchymal stromal cells protects against neonatal hypoxic(-)ischemic brain injury," *International Journal of Molecular Sciences*, vol. 20, 2019.
- [80] Y. Shi, R. K. Leak, R. F. Keep, and J. Chen, "Translational stroke research on blood-brain barrier damage: challenges, perspectives, and goals," *Translational Stroke Research*, vol. 7, pp. 89–92, 2016.
- [81] D. Petrovic-Djergovic, S. N. Goonewardena, and D. J. Pinsky, "Inflammatory disequilibrium in stroke," *Circulation Research*, vol. 119, pp. 142–158, 2016.
- [82] T. Shichita, M. Ito, and A. Yoshimura, "Post-ischemic inflammation regulates neural damage and protection," *Frontiers in Cellular Neuroscience*, vol. 8, p. 319, 2014.
- [83] Y. Wang, X. Chen, W. Cao, and Y. Shi, "Plasticity of mesenchymal stem cells in immunomodulation: pathological and therapeutic implications," *Nature Immunology*, vol. 15, pp. 1009–1016, 2014.
- [84] C. R. Harrell, M. G. Jankovic, C. Fellabaum et al., "Molecular mechanisms responsible for anti-inflammatory and immunosuppressive effects of mesenchymal stem cell-derived factors," *Advances in Experimental Medicine and Biology*, vol. 1084, pp. 187–206, 2019.
- [85] Q. Cheng, Z. Zhang, S. Zhang et al., "Human umbilical cord mesenchymal stem cells protect against ischemic brain injury in mouse by regulating peripheral immunoinflammation," *Brain Research*, vol. 1594, pp. 293–304, 2015.
- [86] S. Glennie, I. Soeiro, P. J. Dyson, E. W. Lam, and F. Dazzi, "Bone marrow mesenchymal stem cells induce division arrest anergy of activated T cells," *Blood*, vol. 105, pp. 2821–2827, 2005.
- [87] M. Li, X. Sun, X. Kuang, Y. Liao, H. Li, and D. Luo, "Mesenchymal stem cells suppress CD8+ T cell-mediated activation by suppressing natural killer group 2, member D protein receptor expression and secretion of prostaglandin E2, indoleamine 2, 3-dioxygenase and transforming growth factor-beta," *Clinical and Experimental Immunology*, vol. 178, pp. 516–524, 2014.
- [88] G. M. Spaggiari, H. Abdelrazik, F. Becchetti, and L. Moretta, "MSCs inhibit monocyte-derived DC maturation and function by selectively interfering with the generation of immature DCs: central role of MSC-derived prostaglandin E2," *Blood*, vol. 113, pp. 6576–6583, 2009.
- [89] Z. Cheng, L. Wang, M. Qu et al., "Mesenchymal stem cells attenuate blood-brain barrier leakage after cerebral ischemia in mice," *Journal of Neuroinflammation*, vol. 15, p. 135, 2018.
- [90] G. Tang, Y. Liu, Z. Zhang et al., "Mesenchymal stem cells maintain blood-brain barrier integrity by inhibiting aquaporin-4 upregulation after cerebral ischemia," *Stem Cells*, vol. 32, pp. 3150–3162, 2014.
- [91] N. Pavlichenko, I. Sokolova, S. Vijde et al., "Mesenchymal stem cells transplantation could be beneficial for treatment of experimental ischemic stroke in rats," *Brain Research*, vol. 1233, pp. 203–213, 2008.
- [92] P. A. Walker, S. K. Shah, F. Jimenez et al., "Intravenous multipotent adult progenitor cell therapy for traumatic brain injury: preserving the blood brain barrier via an interaction with splenocytes," *Experimental Neurology*, vol. 225, pp. 341–352, 2010.
- [93] T. A. Womble, S. Green, M. Shahaduzzaman et al., "Monocytes are essential for the neuroprotective effect of human cord blood cells following middle cerebral artery occlusion in rat," *Molecular and Cellular Neurosciences*, vol. 59, pp. 76–84, 2014.
- [94] H. Offner, S. Subramanian, S. M. Parker, M. E. Afentoulis, A. A. Vandembark, and P. D. Hurn, "Experimental stroke induces massive, rapid activation of the peripheral immune system," *Journal of Cerebral Blood Flow and Metabolism: Official Journal of the International Society of Cerebral Blood Flow and Metabolism*, vol. 26, pp. 654–665, 2006.
- [95] C. C. Leonardo, A. A. Hall, L. A. Collier, C. T. Ajmo Jr., A. E. Willing, and K. R. Pennypacker, "Human umbilical cord blood cell therapy blocks the morphological change and recruitment of CD11b-expressing, isolectin-binding proinflammatory cells after middle cerebral artery occlusion," *Journal of Neuroscience Research*, vol. 88, pp. 1213–1222, 2010.
- [96] R. Das, H. Jahr, G. J. van Osch, and E. Farrell, "The role of hypoxia in bone marrow-derived mesenchymal stem cells: considerations for regenerative medicine approaches," *Tissue Engineering Part B, Reviews*, vol. 16, pp. 159–168, 2010.
- [97] X. Chen, Y. Li, L. Wang et al., "Ischemic rat brain extracts induce human marrow stromal cell growth factor production," *Neuropathology*, vol. 22, pp. 275–279, 2002.
- [98] J. Alder, B. C. Kramer, C. Hoskin, and S. Thakker-Varia, "Brain-derived neurotrophic factor produced by human umbilical tissue-derived cells is required for its effect on hippocampal dendritic differentiation," *Developmental Neurobiology*, vol. 72, pp. 755–765, 2012.
- [99] C. A. Ribeiro, J. S. Fraga, M. Graos et al., "The secretome of stem cells isolated from the adipose tissue and Wharton jelly acts differently on central nervous system derived cell populations," *Stem Cell Research & Therapy*, vol. 3, p. 18, 2012.
- [100] X. Ding, Y. Li, Z. Liu et al., "The sonic hedgehog pathway mediates brain plasticity and subsequent functional recovery after bone marrow stromal cell treatment of stroke in mice," *Journal of Cerebral Blood Flow and Metabolism: Official Journal of the International Society of Cerebral Blood Flow and Metabolism*, vol. 33, pp. 1015–1024, 2013.
- [101] M. Yang, X. Wei, J. Li, L. A. Heine, R. Rosenwasser, and L. Iacovitti, "Changes in host blood factors and brain glia accompanying the functional recovery after systemic administration of bone marrow stem cells in ischemic stroke rats," *Cell Transplantation*, vol. 19, pp. 1073–1084, 2010.
- [102] S. P. Liu, R. H. Fu, H. H. Yu et al., "MicroRNAs regulation modulated self-renewal and lineage differentiation of stem cells," *Cell Transplantation*, vol. 18, pp. 1039–1045, 2009.
- [103] Z. Zhang, J. Yang, W. Yan, Y. Li, Z. Shen, and T. Asahara, "Pretreatment of cardiac stem cells with exosomes derived from mesenchymal stem cells enhances myocardial repair," *Journal of the American Heart Association*, vol. 25, article e002856, 2016.
- [104] H. Xin, Y. Li, Z. Liu et al., "miR-133b promotes neural plasticity and functional recovery after treatment of stroke with

- multipotent mesenchymal stromal cells in rats via transfer of exosome-enriched extracellular particles,” *Stem Cells*, vol. 31, pp. 2737–2746, 2013.
- [105] H. Xin, F. Wang, Y. Li et al., “Secondary release of exosomes from astrocytes contributes to the increase in neural plasticity and improvement of functional recovery after stroke in rats treated with exosomes harvested from microRNA 133b-overexpressing multipotent mesenchymal stromal cells,” *Cell Transplantation*, vol. 26, pp. 243–257, 2017.
- [106] B. Huang, X. C. Jiang, T. Y. Zhang et al., “Peptide modified mesenchymal stem cells as targeting delivery system transfected with miR-133b for the treatment of cerebral ischemia,” *International Journal of Pharmaceutics*, vol. 531, pp. 90–100, 2017.
- [107] G. J. Moon, J. H. Sung, D. H. Kim et al., “Application of mesenchymal stem cell-derived extracellular vesicles for stroke: biodistribution and microRNA study,” *Translational Stroke Research*, vol. 10, pp. 509–521, 2019.
- [108] C. J. Cunningham, E. Redondo-Castro, and S. M. Allan, “The therapeutic potential of the mesenchymal stem cell secretome in ischaemic stroke,” *Journal of Cerebral Blood Flow and Metabolism: Official Journal of the International Society of Cerebral Blood Flow and Metabolism*, vol. 38, pp. 1276–1292, 2018.
- [109] A. Bronckaers, P. Hilken, W. Martens et al., “Mesenchymal stem/stromal cells as a pharmacological and therapeutic approach to accelerate angiogenesis,” *Pharmacology & Therapeutics*, vol. 143, pp. 181–196, 2014.
- [110] Y. C. Lin, T. L. Ko, Y. H. Shih et al., “Human umbilical mesenchymal stem cells promote recovery after ischemic stroke,” *Stroke*, vol. 42, pp. 2045–2053, 2011.
- [111] M. Dao, C. C. Tate, M. McGrogan, and C. C. Case, “Comparing the angiogenic potency of naive marrow stromal cells and Notch-transfected marrow stromal cells,” *Journal of Translational Medicine*, vol. 11, p. 81, 2013.
- [112] A. Zacharek, J. Chen, X. Cui et al., “Angiopoietin1/Tie2 and VEGF/Flk1 induced by MSC treatment amplifies angiogenesis and vascular stabilization after stroke,” *Journal of Cerebral Blood Flow and Metabolism: Official Journal of the International Society of Cerebral Blood Flow and Metabolism*, vol. 27, pp. 1684–1691, 2007.
- [113] E. Diez-Tejedor, M. Gutierrez-Fernandez, P. Martinez-Sanchez et al., “Reparative therapy for acute ischemic stroke with allogeneic mesenchymal stem cells from adipose tissue: a safety assessment: a phase II randomized, double-blind, placebo-controlled, single-center, pilot clinical trial,” *Journal of Stroke and Cerebrovascular Diseases*, vol. 23, pp. 2694–2700, 2014.
- [114] J. Fang, Y. Guo, S. Tan et al., “Autologous endothelial progenitor cells transplantation for acute ischemic stroke: a 4-year follow-up study,” *Stem Cells Translational Medicine*, vol. 8, pp. 14–21, 2019.
- [115] M. L. Levy, J. R. Crawford, N. Dib, L. Verkh, N. Tankovich, and S. C. Cramer, “Phase I/II study of safety and preliminary efficacy of intravenous allogeneic mesenchymal stem cells in chronic stroke,” *Stroke*, vol. 50, pp. 2835–2841, 2019.

Research Article

3D Spheroid Formation Using BMP-Loaded Microparticles Enhances Odontoblastic Differentiation of Human Dental Pulp Stem Cells

Tae-Jun Min,¹ Min Ji Kim,¹ Kyung-Jung Kang,¹ Yeoung Jo Jeoung,¹ Se Heang Oh ¹,
and Young-Joo Jang ^{1,2}

¹Department of Nanobiomedical Science & BK21 FOUR NBM Global Research Center for Regenerative Medicine, Dankook University, Cheonan 31116, Republic of Korea

²Laboratory of Oral Biochemistry, College of Dentistry, Dankook University, Cheonan 31116, Republic of Korea

Correspondence should be addressed to Se Heang Oh; seheangoh@dankook.ac.kr and Young-Joo Jang; yjjang@dankook.ac.kr

Received 26 April 2021; Revised 31 May 2021; Accepted 2 August 2021; Published 2 September 2021

Academic Editor: Adam Ye

Copyright © 2021 Tae-Jun Min et al. This is an open access article distributed under the Creative Commons Attribution License, which permits unrestricted use, distribution, and reproduction in any medium, provided the original work is properly cited.

Human dental pulp stem cells (hDPSCs) are the primary cells responsible for dentin regeneration. Typically, in order to allow for odontoblastic differentiation, hDPSCs are cultured over weeks with differentiation-inducing factors in a typical monolayered culture. However, monolayered cultures have significant drawbacks including inconsistent differentiation efficiency, require a higher BMP concentration than should be necessary, and require periodic treatment with BMPs for weeks to see results. To solve these problems, we developed a 3D-cell spheroid culture system for odontoblastic differentiation using microparticles with leaf-stacked structure (LSS), which allow for the sustained release of BMPs and adequate supply of oxygen in cell spheroids. BMPs were continuously released and maintained an effective concentration over 37 days. hDPSCs in the spheroid maintained their viability for 5 weeks, and the odontoblastic differentiation efficiency was increased significantly compared to monolayered cells. Finally, dentin-related features were detected in the spheroids containing BMPs-loaded microparticles after 5 weeks, suggesting that these hDPSC-LSS spheroids might be useful for dentin tissue regeneration.

1. Introduction

In a normal biological system, stem cells undergo intensive cell-cell contacts to develop tissues with three-dimensional (3D) structures. This is mediated by the microenvironment including the extracellular matrix surrounding cells, which are distinct physiological cues for cell differentiation and proliferation. Two-dimensional (2D) monolayer cultures inadequately reproduce the native microenvironment of stem cells created by intrinsic and extrinsic cellular communications, resulting in an unnatural spatial distribution of signaling molecules, oxygen, and nutrients [1]. Moreover, the normal physiological behaviors of stem cells can be distorted in monolayer cultures, leading to the loss of the multilineage potential and replicative ability [2, 3]. To mimic the physiological environment, various methods have been reported for culturing cells in a 3D structure, including scaffold-free

cultures [4, 5], cultures grown on various scaffold materials [6–8], and cultures embedded in gel materials [9, 10]. 3D cell aggregates, known as spheroids, yield a multicellular mass that mimics the natural cell niche [11]. Scaffold-free 3D culture systems have advantages in preventing the inflammation and infection caused by scaffold material degradation [12] and disadvantages of poor guidance on cells required for cell proliferation and differentiation. Cell spheroids have been utilized in various tissue engineering [13–15] and stem cell applications [10, 16–19]. However, only recently have cell spheroids been investigated for dental tissue regeneration, leaving much data on the topic still to be discovered. Spheroid culturing of human periodontal ligament stem cells (hPDLSCs) significantly enhanced stemness and osteogenic potential compared with hPDLSCs cultured in a monolayer [11, 20]. In addition, osteo/odontoblastic gene expression and mineralization are upregulated in immortalized mouse

dental papilla cells cultured as 3D spheroids when compared with 2D monolayer-cultured cells [21]. In addition to the 3D aspects of the cell culture system, the sustained supply of cytokines or growth factors also plays an important role in mimicking the natural microenvironment and achieving effective differentiation. Biomaterial-based delivery systems in culture have been previously reported to form nanoparticles, microparticles, hydrogels, and tissue engineering scaffolds, improving the pharmacokinetics of retained factors and reducing toxicity [13–15, 22]. Recently, 3D cell culture models, including cell spheroids, have been assessed in terms of drug delivery efficacy [5–7]. In previous studies, signaling pathways stimulated by Wnt proteins, transforming growth factor- β (TGF β)/bone morphogenetic proteins (BMPs), and fibroblast growth factor (FGF) were identified to regulate tooth development [23, 24]; however, the process of dentin formation is not fully understood. Recently, we reported that the combinational treatment of BMP-2 and BMP-4 can maximize the odontoblastic differentiation efficiency of hDPSCs [25]. The induction of odontoblastic differentiation in 3D spheroid cultures via the direct addition of differentiation-inducing factors to the culture medium can be complicated compared to monolayer cultures. In monolayered cultures, oxygen and nutrition are uniformly provided to all cells, whereas in 3D spheroid cultures, the concentrations of oxygen and nutrients can be quite low at the interior of spheroids as limited by diffusion [12, 26]. Our aim was to achieve high efficiency and successful odontoblastic differentiation in a 3D culture system. For this, we established an hDPSC-spheroid complex with accompanying LSS microparticles which allowed for the sustained supply of signaling factors and improved cell adhesiveness. These hDPSCs-spheroid complexes mimicked the natural microenvironment better than conventional monolayered cultures, and even larger-scale structures showed long-lasting differentiation efficiency, more so than any other structures developed thus far (e.g., solid porous matrix- or hydrogel-based scaffold systems and conventional cell only spheroid systems).

2. Materials and Methods

2.1. Cell Culture. Human dental pulp stem cells were obtained from the dental pulp tissues extracted from wisdom teeth under guidelines approved by the IRB of the Dankook University (DKU-NON2019-004). The dental pulp tissues were collected after removing the tooth crown. The tissues were chopped and treated with 3 mg/ml collagenase type-I (Millipore) and 4 mg/ml dispase (Sigma-Aldrich) for 1 h at 37°C. Single-cell suspension was incubated in alpha-modified minimum essential medium (α -MEM, Hyclone) containing 20% fetal bovine serum (Hyclone) and antibiotics (Lonza) at 37°C in 5% CO₂. For induction of odontoblastic differentiation in 2D monolayer culture, hDPSCs were treated with BMP-2 and BMP-4 as indicated concentrations in every 3 days. Stemness and differentiation potentials of independently isolated hDPSCs from patients were verified by expression of the representative mesenchymal stem cell markers and odontoblastic markers (Figure S1 and S2).

Each cell batch was not combined and used separately in experiments.

2.2. Preparation of Microparticles with BMPs and the Release Behavior Analysis. Microparticles with leaf-stacked structure (LSS) were fabricated by a heating and cooling method as described in our previous studies [27]. In brief, polycaprolactone (PCL, 81 kDa, Lakeshore Biomaterials) was dissolved in tetraglycol (Sigma-Aldrich) in 15% at 90°C, and the solution was stored at 4°C to obtain LSS microparticles. LSS particles in the size range of 25–53 μ m were collected using standard testing sieves. For morphological observation of LSS microparticles, a scanning electron microscope (S-4300, Hitachi) was used. For immobilization of BMP-2 and BMP-4 in LSS microparticles, a mixture of 1 ml LSS particles and 1 ml BMP solution (1 μ g/ml BMP in PBS supplemented with 1% bovine serum albumin) was stored at 4°C for 3 h under positive pressure. Excess BMP solutions were removed and freeze-dried. To investigate the release behavior of BMPs from LSS microparticles, 5 mg BMPs-loaded LSS microparticles were incubated in 1 ml PBS at 37°C, and supernatant was collected every 24 h. The amount of BMPs released from LSS microparticles was detected by the ELISA kit (DuoSet, R&D Systems).

2.3. Spheroid Formation. To prepare hDPSC-spheroids containing BMPs-loaded LSS microparticle, suspension of cell (2.7×10^6 cells) and microparticle (0.3×10^6 particles) was seeded onto agarose mold with concave microstructure (800 μ m in diameter and 400 μ m in depth). A hemocytometer was used to count cells and microparticles. 144 concaves per experiment were prepared. The spheroids were incubated in a growth medium for 1 week and, then, incubated for additional 4 weeks to induce odontoblastic differentiation. Size and morphological changes of spheroids were observed using a light microscope (CKX41, Olympus) and a scanning electron microscope (S-4300, Hitachi).

2.4. Immunocytochemistry and Immunohistochemistry. For histological observation, cell spheroids were fixed with 4% paraformaldehyde for 20 min at 4°C. After freezing at -70°C, the specimens were cut into sections of 8- μ m thickness and, then, stained with Hematoxylin and Eosin (H&E) staining for observation by a light microscope (CKX41, Olympus). To visualize protein expression, immunocytochemical (ICC) staining was conducted on cell spheroids. A slice cut from spheroid was washed with Tris-Buffered Saline (TBS), permeabilized with 0.1% Triton X-100 for 5 min, and blocked with 10% normal serum (in TBS containing 1% BSA) for 2 h, consecutively. Specimens were incubated with anti-BSP (ab125227, Abcam) and anti-DSPP antibodies (Santa Cruz, sc-73642) at 4°C for 12 h, followed by incubation with Alexa Fluor® 488 (Abcam) as secondary antibody for 1 h. Cell nuclei were stained with 4',6-diamidino-2-phenylindole (DAPI, Vector Laboratories) and observed using a fluorescence microscope (Eclipse Ts2R, Nikon).

2.5. Quantification of Calcium Contents. For quantification of mineralization, cells or spheroids were collected and incubated in 0.6N HCl for 24 h for decalcification. Calcium

TABLE 1: Primer sequences.

Genes	Forward primers	Reverse primers
BSP	5'-TACCGAGCCTATGAAGATGA-3'	5'-CTTCTGAGTTGAACTTCGA-3'
COL1	5'-GGAGGAGAGTCAGGAAGG-3'	5'-TCAGCAACACAGTTACACAA-3'
DMP-1	5'-GACTCTCAAGAAGACAGCAA-3'	5'-GACTCACTACCACCTCT-3'
OCN	5'-TGAGTCCTGAGCAGCAG-3'	5'-TCTCTTCACTACCTCGCT-3'
OPN	5'-GTGGGAAGGACAGTTATGAA-3'	5'-CTGACTTTGGAAAAGTTCTTG-3'
OSX	5'-TTGACATGTACCCCTTCTG-3'	5'-CAATACCCCTGATGAAGAGG-3'
GAPDH	5'-GTATGACAACAGCCTCAAGAT-3'	5'-CCTTCCACGATACCAAAGTT-3'

amounts were quantified using Calcium Colorimetric Assay Kit (Sigma-Aldrich). A chromogenic complex was formed between calcium ions and O-cresolphthalein, and its absorbance intensity was measured at 575 nm. The calcium amounts were calculated according to the absorbance.

2.6. Real-Time Polymerase Chain Reaction. Total RNA was extracted from cells or spheroids using Easy-Spin Kit (Intron), and cDNA was synthesized using ReverTra Ace qPCR RT Mix (Toyobo). The qRT-PCR was conducted with iTaq Universal SYBR Green Supermix (Bio-Rad) using specific primers (Table 1). qPCR amplifying condition consisted of 1 cycle for 30 sec at 95°C, and 40 cycles for 15 sec at 95°C of denaturation and 60 sec at 55-60°C of annealing/extension. A melt curve was constructed in the range of 65°C to 95°C with 0.5°C increments per step. The relative comparison of each gene was analyzed, and glyceraldehyde 3-phosphate dehydrogenase (GAPDH) was used for normalizing gene expression as an internal control. Three samples were analyzed for each target gene.

2.7. Statistical Analysis. The differences between two samples were evaluated by the *t*-test as a statistical method. A *P* value of less than 0.05 was considered statistically significant.

3. Results

3.1. Development of BMPs-Loaded Microparticles for Sustainable Delivery. Microparticles with a leaf-stacked structure (LSS) were developed to provide an appropriate microenvironment with a continuous supply of factors and sufficient surface for cell adhesion [27]. Diameters of these particles were 25~53 μm. SEM imaging (Figure 1(a)) revealed that the surfaces of these particles were covered with a laminated structure. Such laminated porous structures not only can offer a sustained release of bioactive molecules but also can improve cell adhesion and permeation of oxygen and nutrients.

To induce odontoblastic differentiation of monolayered hDPSCs, cultures were cotreated with BMP-2 and BMP-4 [25]. To facilitate odontoblastic differentiation in a 3D culture system, LSS microparticles loaded with either BMP-2 or BMP-4 were prepared. When 5 mg of microparticles was resuspended in 10 μg/ml each BMP solution, maximal loading amounts of BMP-2 and BMP-4 were 206.16 ng/5 mg par-

ticles and 194.26 ng/5 mg particles, respectively. After a high initial release of factors between day 1 and day 7, the total duration of release above the effective concentration of 0.2 ng/ml was 39 days in case of BMP-2 and 37 days in case of BMP-4 (Figure 1(b), A and B). Based on the release behavior, total accumulated amounts of released BMP-2 and BMP-4 were estimated to be 174.93 ng/5 mg particles and 150.64 ng/5 mg particles, respectively (Figure 1(c), A and B). To sum up, 84.85% and 77.55% of total loading amounts of BMP-2 and BMP-4 were released over 37 and 39 days, respectively. These data suggested that BMPs were continuously released from LSS microparticles for at least 37 days, allowing them to achieve continuous differentiation induction without an intermittent stimulation.

3.2. Formation of hDPSC Spheroids with BMP-Loaded LSS Microparticles. To construct cell aggregates, 2.7×10^6 hDPSCs and 0.3×10^6 BMPs-loaded LSS particles were mixed in an agarose concave microwell. In our previous report [25], monolayered hDPSCs required treatment with both 33.3 ng/ml BMP-2 and 3.3 ng/ml BMP-4 per day to produce odontoblastic differentiation. To induce odontoblastic differentiation under conditions similar to a two-dimensional culture, 3.2 mg BMP-2-loaded LSS particles (0.270×10^6 particles) and 0.32 mg BMP-4-loaded LSS particles (0.027×10^6 particles) were used for spheroid formation. These particles released either 1.17 ng/ml BMP-2 or 0.12 ng/ml BMP-4 per day. One spheroid body was constructed per well (Figures 2(a) and 2(b)), resulting in a total of 144 cell spheroids. Cell spheroids without LSS particles decreased in size over time. They almost disappeared after five weeks (Figure 2, A in (a) and (b)). This phenomenon might be due to cell death as cell necrosis in the central region of spheroids has been occasionally observed in larger spheroid structures [28]. However, cell spheroids with LSS microparticles (Cell/LSS and Cell/LSS/BMPs) did not shrink much during incubation (Figure 2, A and C in (a) and (b)). To analyze cell viability, an MTT assay was performed with 30 spheroids containing LSS particles. By the first week, cells in spheroids without particles sharply decreased in number, while cells in Cell/LSS and Cell/LSS/BMPs proliferated and cell numbers increased (Figure 2(c)). Over a period of longer than three weeks, the number of cells remained somewhat unchanged except for spheroids with only cells which showed decreased number over the same period

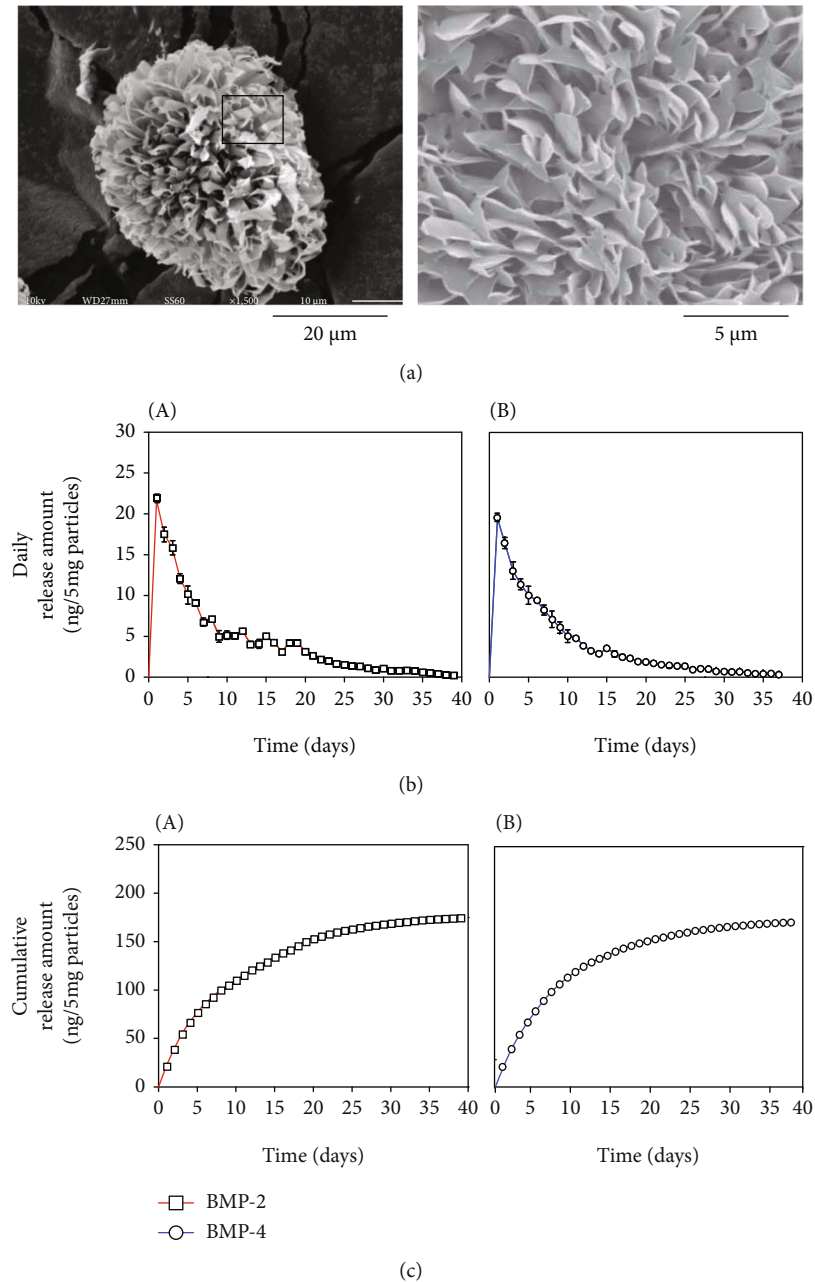


FIGURE 1: Sustainable release of BMP-2 and BMP-4 by using the microparticles of the entire leaf-stacked structure (LSS). (a) Scanning electron microscopic structure of the surface of an ELSS microparticle. (b) Daily release amounts of BMP-2 (A) and BMP-4 (B). The release behavior was analyzed daily using 5 mg of particles and continued until 0.2 ng of each BMP was released. The releases of BMP-2 and BMP-4 were analyzed for 39 days and 37 days, respectively. (c) Cumulative release amounts of BMP-2 (A) and BMP-4 (B). Over 39 days and 37 days, the cumulative release amounts of BMP-2 and BMP-4 per 5 mg of particles were 174.93 ng and 194.26 ng, respectively.

(Figure 2(c), bars in 3-5 wks). Therefore, mixed hDPSCs and LSS particle spheroid system was appropriate for a long-term differentiation of hDPSCs. Hematoxylin and eosin (H&E) staining revealed cells in the core region of spheroids due to a high survival rate. It also revealed that the gap between cells and particles narrowed as the incubation time increased (Figure 2(d)). In both LSS particles and BMPs-loaded LSS particles, cells either wrapped close to particles or hung between particles.

3.3. Enhancement of Odontoblastic Differentiation in hDPSC/LSS Spheroids Releasing BMP-2 and BMP-4. Odonto/osteoblastic differentiation of hDPSCs cultured in spheroids was evaluated based on the transcriptional expression of odonto/osteogenic markers. Overall, gene expression levels of representative markers were increased in spheroids even without BMP-2 or BMP-4 (Figure 3(a), LSS in a-f), although their expression levels were increased more in spheroids with BMPs-loaded LSS particles (Figure 3(a),

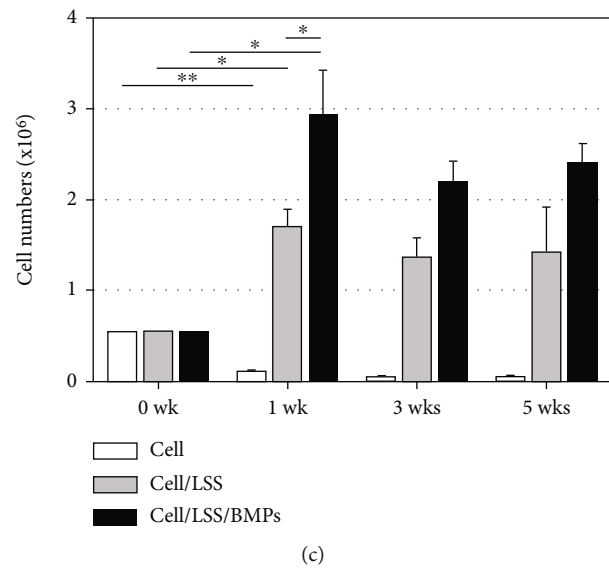
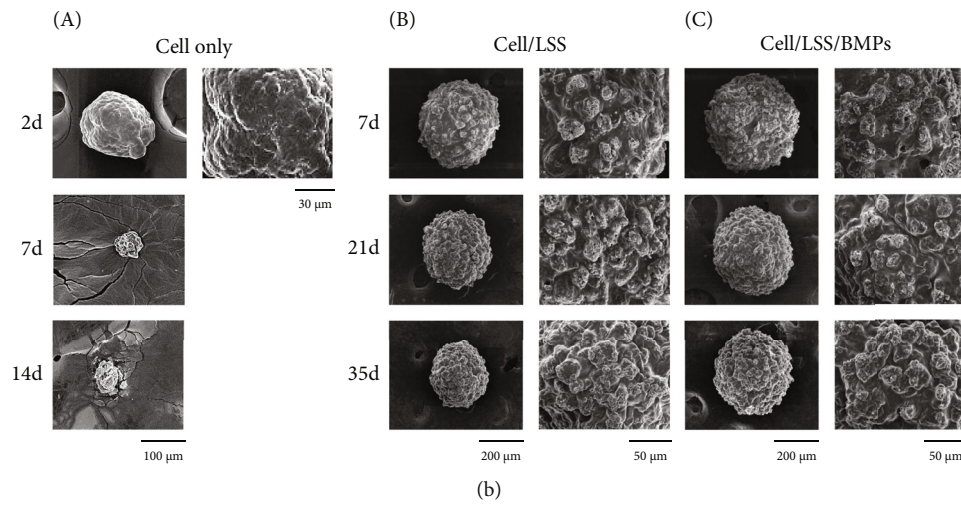
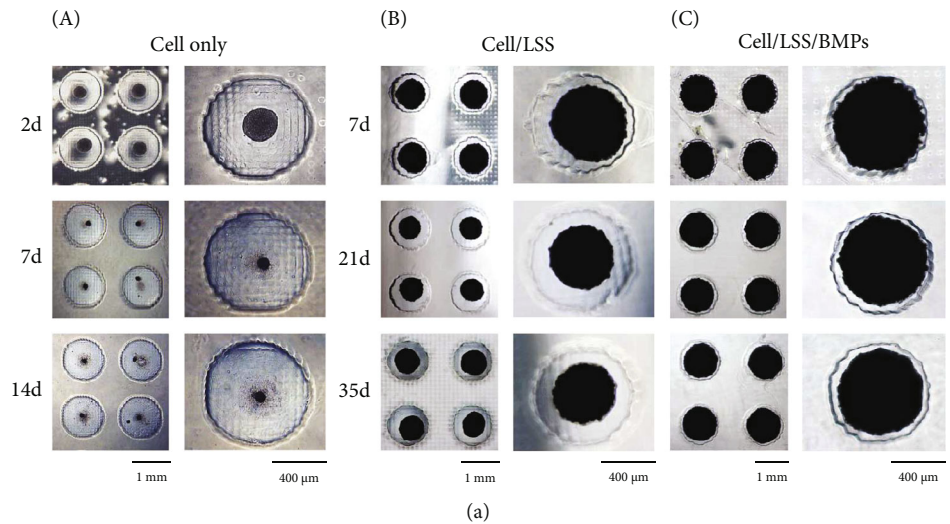


FIGURE 2: Continued.

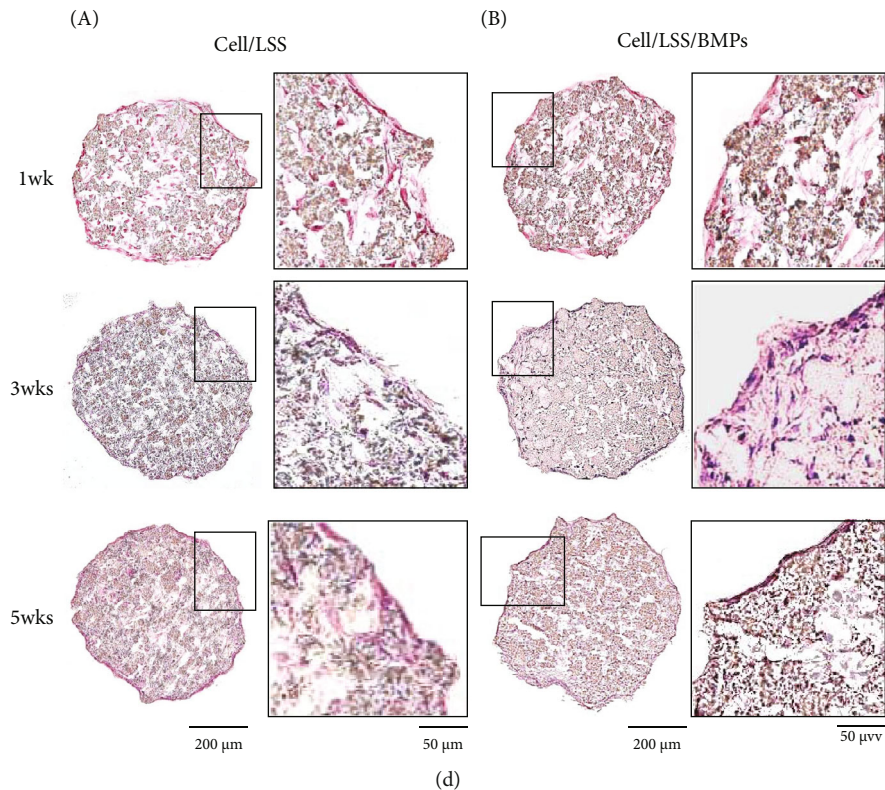


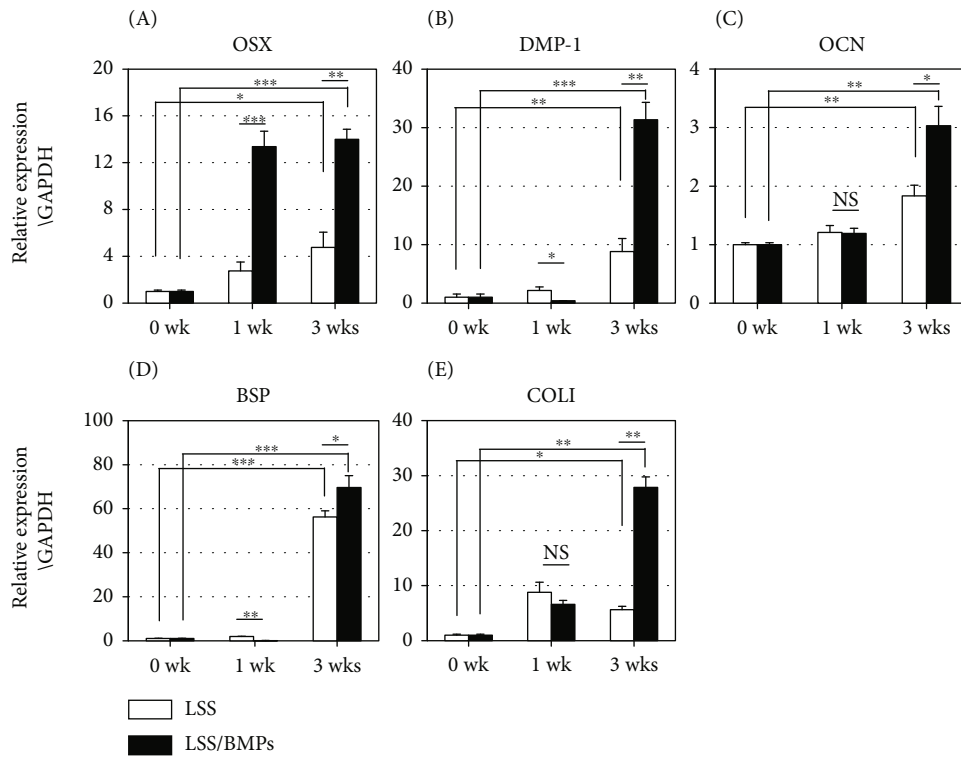
FIGURE 2: Formation of hDPSC spheroids containing the BMPs-loaded LSS microparticles. (a, b) Photographic and scanning electron microscopic image of hDPSC spheroids. (A) hDPSC spheroid without particles. (B) hDPSC spheroid with particles. (C) hDPSC spheroid with BMPs-loaded particles. (c) Cell proliferation of hDPSCs in spheroids containing microparticles after culturing for 1, 3, and 5 weeks. 0 wk indicated the cell numbers added for spheroid formation. White bars, cell numbers in spheroids containing particles without BMPs; black bars, cell numbers in spheroids containing particles loaded BMPs. * $P < 0.05$; ** $P < 0.01$; *** $P < 0.001$; NS: not significant. (d) H&E staining of paraffin section of hDPSC-spheroids containing LSS particles. As well as covering on spheroid by cell layers, cells were detected inside of spheroid. (A) hDPSC spheroid with particles. (B) hDPSC spheroid with BMPs-loaded particles.

LSS/BMPs in a-f). After 3 weeks of differentiation, expression levels of osterix (OSX) and dentin matrix protein-1 (DMP-1) were significantly increased in spheroids with BMPs-loaded LSS particles than in spheroids without LSS particles (Figure 3(a), A and B). Expressions levels of osteocalcin (OCN), bone morphogenetic protein (BSP), and type I collagen (COL1) in spheroids with BMPs-loaded particles were also increased than in those without BMPs (Figure 3(a), C–E). Calcium deposition is known to be an important indicator of odonto/osteoblastic differentiation. Thus, calcium content was quantified for 30 spheroids. It was found that spheroids containing both LSS and LSS/BMPs particles showed a significant time-dependent increase in calcium deposition (Figure 3(b)). However, the amount of calcium accumulated in spheroids with ELSS/BMPs was more than doubled compared to that in spheroids without BMPs over five weeks (Figure 3(b), bars in 5wks). In addition, the immunohistochemical analysis clearly showed that BSP and DSPP as two representative odonto/osteogenic markers were strongly increased in spheroids with LSS/BMPs after 5 weeks (Figure 3(c), A and B).

3.4. Odontoblastic Differentiation of hDPSCs in Monolayered Cultures and LSS/Cell Spheroid Cultures.

In traditional

monolayered cultures, BMP-2 and BMP-4 are added to hDPSCs once every two or three days to facilitate odonto/osteoblastic differentiation [25]. To compare differentiation efficacies of hDPSCs cultured in 2D monolayers and 3D spheroid systems, monolayered cells were treated with these two BMPs at concentrations approximately equal to the concentration of BMPs released from LSS microparticles. Average amounts of BMP-2 and BMP-4 added into the 2D culture during the first three days at a concentration ratio of 10:1 were 33.3 ng/ml and 3.3 ng/ml, respectively. After that, monolayered cultures were treated with BMPs once every three days for five weeks in a manner mimicking the release behavior from 3D spheroids (Figure 4(a)). Compared to spheroid cultures, the amount of BMPs required in 2D cultures was doubled. However, they were treated to decrease at the same ratio with releasing behavior of LSS particles. When expression levels of odonto/osteogenic markers were evaluated, all markers were significantly increased in 3D spheroid-cultured hDPSCs after 3 weeks of differentiation than in monolayered cells (Figure 4(b)). In addition, based on the same number of cells, the calcium content in 3D spheroids was increased 1.5 times compared to that in monolayered cultures (Figure 4(c)), suggesting a higher differentiation efficiency could be achieved with our LSS/hDPSCs



(a)

FIGURE 3: Continued.

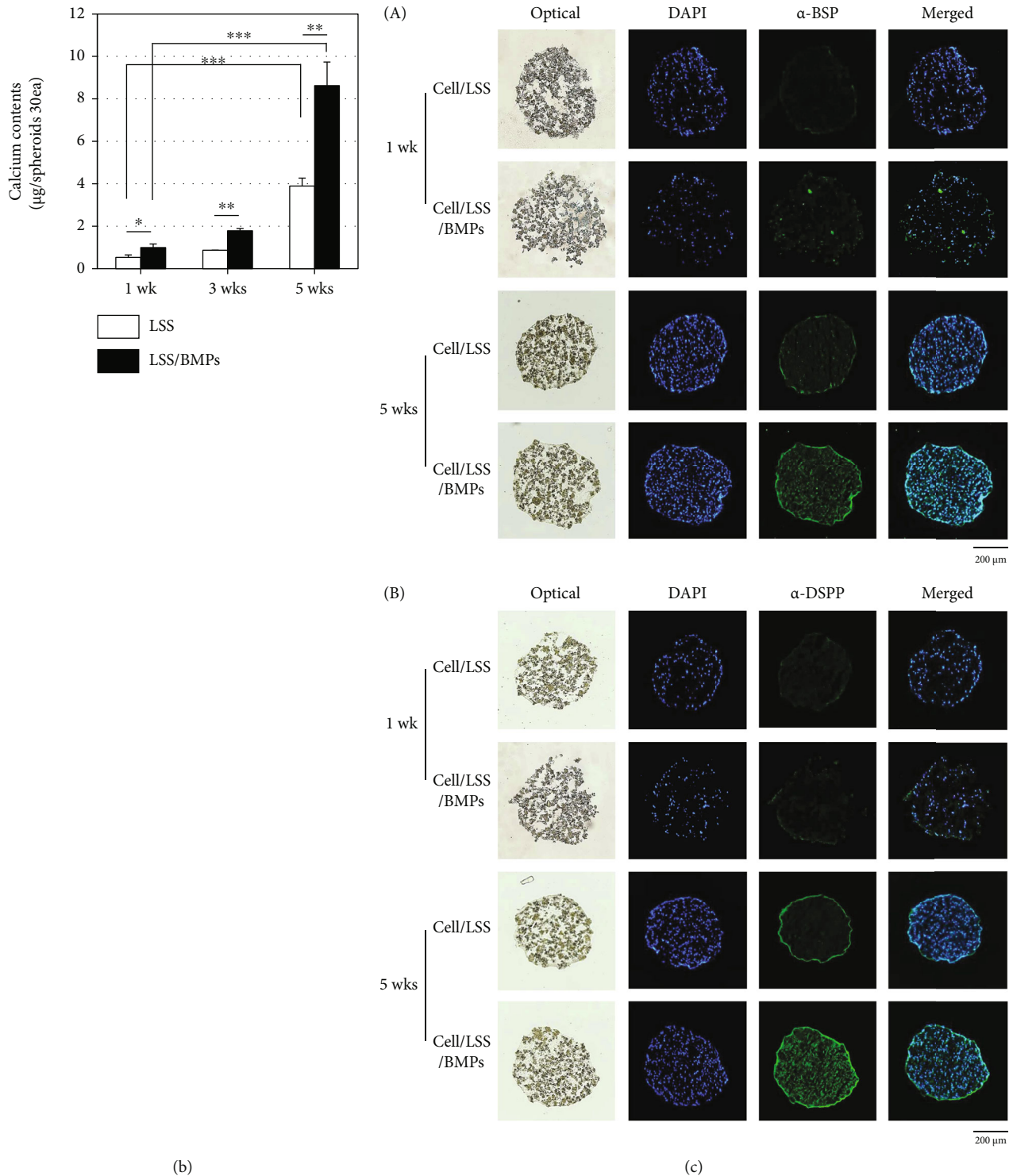


FIGURE 3: Odonto/osteoblastic differentiation of 3D spheroid-cultured hDPSCs improves by the sustainably released BMP-2 and BMP-4. (a) Odonto/osteoblastic marker gene expression of hDPSC spheroids. (A) Osterix. (B) Dentin matrix protein-1. (C) Osteocalcin. (D) Bone sialoprotein. (E) Collagen type-1. * $P < 0.05$; ** $P < 0.01$; *** $P < 0.001$; NS: not significant. (b) Calcium deposition in spheroids. 30 spheroids were collected to analyze the amounts of calcium as followed in Experimental procedures. White bars, cell numbers in spheroids containing particles without BMPs; black bars, cell numbers in spheroids containing particles loaded BMPs. * $P < 0.05$; ** $P < 0.01$; *** $P < 0.001$. (c) Immunohistochemical staining of hDPSCs spheroids for two representative odontoblastic markers such as bone sialoprotein (A) and dentin sialophosphoprotein (B). The paraffin section of hDPSC-spheroids collected at an indicated time was treated with the primary antibody, followed by FTIC-conjugated secondary antibody. LSS: spheroids containing particles without BMPs; LSS/BMPs: spheroids containing particles loaded BMPs.

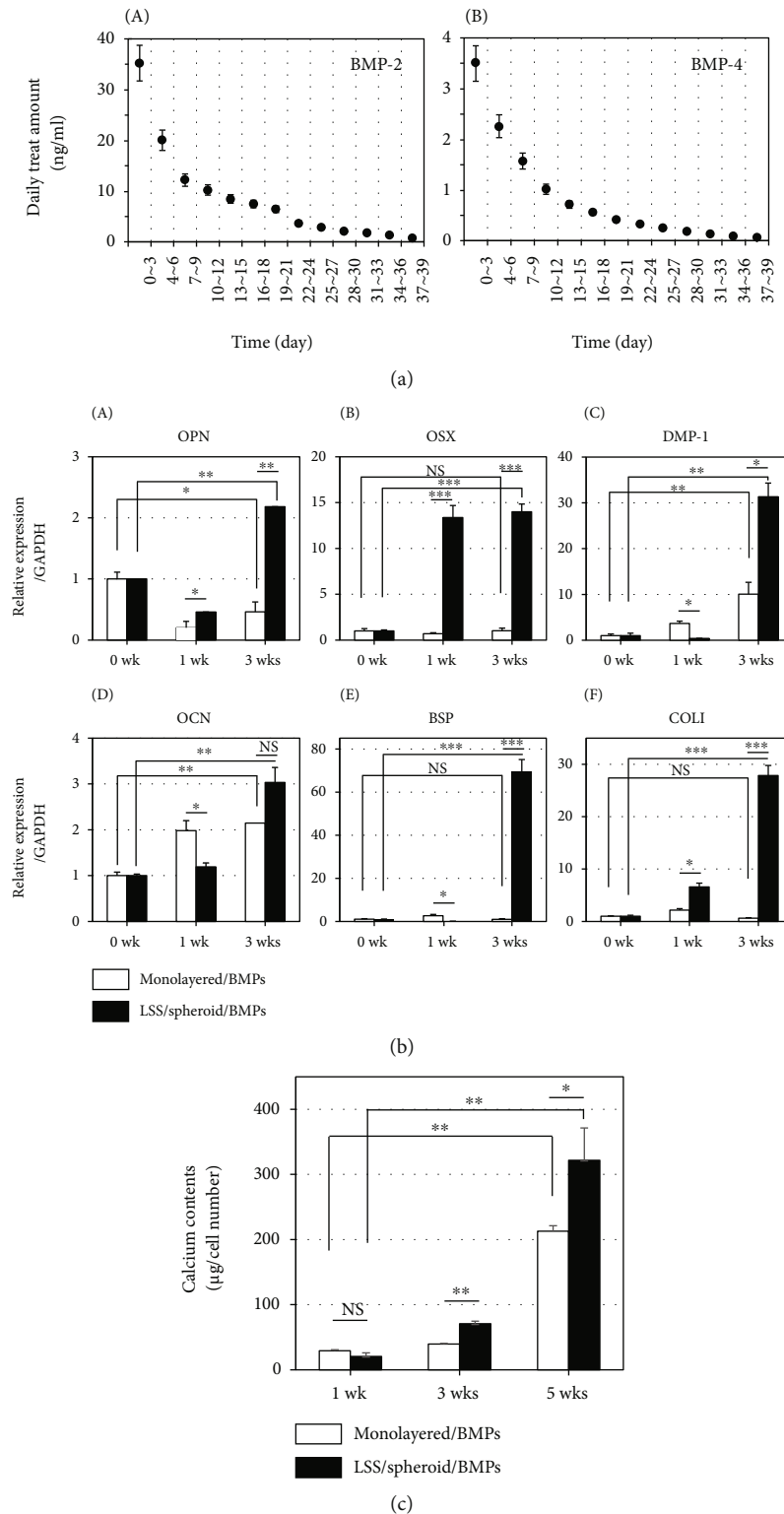


FIGURE 4: Comparison of odonto/osteoblastic differentiation of 2D monolayer-cultured hDPSCs and 3D spheroid-cultured hDPSCs. (a) Daily treat amounts of BMP-2 (A) and BMP-4 (B) in 2D monolayered culture. hDPSCs on culture dish were treated with BMPs once every 3 days. Based on the release behavior from LSS particles (Figure 1(b)), the daily average value was calculated from the sum of three days' values and displayed on the graph as a point. (b) Odonto/osteoblastic marker gene expression in hDPSCs cultured in 2D monolayer and in 3D spheroids. (A) Osteopontin. (B) Osterix. (C) Dentin matrix protein-1. (D) Osteocalcin. (E) Bone sialoprotein. (F) Collagen type-1. * $P < 0.05$; ** $P < 0.01$; *** $P < 0.001$; NS: not significant. (c) Calcium deposition in hDPSCs cultured in 2D monolayer and in 3D spheroids. 30 spheroids were collected to analyze the amounts of calcium as followed in Experimental procedures. White bars, 2D monolayer culture treated with BMPs; black bars, 3D spheroids containing particles loaded BMPs. * $P < 0.05$; ** $P < 0.01$; NS: not significant.

spheroid system using vastly smaller amounts of cytokines than in traditional monolayered cultures.

4. Discussion

3D spheroid cultures are excellent for enhancing cell-cell and cell-extracellular matrix (ECM) interactions, mimicking the natural environment of tissues. In this study, we present an exciting spheroid culture system combined with a drug delivery system for the odonto/osteoblastic differentiation of hDPSCs. Without additional treatment with differentiation factors, hDPSCs do not differentiate well into odontoblasts or osteoblasts in traditional monolayered cultures [25]. On the other hand, it was recently reported that 3D culture systems can induce differentiation without additional inducing factors in both spheroids and scaffold-embedded cultures [11, 20, 21, 26, 29]. Nevertheless, because growth factors and cytokines are important for modulating cell proliferation, differentiation, and cell adhesion, the addition of inducers is still essential for proper differentiation. However, growth factors and cytokines only act locally and possess short half-lives and short diffusion distances through ECMs. For example, FGF and PDGF have a half-life of only 3 minutes and less than 2 minutes, respectively, due to enzymatic degradation and inactivation in physiological culture conditions [15]. Therefore, 3D cultures should be constructed in conjunction with additional drug delivery systems to sustainably release adequate growth factors and cytokines. The microparticles with the leaf-stacked structure (LSS) used in this study were suitable for cell attachment as well as the sustainable release of differentiation-inducing factors. In our recent study, we demonstrated that the microparticles with the leaf-stacked structure (LSS) significantly prevent cell necrosis in human bone marrow-derived mesenchymal stem cells (hBMSCs) (data not shown). Therefore, we can assume that cell viability in hDPSCs-spheroids with LSS particles was greatly improved in this experiment.

As shown in Figure 2, the cells in spheroid structures with LSS particles had increased viability compared to cell aggregates formed without LSS particles, and the spheroid size did not shrink even after 5 weeks of incubation. The findings were very surprising in light of the fact that more than a week or two of cell differentiation experiments were difficult when spheroids made from simple lumps of cells were used in previous studies [20, 21].

Previously, we determined the optimal concentration of BMP-2 and BMP-4 to maximize the efficiency of odontoblastic differentiation of hDPSCs: 33.2 ng/ml BMP-2 and 3.3 ng/ml BMP-4 per day [25]. Because the concentrations of BMP-2 and BMP-4 have treated at 10:1, two types of LSS particles loaded with BMP-2 or BMP-4 were mixed in a 10:1 ratio to meet proper differentiation conditions. The biggest advantage of the LSS/hDPSCs spheroid system was that it could be applied to experiments by counting the number of spheroids directly. Other studies that may reflect dual-delivery systems have recently been published. A novel drug-delivery system based on double-layered microspheres differentially released SDF-1 and BMP-2 [30]. The mesoporous silica nanoparticles-embedded core-shell nanofiber membrane

provides for an effective delivery of dual drugs [31]. Together with our results, these reports will provide useful information for guided tissue regeneration.

Although the amounts of BMPs released from LSS microparticles were much less than those required in 2D monolayered cultures, the odonto/osteoblastic differentiation and mineral formation in LSS/cell spheroid-cultured hDPSCs were significantly increased after 3-5 weeks of culture compared to the monolayered but more heavily treated cells (Figure 3). These results suggest that the differentiation efficiency of hDPSCs can be enhanced in this 3D spheroid culture system using much smaller amounts of cytokines compared to 2D cultures. Previously, Chen et al. reported that periodontal ligament fibroblasts in scaffolds containing a mixture of BMP-2 and IGF-1 showed a high osteoblastic differentiation efficiency [26]. As one step further from the previous research, our dual-microparticle containing spheroids can be used to release multiple growth factors or cytokines in a controlled and independent fashion, thereby representing a promising 3D culture system for tissue engineering. In the future, multiple cell spheroids constructed with different cell types and LSS microparticles loaded with various factors could serve as building blocks in complex tissue engineering applications.

5. Conclusions

We established a 3D-spheroid culture system of hDPSCs for odontogenic differentiation. In this spheroid system, the microparticles with leaf-stacked structure (LSS) were used. LSS-microparticles allowed sustained release of BMPs and oxygen supply for 40 days. Odontogenic differentiation and mineralization increase significantly compared to monolayered cells, suggesting that these large-scale hDPSCs-LSS spheroids containing long-lasting viability might be useful for dentin regeneration.

Data Availability

All the data in this study are available from the corresponding authors on reasonable request.

Disclosure

Kyung-Jung Kang recent address is Eutilex, Catholic University School of Medicine, Seoul, 06591, Korea.

Conflicts of Interest

The authors declare that they have no competing financial interests to declare.

Authors' Contributions

Tae-Jun Min performed the collection and/or assembly of data and data analysis. Min Ji Kim performed the collection and/or assembly of data and data analysis. Kyung-Jung Kang performed the collection and/or assembly of data. Yeoung Jo Jeoung performed the collection and/or assembly of data. Se Heang Oh performed the conception and design, data

analysis and interpretation, and manuscript writing. Young-Joo Jang performed the conception and design, financial support, data analysis and interpretation, and manuscript writing. Tae-Jun Min and Min Ji Kim contributed equally to this work.

Acknowledgments

We thank Dr. Yoo Tae-Min in Dankook Dental Hospital and Dr. Lee Kyu-Tae in Yonsei Woil Dental Hospital for Provision of research materials. This research was supported by the Bio & Medical Technology Development Program (NRF-2015M3A9C6029130) (Y.-J.J. & S.O.) and by the Mid-Career Researcher Program (NRF-2019R1A2C1084524) of the NRF funded by MSIT (Y.-J.J.).

Supplementary Materials

Figure S1: verification of stem cell potentials in human dental pulp primary cells (hDPSCs). CD Antibodies against the following mesenchymal stem cell antigens were treated with cells: CD44, CD90, CD146, and STRO-1. CD24 and CD106 were used as negative markers. After incubation with the primary antibodies, FITC labeled anti-mouse secondary antibody was treated. CD expression of hDPSCs was analyzed by Flow cytometry. hDPSCs independently cultivated from six different patients were used in FACS analysis. Red peaks indicated cells treated with FITC-secondary antibody only. Figure S2: verification of odontogenic differentiation potential in human dental pulp primary cells (hDPSCs). Osteo/odontogenic gene expressions in hDPSCs treated with BMP-2 and BMP-4 for 2 weeks. hDPSCs independently cultivated from six different patients were used in Quantitative RT-PCR analysis. According to the data of relative expression between undifferentiated and differentiated cells, three cell batches isolated from patients #165, #280, and #311 were selected and used in this experiment. (*Supplementary materials*)

References

- [1] M. A. Kinney, T. A. Hookway, Y. Wang, and T. C. McDevitt, "Engineering three-dimensional stem cell morphogenesis for the development of tissue models and scalable regenerative therapeutics," *Annals of Biomedical Engineering*, vol. 42, no. 2, pp. 352–367, 2014.
- [2] E. Park and A. N. Patel, "Changes in the expression pattern of mesenchymal and pluripotent markers in human adipose-derived stem cells," *Cell Biology International*, vol. 34, no. 10, pp. 979–984, 2010.
- [3] P. C. Baer, N. Griesche, W. Luttmann, R. Schubert, A. Luttmann, and H. Geiger, "Human adipose-derived mesenchymal stem cells *in vitro*: evaluation of an optimal expansion medium preserving stemness," *Cytotherapy*, vol. 12, no. 1, pp. 96–106, 2010.
- [4] T. Vermonden, R. Censi, and W. E. Hennink, "Hydrogels for protein delivery," *Chemical Reviews*, vol. 112, no. 5, pp. 2853–2888, 2012.
- [5] C. R. Thoma, M. Zimmermann, I. Agarkova, J. M. Kelm, and W. Krek, "3D cell culture systems modeling tumor growth determinants in cancer target discovery," *Advanced Drug Delivery Reviews*, vol. 69-70, pp. 29–41, 2014.
- [6] N. Eritja, X. Dolcet, and X. Matias-Guiu, "Three-dimensional epithelial cultures: a tool to model cancer development and progression," *Histology and Histopathology*, vol. 28, pp. 1245–1256, 2013.
- [7] B. Weigelt, C. M. Ghajar, and M. J. Bissell, "The need for complex 3D culture models to unravel novel pathways and identify accurate biomarkers in breast cancer," *Advanced Drug Delivery Reviews*, vol. 69-70, pp. 42–51, 2014.
- [8] N. Chaicharoenaudomrung, P. Kunhorm, and P. Noisa, "Three-dimensional cell culture systems as an *in vitro* platform for cancer and stem cell modeling," *World Journal of Stem Cells*, vol. 11, no. 12, pp. 1065–1083, 2019.
- [9] A. Shehzad, V. Ravinayagam, H. AlRumaih et al., "Application of three-dimensional (3D) tumor cell culture systems and mechanism of drug resistance," *Current Pharmaceutical Design*, vol. 25, no. 34, pp. 3599–3607, 2019.
- [10] J. K. Lukowski, E. M. Weaver, and A. B. Hummon, "Analyzing liposomal drug delivery systems in three-dimensional cell culture models Using MALDI imaging mass spectrometry," *Analytical Chemistry*, vol. 89, no. 16, pp. 8453–8458, 2017.
- [11] Y. Moritani, M. Usui, K. Sano et al., "Spheroid culture enhances osteogenic potential of periodontal ligament mesenchymal stem cells," *Journal of Periodontal Research*, vol. 53, no. 5, pp. 870–882, 2018.
- [12] R. Edmondson, J. J. Broglie, A. F. Adcock, and L. Yang, "Three-dimensional cell culture systems and their applications in drug discovery and cell-based biosensors," *Assay and Drug Development Technologies*, vol. 12, no. 4, pp. 207–218, 2014.
- [13] P. B. Malafaya, G. A. Silva, and R. L. Reis, "Natural-origin polymers as carriers and scaffolds for biomolecules and cell delivery in tissue engineering applications," *Advanced Drug Delivery Reviews*, vol. 59, no. 4-5, pp. 207–233, 2007.
- [14] S. K. Nitta and K. Numata, "Biopolymer-based nanoparticles for drug/gene delivery and tissue engineering," *International Journal of Molecular Sciences*, vol. 14, no. 1, pp. 1629–1654, 2013.
- [15] R. Censi, P. Di Martino, T. Vermonden, and W. E. Hennink, "Hydrogels for protein delivery in tissue engineering," *Journal of Controlled Release*, vol. 161, no. 2, pp. 680–692, 2012.
- [16] X. Liu, E. M. Weaver, and A. B. Hummon, "Evaluation of therapeutics in three-dimensional cell culture systems by MALDI imaging mass spectrometry," *Analytical Chemistry*, vol. 85, no. 13, pp. 6295–6302, 2013.
- [17] H. Li and A. B. Hummon, "Imaging mass spectrometry of three-dimensional cell culture systems," *Analytical Chemistry*, vol. 83, no. 22, pp. 8794–8801, 2011.
- [18] L. Roncoroni, L. Elli, M. T. Bardella et al., "Cytogenetic characterization and cell cycle analysis of three human colon adenocarcinoma cell lines: comparison between two- and three-dimensional cell culture systems," *Cancer Investigation*, vol. 28, no. 1, pp. 7–12, 2010.
- [19] C. Agbunag, K. E. Lee, S. Buontempo, and D. Bar-Sagi, "Pancreatic Duct Epithelial Cell Isolation and Cultivation in Two-Dimensional and Three-Dimensional Culture Systems," *Methods in Enzymology*, vol. 407, pp. 703–710, 2006.
- [20] K. Iwasaki, M. Nagata, K. Akazawa, T. Watabe, and I. Morita, "Changes in characteristics of periodontal ligament stem cells in spheroid culture," *Journal of Periodontal Research*, vol. 54, no. 4, pp. 364–373, 2019.

- [21] M. Yamamoto, N. Kawashima, N. Takashino et al., “Three-dimensional spheroid culture promotes odonto/osteoblastic differentiation of dental pulp cells,” *Archives of Oral Biology*, vol. 59, no. 3, pp. 310–317, 2014.
- [22] J. W. Yoo, D. J. Irvine, D. E. Discher, and S. Mitragotri, “Bio-inspired, bioengineered and biomimetic drug delivery carriers,” *Nature Reviews of Drug Discovery*, vol. 10, no. 7, pp. 521–535, 2011.
- [23] I. Thesleff and M. Mikkola, “The role of growth factors in tooth development,” *International Review of Cytology*, vol. 217, pp. 93–135, 2002.
- [24] M. Tummers and I. Thesleff, “The importance of signal pathway modulation in all aspects of tooth development,” *Journal of Experimental Zoology. Part B*, vol. 312B, no. 4, pp. 309–319, 2009.
- [25] K. J. Kang, C. J. Ryu, and Y. J. Jang, “Identification of dentinogenic cell-specific surface antigens in odontoblast-like cells derived from adult dental pulp,” *Stem Cell Research and Therapy*, vol. 10, no. 1, p. 128, 2019.
- [26] F. M. Chen, R. Chen, X. J. Wang, H. H. Sun, and Z. F. Wu, “_In vitro_ cellular responses to scaffolds containing two microencapsulated growth factors,” *Biomaterials*, vol. 30, no. 28, pp. 5215–5224, 2009.
- [27] M. J. Kim, J. H. Lee, J. S. Kim et al., “Intervertebral disc regeneration using stem cell/growth factor-loaded porous particles with a leaf-stacked structure,” *Biomacromolecules*, vol. 21, no. 12, pp. 4795–4805, 2020.
- [28] J. Friedrich, W. Eder, J. Castaneda et al., “A reliable tool to determine cell viability in complex 3-d culture: the acid phosphatase assay,” *Journal of Biomolecular Screening*, vol. 12, no. 7, pp. 925–937, 2007.
- [29] S. Na, H. Zhang, F. Huang et al., “Regeneration of dental pulp/dentine complex with a three-dimensional and scaffold-free stem-cell sheet-derived pellet,” *Journal of Tissue Engineering and Regenerative Medicine*, vol. 10, no. 3, pp. 261–270, 2016.
- [30] C. Xu, J. Xu, L. Xiao et al., “Double-layered microsphere based dual growth factor delivery system for guided bone regeneration,” *RSC Advances*, vol. 8, no. 30, pp. 16503–16512, 2018.
- [31] C. Xu, Y. Cao, C. Lei et al., “Polymer-mesoporous silica nanoparticle core-shell nanofibers as a dual-drug-delivery system for guided tissue regeneration,” *ACS Applied Nano Materials*, vol. 3, no. 2, pp. 1457–1467, 2020.

Research Article

Interleukin-20 Acts as a Promotor of Osteoclastogenesis and Orthodontic Tooth Movement

Yuanbo Liu ^{1,2}, Yilong Ai ³, Xuan Sun ^{1,2}, Bowen Meng ^{1,2}, Xi Chen ^{1,2},
Dongle Wu ^{1,2}, Lei Gan ^{1,2}, Benyi Yang ^{1,2}, Chaoran Fu ^{1,2}, Yilin Wu ^{1,2},
and Yang Cao ^{1,2}

¹Hospital of Stomatology, Guanghua School of Stomatology, Sun Yat-sen University, Guangzhou, China

²Guangdong Provincial Key Laboratory of Stomatology, Guangzhou, China

³Foshan Stomatological Hospital, School of Stomatology and Medicine, Foshan University, Foshan, Guangdong, China

Correspondence should be addressed to Yang Cao; caoyang@mail.sysu.edu.cn

Received 23 February 2021; Revised 16 April 2021; Accepted 10 May 2021; Published 26 May 2021

Academic Editor: Adam Ye

Copyright © 2021 Yuanbo Liu et al. This is an open access article distributed under the Creative Commons Attribution License, which permits unrestricted use, distribution, and reproduction in any medium, provided the original work is properly cited.

Objectives. Bones constitute organs that are engaged in constant self-remodelling. Osteoblast and osteoclast homeostasis during remodelling contribute to overall skeletal status. Orthodontics is a clinical discipline that involves the investigation and implementation of moving teeth through the bone. The application of mechanical force to the teeth causes an imbalance between osteogenesis and osteogenesis in alveolar bone, leading to tooth movement. Osteoimmunology comprises the crosstalk between the immune and skeletal systems that regulate osteoclast-osteoblast homeostasis. Interleukin- (IL-) 20, an IL-10 family member, is regarded as a proinflammatory factor for autoimmune diseases and has been implicated in bone loss disease. However, the mechanism by which IL-20 regulates osteoclast differentiation and osteoclastogenesis activation remains unclear. This study investigated the effects of IL-20 on osteoclast differentiation in a rat model; it explored the underlying molecular mechanism in vitro and the specific effects on orthodontic tooth movement in vivo. **Methods.** For in vitro analyses, primary rat bone marrow-derived macrophages (BMMs) were prepared from Sprague–Dawley rats for osteoclast induction. After BMMs had been treated with combinations of recombinant IL-20 protein, siRNA, and plasmids, the expression levels of osteoclast-specific factors and signalling pathway proteins were detected through real-time polymerase chain reaction, western blotting, and immunofluorescence staining. For in vivo analyses, IL-20 was injected into the rat intraperitoneal cavity after the establishment of a rat orthodontic tooth movement (OTM) model. OTM distance was detected by Micro-CT and HE staining; the expression levels of protein were detected through immunofluorescence staining. **Results.** In vitro analyses showed that a low concentration of IL-20 promoted preosteoclast proliferation and osteoclastogenesis. However, a high concentration of IL-20 inhibited BMM proliferation and osteoclastogenesis. IL-20 knockdown decreased the expression of osteoclast specific-markers, while IL-20 overexpression increased the expression of osteoclast specific-markers. Furthermore, IL-20 regulated osteoclast differentiation through the OPG/RANKL/RANK pathway. Overexpression of IL-20 could significantly upregulate RANKL-mediated osteoclast differentiation and osteoclast specific-marker expression; moreover, RANKL/NF- κ B/NFATc1 acted as downstream signalling molecule for IL-20. In vivo analysis showed that OTM speed was significantly increased after intraperitoneal injection of IL-20; additionally, mechanical stress sensing proteins were markedly activated. **Conclusions.** IL-20 augments osteoclastogenesis and osteoclast-mediated bone erosion through the RANKL/NF- κ B/NFATc1 signalling pathway. IL-20 inhibition can effectively reduce osteoclast differentiation and diminish bone resorption. Furthermore, IL-20 can accelerate orthodontic tooth movement and activate mechanical stress sensing proteins.

1. Introduction

Osteoclasts constitute a core component of the bone multicellular unit. They have a vital role in bone remodelling and

are an essential role in the maintenance of skeletal structural integrity and metabolic capacity [1–3]. The coordinated functions of skeletal cells are regulated by multiple hormones, growth factors, chemokines, and cytokines that act

via interconnected signalling networks, resulting in the activation of specific transcription factors and their corresponding target genes [4]. Receptor activator of NF- κ B ligand (RANKL) and macrophage colony-stimulating factor (M-CSF) are secreted and expressed by various cells including osteoblasts; these are key factors in osteoclastogenesis and bone resorption [5, 6].

In the context of osteoimmunology, cytokine crosstalk during osteoclast differentiation is receiving increasing attention. Many studies have indicated that immune cells, such as macrophages and T cells, secrete proinflammatory cytokines (e.g., IL-1, IL-6, IL-10, IL-17, IL-18, IL-22, IL-33, and TNF), which are involved in mediating osteoclastogenesis [7–13]. IL-20 is considered a proinflammatory factor in the context of autoimmune diseases; it also acts as an IL-10-related immunoregulatory molecule [14]. Notably, IL-20 can induce synovial fibroblasts to produce proinflammatory molecules, including TNF- α , IL-1 β , MMP-1, MMP-13, and MCP-1. This effect activates T cells, monocytes, dendritic cells, and neutrophils, thus, causing tissue and bone damage [15, 16]. Studies have shown that the median serum levels of IL-20 in patients with osteoporosis and osteopenia are 209.5 pg/mL and 181.3 pg/mL, respectively; however, healthy people exhibited a median serum level of 15.38 pg/mL. Furthermore, the use of a mouse anti-human IL-20 monoclonal antibody protected ovariectomised (OVX) mice against bone destruction, while facilitating increased bone mineral density. This antibody also inhibited IL-20-induced RANKL expression in osteoblasts [17]. These data indicate that IL-20 can inhibit osteoblasts and promote osteoclast formation. IL-20 is a decisive factor in the balance between osteoclast and osteoblast differentiation. Bone homeostasis is achieved through combined osteoclast and osteoblast activity. Additionally, we previously found that IL-20 has an inhibitory effect on the osteoblast maturation of mouse preosteogenic MC3T3-E1 cells [18]. These findings confirmed the influence of IL-20 on osteoclast differentiation and function.

Orthodontic tooth movement depends on the coordinated absorption and formation of surrounding bone and periodontal ligament tissue. Tooth loading causes local hypoxia and fluid flow, which triggers a sterile inflammatory cascade that ultimately leads to osteoclast resorption in the compression side and osteoblast deposition in the tension side. During orthodontic tooth movement, the imbalance between osteoblastogenesis and osteoclastogenesis is the basis for alveolar bone reconstruction and tooth movement [19–21]. We hypothesise that IL-20 can accelerate the speed of orthodontic tooth movement.

In this study, we investigated the effects of IL-20 on osteoclast differentiation and function through the RANKL/NF- κ B/NFATc1 signalling pathway. Notably, IL-20RB knockdown led to partial inhibition of the ability of IL-20 to promote osteoclast differentiation. Although the expression of NF- κ B did not significantly change, the expression levels of TRAF6 and NFATc1 were significantly reduced. These findings showed that IL-20 affects osteoclast differentiation by regulating the TRAF6/NFATc1 signalling pathway. Furthermore, *in vivo* analyses demonstrated that IL-20 can significantly enhance the orthodontic movement of teeth, and the expression levels

of IL-20, TRAP, and YAP in the periodontal ligament were significantly increased in teeth undergoing orthodontic movement.

This study proved the effect of IL-20 on the differentiation and function of osteoclasts and its mechanism; it demonstrates that IL-20RB is a key factor in the effects of IL-20 on osteoclast differentiation, while providing important information for the experimental analysis of orthodontic tooth movement.

2. Materials and Methods

2.1. Cytokines, Reagents, and Antibodies. Recombinant rat M-CSF and RANKL were obtained from PeproTech (USA) and R&D Systems (USA), respectively. Recombinant rat IL-20 was purchased from Sino Biological Inc. (China). Dulbecco's modified Eagle's medium (DMEM; high glucose formulation), fetal bovine serum (FBS), phosphate-buffered saline (PBS), penicillin, and streptomycin were purchased from Invitrogen (USA). Red blood cell (RBC) lysis buffer was purchased from CWBIO (China). Primary antibodies against GRB2, ERK, NF- κ B, TRAP, CTSK, JNK, TRAF6, I κ K, and p-38 were obtained from Cell Signalling Technology Inc. (USA). Primary antibodies against RANKL, OPG, MMP-9, NFATc1, IL-20, IL-20RB, HIF- α , CXCR-4, CCR7, and VEGF-R2 were obtained from Abcam (USA).

2.2. Animals and Animal Ethics. Four-week-old Sprague-Dawley rats ($n = 120$) were obtained from the Animal Experimental Center of Sun Yat-sen University and used in this study. Rats were fed, anaesthetised, and killed in accordance with the guidelines of the Institutional Animal Care and Use Committee (IACUC) of Sun Yat-sen University. All experimental protocols were approved by the Animal Ethical and Welfare Committee of Sun Yat-sen University (SYSU-IACUC-2018-000099, Guangzhou, China).

2.3. Cell Isolation and Culture. Primary rat bone marrow-derived macrophages (BMMs) were obtained from the femurs and tibiae of 4-week-old Sprague-Dawley rats. The methods for BMM collection were performed as described previously [22], with minor modifications. Briefly, the femur and tibia of each rat were separated; then, bone marrow cells were extracted. The cells were centrifuged at 450 g for 5 minutes and then resuspended in RBC lysis buffer on ice for 15 minutes to enable purification of bone marrow cells. Resuspended cells were centrifuged at 500 g for 10 minutes to collect BMMs and remove RBCs. Resuspended cells with primary culture medium composed of 10% FBS and DMEM (high glucose formulation) and then cultured in a humidified environment of 5% carbon dioxide and 37°C. After 48 hours of culture, nonadherent cells were collected and resuspended in an antibiotic-free complete medium containing 10% FBS and 15 ng/mL M-CSF; cells were plated in 24-well plates (2×10^6 cells/well) for 2–3 days to induce BMMs to differentiate into preosteoclasts. To induce osteoclastogenesis, the osteoclast culture medium was replaced with an antibiotic-free complete medium containing M-CSF (30 ng/mL) and

RANKL (50 ng/mL) at 2-day intervals for 6-8 days until the osteoclasts differentiated and matured.

2.4. Cell Viability Assay. Cell Counting Kit-8 reagents were purchased from Dojindo. Briefly, preosteoclasts were cultured in 96-well plates with antibiotic-free complete medium supplemented with varying concentrations of IL-20 (0.02–100 ng/mL). The absorbance in each well was measured at 450 nm with a microplate reader (Tecan SUNRISE microplate reader, Tecan, Switzerland) after 1, 3, 5, and 7 days of culture.

2.5. TRAP-Positive Staining and Bone Resorption Pit Assay. After culture with M-CSF and RANKL, mature osteoclasts were treated in 4% paraformaldehyde and stained with an Acid Phosphatase Leukocyte (TRAP) Kit (Sigma-Aldrich, USA), in accordance with the manufacturer's protocol. Using an inverted microscope (Zeiss, Germany), the numbers of TRAP-positive multinucleated cells with ≥ 3 nuclei were then counted to determine the number of osteoclast-like cells. To observe the bone resorption activity of mature osteoclasts, BMMs were cultured with M-CSF and RANKL in a 24-well osteo assay surface multiple-well plate (Corning Life Sciences, USA) coated with a thin inorganic three-dimensional crystalline material. After 6-8 days of culture, a pit formation assay was performed, and 100 μ L of 10% bleach solution was added to each well. Cells were then incubated in the bleach solution for 10 minutes at room temperature. The wells were rinsed twice with distilled water and allowed to air dry at room temperature for 2 hours. Using an inverted microscope (Zeiss), analyses of the individual pits or multiple pit clusters were performed at 5 \times magnification.

2.6. qRT-PCR Analysis. Primer pairs were purchased from Takara and RiboBio, and the primer sequences used for this experiment are shown in Table 1. Total mRNA was extracted with an RNA Rapid Purification Kit (ES Science, China), in accordance with the manufacturer's protocol. Assessments of extracted RNA concentration and quality were performed using NanoDrop ND-1000 Spectrophotometer analysis (NanoDrop Technologies, USA). PrimeScript™ RT Master Mix (Perfect Real Time) (Takara, Japan) was used for reverse transcription to generate cDNA. Quantitative reverse transcription-polymerase chain reaction (qRT-PCR) was performed with SYBR® Premix Ex Taq™ (Tli RNaseH Plus) (Takara, Japan) using a MicroAmp Optical 394-Well Reaction Plate with Barcodes (Thermo Fisher Scientific) on a QuantStudio 7 Flex Real-Time PCR System (Applied Biosystems™). Relative mRNA expression of target genes was calculated using the $2^{-\Delta\Delta C_t}$ method and normalised against the expression of the *GAPDH* housekeeping gene.

2.7. Western Blotting Analysis. Cell lysates were prepared using ice-cold RIPA lysis buffer in the presence of a protease-/phosphatase inhibitor cocktail (Cell Signalling Technology), and the supernatants were collected for further experiments. Briefly, equal amounts (50 μ g) of protein samples were resolved using sodium dodecyl sulfate-polyacrylamide through 8% gel electrophoresis and then transferred to an Immobilon®-P Transfer Membrane (Millipore, USA). The membrane was blocked with 5% (*w/v*) bovine serum albumin (BSA) at 4°C

overnight and then incubated with primary antibodies and secondary antibodies. Immunoreactivity was visualised with the Immobilon™ Western Chemiluminescent HRP substrate (Millipore).

2.8. Small Interfering RNA Transfection. Bone marrow-derived macrophages were transfected with Cy3-conjugated small interfering RNA (siRNA) targeting IL-20 and IL-20RB, or comprising negative control siRNA. The IL-20- and IL-20RB-targeting siRNAs and negative control siRNA were purchased from RiboBio (Guangzhou, China). The siRNA sequences are shown in Tables 2 and 3. The siRNA transfection mixture was mixed with Lipofectamine 3000 transfection reagent (Thermo Fisher Scientific, USA) in serum-free DMEM. Rat BMMs were inoculated into six-well plates (2×10^6 cells/well) with antibiotic-free complete medium. After 4–6 hours, the cells were adherent; the complete medium was removed and cells were washed twice with PBS and then incubated with the transfection mixture for 6–8 hours. After incubation, the transfected cells were cultured with DMEM containing 10% FBS for 48 hours. qRT-PCR and western blotting analysis were performed as described above.

2.9. Plasmid Extraction and Overexpression of IL-20. Design and synthesis of overexpression gene sequences were performed by RiboBio. Sequence details are provided in Table 4. An overexpression plasmid was extracted from *Escherichia coli* DH5 α using an EndoFree Maxi Plasmid Kit (Tiangen, China), and its concentration and quality were determined using NanoDrop ND-1000 Spectrophotometer analysis (NanoDrop Technologies). The plasmid transfection mixture was mixed with Lipofectamine 3000 transfection reagent (Thermo Fisher Scientific) in serum-free DMEM. BMM culture and analysis were performed as described above. The sequencing blow is cloned fragment sequencing results. The underlined part of the sequence is the cloned target sequence, and the upstream and downstream regions are the sequences of the vector frame.

CTATATAAGCAGAGCTCTCTGGCTAACTAGAGAAA
 CCCACTGCTTACTGGCTTATCGAAAGCTGTAATACG
 ACTCACTATAGGGATCCCAGGAATTCGCCGCCACCA
 TGAGAGGCTTTCGTCTTGCCTTTGGACTGTTCTCCGT
 TGTGGGTTTTCTTCTCTGGACTCCTTAACTGGGCTC
 AAGACCCTTCATTTGGGAAGCTGTGTAATCACTGCA
 AACCTACAGGCGATACAAAAGGAATTTTCTGAGATT
 CGGCATAGTGTGCAAGCTGAAGATGAAAATATCGAC
 GTCAGGATTTTAAGGACGACTGAGTCCCTGAAAGAC
 ACAAAGCTTTCGGATAGGTGCTGCTTTCTCCGCCAT
 CTAGTGAGGTTCTATCTGGACAGGGTGTCAAAGTC
 TACCAGACCCCTGACCATCATACCCTGCGAAAGATC
 AGCAGCCTCGCCAATTCTTTTCTTATCATCAAGAAG
 GACCTCTCAGTCTGTCATTCTCACATGGCATGTCATT
 GTGGCGAAGAAGCAATGGAGAAAATACAACCAAATTC
 TCAGTCATTTACAGAGCTTGAGCTCCAGGCAGCCG
 TGGTGAAGGCTTTGGGGGAAGTGGCATTCTTCTGA
 GATGGATGGACTCGAGTCTAGAGGGCCCCGTTAAAC
 CCGCTGATCAGCCTCGACTGTGCCTTCTAGTGCC.

TABLE 1: Primer sequences used for real-time PCR.

Gene	Forward primer sequence (5'-3')	Reverse primer sequence (5'-3')
GAPDH	GGCACAGTCAAGGCTGAGAATG	ATGGTGGTGAAGACGCCAGTA
IL-20	ACTGCAAACCTACAGGCGATACAA	AGAACCTCACTAGATGGCGGAGA
IL-20RB	AGCACTTGATGGGTTAACAGCC	GAAAACAGAGACACAGCCCTCC
RANK	CAGGACAGGGCTGATGCAA	TGACTGACGTACACCACGATGA
RANKL	CTCATGCAGGAGAATCAAAC	TTCCATCATAGCTGGAAGTC
OPG	GACCAAAGTGAATGCCGAGAG	CGCTGCTTTTACAGAGGTCAA

TABLE 2: siRNA IL-20.

Target gene name	Target gene sequence
si-r-IL20_001	CAACCAAATTCTCAGTCAT
si-r-IL20_002	GGATGGAGGAGATGTTATA
si-r-IL20_003	CTTCTCTGGACTCCTTTAA

TABLE 3: siRNA IL-20RB.

Target gene name	Target gene sequence
si-r-IL20rb_001	TCTCTGTACGGTCAACCAA
si-r-IL20rb_002	ATTCCGGTGCACCTAGAAA
si-r-IL20rb_003	CCTGACACCTTGAAAGTAA

TABLE 4: Overexpression plasmid.

Target sequence name	r-IL20 (NM_001143881.1 complete CDS)-WT
Clone length	518 bp (NM_001143881.1 complete CDS)
5' restriction site	EcoRI
3' restriction site	XhoI
Vector name	pEXP-RB-Mam-EGFP
Frame size	4.8 kb
Host bacteria	<i>E. coli</i> DH5 α
Antibiotic resistance	Ampicillin
Copy number	High copy

2.10. Gene Ontology (GO) Analysis and Pathway Analysis. mRNA analysis included GO analysis (<http://www.geneontology.org>), which provides three structured networks of defined terms that describe gene product attributes. *P* values denote the significance of GO term enrichment in the predicted mRNA list, where $P < 0.05$ was considered statistically significant. The most enriched GO terms ranked by fold enrichment and enrichment score among the three groups were identified. Pathway analysis was also performed using the most current Kyoto Encyclopedia of Genes and Genomes (KEGG) database. This functional analysis allowed the identification of biological pathways for which there was a significant enrichment of differentially expressed mRNAs. As noted above, $P < 0.05$ was considered statistically significant.

2.11. Establishment of Rat Orthodontic Tooth Movement Model. Rats were fixed in the supine position after routine anaesthesia. We used a custom-designed force applying device, comprising a tension spring cut into small sections of approximately 5 mm, with two 0.1 mm diameter ligature wires tied to the ends of the tension springs, while the ends were permitted to remain long for ligation and fixation to the teeth. The left maxillary first molar and left maxillary incisor were cleaned and dried. One end of the force device was fixed to the maxillary first molar, and one end of the ligature was passed through the gap between the maxillary first and second molars; it was then tightened and cut. The maxillary first molar was then cleaned with alcohol, dried, and treated with an acid etching agent for 40 seconds. After full removal of the etching agent, the resin was bonded to the proximal surface of the first molar and then shaped with an oral applicator as follows. The connection between the ligation wire and tension spring was wrapped to prevent the device from loosening; the end of the ligature wire was also wrapped to prevent the end from damaging the rat's mouth. Concurrently, a small amount of resin was bonded to the occlusal surface of the molar to strengthen the retention. An orthodontic dynamometer was used to measure and record the position of the ligature wire at a tension of 50 g. The other end of the force device was then ligated and fixed to the maxillary central incisor, and the end was cut to prevent detachment of the device. Then, we used Micro-CT and HE staining to assess the rat orthodontic tooth movement model.

2.12. Statistical Analysis. All results are expressed as the mean \pm standard deviation, and reported values were obtained from at least three experiments. Statistical differences were evaluated with GraphPad Prism software, version 7.04, using Student's *t*-test or one-way ANOVA with Tukey's post hoc analysis. $P < 0.05$ was considered statistically significant.

3. Results

3.1. BMM Proliferation Is Influenced by the Concentration of IL-20. To determine whether IL-20 can affect BMM proliferation, we treated BMMs with various concentrations of IL-20 and used a CCK-8 assay to detect cell proliferation activity on days 1, 3, 5, and 7. We found that an IL-20 concentration of 20 ng/mL was sufficient to promote BMM proliferation (Figure 1(a)). However, an IL-20 concentration of >100 ng/mL caused inhibition of BMM proliferation. Western blotting

analysis confirmed that, at an IL-20 concentration of 20 ng/mL, BMM proliferation signalling factors (e.g., *GRB2*, *ERK*, and *NF- κ B*) were significantly upregulated during early osteoclast differentiation (Figure 1(b)). Using the same cell treatment method, we administered various concentrations of IL-20 to M-CSF-induced preosteoclasts with RANKL and then identified the osteoclast number and size by TRAP staining after 6–8 days of cell culture. We found that an IL-20 concentration of 20 ng/mL led to significant increases in the number and size of TRAP-positive osteoclasts, compared with the control group; conversely, an IL-20 concentration of 100 ng/mL significantly reduced the number of TRAP-positive osteoclasts (Figure 1(c)). In addition, we incubated M-CSF-induced preosteoclasts with RANKL in osteo assay surface plates treated with various concentrations of IL-20. Using a bone resorption pit assay, we found that an IL-20 concentration of 20 ng/mL significantly enhanced the size of the bone resorption pit, compared with the pit sizes in other groups; however, an IL-20 concentration of 100 ng/mL led to minimal changes in the bone resorption pit area (Figure 1(d)). These results indicated that IL-20 regulated osteoclastogenesis and function in a dose-dependent manner.

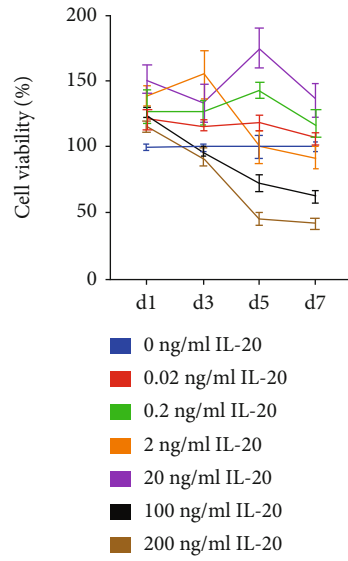
Subsequently, we treated M-CSF-induced preosteoclasts with RANKL and IL-20 at a concentration of 20 ng/mL for 6–8 days. Western blotting analyses indicated that IL-20 modulated the expression patterns of osteoclast-specific and bone resorption functional proteins (e.g., TRAP, CTSK, and MMP-9) (Figures 1(e) and 1(f)). To confirm the effect of IL-20 on early osteoclast differentiation, we treated M-CSF-induced preosteoclasts with RANKL and IL-20 for 2–3 days. Western blotting analyses revealed the expression of marker genes (e.g., *RANK*, *CTSK*, *TRAP*, *ATP60*, and *c-Fos*) in early osteoclast differentiation (Figures 1(g) and 1(h)). These results indicated that, during early osteoclast differentiation, a low concentration of IL-20 upregulated the expression of *RANK* and *CTSK*, whereas it downregulated the expression of *c-Fos*; moreover, a high concentration of IL-20 downregulated the expression of *RANK*, *CTSK*, and *ATP60*. Notably, IL-20 had no effect on *TRAP* expression. These results indicated that a low concentration of IL-20 promotes early osteoclast differentiation. Furthermore, TRAP is a protein specifically expressed in mature osteoclasts; our results indicate that it exhibits minimal or no expression during early osteoclast differentiation.

3.2. IL-20 Modulated the Expression of Osteoclast-Specific Proteins and Promoted Osteoclastogenesis through the OPG/RANKL/RANK Axis. Using TRAP-positive staining and bone resorption pit assays, we found that IL-20 influenced osteoclastogenesis and bone resorption ability. Cellular immunohistochemistry analysis confirmed the presence of IL-20 and its receptor IL-20RB in bone marrow stromal cells (BMSCs) and bone marrow monocytes (Figure 2(a)). These results provided an experimental basis for using siRNA to knock down IL-20 and its receptor IL-20RB; it also provided a basis for performing IL-20 overexpression assays with liposomes. The OPG/RANKL/RANK axis has various cell regulatory functions, but its most well-known point is the osteoclast differentiation upstream signalling pathway. This biological axis

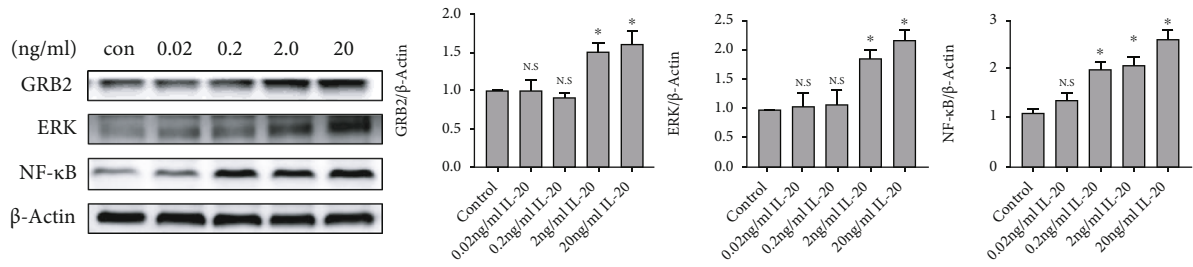
regulates osteoclast differentiation through the antagonistic action of OPG and RANKL [8, 10, 23–27]. To investigate whether IL-20 can regulate osteoclast differentiation through the OPG/RANKL/RANK axis, we constructed an IL-20 overexpression plasmid using *E. coli* DH5 α and then transfected the plasmid into BMMs. The expression of IL-20 in BMMs after transfection was detected by qRT-PCR and western blotting (Figures 2(b) and 2(c)). After transfection, the cells were stimulated to differentiate into osteoclasts, and the expression patterns of OPG, RANK, and RANKL were investigated using qRT-PCR and western blotting (Figures 2(d) and 2(e)). Compared with the control group, the expression levels of RANK and RANKL were significantly increased in the IL-20 overexpression group, while the expression level of OPG was significantly reduced; moreover, the RANKL/OPG ratio was significantly increased. These results clearly showed that increased expression of IL-20 could regulate the expression of RANKL and OPG, indicating that IL-20 can modulate osteoclast differentiation through the OPG/RANKL/RANK axis.

3.3. GO Analysis and Pathway Analysis following the Overexpression of IL-20 in Bone Marrow-Derived Mononuclear Cells. The above findings indicated that IL-20 can modulate the OPG/RANKL/RANK pathway to promote osteoclast differentiation. To further investigate the effects of IL-20 on monocytes and osteoclasts, we used high-throughput transcriptome sequencing (RNA-seq) to detect differences in mRNA expression between normal BMMs and IL-20-overexpressing BMMs. The results showed a large difference between groups, indicating that IL-20 overexpression had a significant effect on preosteoclasts (Figure 3(a)). Volcano diagram depiction revealed that, compared with normal BMMs, IL-20-overexpressing BMMs exhibited 994 significantly upregulated genes and 1203 significantly downregulated genes (Figure 3(b)). GO analysis and pathway analysis were performed to evaluate the roles of IL-20 in biological processes, cellular components, molecular functions, and pathways. GO analysis demonstrated that IL-20 overexpression had a strong effect on the monocyte biological process, and the impact was concentrated mainly on the cellular immune response and the cellular response to stimuli. Notably, IL-20 overexpression in BMMs substantially changed their response to stress, which implies that IL-20 is important in both distraction osteogenesis and orthodontic alveolar bone reconstruction (Figure 3(c)). KEGG analysis demonstrated that IL-20 overexpression in BMMs had substantial effects on osteoclast differentiation and chemokine interactions. It also had robust effects on arthritis pathogenesis, the downstream osteoclast differentiation pathway induced by RANKL, and the HIF- α signalling pathway and apoptosis (Figure 3(d)).

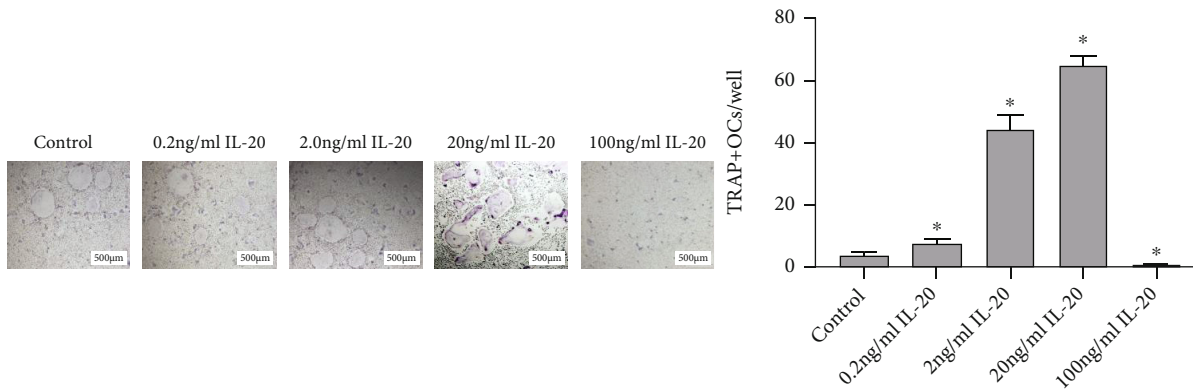
3.4. IL-20 Regulated RANKL-Mediated Osteoclastogenic Downstream Signal Transduction. To explore the mechanism by which IL-20 regulates RANKL-mediated osteoclast differentiation, bone marrow-derived mononuclear cells were transfected with siRNA fluorescence staining showed high transfection efficiency (Figure 4(a)). qRT-PCR and western blotting analyses showed that siRNA had significant transfection efficiency with respect to target genes (Figures 4(b) and



(a)

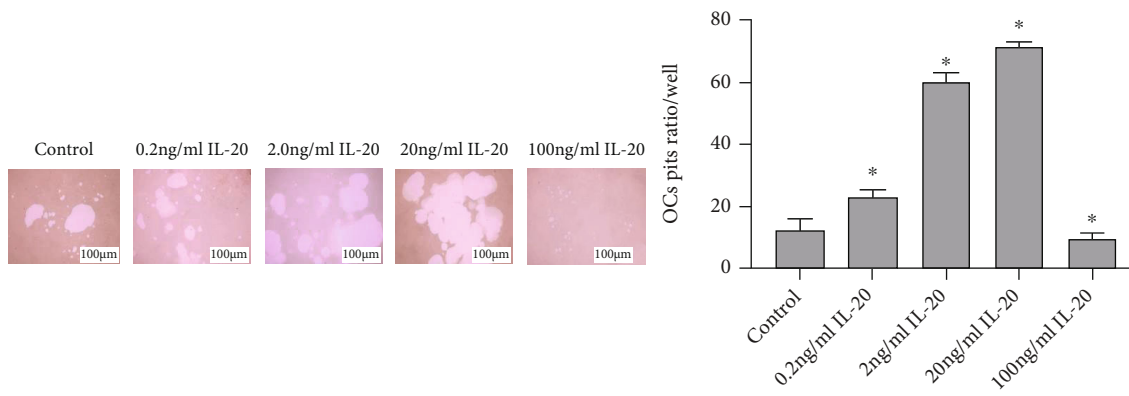


(b)

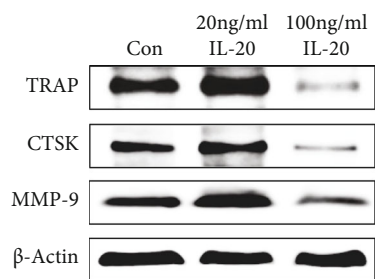


(c)

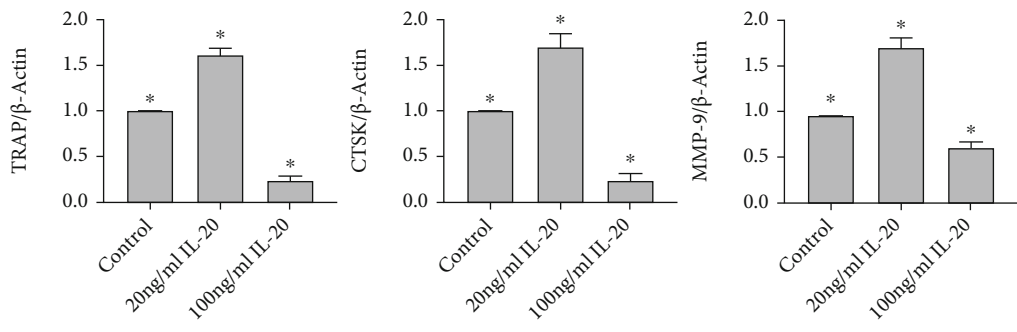
FIGURE 1: Continued.



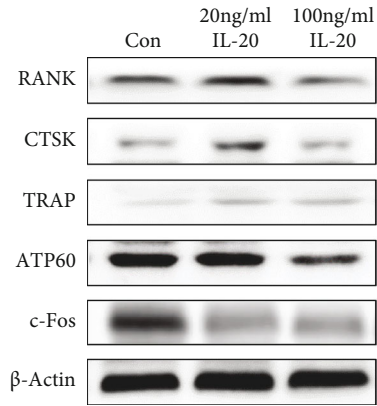
(d)



(e)



(f)



(g)

FIGURE 1: Continued.

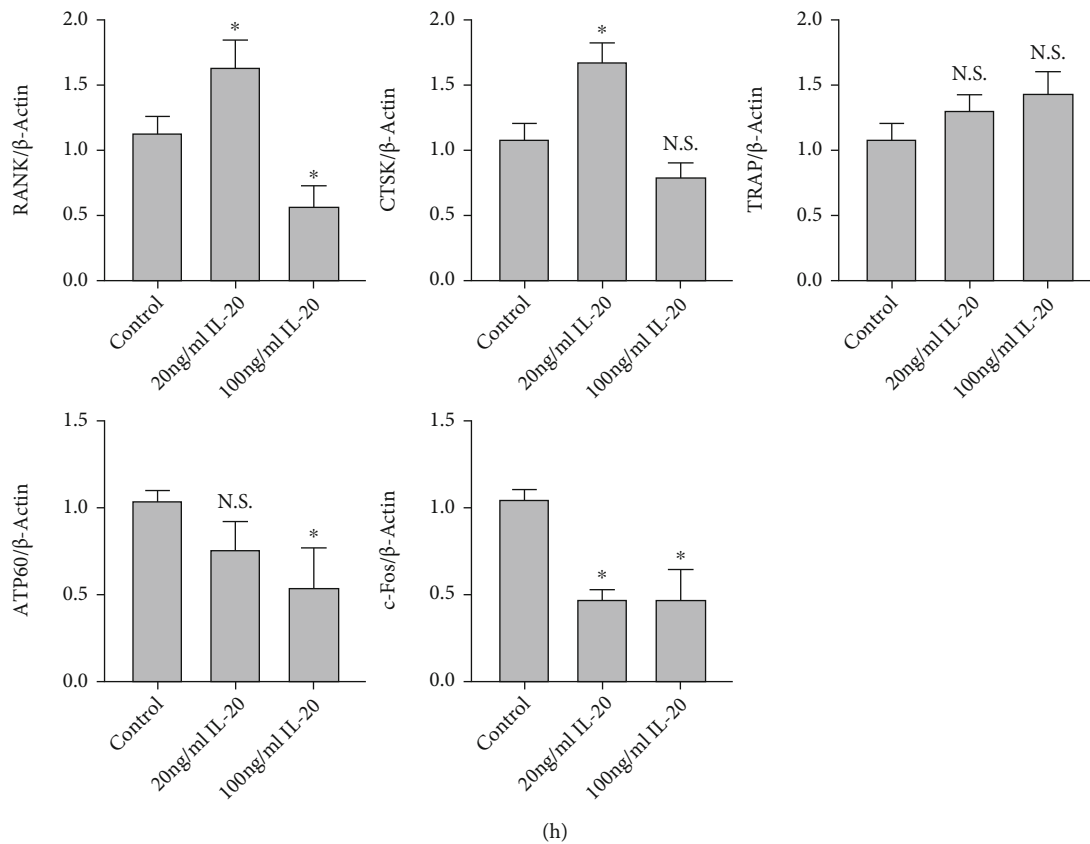


FIGURE 1: IL-20 concentration differentially regulates BMM activity, and a low concentration of IL-20 can activate ERK signalling to promote cell proliferation. BMM viability was detected by CCK8 assay. IL-20 concentration differentially regulates osteoclast formation and bone resorption capacity. (a) Cell viability analysis of IL-20-treated BMMs on days 1, 3, 5, and 7. Bars represent the mean \pm SEM of six independent experiments ($n = 12$). (b) BMMs treated with various concentrations of IL-20 were used to investigate the protein expression levels of ERK, GRB2, and NF- κ B by western blotting during early osteoclast differentiation. Bars represent the mean \pm SEM of three independent experiments ($n = 12$). * $P < 0.05$ vs. control group; ns: not significant. (c) M-CSF-induced preosteoclasts were cultured with 30 ng/mL RANKL and various concentrations of IL-20. The control group comprised M-CSF-induced preosteoclasts cultured with 30 ng/mL M-CSF, 30 ng/mL RANKL, and 0 ng/mL IL-20; TRAP-positive staining was used to examine and measure the number of TRAP-positive osteoclasts with ≥ 3 nuclei. (d) A bone resorption pit assay was performed to examine osteoclast function. M-CSF-induced preosteoclasts in the control group were treated as described for the TRAP staining assay; the areas of bone resorption pits were quantified. (e and f) Expression levels of osteoclast-specific proteins (TRAP, CTSK, and MMP-9) were examined using western blotting. (g and h) Expression levels of osteoclast marker genes (*RANK*, *CTSK*, *TRAP*, *ATP60*, and *c-Fos*) during early osteoclast differentiation after supplementation of IL-20 at 20 ng/mL or 100 ng/mL. Bars represent the mean \pm SEM of six independent experiments ($n = 18$). * $P < 0.05$ vs. control group; N.S.: not significant.

4(c)). After transfection, BMMs were cultured in antibiotic-free complete medium with M-CSF and RANKL for 3 days. Western blotting revealed that, compared with the control group, cells in the IL-20 overexpression group exhibited activation of the RANK/RANKL downstream signalling effectors in osteoclastogenesis (e.g., JNK, NF- κ B, TRAF6, I κ K, NFATc1, and p38) (Figure 4(d)). In contrast, the group that received siRNA to suppress IL-20 expression showed significant inhibition of the above signalling pathways; in particular, p-I κ k α was significantly activated, indicating inhibition of the NF- κ B signalling pathway. In addition, we used siRNA to reduce the expression of IL-20RB and cultured the cells with an antibiotic-free complete medium containing 20 ng/mL IL-20 (Figure 4(d)). Western blotting demonstrated that the I κ K and NF- κ B signalling pathways were activated, whereas the JNK, TRAF6, NFATc1, and p-38 path-

ways were not (Figure 4(e)). Similar to inhibition of IL-20, the inhibition of IL-20RB also inhibited the activation of TRAF6/NFATc1 signalling pathways; this indicated that the key IL-20 receptor, IL-20RB, can regulate activation of the osteoclast differentiation signalling pathway.

3.5. IL-20 Feedback Regulates BMSC Involvement in Osteoclastogenesis through the OPG/RANKL/RANK Axis and Downstream Signal Transduction. BMSCs are cells with self-renewal ability, capable of producing at least one type of highly differentiated progeny cell with multidirectional differentiation potential; BMSCs can also produce cytokines involved in immune responses. After BMSCs differentiate into osteoblasts, M-CSF and RANKL can be secreted, and these factors can induce the formation of osteoclasts [5]. In this experiment, we used siRNA to knock down IL-20 and

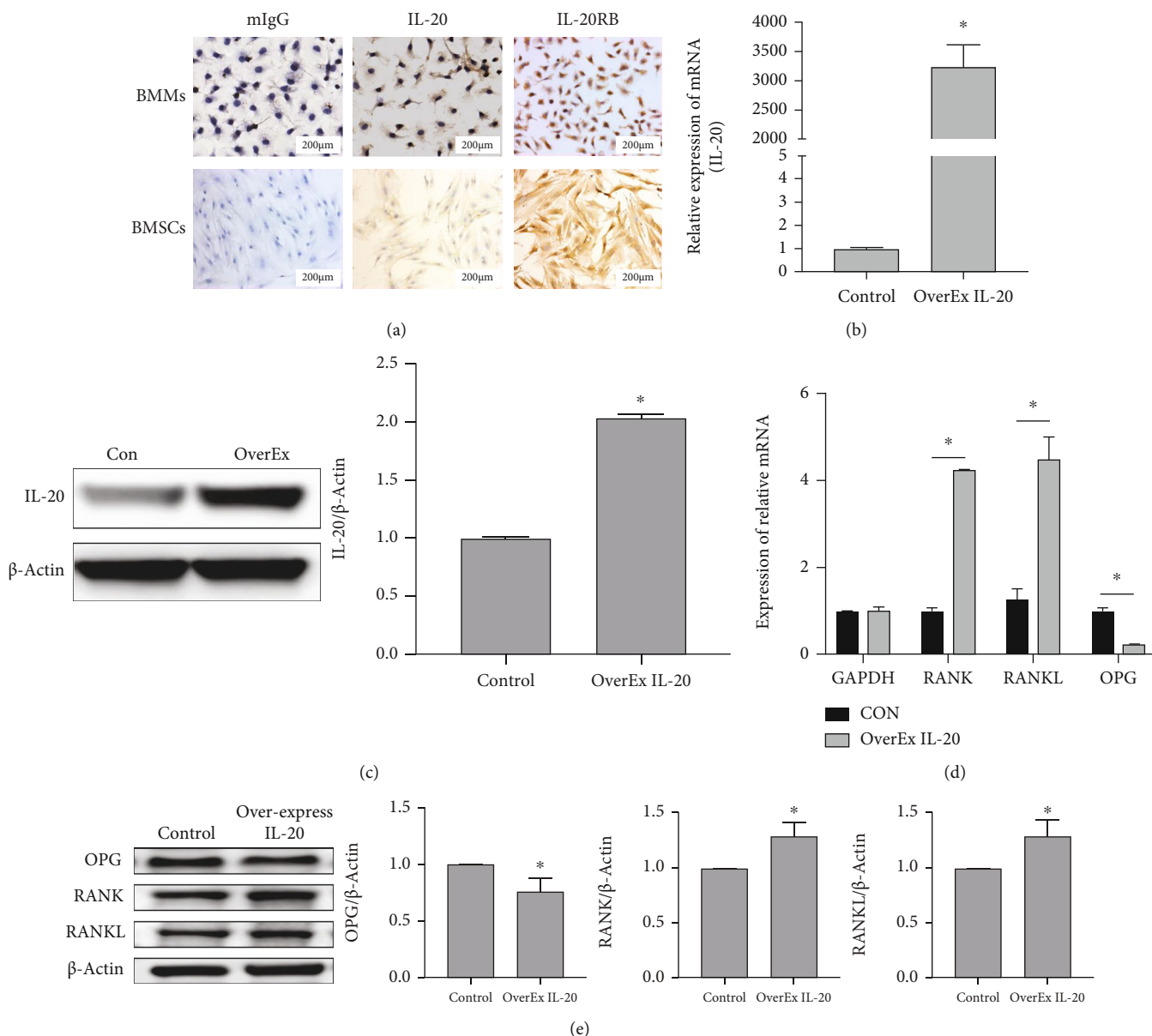
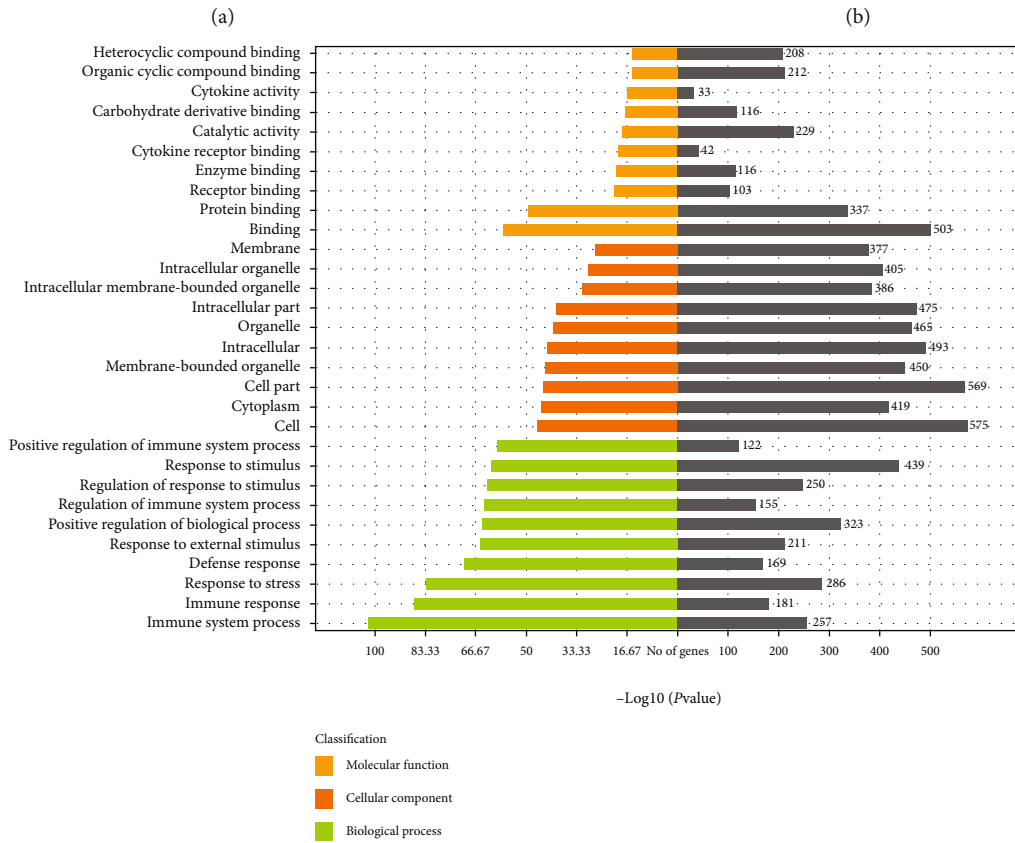
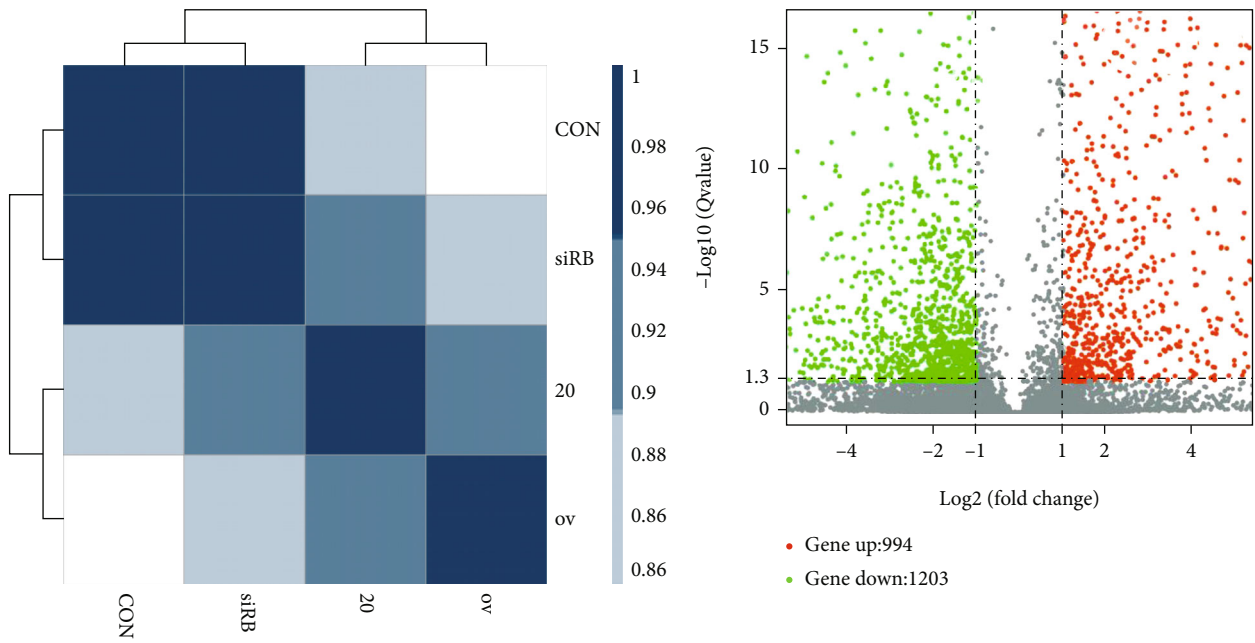


FIGURE 2: Overexpression of IL-20 regulates the expression of RANKL and OPG, indicating that IL-20 can modulate osteoclast differentiation through the OPG/RANKL/RANK axis. (a) Expression levels of IL-20 and its receptor IL-20RB in BMSCs and BMMs were determined by immunohistochemical staining. The use of an overexpression plasmid to enhance IL-20 expression in BMMs led to increased expression levels of RANKL and RANK, whereas it led to a decreased expression level of OPG. (b and c) BMMs were transfected with overexpression plasmids to increase the expression of IL-20, and the expression level of IL-20 was detected by qRT-PCR and western blotting; the control group received no plasmid. * $P < 0.05$ vs. control group. (d) mRNA expression levels of RANK, RANKL, and OPG were evaluated by qRT-PCR after 2 days of transfection. * $P < 0.05$ vs. control group; (e) protein expression levels of OPG, RANK, and RANKL were examined by western blotting. Bars represent the mean \pm SEM of three independent experiments ($n = 12$). * $P < 0.05$ vs. control group; N.S.: not significant.

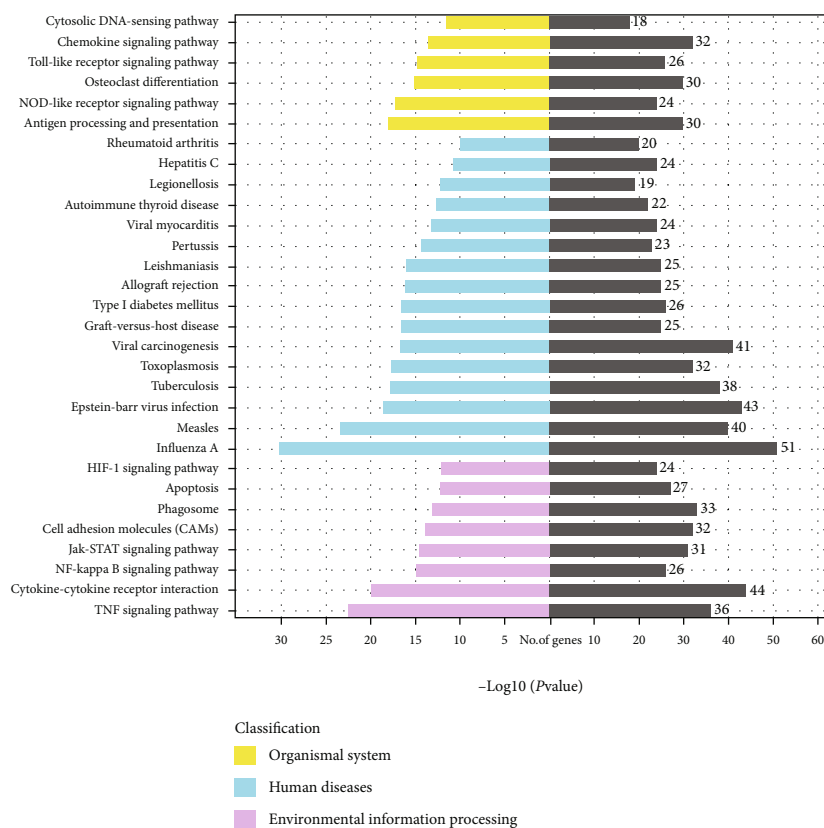
its key receptor IL-20RB in BMSCs; we also used a plasmid to induce BMSCs to overexpress IL-20. After transfection, BMSCs were continuously cultured for 48 hours; we then collected and used BMSC conditioned medium- (CM-) cultured BMMs. Fluorescence staining showed high transfection efficiency (Figure 5(a)). Western blotting analyses showed that siRNA had significant transfection efficiency with respect to target genes (Figures 5(b) and 5(c)). Western blotting analysis of bone marrow-derived mononuclear cells after 3 days of

culture with BMSC CM showed that, compared with the control group, the expression levels of RANK and RANKL were significantly increased in BMMs cultured with IL-20-overexpressing BMSC CM; moreover, the expression of OPG was significantly reduced and the RANKL/OPG ratio was significantly enhanced (Figures 5(d) and 5(e)). BMMs cultured with BMSC CM treated with IL-20 siRNA showed significantly elevated OPG expression levels. In addition, BMMs cultured with IL-20-overexpressing BMSC CM



(c)

FIGURE 3: Continued.



(d)

FIGURE 3: GO analysis and KEGG analysis of the difference between the mRNA of BMMs overexpressing IL-20 and normal BMMs. (a) Significant differences between cells in the control and IL-20 overexpression groups. (b) Volcano charts of differential mRNA expression. Red and green denote high and low expression levels, respectively. Each mRNA transcript is represented by a single row of coloured boxes, and each sample is represented by a single column. (c) Most significantly enriched GO ($-\log_{10}(P \text{ value})$) terms of mRNA gene symbols according to biological process, cellular component, and molecular function. (d) Bar plot shows the top ten enrichment scores ($-\log_{10}(P \text{ value})$) of significantly enriched pathways.

demonstrated activation of downstream osteoclastogenesis signalling pathways mediated by the RANK/RANKL axis (e.g., NF- κ B and TRAF6 pathways); however, the p38 and JNK pathways were not activated. BMMs cultured with IL-20 siRNA-treated BMSC CM exhibited downregulation of the p38, TRAF6, and JNK pathways. These results indicated that IL-20 could directly induce preosteoclast differentiation into osteoclasts. Moreover, it regulated the expression of OPG and RANKL by induction of BMSCs and activation of some downstream signalling pathways that are activated by the OPG/RANK/RANKL axis in osteoclastogenesis [28], thereby indirectly promoting preosteoclast differentiation into osteoclasts.

3.6. IL-20 Can Accelerate the Speed of Rat Orthodontic Tooth Movement. The above results confirmed that IL-20 promotes osteoclast differentiation by regulating the upstream RANK/RANKL/OPG pathway and the RANKL-mediated downstream signalling pathway. “Orthodontic tooth movement” is a unique bone remodelling process within the jaw, which mainly manifests through bone formation on the tension side and bone resorption on the compression side. This mechanism has received extensive attention in the field of oral bio-

mechanics [29]. To investigate whether IL-20 can accelerate bone resorption and bone remodelling in rats, we established a rat orthodontic tooth movement model (Figure 6(e)), with maxillary incisors as a base point, that used an orthodontic treatment spring with consistent force (50 g) along a first molar. Micro-CT of the maxilla showed that, compared with the control group, the gap between the first and second molars was increased in the OTM group; thus, the transverse and longitudinal sections of the first molars were both visible in the OTM group (Figure 6(b)). HE staining of the transverse plane of the first molars showed that the compressed side of the periodontal ligament of the molars was narrower in the OTM group than in the control group (Figures 6(d), 6(f), 6(h), and 6(i)). Based on the results of vitro experiments, we injected IL-20 into the intraperitoneal cavities of rats that had been subjected to orthodontic force. Three days before modelling, rats in the OTM + IL-20 group received IL-20 solution at a rate of 40 mg/kg body weight. Intraperitoneal injections were performed at 2-day intervals before 3 days of modelling; on the 10th day, the rats were sacrificed and micro-CT was performed (Figure 6(a)) to analyse the first molar movement distance. Compared with the OTM + vehicle group (Figure 6(c)), the OTM + IL-20 group had greater

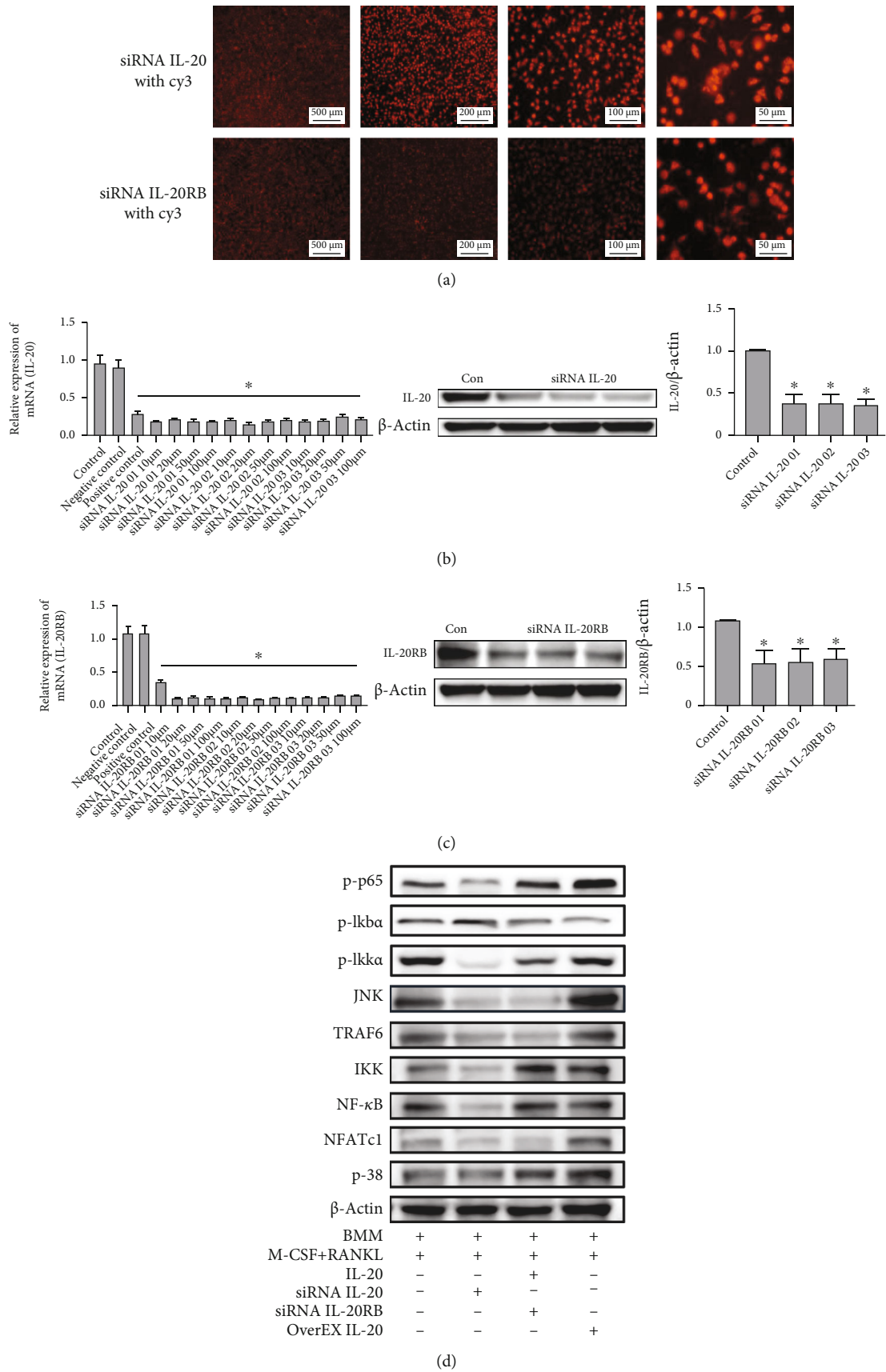


FIGURE 4: Continued.

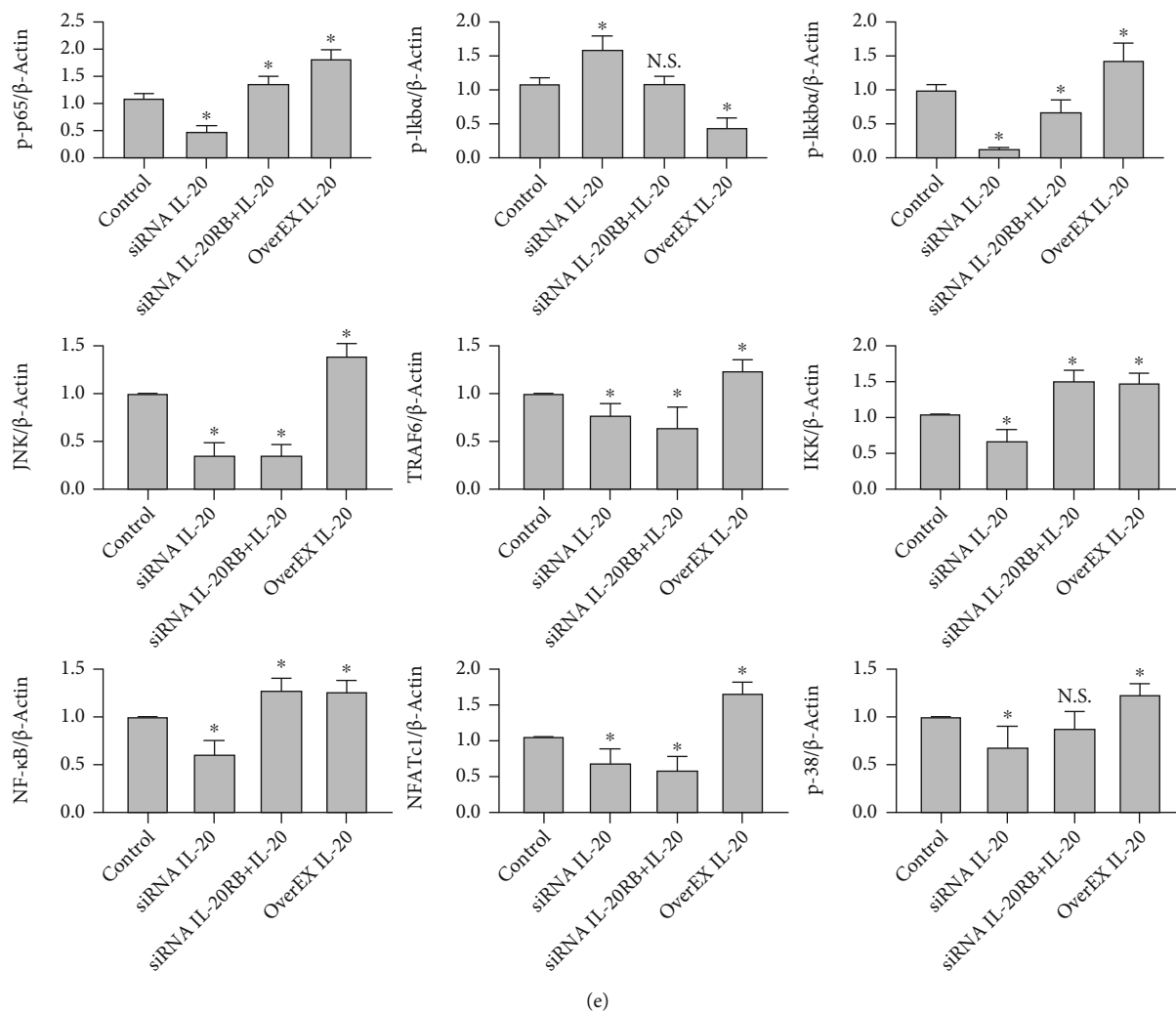


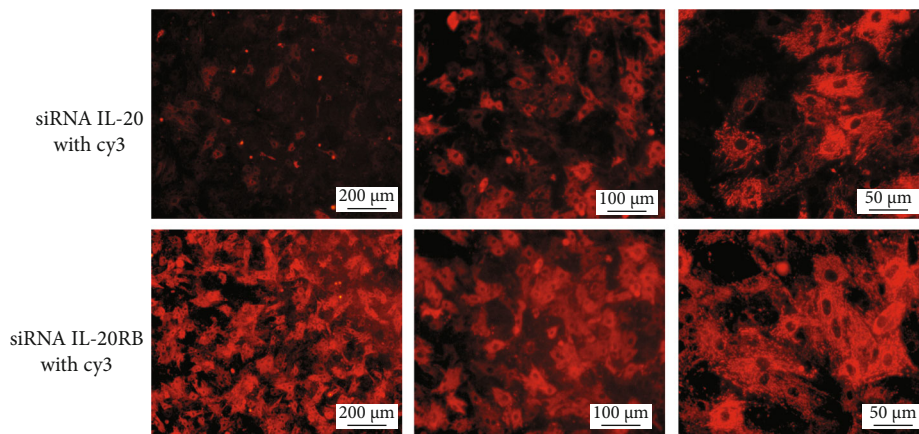
FIGURE 4: Robust expression of IL-20 significantly activated the RANKL-mediated downstream signalling pathway. siRNA reduction of IL-20 expression in BMMs led to significant inhibition of the RANKL-mediated downstream signalling pathway; moreover, siRNA reduction of IL-20RB, a key receptor for IL-20, in BMMs led to inhibition of IL-20-modulated downstream signalling pathways. (a) Bone marrow-derived mononuclear cells were transfected with siRNA carrying Cy3 dye and imaged with a fluorescence-inverted microscope to confirm the presence of siRNA within the cells. (b and c) qRT-PCR and western blotting analyses verified the inhibition of IL-20 and IL-20RB expression by siRNA at different concentrations (10–100 μ M of each siRNA sequence); three siRNA sequences were designed and synthesised for each gene. (d and e) Western blotting analysis was used to detect the RANKL-mediated downstream signalling pathway protein expression levels in BMMs transfected with IL-20 siRNA, IL-20RB siRNA with 20 ng/mL IL-20, and the IL-20 overexpression plasmid for 2 days; examined proteins included p-I κ B, p-I κ B β , p-p65, JNK, TRAF6, I κ K, NF- κ B, NFATc1, and p-38. Bars represent the mean \pm SEM of three independent experiments ($n = 12$). * $P < 0.05$ vs. control group; N.S.: not significant.

tooth movement distance over 7 days of exposure to similar force for a similar duration (Figure 6(b)); bone resorption was also greater in the OTM + IL-20 group. These findings suggested that IL-20 accelerates the formation of bone fractures and the speed of bone reconstruction. To test this hypothesis, double-labelling immunofluorescence staining of the periodontal ligament of the maxillary first molar was performed. The results indicated that the expression of IL-20 in the periodontal ligament increased after orthodontic tooth movement with IL-20 injection, compared with the control group; moreover, the expression levels of TRAP and YAP also increased in the group with IL-20 injection (Figure 6(g)). TRAP is an osteoclast-specific protein, while YAP is a protein that responds to mechanical stress. The

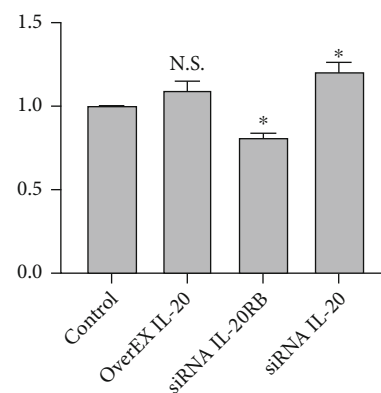
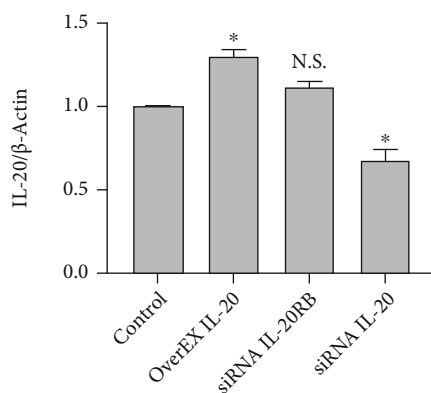
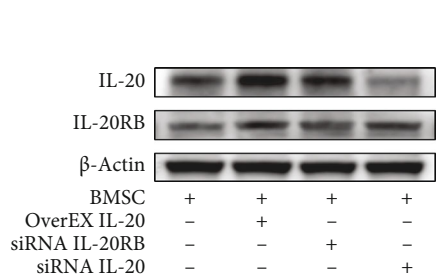
increased expression level of IL-20 in the periodontal ligament of teeth undergoing orthodontic movement implied that IL-20 is important in alveolar bone reconstruction. The increased expression levels of TRAP and YAP in the region near IL-20 expression suggest that, while IL-20 promotes osteoclast differentiation and accelerates bone remodelling, it can also enable periodontal ligament cells to more robustly respond to orthodontic force, further accelerating alveolar bone remodelling.

4. Discussion

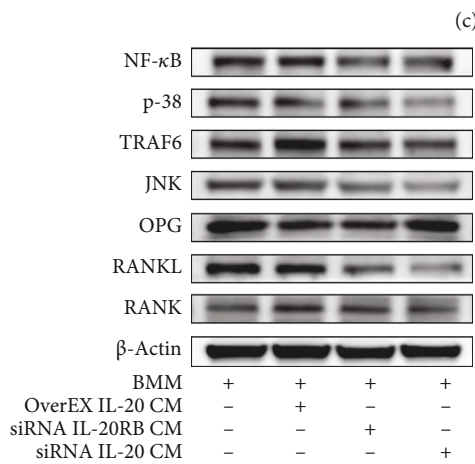
IL-20 is a powerful proinflammatory, chemotactic, and angiogenic cytokine of the IL-10 family. In chronic



(a)



(b)



(d)

FIGURE 5: Continued.

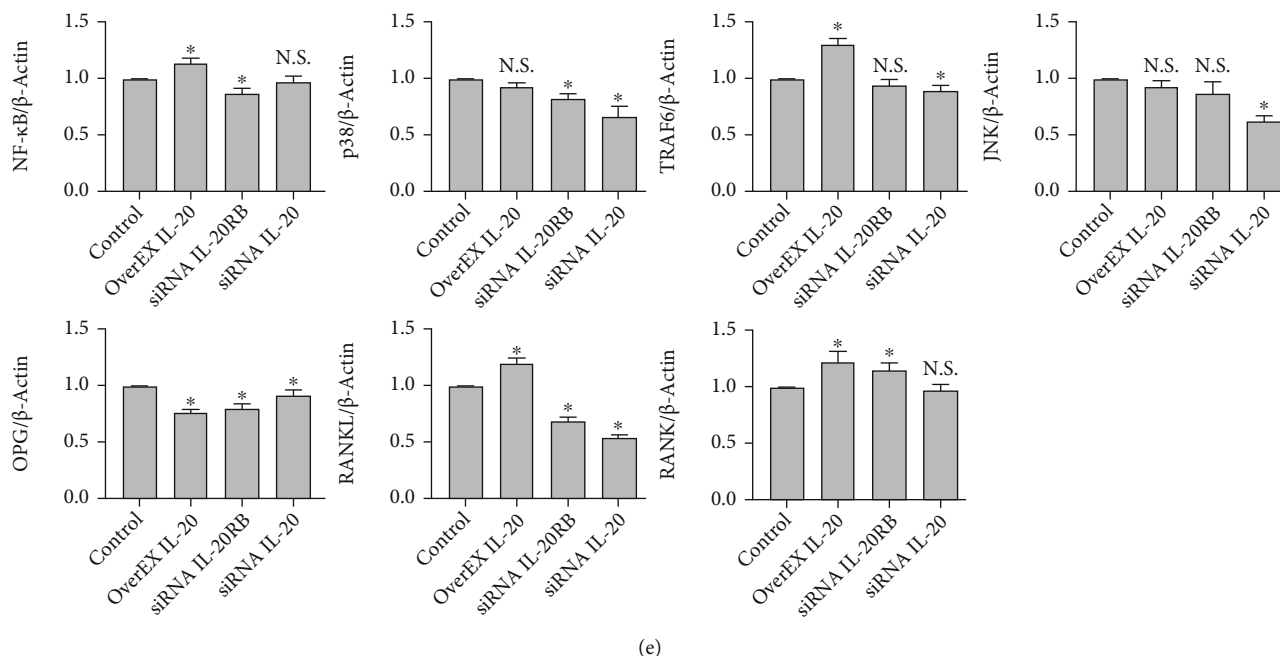


FIGURE 5: IL-20 can induce BMSCs to regulate the expression of OPG and RANKL and then influence osteoclastogenesis through the OPG/RANKL/RANK axis. (a) BMSCs were transfected with siRNA carrying Cy3 dye and imaged with a fluorescence-inverted microscope to confirm that siRNA had been transfected into the cells. (b and c) Western blotting analysis verified the inhibition of IL-20 and IL-20RB expression by siRNA and the overexpression of IL-20 using a plasmid. (d and e) Western blotting analysis detected protein levels of OPG/RANK/RANKL axis components and a subset of RANKL-mediated downstream signalling pathway components in BMMs cultured with BMSC CM treated with IL-20 siRNA, IL-20RB siRNA, and an IL-20 overexpression plasmid. Bars represent the mean \pm SEM of three independent experiments ($n = 12$). * $P < 0.05$ vs. control group; N.S.: not significant.

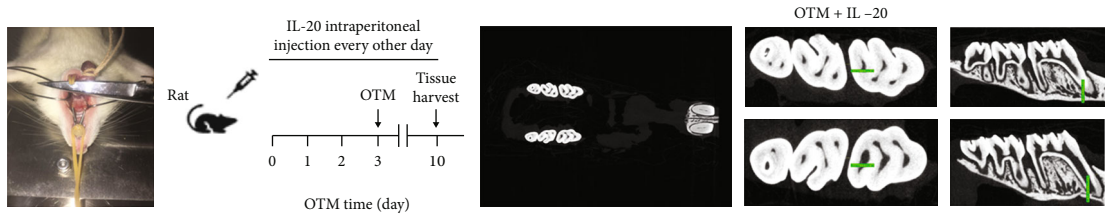
inflammatory diseases (e.g., psoriasis, atherosclerosis, and rheumatoid arthritis), IL-20 has been shown to exhibit robust proinflammatory, vascular regenerative, and cell chemotactic effects [30, 31]. The IL-20 family of cytokines can strengthen tissue remodelling and wound healing, maintain tissue integrity, and maintain and restore homeostasis in the context of infection and inflammation [32]. Some studies have shown that IL-20 plays important roles in osteoporosis and bone loss-related diseases; moreover, studies in ovariectomised mice have shown that anti-IL-20 antibodies can prevent bone resorption by blocking osteoclast formation and inducing osteoblast formation [17, 18]. Because of breakthroughs in the osteoclastogenesis molecular mechanism by means of coculture systems comprising BMSCs and BMMs or T cells, many cytokines and chemokines involved in bone remodelling and bone resorption have been identified; these include TNF- α , IL-1, IL-6, IL-10, IL-17, and IL-22 [33–40].

An IL-20 receptor (IL-20R) cytokine is reportedly expressed by immune cells. IL-20R cytokines are presumably related to the pathogenesis of chronic inflammation and autoimmune diseases. Some studies have shown that IL-20R cytokines play a suppressive role in regulating immune cells, such as innate and adaptive T cell responses [41]; thus, the functions and roles of IL-20R cytokines in autoimmunity are presumably complex. IL-20 and its family of cytokines share three receptors (IL-20RA, IL-20RB, and IL-22RA1); because of the promiscuity of the type I (IL-20RA and IL-20RB heterodimer) and type II (IL-20RAI and IL-20RB heterodimer) receptors, IL-20 and its family have some dis-

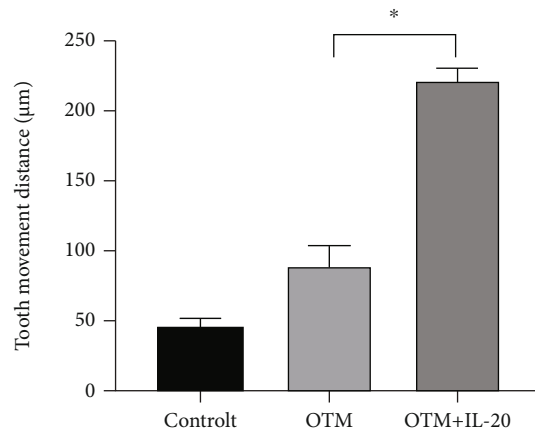
tinctive features [31]. IL-20 can signal through both type I receptor heterodimers and type II receptor heterodimers, and both receptor heterodimers share the common receptor subunit IL-20RB [42]. Therefore, IL-20RB may have an important effect on the cellular roles of IL-20.

We used siRNA knockdown to reduce the expression of IL-20 in rat BMMs and found that RANKL-induced osteoclastogenesis decreased. However, our findings demonstrated that IL-20 has a dual effect on osteoclast differentiation and function. A low concentration of IL-20 promoted both preosteoclast proliferation and osteoclastogenesis, whereas a high concentration of IL-20 inhibited BMM proliferation and osteoclastogenesis. Notably, transfection with an IL-20-overexpression plasmid did not cause inhibition of osteoclast differentiation; in contrast, it activated the RANKL-mediated osteoclastogenic downstream signalling pathway and promoted osteoclast differentiation. These findings suggest that IL-20 binds to two receptor complexes: IL-20R1/IL-20R2 and IL-22R1/IL-20R2. Both heterodimeric receptor complexes partially signal through the JAK/STAT pathway. Moreover, IL-20 binds to its receptor and enters the cell to activate STAT1. Our KEGG pathway analyses revealed that this activation of the JAK/STAT signalling pathway and STAT1 are sufficient to inhibit the osteoclast differentiation by inhibiting both c-Fos and TRAF6. We presume that the enhanced expression of IL-20 can directly upregulate on the TRAF6/NF- κ B/NFATc1 signal pathway to promote osteoclast differentiation.

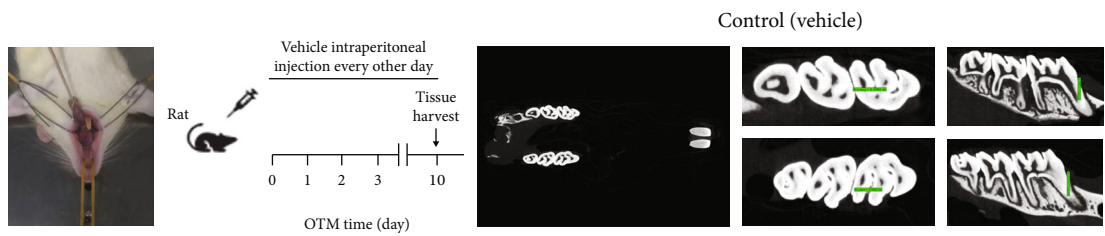
In accordance with previous findings, we added recombinant IL-20 protein to rat BMMs that had knocked down



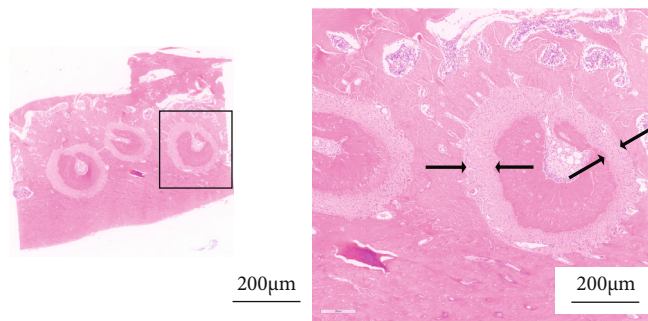
(a)



(b)



(c)



(d)



(e)

FIGURE 6: Continued.

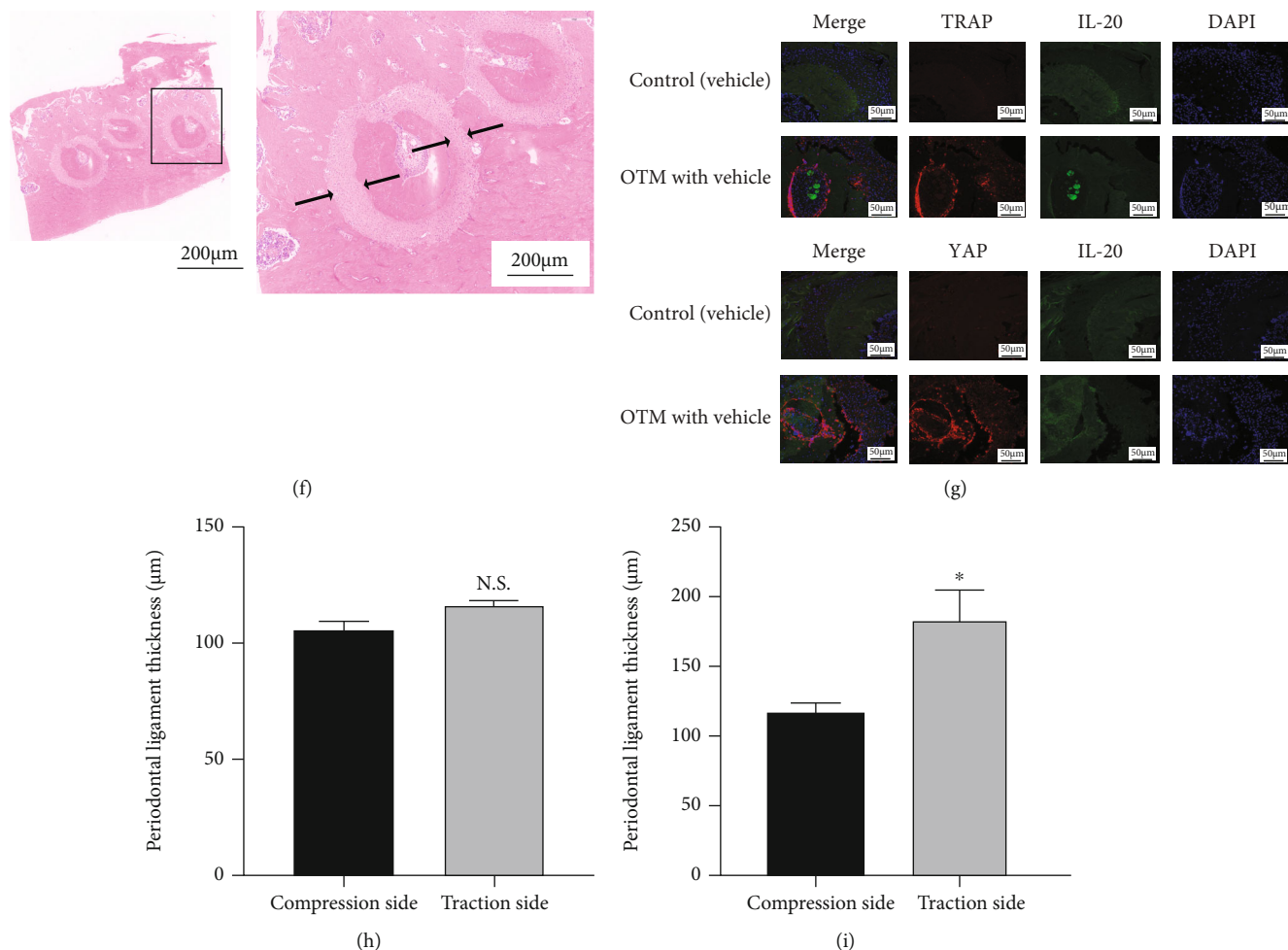


FIGURE 6: (a) OTM + IL-20 group: during the application of orthodontic force, an IL-20 solution with a concentration of 40 mg/kg body weight was injected at 2-day intervals. Seven days after the application of orthodontic force, micro-CT showed larger gaps between first and second molars. (b) Micro-CT measurement revealed that the gap between the first and second molars was significantly greater in the OTM + IL-20 group than in the OTM group. Bars represent the mean \pm SEM of three independent experiments ($n = 12$). * $P < 0.05$ vs. OTM group; ns: not significant. (c) Control group: no orthodontic force was applied, and 0.9% saline alone was injected at 2-day intervals. Micro-CT showed no obvious gap between first and second molars. (d and f) HE staining showed significant changes in first molar periodontal ligament thickness. (e) OTM group: during the application of orthodontic force, 0.9% saline was injected at 2-day intervals. Seven days after the application of orthodontic force, micro-CT showed obvious gaps between first and second molars. (g) Double-labelled immunofluorescence staining showed that, in the context of orthodontic force, the expression levels of TRAP and YAP increased in the first molar periodontal ligament; both showed high expression in the region near IL-20 expression. (h) There was no significant change in the periodontal ligament in the control group. (i) HE staining was used to measure the periodontal ligament on the compressed and traction sides of the first molar in the control and OTM groups. The periodontal ligament thickness in the OTM group was significantly thinner on the compressed side than on the traction side. Bars represent the mean \pm SEM of three independent experiments ($n = 12$). * $P < 0.05$ vs. OTM group; N.S.: not significant.

IL-20RB and cocultured. The results suggested that the expression of NF- κ B was increased, although the RANKL-mediated TRAF6/NFATc1 signalling pathway did not significantly change. Thus, in the absence of IL-20RB, IL-20 does not influence osteoclast differentiation. These data indicate that IL-20RB has an important effect on the cellular functions of IL-20. Our findings indicate that IL-20RB offers a potential therapeutic target for patients with bone loss disease and osteoporosis, which may effectively inhibit bone loss.

Osteoblast–osteoclast communication, regulated by various molecules, cytokines, and signalling pathways, is important for bone homeostasis. The OPG/RANK/RANKL axis is

an important signalling pathway in this communication, and IL-20 is an important regulator of the balance between osteoblastogenesis and osteoclastogenesis [37, 38]. Studies have shown that bone-associated immune mediators target IL-20 in MC3T3-E1 cells (mouse osteoblasts) and mature osteoclasts; moreover, IL-20 acts as an important regulator of osteoblasts and osteoclasts by activating OPG/RANK/RANKL, which are essential components in the osteoclast signalling pathway [43, 44]. In this study, we confirmed that IL-20 can induce BMSCs to regulate the expression of OPG and RANKL and then affect osteoclastogenesis through the OPG/RANKL/RANK axis. Subsequently, we found that the

RANKL/TRAF6/NF- κ B and JNK/p38/MAPK signalling pathways were activated during osteoclast differentiation in BMMs, following culture with CM from IL-20-overexpressing BMSCs. However, the RANKL/TRAF6/NF- κ B and JNK/p38/MAPK signalling pathways were not activated during osteoclast differentiation in BMMs, following culture with CM from IL-20 and IL-20RB knockdown BMSCs. Overall, our findings indicated that RANKL and OPG in BMSCs were endogenously induced by IL-20, which supports the notion of regulatory feedback during osteoclast differentiation through the OPG/RANKL/RANK axis.

“Orthodontic tooth movement” is the application of appropriate “biological force” to the teeth, alveolar bone, and jaw to cause physiological movement, thereby correcting malocclusion (occlusion) deformities. The imbalance between osteoblasts and osteoclasts is the biological basis of tooth movement and alveolar bone reconstruction [29]. Through in vitro experiments, we clarified the effects of IL-20 and its key receptor, IL-20RB, on osteoclast differentiation and functions. Additionally, we found that IL-20 stimulates BMSCs to participate in feedback regulation of osteoclast formation through the OPG/RANKL/RANK axis. Moreover, IL-20 can change the local immune environment and affect osteoclast differentiation. Our in vitro findings implied that IL-20 can affect orthodontic tooth movement. Using a rat model of tooth movement, we injected IL-20 solution into the abdominal cavity. Notably, rats that had been injected with IL-20 solution exhibited significant enhancements of tooth movement speed and distance. These findings indicate that IL-20 accelerates the speed of osteoclast differentiation and alveolar bone reconstruction. Through double-labelling immunofluorescence staining of the periodontal ligament during orthodontic tooth movement, we found that IL-20 in the periodontal ligament is closely associated with the osteoclast-specific protein, TRAP, and the mechanical stress response protein, YAP. Thus, IL-20 can promote osteoclast differentiation and accelerate the speed of orthodontic tooth movement; it can also enable the periodontal ligament to better respond to the mechanical force of the load and accelerate the reconstruction of alveolar bone.

In conclusion, we found that IL-20 can differentially regulate osteoclast formation and osteoclast-mediated bone resorption capacity. IL-20 acts on the upstream differential regulation of primary cell osteoclastogenesis by regulating the OPG/RANKL/RANK axis. In addition, we demonstrated that IL-20 may activate the OPG/RANKL/RANK axis, and we revealed a possible molecular mechanism involving the RANKL/NF- κ B/NFATc1 pathway. Using IL-20 at a concentration of 20 ng/mL, combined with siRNA transfection to reduce the expression of IL-20RB, a key receptor of IL-20, we achieved partial inhibition of the RANKL-mediated downstream signalling pathway regulated by IL-20. We also used high-throughput transcriptome sequencing to confirm that enhanced expression of IL-20 can substantially influence the cellular immune response, stimulus feedback, and cellular response to stress; these effects are in addition to its role in the osteoclast differentiation pathway. Our in vivo analyses confirmed that IL-20 could promote osteoclast differentiation, thereby accelerating the speed of orthodontic tooth movement. In addition, IL-20 promoted the expression of

mechanical force response proteins, which may enable the periodontal ligament to more effectively adapt to the mechanical force load and may improve the speed of bone remodelling. Our findings imply that targeting IL-20 may be a promising therapeutic approach for diseases with bone loss; they also support a new perspective regarding the investigation of orthodontic tooth movement.

Abbreviations

IL:	Interleukin
siRNA:	Small interfering RNA
mRNA:	Messenger ribonucleic acid
GO:	Gene Ontology
KEGG:	Kyoto Encyclopedia of Genes and Genomes
OTM:	Orthodontic tooth movement
qRT-PCR:	Real-time quantitative polymerase chain reaction
FBS:	Fetal bovine serum
cDNA:	Complementary DNA
PBS:	Phosphate buffer saline
DMEM:	Dulbecco's modified eagle medium
OMEM:	Opti modified eagle medium
SD:	Standard deviation
M-CSF:	Macrophage colony-stimulating factor
RANK:	Receptor activator of NF- κ B
RANKL:	Receptor activator of NF- κ B ligand
CCK-8:	Cell counting kit-8
OverEx:	Overexpression
OPG:	Osteoclastogenesis inhibitory factor
TRAP:	Tartrate resistant acid phosphatase
CTSK:	Cathepsin K
MMP-9:	Matrix metalloprotein-9
RBC:	Red blood cell
BMSC:	Bone marrow mesenchymal stem cell
BMM:	Marrow-derived macrophage
RIPA:	Radio immunoprecipitation assay
SDS-PAGE:	Sodium dodecyl sulfate-polyacrylamide gel electrophoresis
BSA:	Bovine albumin
IL-20RA:	Interleukin 20 receptor subunit alpha
IL-20RB:	Interleukin 20 receptor subunit beta
IL-22RA1:	Interleukin 22 receptor subunit alpha 1
GRB2:	Growth factor receptor-bound protein 2
ERK:	Extracellular regulated MAP kinase
JNK:	c-Jun N-terminal kinase
TRAF6:	Tumor necrosis factor receptor-associated factor 6
IKK:	Inhibitor of kappa B kinase beta
NFATc1:	Nuclear factor of activated T cells 1
p-38:	p38 kinase
HIF- α :	Hypoxia-inducible factor 1 subunit alpha a
CXCR4:	C-X-C motif chemokine receptor 4
CCR7:	C-C motif chemokine receptor 7
VEGF-R2:	Vascular endothelial growth factor receptor 2.

Data Availability

The data that support the findings of this study are available from the corresponding author upon reasonable request.

Conflicts of Interest

The authors declare no conflict of interest.

Authors' Contributions

Yang Cao, Yuanbo Liu, and Yilong AI designed the experiments. Yuanbo Liu, Yilong AI, and Bowen Meng carried out the experiments. Yuanbo Liu, Xuan Sun, Xi Chen, Dongle Wu, Benyi Yang, Chaoran Fu, Yilin Wu, and Lei Gan collected and analysed the data. Yuanbo Liu, Yilong AI, and Yang Cao wrote and revised the manuscript. Yuanbo Liu, Yilong AI, and Xuan Sun were co-first authors.

Acknowledgments

This study was supported by grants from the Natural Science Foundation of Guangdong Province (grant number 2017A030313529), National Natural Science Foundation of China (grant number 81970963), and Guangdong Financial Fund for High-Caliber Hospital Construction.

References

- [1] A. H. Hassan, S. H. Al-Saeed, B. A. Al-Maghlouth, M. A. Bahammam, A. I. Linjawi, and T. H. El-Bialy, "Corticotomy-assisted orthodontic treatment," *Saudi Medical Journal*, vol. 36, no. 7, pp. 794–801, 2015.
- [2] S. R. Taddei, I. Andrade Jr., C. M. Queiroz-Junior et al., "Role of CCR2 in orthodontic tooth movement," *American Journal of Orthodontics and Dentofacial Orthopedics*, vol. 141, no. 2, pp. 153–160.e1, 2012.
- [3] K. J. Suchacki, F. Roberts, A. Lovdel et al., "Skeletal energy homeostasis: a paradigm of endocrine discovery," *The Journal of Endocrinology*, vol. 234, no. 1, pp. R67–R79, 2017, Epub 2017 Apr 28.
- [4] J. C. Crockett, M. J. Rogers, F. P. Coxon, L. J. Hocking, and M. H. Helfrich, "Bone remodelling at a glance," *Journal of Cell Science*, vol. 124, no. 7, pp. 991–998, 2011.
- [5] K. Matsuo and N. Irie, "Osteoclast-osteoblast communication," *Archives of Biochemistry and Biophysics*, vol. 473, no. 2, pp. 201–209, 2008, Epub 2008 Mar 29.
- [6] I. Ushach and A. Zlotnik, "Biological role of granulocyte macrophage colony-stimulating factor (GM-CSF) and macrophage colony-stimulating factor (M-CSF) on cells of the myeloid lineage," *Journal of Leukocyte Biology*, vol. 100, no. 3, pp. 481–489, 2016.
- [7] E. R. Stanley, M. Cifone, P. M. Heard, and V. Defendi, "Factors regulating macrophage production and growth: identity of colony-stimulating factor and macrophage growth factor," *Journal of Experimental Medicine*, vol. 143, no. 3, pp. 631–647, 1976.
- [8] W. S. Simonet, D. L. Lacey, C. R. Dunstan et al., "Osteoprotegerin: a novel secreted protein involved in the regulation of bone density," *Cell*, vol. 89, no. 2, pp. 309–319, 1997.
- [9] E. Tsuda, M. Goto, S. Mochizuki et al., "Isolation of a novel cytokine from human fibroblasts that specifically inhibits osteoclastogenesis," *Biochemical and Biophysical Research Communications*, vol. 234, no. 1, pp. 137–142, 1997.
- [10] H. Yasuda, N. Shima, N. Nakagawa et al., "Identity of osteoclastogenesis inhibitory factor (OCIF) and osteoprotegerin (OPG): a mechanism by which OPG/OCIF inhibits osteoclastogenesis in vitro," *Endocrinology*, vol. 139, no. 3, pp. 1329–1337, 1998.
- [11] M. Tsukasaki and H. Takayanagi, "Osteoimmunology: evolving concepts in bone-immune interactions in health and disease," *Nature Reviews. Immunology*, vol. 19, no. 10, pp. 626–642, 2019, Epub 2019 Jun 11.
- [12] K. W. Kim, H. R. Kim, J. Y. Park et al., "Interleukin-22 promotes osteoclastogenesis in rheumatoid arthritis through induction of RANKL in human synovial fibroblasts," *Arthritis and Rheumatism*, vol. 64, no. 4, pp. 1015–1023, 2012, Epub 2011 Oct 27.
- [13] J. Schulze, T. Bickert, F. T. Beil et al., "Interleukin-33 is expressed in differentiated osteoblasts and blocks osteoclast formation from bone marrow precursor cells," *Journal of Bone and Mineral Research*, vol. 26, no. 4, pp. 704–717, 2011.
- [14] Y. Xue, Z. Liang, X. Fu, T. Wang, Q. Xie, and D. Ke, "IL-17A modulates osteoclast precursors' apoptosis through autophagy-TRAF3 signaling during osteoclastogenesis," *Biochemical and Biophysical Research Communications*, vol. 508, no. 4, pp. 1088–1092, 2019, Epub 2018 Dec 12.
- [15] K. Yokota, K. Sato, T. Miyazaki et al., "Combination of tumor necrosis factor α and interleukin-6 induces mouse osteoclast-like cells with bone resorption activity both in vitro and in vivo," *Arthritis & Rheumatology*, vol. 66, no. 1, pp. 121–129, 2014.
- [16] A. Paradowska-Gorycka, A. Grzybowska-Kowalczyk, E. Wojtecka-Lukasik, and S. Maslinski, "IL-23 in the Pathogenesis of Rheumatoid Arthritis," *Scandinavian Journal of Immunology*, vol. 71, no. 3, pp. 134–145, 2010.
- [17] Y. H. Hsu, W. Y. Chen, C. H. Chan, C. H. Wu, Z. J. Sun, and M. S. Chang, "Anti-IL-20 monoclonal antibody inhibits the differentiation of osteoclasts and protects against osteoporotic bone loss," *Journal of Experimental Medicine*, vol. 208, no. 9, pp. 1849–1861, 2011.
- [18] Y. H. Hsu, Y. S. Chiu, W. Y. Chen et al., "Anti-IL-20 monoclonal antibody promotes bone fracture healing through regulating IL-20-mediated osteoblastogenesis," *Scientific Reports*, vol. 6, no. 1, 2016.
- [19] T. C. Dandajena, M. A. Ihnat, B. Disch, J. Thorpe, and G. F. Currier, "Hypoxia triggers a HIF-mediated differentiation of peripheral blood mononuclear cells into osteoclasts," *Orthodontics & Craniofacial Research*, vol. 15, no. 1, pp. 1–9, 2012.
- [20] H. Huang, R. C. Williams, and S. Kyrkanides, "Accelerated orthodontic tooth movement: molecular mechanisms," *American Journal of Orthodontics and Dentofacial Orthopedics*, vol. 146, no. 5, pp. 620–632, 2014, Epub 2014 Oct 28.
- [21] H. J. Park, K. H. Baek, H. L. Lee et al., "Hypoxia inducible factor-1 α directly induces the expression of receptor activator of nuclear factor- κ B ligand in periodontal ligament fibroblasts," *Molecules and Cells*, vol. 31, no. 6, pp. 573–578, 2011.
- [22] D. E. Maridas, E. Rendina-Ruedy, P. T. Le, and C. J. Rosen, "Isolation, Culture, and Differentiation of Bone Marrow Stromal Cells and Osteoclast Progenitors from Mice," *Journal of Visualized Experiments*, no. 131, p. 56750, 2018.
- [23] N. Takahashi, T. Akatsu, N. Udagawa et al., "Osteoblastic cells are involved in osteoclast formation," *Endocrinology*, vol. 123, no. 5, pp. 2600–2602, 1988.
- [24] H. Yoshida, S. Hayashi, T. Kunisada et al., "The murine mutation osteopetrosis is in the coding region of the macrophage colony stimulating factor gene," *Nature*, vol. 345, no. 6274, pp. 442–444, 1990.

- [25] H. Yasuda, N. Shima, N. Nakagawa et al., "Osteoclast differentiation factor is a ligand for osteoprotegerin/osteoclastogenesis-inhibitory factor and is identical to TRANCE/RANKL," *Proceedings of the National Academy of Sciences*, vol. 95, no. 7, pp. 3597–3602, 1998.
- [26] T. Suda, N. Takahashi, N. Udagawa, E. Jimi, M. T. Gillespie, and T. J. Martin, "Modulation of osteoclast differentiation and function by the new members of the tumor necrosis factor receptor and ligand families," *Endocrine Reviews*, vol. 20, no. 3, pp. 345–357, 1999.
- [27] Y. Y. Kong, H. Yoshida, I. Sarosi et al., "OPGL is a key regulator of osteoclastogenesis, lymphocyte development and lymph-node organogenesis," *Nature*, vol. 397, no. 6717, pp. 315–323, 1999.
- [28] D. L. Lacey, W. J. Boyle, W. S. Simonet et al., "Bench to bedside: elucidation of the OPG–RANK–RANKL pathway and the development of denosumab," *Nature Reviews Drug Discovery*, vol. 11, no. 5, pp. 401–419, 2012.
- [29] Y. Li, L. A. Jacox, S. H. Little, and C. C. Ko, "Orthodontic tooth movement: the biology and clinical implications," *The Kaohsiung Journal of Medical Sciences*, vol. 34, no. 4, pp. 207–214, 2018, Epub 2018 Feb 3.
- [30] M. V. Autieri, "IL-19 and Other IL-20 Family Member Cytokines in Vascular Inflammatory Diseases," *Frontiers in Immunology*, vol. 9, p. 700, 2018.
- [31] U. M. Wegenka, "IL-20: biological functions mediated through two types of receptor complexes," *Cytokine & Growth Factor Reviews*, vol. 21, no. 5, pp. 353–363, 2010, Epub 2010 Oct 16.
- [32] W. Ouyang, S. Rutz, N. K. Crellin, P. A. Valdez, and S. G. Hymowitz, "Regulation and functions of the IL-10 family of cytokines in inflammation and disease," *Annual Review of Immunology*, vol. 29, no. 1, pp. 71–109, 2011.
- [33] D. Medhat, C. I. Rodríguez, and A. Infante, "Immunomodulatory Effects of MSCs in Bone Healing," *International Journal of Molecular Sciences*, vol. 20, no. 21, p. 5467, 2019.
- [34] R. Lieder and O. E. Sigurjonsson, "The effect of recombinant human interleukin-6 on osteogenic differentiation and YKL-40 expression in human, bone marrow-derived mesenchymal stem cells," *Biores Open Access*, vol. 3, no. 1, pp. 29–34, 2014.
- [35] L. Ma, R. Aijima, Y. Hoshino et al., "Transplantation of mesenchymal stem cells ameliorates secondary osteoporosis through interleukin-17-impaired functions of recipient bone marrow mesenchymal stem cells in MRL/lpr mice," *Stem Cell Research & Therapy*, vol. 6, no. 1, p. 104, 2015.
- [36] A. A. El-Zayadi, E. A. Jones, S. M. Churchman et al., "Interleukin-22 drives the proliferation, migration and osteogenic differentiation of mesenchymal stem cells: a novel cytokine that could contribute to new bone formation in spondyloarthropathies," *Rheumatology*, vol. 56, no. 3, pp. 488–493, 2016.
- [37] H. Liu, G. W. Xu, Y. F. Wang et al., "Composite scaffolds of nano-hydroxyapatite and silk fibroin enhance mesenchymal stem cell-based bone regeneration via the interleukin 1 alpha autocrine/paracrine signaling loop," *Biomaterials*, vol. 49, pp. 103–112, 2015, Epub 2015 Feb 14.
- [38] Z. Chen, L. Su, Q. Xu et al., "IL-1R/TLR2 through MyD88 divergently modulates osteoclastogenesis through regulation of nuclear factor of activated T cells c1 (NFATc1) and B lymphocyte-induced maturation protein-1 (Blimp1)," *Journal of Biological Chemistry*, vol. 290, no. 50, pp. 30163–30174, 2015.
- [39] K. Tanaka, K. Yamagata, S. Kubo et al., "Glycolaldehyde-modified advanced glycation end-products inhibit differentiation of human monocytes into osteoclasts via upregulation of IL-10," *Bone*, vol. 128, p. 115034, 2019.
- [40] N. Udagawa, N. Takahashi, E. Jimi et al., "Osteoblasts/stromal cells stimulate osteoclast activation through expression of osteoclast differentiation factor/RANKL but not macrophage colony-stimulating factor," *Bone*, vol. 25, no. 5, pp. 517–523, 1999.
- [41] J. Chen, R. R. Caspi, and W. P. Chong, "IL-20 receptor cytokines in autoimmune diseases," *Journal of Leukocyte Biology*, vol. 104, no. 5, pp. 953–959, 2018.
- [42] N. J. Logsdon, A. Deshpande, B. D. Harris, K. R. Rajashankar, and M. R. Walter, "Structural basis for receptor sharing and activation by interleukin-20 receptor-2 (IL-20R2) binding cytokines," *Proceedings of the National Academy of Sciences*, vol. 109, no. 31, pp. 12704–12709, 2012.
- [43] W. Zhang, S. Magadi, Z. Li, C. W. Smith, and A. R. Burns, "IL-20 promotes epithelial healing of the injured mouse cornea," *Experimental Eye Research*, vol. 154, pp. 22–29, 2017.
- [44] Y. Ikebuchi, S. Aoki, M. Honma et al., "Coupling of bone resorption and formation by RANKL reverse signalling," *Nature*, vol. 561, no. 7722, pp. 195–200, 2018, Epub 2018 Sep 5.

Research Article

Biocompatibility and Angiogenic Effect of Chitosan/Graphene Oxide Hydrogel Scaffolds on EPCs

Lifang Zhang ¹, Xinping Li,¹ Congying Shi ², Gaoying Ran,¹ Yuting Peng,¹ Shuguang Zeng ¹ and Yan He³

¹Department of Oral and Maxillofacial Surgery, Stomatological Hospital, Southern Medical University, 510000 Guangzhou, Guangdong, China

²Clinical Application Center, Guangdong Cord Bank, 510000 Guangzhou, Guangdong, China

³Skeletal Biology Research Center, Department of Oral Maxillofacial Surgery, Harvard School of Dental Medicine, Boston, 02114 MA, USA

Correspondence should be addressed to Shuguang Zeng; sunrisezdoctor@smu.edu.cn

Received 28 February 2021; Revised 29 March 2021; Accepted 22 April 2021; Published 19 May 2021

Academic Editor: Jing Yan

Copyright © 2021 Lifang Zhang et al. This is an open access article distributed under the Creative Commons Attribution License, which permits unrestricted use, distribution, and reproduction in any medium, provided the original work is properly cited.

Angiogenesis in the field of tissue engineering has attracted significant attention. Graphene oxide has become a promising nanomaterial in tissue engineering for its unique biochemical properties. Therefore, herein, a series of chitosan (CS)/graphene oxide (GO) hydrogel scaffolds were synthesized by crosslinking CS and GO at different concentrations (0.1, 0.5, and 1.0 wt.%) using genipin. Compared with the CS hydrogel scaffolds, the CS/GO hydrogel scaffolds have a better network structure and mechanical strength. Then, we used endothelial progenitor cells (EPCs) extracted from human umbilical cord blood and cocultured these EPCs with the as-prepared scaffolds. The scaffolds with 0.1 and 0.5 wt.%GO showed no considerable cytotoxicity, could promote the proliferation of EPCs and tube formation, and upregulated the expressions of CD34, VEGF, MMP9, and SDF-1 in EPCs compared to the case of the scaffold with 1.0 wt.%GO. This study shows that the addition of graphene oxide improves the structure of chitosan hydrogel and enhances the proliferation activity and angiogenic capacity of EPCs.

1. Introduction

Tissue defects caused by trauma, infection, and tumor resection have become a serious problem in healthcare worldwide [1]. Although surgery is the most valid method to treat these defects, it has certain limitations. In this regard, tissue engineering has attracted significant attention. However, as tissue regeneration relies on blood vessels for the transport of nutrients and metabolic wastes, engineered tissues cannot be widely used because they lack a vascular system [2]. Without perfusion from implanted microvasculature, the thickness of engineered tissue constructs in vitro is limited to approximately 200 μm , which is the oxygen diffusional limit [3]. Therefore, sufficient angiogenesis can promote the survival and repair of damaged tissues [4]. Although several studies have been reported on the osteogenesis of scaffold materials,

studies on the angiogenesis of these materials are in their infancy at present [5, 6]. Hence, researchers in the field of tissue engineering have started to focus on improving the angiogenesis of tissue-engineered structures [7, 8].

A three-dimensional porous structure is conducive to the growth of endothelial cells and the formation of vascular structures [9, 10]. Hydrogels, as a three-dimensional porous structure, acquire good biocompatibility, degradability, and suitable mechanical properties, and it can be developed and improved to achieve more potential scaffold materials [11, 12]. Chitosan (CS) is a deacetylated product of chitin, which has the advantages of widespread availability and nontoxicity [13]. Hydrogels composed of CS have good biocompatibility and degradability and are widely used as scaffold materials for tissue engineering [14, 15]. However, the weak mechanical strength and low bone conductivity of CS limit the

application of these scaffold materials in tissue engineering [16]. To overcome these limitations, many researchers have developed CS composite materials [17, 18] by incorporating inorganic bioactive materials, such as β -tricalcium phosphate and hydroxyapatite (HA), using CS to promote bone regeneration [19, 20]. However, the application of these materials is hindered by their insufficient osteoinduction and angiogenesis [21].

In addition, graphene derivatives have gradually become a research hotspot in the field of nanobiomedicine as they can provide a favorable physical and chemical environment for bone formation [22]. Graphene oxide (GO) has shown considerable potential for biomedical applications, including bone tissue engineering, due to its excellent physical and chemical properties and biological activity [23, 24]. GO at an appropriate concentration can induce angiogenesis without significant cytotoxicity [25, 26]. Moreover, GO has abundant oxygen-containing groups, which can increase the deposition of HA [27]. Many researchers have introduced GO into tissue-engineered implants and found that GO is effective in promoting angiogenesis [27–29]. Thus, the addition of GO nanoparticles to the CS hydrogel can overcome the abovementioned limitations of this hydrogel.

In addition to having a suitable three-dimensional scaffold, the growth and proliferation of seed cells are crucial. Endothelial progenitor cells (EPCs), which are precursors of endothelial cells, can stimulate the growth of collateral vessels in ischemic tissues and thus promote angiogenesis [30]. EPCs can be noninvasively obtained from umbilical cord blood and adult peripheral blood, thereby eliminating immunogenicity [31]. Therefore, the angiogenic capacity of a tissue-engineered implant can be enhanced by introducing EPCs into it.

Furthermore, genipin (GNP) is a nontoxic, easily degradable natural substance, which has been widely used for crosslinking biological materials [32]. It was predicted that CS can react with genipin by nucleophilic ring-opening reactions, which is more conducive to the formation of spatial network structures in studies [33, 34]. Several studies have shown that the cytotoxicity of GNP is significantly lower than that of the classical crosslinking agent glutaraldehyde *in vitro* [35], and GNP has been continuously applied to manufacture biopolymer scaffolds in bone tissue engineering [36, 37].

Accordingly, in this study, a series of CS/GO hydrogel scaffolds were fabricated by crosslinking CS and GO at different concentrations using GNP. These hydrogel scaffolds exhibited significantly improved stability. Subsequently, we investigated the physical and chemical properties of these scaffolds. Moreover, the angiogenic potential of these scaffolds was evaluated by coculturing them with human EPCs, and the possible mechanisms have been discussed.

2. Materials and Methods

2.1. Hydrogel Production. Herein, 2.0 g CS (degree of deacetylation $\geq 95\%$, Macklin, Shanghai, China) was dissolved in 100 mL aqueous hydrochloric acid (0.1 mol/L, Sigma-Aldrich, St. Louis, State of Missouri, USA) under sterile conditions. The pH of the resulting solution was adjusted

to approximately 7.25 by β -glycerophosphate sodium solution (70% *w/v*, Solarbio, Beijing, China). Then, appropriate amounts of GNP solution (1% *w/v*, Sigma-Aldrich) and GO aqueous solution (3 mg/mL, Macklin) were added to the abovementioned solution. By mechanical stirring and ultrasonic breaking, CS/GO mixed solutions with different GO concentrations were prepared. Thereafter, these mixed solutions were centrifuged at 4°C and 3000 r/min for 10 min and then placed in a biochemical incubator at 37°C to form the hydrogels. Finally, these hydrogels were frozen at -80°C for 4 h and then placed in a vacuum freeze dryer (Biobase, Jinan, Shandong province, China) to construct hydrogel scaffolds.

2.2. Scanning Electron Microscopy (SEM). All lyophilized hydrogel scaffolds were cut into cubes with a side length of 0.5 cm followed by sputter coating with gold in liquid nitrogen. The internal structure and morphology of the scaffold sections were examined by SEM (Hitachi S-3700N, Chiyoda, Tokyo). Three samples of each group were chosen, and pictures were taken under an electron microscope. Three areas of each sample were selected randomly and measured by ImageJ. Typically, the average pore size was calculated.

2.3. Fourier Transform Infrared Spectroscopy (FTIR). Hydrogel scaffolds in appropriate amounts were ground and mixed with KBr (Macklin) particles in a 1:300 ratio. Then, they were scanned 64 times using a Fourier transform infrared spectrometer (SENSOR 27, Bruker, Karlsruhe, Baden-Wuerttemberg, Germany) in the range of 4000–400 cm^{-1} at a resolution of 2 cm^{-1} , and Fourier transform infrared spectra were recorded.

2.4. X-Ray Powder Diffraction (XRD). The abovementioned samples were analyzed using an X-ray diffractometer (D8X, Bruker), and the corresponding XRD patterns were acquired. The scanning area was in the 2θ range of 0–40°, and the scanning speed was 2°/min.

2.5. Tensile Properties. Lyophilized scaffolds were cut into 2 cm \times 0.5 cm strips, and their tensile properties were measured using an electronic universal material testing machine (Qingji Instrument Technology Co., Ltd, Shanghai, China) and a 100 N load cell at a loading rate of 10 mm/min. The measurement was performed five times, and the average value was calculated.

2.6. Swelling Rate (SR). Suitable amounts of lyophilized scaffolds were weighed, immersed in a large amount of ultrapure water at 25°C for 24 h, and then weighed again after removing the surface moisture:

$$SR = 100\% \times \frac{W_s - W_d}{W_d}, \quad (1)$$

where W_s and W_d are the weights of the wet and dry hydrogel scaffolds, respectively.

2.7. Porosity (ϵ) Test. The specific method was as follows [38]: hydrogels (dry mass M_0) were immersed in ethanol in a

weighing bottle. The bottle was weighed before (Ma) and after (Mb) removing the wet scaffold. Meanwhile, a 50 mL pycnometer filled with ethanol was weighed with the weight denoted as M1. The ethanol was poured out, and the wet scaffold previously soaked in ethanol was placed in the pycnometer, and ethanol was added until the pycnometer was filled to the same mark. The pycnometer was weighed again with weight denoted as M2. Porosity was calculated according to the following equations (ρ is the density of ethanol):

$$\begin{aligned} V1 &= (Ma - Mb - M0)/\rho, \\ V2 &= [(Ma - Mb) - (M2 - M1)]/\rho, \\ \varepsilon &= [V1/V2] \times 100\% = (Ma - Mb - M0)/[(Ma - Mb) \\ &\quad - (M2 - M1)] \times 100\%, \end{aligned} \quad (2)$$

where V1 is the volume of scaffold pores, V2 is the apparent volume of the scaffold, and ε is the porosity of the scaffold. Measurements were repeated three times for the same sample, and the average value was obtained.

2.8. Cell Subculture

2.8.1. Subculture of EPCs. After the EPCs (purchased from the Guangdong Cord Blood Bank, Guangzhou, Guangdong province, China) adhere to the wall, the medium was changed every two days. The cells can be subcultured when they have grown to 80%. After removing the original medium, rinse with PBS (Thermo Fisher Scientific, Waltham, Massachusetts, USA) twice and add 0.5 mL 0.25% trypsin (Sigma-Aldrich). When the cells are round, add medium to stop the digestion. After centrifugation at 800 rpm for 3 min, resuspension with Endothelial Cell Growth Medium (EGM) was used to inoculate in a culture flask and then cultured in a 37°C, 5% CO₂ incubator (Thermo Fisher Scientific).

2.9. Cell Identification. Herein, 1×10^6 EPCs were collected, and fluorescent dyes were used to conjugate cell surface markers: CD45/FITC, CD14/PE, CD34/PE, CD133/PE, CD31/FITC, CD105/FITC, and KDR-PE (Thermo Fisher Scientific). Cells were fixed with 4% paraformaldehyde (Beyotime Biotechnology). After being stained and washed with flow cytometry staining buffer (PBS + 1%BSA + 0.1%NaN₃), the cells were analyzed using a flow cytometer (BD Biosciences, Franklin Lakes, New Jersey, USA).

2.10. Tube Formation Experiment. Matrigel (Corning, New York, USA) was melted at 4°C and added to a 96-well plate precooled at -20°C followed by the removal of air bubbles. Then, this plate was placed in a cell incubator at 37°C for 1 h. The EPCs were treated with serum-free Endothelial Cell Growth Medium (EGM) for 1 h and then placed on a 96-well plate covered with Matrigel at 5×10^4 cells/well; thereafter, this plate was placed in a 37°C, 5% CO₂ humidified incubator. After 8 h, tube formation was observed using a microscope (Olympus IX51, Japan), and images were acquired.

2.11. Cocultivation and Grouping of EPCs and Hydrogel Scaffolds. Hydrogel scaffolds were placed in a well plate, and then, an appropriate amount of EPCs was inoculated into these scaffolds according to the experimental requirements. Based on the concentration of GO in the scaffolds, the coculture system was divided into five groups: EPCs, CS; EPCs, CS/0.1 wt.%GO; EPCs, CS/0.5 wt.%GO; EPCs, CS/1.0 wt.%GO; and EPCs.

2.12. Cell Counting Kit-8 (CCK-8) Assay. Scaffolds in appropriate amounts were fabricated under aseptic conditions and spread on a 24-well plate; then, 500 mL of a medium containing 5×10^4 EPCs was seeded in each well, and 50 μ L CCK-8 solution (Dojindo, Kumamoto, Japan) was added to each well every 36 h. After incubation at 37°C for 2 h, 100 μ L medium was withdrawn and added to a 96-well plate for absorbance measurement at 450 nm using a microplate reader (Bio-Rad, Hercules, California, USA). In each test, three duplicate wells were set for all specimens.

2.13. Lactate Dehydrogenase (LDH) Toxicity Assay. Scaffolds were synthesized under aseptic conditions and spread in 96-well plates. The EPCs were digested and seeded at 1×10^4 cells/well. After 1, 3, and 5 days, three wells of cells for each group were centrifuged at 400 g for 5 min, and the supernatants were obtained. LDH working solution (Beyotime Biotechnology) was prepared according to the instructions of the LDH. The LDH working solution was completely mixed with the test solution. Approximately 120 μ L of supernatant was withdrawn from each well and put in a new 96-well plate. At room temperature, the 96-well plate wrapped with aluminum foil was placed on a horizontal shaker for slow shaking followed by incubation in the dark for 30 min. Then, the absorbance was measured at 490 nm using the abovementioned microplate reader.

2.14. Live/Dead Staining. The EPCs were seeded on 12-well plates at 5×10^5 cells/well. After culturing in a cell incubator, the culture solution was withdrawn and gently soaked three times with PBS to ensure the removal of the active esterase present in the culture medium.

2.14.1. Configuration of the Staining Working Solution (Beyotime Biotechnology). Calcein and propidium iodide were equilibrated at room temperature for 30 min, and the staining working solution was configured according to the instructions. The staining working solution (200 μ L) was added to each well to cover the bottom of the well plate, followed by incubation in the dark for 30 min and gentle washing three times with PBS for 5 min each time. The green and red fluorescence of the same region was examined using a fluorescence microscope (Olympus IX51, Japan).

2.14.2. Measurement of the Number of Dead and Live Cells. Trypsin without ethylenediaminetetraacetic acid was used to digest the previously seeded and soaked EPCs, followed by centrifugation and washing twice with PBS to resuspend the cells. Then, the cells of each group were stained by the abovementioned process followed by washing and

TABLE 1: Sequences of primers for qRT-PCR.

Gene symbol	Forward primer (5'-3')	Reverse primer (5'-3')
CD34	AGACTGTGCAGTGATGTGGT	CCCTGGTACATTCGGGTCTG
MMP9	CCTGGGCAGATTCCAAACCT	GTACACGCGAGTGAAGGTGA
VEGF	GGCAAAAACGAAAGCGCAAG	GAGGCTCCAGGGCATTAGAC
SDF-1	TGCCCTTCAGATTGTAGCCC	GCGTCTGACCCTCTCACATC
GAPDH	GGAGTCCACTGGCGTCTTCA	GTCATGAGTCCTTCCACGATACC

centrifugation with PBS. Finally, the measurement was conducted using the flow cytometer.

2.15. Tube Formation Assay. Cells were inoculated according to the instructions provided on the CCK-8 kit and continuously cultured for 7 days. The Matrigel basement membrane matrix (BD Biosciences, Franklin Lakes, New Jersey, USA) was thawed at 4°C, mixed with the basal medium in equal proportion, pipetted into precooled 96-well plates, and incubated at 37°C for 30 min. After Matrigel polymerization, EPCs were treated with serum-free EGM for 1 h and then digested and reseeded on Matrigel in 96-well plates at 1×10^4 cells/well. After being incubated at 37°C for 8 h, the cells were imaged using a microscope (Leica, Wetzlar, Hesse-Darmstadt, Germany), and the images were analyzed and interpreted using ImageJ software.

2.16. Quantitative Reverse Transcription Polymerase Chain Reaction (qRT-PCR). The EPCs were seeded in 6-well plates at 1×10^6 cells/well and continuously cultured for 7 days. Total RNAs of the cells of each group were extracted with the TRIzol reagent (Sigma, Missouri, USA) and reverse transcribed into cDNA using an Evo M-MLV RT Premix kit (Accurate Biology, Changsha, Hunan, China). The SYBR® Green Premix Pro Taq HS qPCR Kit (Accurate Biology, Changsha, Hunan, China) was used for PCR amplification, and the total volume of the reaction system was 20 µL. PCR was performed employing the ABI PRISM® 7500 sequence detection system. The reaction conditions were as follows: 95°C for 30 s, followed by 40 cycles of 95°C for 5 s and 60°C for 30 s. Thereafter, the 2- $\Delta\Delta$ CT method was used to calculate the relative DNA expression. All primers used in this experiment were synthesized by TsingKe (Beijing, China) and are listed in Table 1.

2.17. Western Blot Analysis. Cells were seeded and cultured as mentioned in Section 2.15. The cells were lysed with RIPA Lysis Buffer (Sigma, Missouri, USA), placed on ice for 30 min, and then centrifuged at 12000 g for 15 min at 4°C, and the supernatant was aspirated. The bicinchoninic acid protein kit (China Biyuntian Biotechnology Co., Ltd) was used to determine the protein concentration of cells. Sodium dodecylsulphate-polyacrylamide gel electrophoresis (SDS-PAGE) loading buffer (YongJin, Guangzhou, Guangdong, China) was added to the cells in a 4:1 ratio followed by heating at 100°C for 10 min. The sample (20 µg) was subjected to SDS-PAGE and then transferred to a polyvinylidene difluoride membrane (Millipore, Billerica, MA, USA), which was then blocked with 5% skim milk at room temperature for

2 h. The resulting membrane was incubated with the primary antibody at 4°C overnight and then with the specific secondary antibody at room temperature for 2 h. Thereafter, ChemiDoc XRS+ (Bio-Rad) was employed to detect the protein band by chemiluminescence, and the images were analyzed using the Quantity One software. The following antibodies were used: CD34 (1:1000; Proteintech, 3C8G12), VEGF (1:1000; Thermo Fisher, MA5-13182), SDF-1 (1:1000; Abcam, ab9797), MMP9 (1:3000; Thermo Fisher, PA5-83748), and GAPDH (1:5000; Fude Biotechnology, FD0063-100).

2.18. Statistical Analysis. Statistical analyses were carried out using SPSS 22.0 software. All experimental data were expressed as the mean difference \pm standard deviation. Comparisons between different groups were conducted using an independent sample *t*-test. Moreover, for multiple specimens, initially, the homogeneity of variance was calculated by Levene's test. If the variance was uniform, one-way analysis of variance (ANOVA) was simultaneously performed using SNK multiple comparisons between groups; if the variance was uneven, Welch's robust ANOVA was conducted, and Dunnett's T3 test was employed for multiple comparisons between groups. $P < 0.05$ was considered statistically significant.

3. Results

3.1. Features and Structural Characterization of CS/GO Hydrogel Scaffolds. The as-prepared CS/GO hydrogel scaffolds were dark blue, jelly-like, and elastic (as observed by the naked eye), and their internal structure was loose, which recovered after deformation under light pressure (Figures 1(a)–1(d)). After vacuum freeze-drying, their texture became hard and brittle, and the pure CS hydrogel scaffold was not suitable for clamping and had low mechanical strength (Figure 1(e)).

The structure of the pure CS hydrogel scaffold is disordered and irregularly curled. With an increase in the GO concentration, the internal shape of this scaffold slowly became uniform, and the irregular curling gradually improved (Figure 2(a)), indicating that the addition of GO improved the internal structure of the CS hydrogel scaffold. SEM images also show that all the hydrogel scaffolds are highly porous and interconnected, with pore size in the range of 100–150 µm (Figures 2(b) and 2(c)).

We used a series of experiments to further characterize the physical and chemical properties of the CS/GO hydrogel scaffolds. FTIR spectra of the CS hydrogel scaffold exhibited two characteristic absorption bands at 1636 and 1597 cm⁻¹,

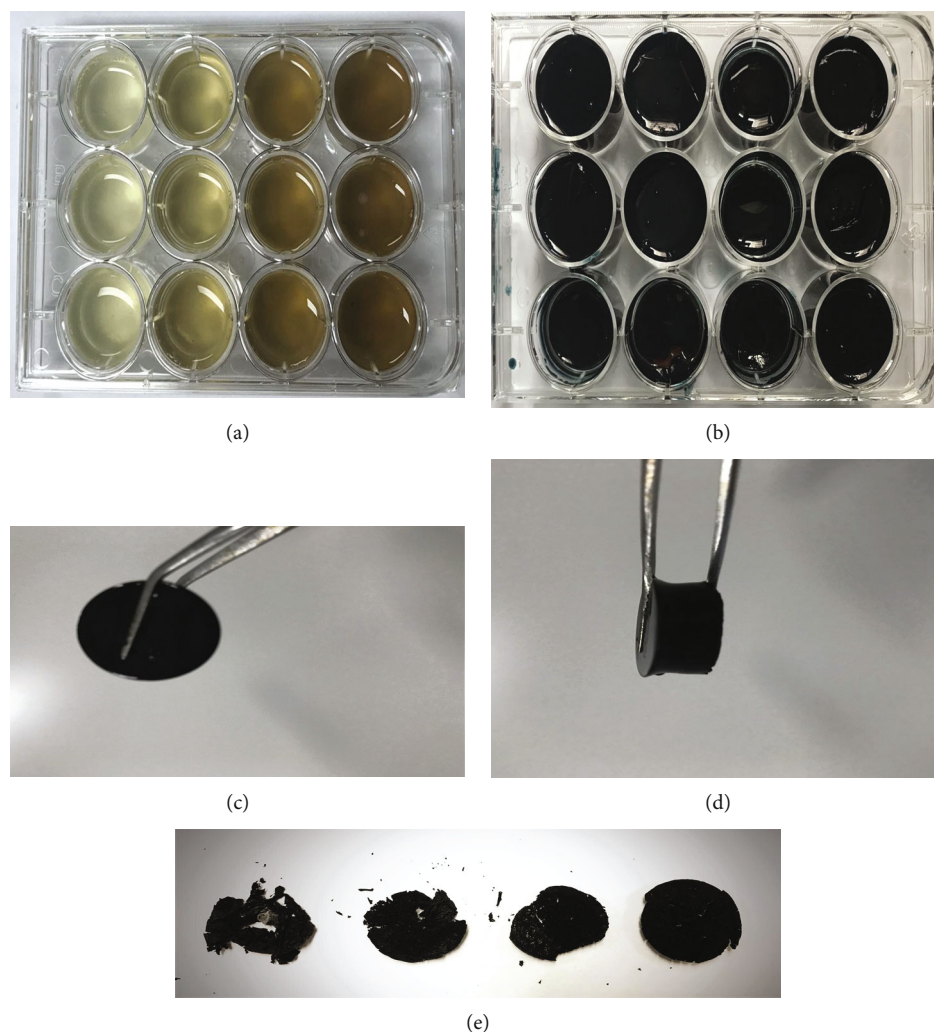


FIGURE 1: Features of CS/GO hydrogel scaffolds (from left to right: the hydrogel scaffolds with 0, 0.1, 0.5, and 1.0 wt.%GO): (a) CS/GO hydrogel scaffolds directly spread on a 12-well plate. (b) CS/GO hydrogel scaffolds crosslinked for 24 h. (c) Front view of the hydrogel scaffolds. (d) Side view of the hydrogel scaffolds. (e) CS/GO hydrogel scaffolds after vacuum freeze-drying.

corresponding to the C-O tensile vibration of the acetylated amino group (-NHCO-) and the N-H bending of -NH₂, respectively. In the case of the CS/GO hydrogel scaffolds, the -NH₂ absorption band shifted to a lower value, whereas the intensity of the -NHCO- band increased; this may be because the -NH₂ group of CS reacts with the -COOH group of GO, leading to the formation of an -NHCO- graft point (Figure 3(a)).

XRD patterns of each group of scaffolds showed the characteristic peak of CS at $2\theta = 20.1^\circ$, which indicated the crystallinity of CS (Figure 3(b)). With an increase in the GO concentration, the intensity of this peak gradually decreased, and a new sharp peak appeared near $2\theta = 11.0^\circ$, which became more evident with an increase in the GO concentration. All these results suggest that the introduction of GO indeed changes the crystal structure of CS and is consistent with the FTIR results.

3.2. Physical and Chemical Properties of the CS/GO Hydrogel Scaffolds. The porosity test indicated that the porosity of each group of scaffolds was ranged from 92% to 95%. However, it

slowly increased with an increase in the concentration of GO from 0.1 to 1.0 wt.% (Figure 3(c)). There are no differences in porosity among each group ($P = 0.095 > 0.05$).

As shown in Figure 3(c), the CS hydrogel scaffold has a higher SR than that of the CS/GO hydrogel scaffolds, and the SR of the CS/GO hydrogel scaffolds gradually decreased with an increase in the GO concentration from 0.1 to 1.0 wt.%.

To further explore the influence of GO on the properties of the CS hydrogel scaffold, the tensile properties of the CS/GO hydrogel scaffolds were investigated. The tensile stress-strain curves for each group of scaffolds are shown in Figure 3(e), and the mechanical properties are summarized in Table 2. Results suggest that when the GO concentration was increased from 0 to 1.0 wt.%, the elastic modulus, tensile strength, and elongation at break increased from 0.829 to 22.026 MPa, from 1.363 to 7.153 MPa, and from 61.3 to 161.5%, respectively.

3.3. Identification of EPCs. To verify the hypothesis that the CS/GO hydrogel scaffold can improve the angiogenesis of

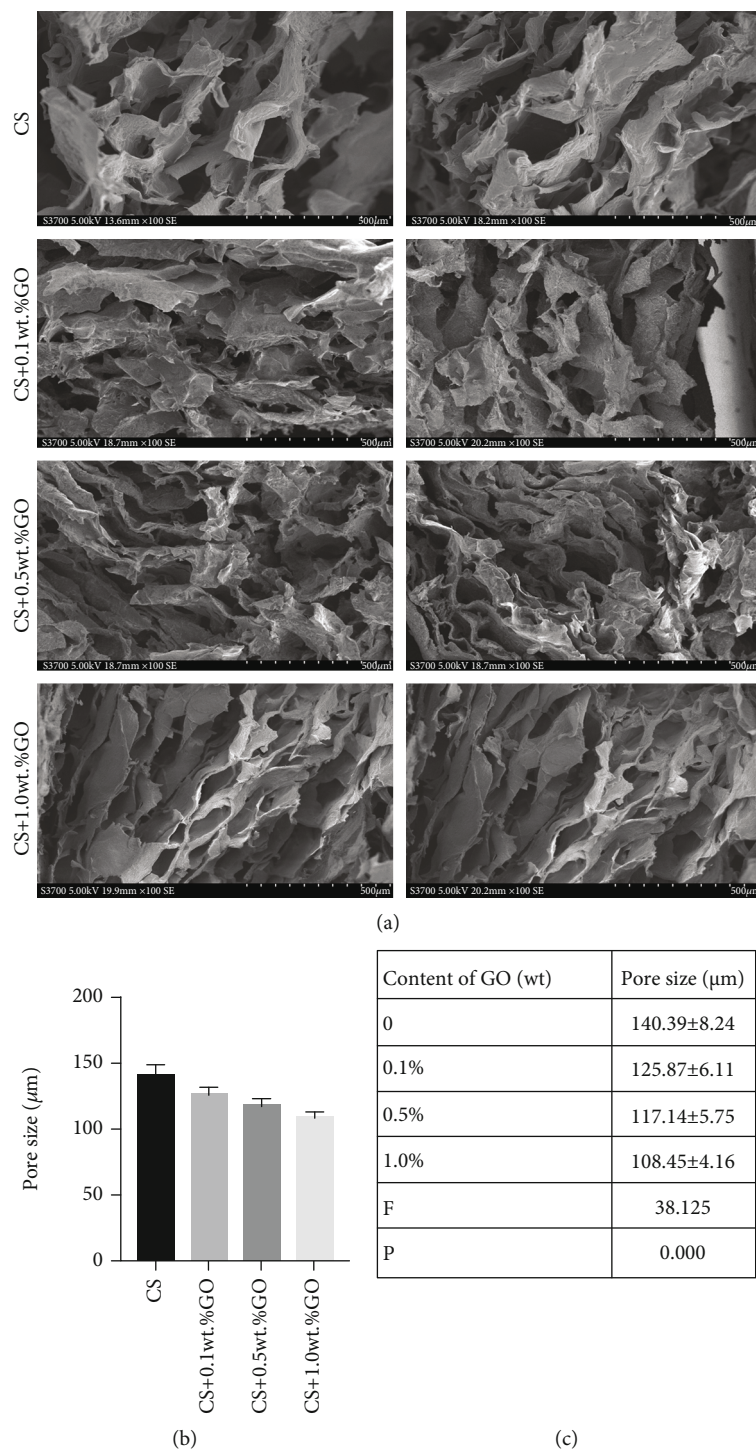


FIGURE 2: SEM images of the CS/GO hydrogel scaffolds. (a) SEM image of the cross-section of the scaffolds of each group (bar = 500 μm). (b, c) Aperture size of each group randomly measured by ImageJ. * $P < 0.05$ compared with the cases of other groups.

cells, we used EPCs from human umbilical cord blood as seed cells for investigation. The freshly isolated primary cells were round (Figure 4(a)). After being cultured for 3–5 days, the cells proliferated, grew into nearly spindle-shaped cells, and demonstrated “colony-like growth” (Figure 4(b)). After 7 days, the cells rapidly proliferated and were connected to each other in a typical “paving stone” pattern (Figure 4(c)). Flow cytometry results showed that the third-generation

EPCs had low expressions of CD45 (0.11%), CD14 (0.21%), CD34 (4.21%), and CD133 (1.16%) and high expressions of the endothelial cell markers CD31 (99.76%), CD105 (98.45%), and KDR (92.55%) (Figure 4(d)). The results of the tubule formation experiments suggested that the cells connected end-to-end during incubation with Matrigel to form a tubule-like structure, and each tubule was connected to form a tube-like structure similar to that of the vascular

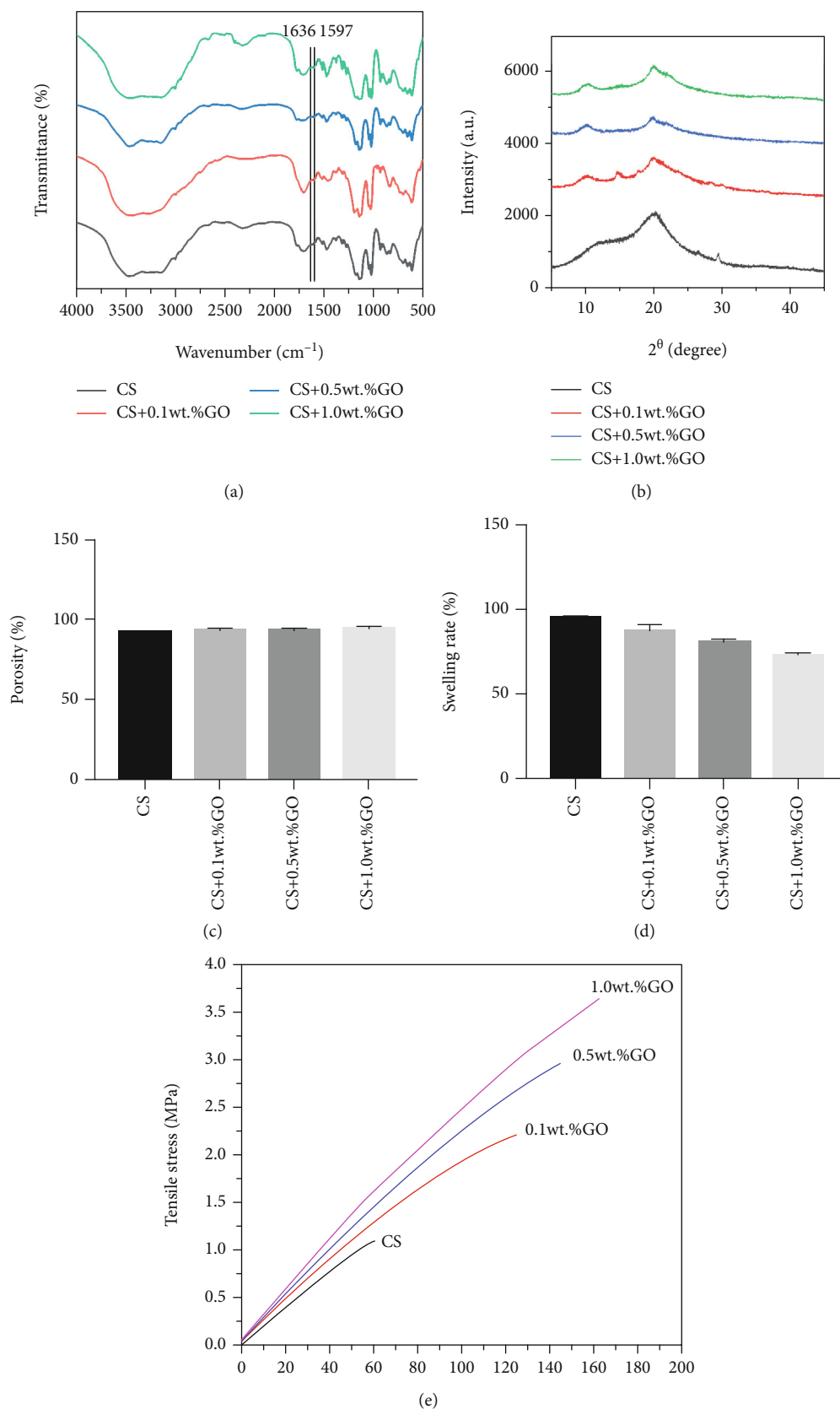


FIGURE 3: Physical and chemical properties of CS/GO hydrogel scaffolds. (a) FTIR spectra, (b) XRD patterns, and (c) porosity of the hydrogel scaffolds of each group (**P* > 0.05). (d) Swelling rate of the hydrogel scaffolds of each group (**P* < 0.05). (e) Tensile properties of the hydrogel scaffolds of each group.

TABLE 2: Physical properties of the CS/GO hydrogel scaffolds with different contents of GO.

Group	Tensile strength (MPa)	Modulus of elasticity (MPa)	Elongation at break (%)
CS	1.363 ± 0.367	0.829 ± 0.590	61.3
CS+0.1 wt.%GO	4.053 ± 0.526	6.863 ± 0.940	122.3
CS+0.5 wt.%GO	5.627 ± 0.343	12.460 ± 2.120	140.6
CS+1.0 wt.%GO	7.153 ± 0.383	22.026 ± 2.752	161.5

lumen (Figure 4(e)). These results confirm that the EPCs extracted in this experiment are a class of progenitor cells that can differentiate into endothelial cells and have the ability to form tubules.

3.4. Evaluation of the Effect of CS/GO Hydrogel Scaffolds on the Proliferation of EPCs and Cytotoxicity of These Scaffolds.

During the coculture of the hydrogel scaffolds with EPCs, we explored the effect of the CS/GO hydrogel scaffolds on the proliferation of EPCs and the cytotoxicity of these scaffolds (Figures 5(a) and 5(b)). First, the proliferation of the EPCs in the five culture groups was analyzed by the CCK-8 assay on 1, 3, and 5 days after culture. Cell proliferation was considerably inhibited when the concentration of GO was increased to 1.0 wt.%, whereas it was promoted when the concentration of GO was increased from 0 to 0.5 wt.%. The LDH toxicity assay again confirmed that the group containing 1.0 wt.%GO indeed had clear cytotoxicity, which indicated that GO over a certain concentration caused cytotoxicity.

To further confirm the cytotoxicity of the hydrogel scaffold with 1.0 wt.%GO, a live/dead staining was performed, and images were obtained using the fluorescence microscope, and the numbers of dead and live cells were recorded by flow cytometry (Figure 6). The proportion of dead cells in the EPCs, CS; EPCs, CS/0.1 wt.%GO; EPCs, CS/0.5 wt.%GO; EPCs, CS/1.0 wt.%GO; and EPC groups was less than 10% ($P < 0.05$, compared with the case of the EPCs, CS/1.0 wt.%GO group), and there was no statistical difference in the proportion of dead cells between the EPCs; EPCs, CS; EPCs, CS/0.1 wt.%GO; and EPCs, CS/0.5 wt.%GO groups ($P > 0.05$). In the EPCs, CS/1.0 wt.%GO group, the proportion of dead cells was up to 16.5% ($P < 0.05$, compared with the cases of other groups). All these results clearly confirm that the hydrogel scaffold with 1.0 wt.%GO has substantial cytotoxicity.

3.5. Effect of the CS/GO Hydrogel Scaffold on the Angiogenesis of EPCs.

Results of the tube formation analysis (Figures 5(c)–5(f)) demonstrated that on the seventh day of coculture, the EPCs in the EPCs, CS/0.5 wt.%GO group had most significant tube formation ability, whereas those in the EPCs, CS/1.0 wt.%GO group had the lowest tube formation ability ($P < 0.05$). Moreover, the tube formation abilities of EPCs in the EPCs and EPCs, CS groups were not significant ($P > 0.05$).

To further study the role of CS/GO hydrogel scaffolds in promoting angiogenesis, qRT-PCR and Western blot analysis were conducted, and the results showed that on the seventh day of coculture, the expressions of CD34, VEGF,

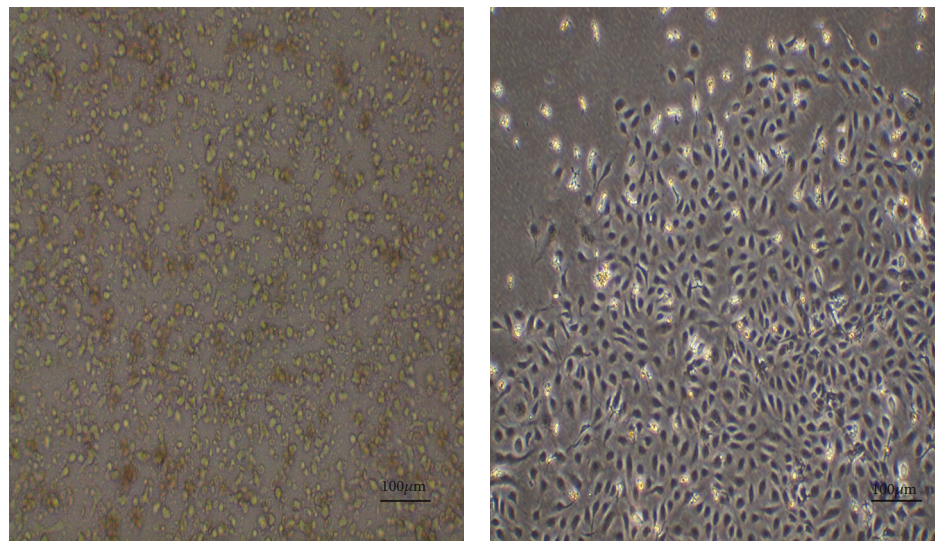
MMP9, and SDF-1 in EPCs were considerably upregulated with an increase in the GO concentration when compared with the case of the EPC group. However, the expressions of CD34, VEGF, MMP9, and SDF-1 were inhibited in the EPCs, CS/1.0 wt.%GO group (Figure 7). As shown in Figure 7(a), the relative mRNA expressions of the EPCs, CS and EPC groups were not significant ($P > 0.05$), whereas those of the other groups had statistical significance in multiple comparisons ($*P < 0.05$, compared with that of the EPC group). The results of Western blot analysis are similar to those of the qRT-PCR (Figures 7(b) and 7(c)). All these results indicate that in an appropriate concentration range, GO can promote the proliferation and angiogenic ability of EPCs, which will contribute to improving angiogenesis in tissue engineering.

4. Discussion

In 1993, tissue engineering was proposed by American scholars and subsequently brought a new dawn to the reconstruction and repair of tissue defects [39]. Tissue engineering is a discipline that covers multidisciplinary fields such as biology, medicine, and engineering. It develops new biological materials to develop biological substitutes that can repair or improve defective tissues, organs, or parts of the human body [40, 41]. Although the existing biomaterials have made some progress in the repair of tissue defects, the angiogenesis of regenerated tissue is still a research problem. Although currently different studies promote tissue regeneration through angiogenesis, none of the methods have been successfully applied clinically [5, 8, 42]. Therefore, continuous exploration and development of scaffold materials that promote tissue angiogenesis and the success rate of tissue defect repair have important medical value.

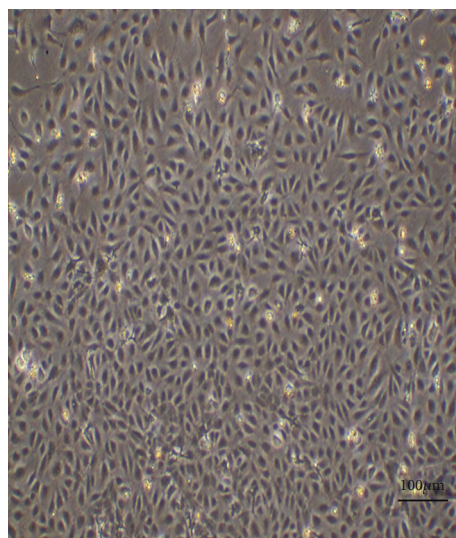
GO was brought into tissue engineering for its good mechanical properties and angiogenesis properties [43, 44]. So, we added GO into chitosan hydrogel in order to make an ideal hydrogel scaffold material. A single biomaterial has limitations due to its own performance. Therefore, the composite materials have their superior performance due to multiple materials being mutually reconstructed and will play a vital role in tissue engineering scaffolds to repair tissue defects. The application of crosslinking and covalent bonding significantly improves the stability of the hydrogel [45, 46]. So, genipin was used as the crosslinking agent in this study. Accordingly, a series of CS/GO hydrogel scaffolds were fabricated by crosslinking CS and GO at different concentrations using GNP in our research.

Analyzing the features and structural characterization of CS/GO hydrogel scaffolds, we attained the conclusions as



(a)

(b)



(c)

FIGURE 4: Continued.

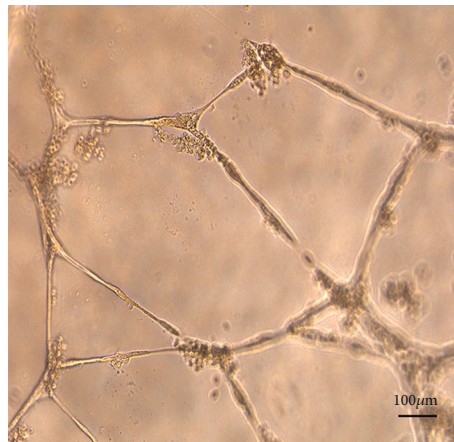
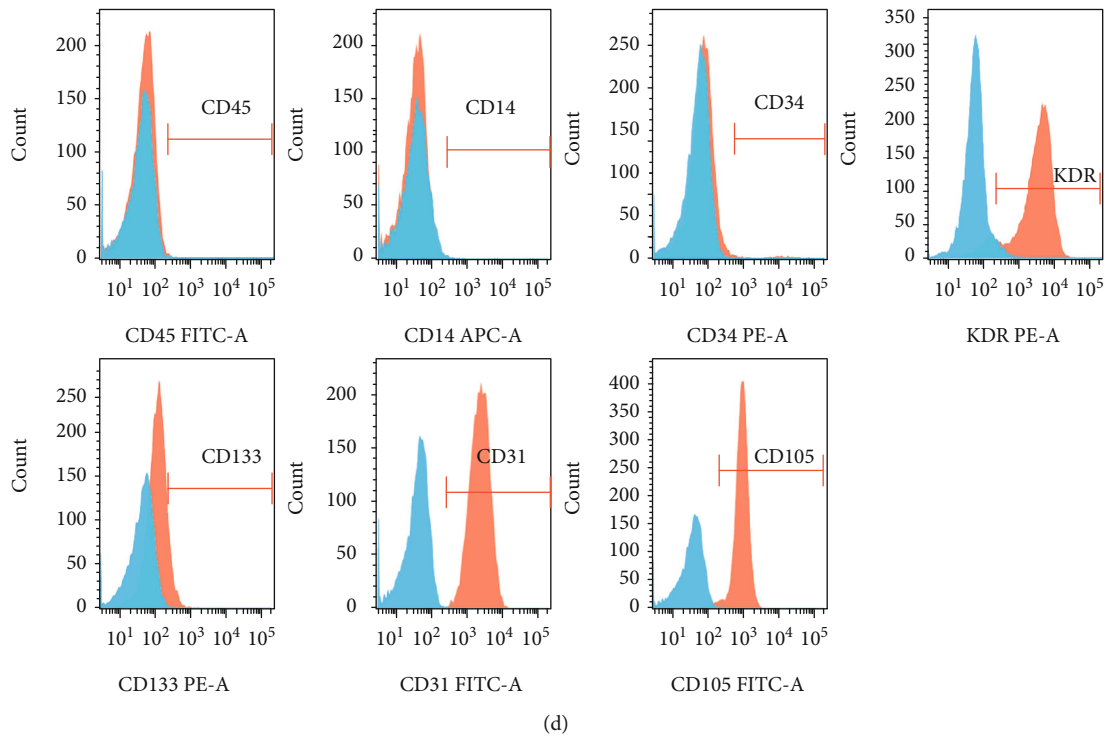


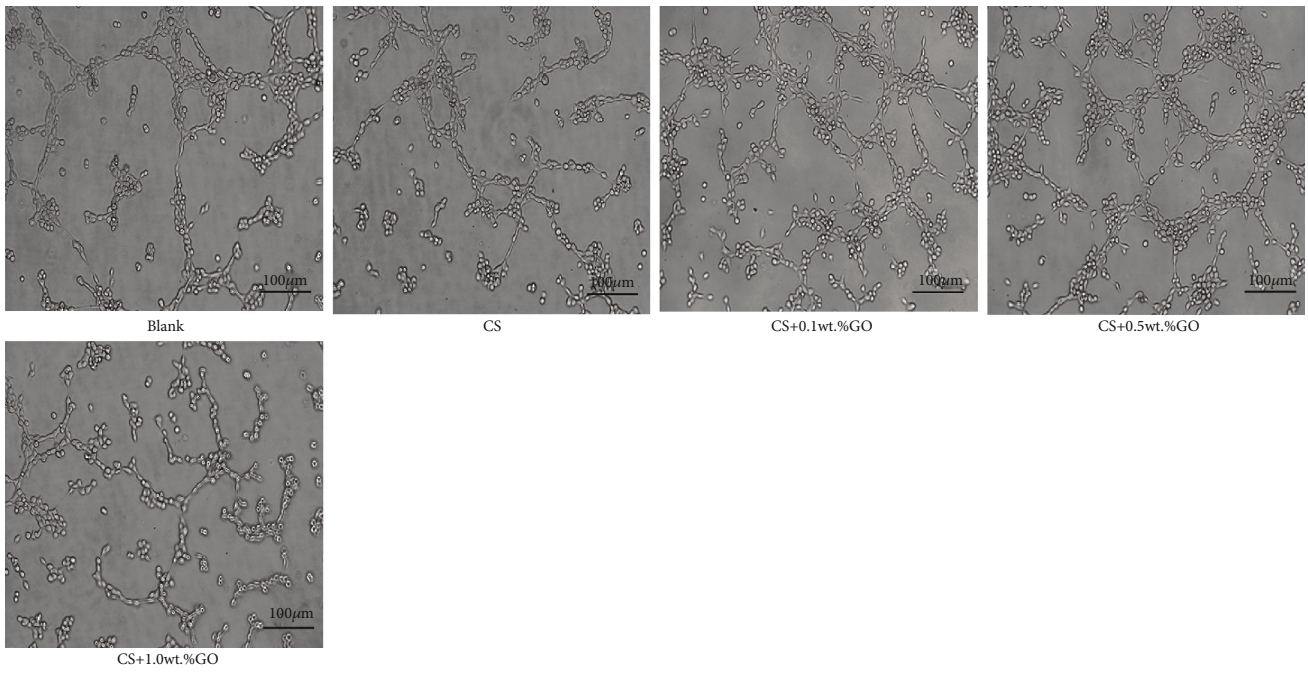
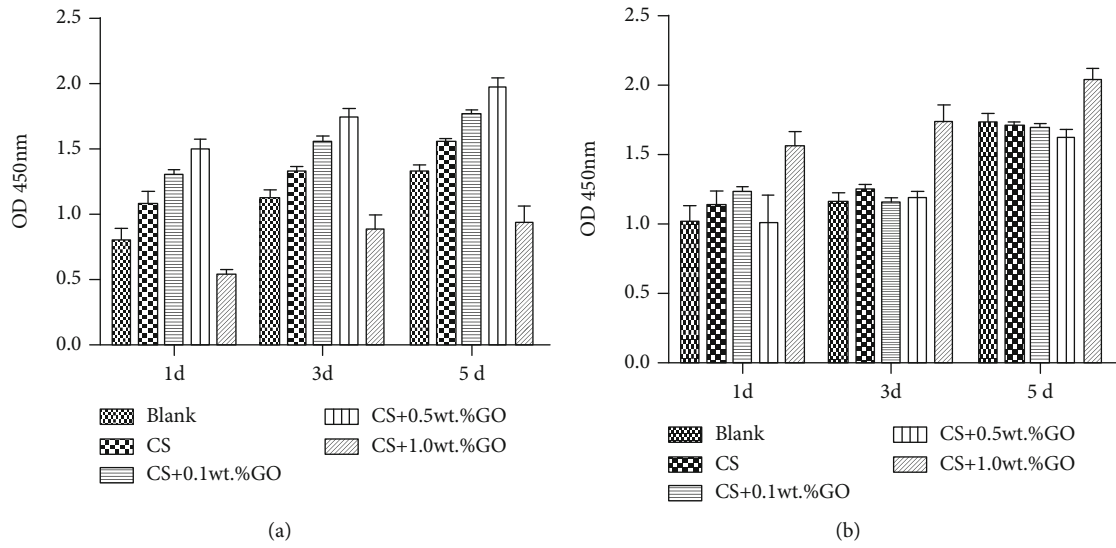
FIGURE 4: Isolation, culture, and identification of EPCs (provided by Guangdong Cord Blood Bank). Newly isolated primary cells (a) and cells cultured for 3–5 (b) and 7 (c) days. (d) Flow cytometry identification results of primary cells. (e) Matrigel tubule formation experiment of primary cells.

follows. With an increase in the GO concentration, the strength of the scaffold gradually increased. Therefore, the addition of GO to the CS hydrogel scaffold is effective in increasing the hardness of this scaffold. Furthermore, the pore size of the scaffold slowly decreased with an increase in the concentration of GO. This further showed that the addition of GO improved the structure of the CS hydrogel scaffold, making the spatial network structure inside the scaffold more uniform and porous.

We used a series of experiments to further characterize the physical and chemical properties of the CS/GO hydrogel scaffolds. From the FTIR and XRD, the introduction of GO indeed changed the crystal structure of CS. We predicted a

possible schematic diagram of the material structure in the Figure 8.

The porosity test simply confirms that the introduction of GO increases the porosity of the CS hydrogel scaffold. Furthermore, a better porosity can promote cell spreading and facilitate cell proliferation [47, 48]. In addition, SEM images show that the introduction of GO makes the structure of the CS hydrogel scaffold more uniform, reduces the pore size, and increases the porosity. Considering that the porosity increased and the structure of the hydrogel became more uniform by adding GO, it is attributed to physical crosslinking between $-\text{COOH}$ and $-\text{OH}$ of GO and $-\text{NH}_2$ of CS, which may even chemically crosslink upon the addition of GNP.



(c)

FIGURE 5: Continued.

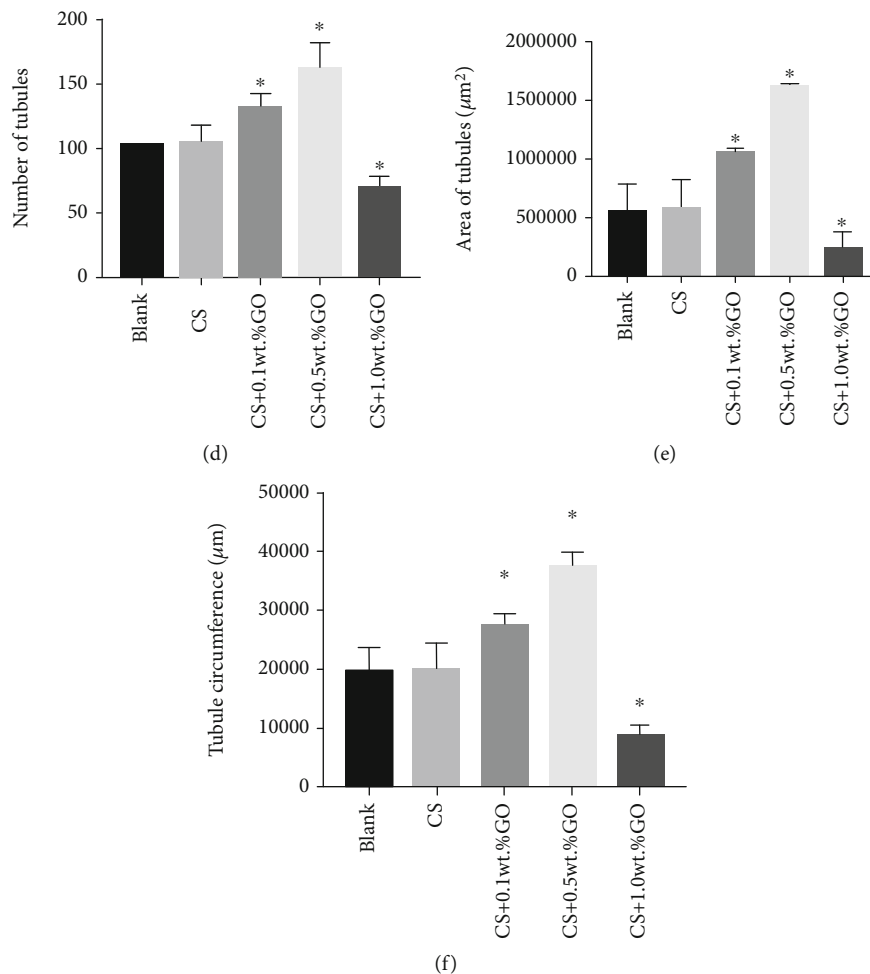


FIGURE 5: Effect of CS/GO hydrogel scaffolds on the proliferation and angiogenesis of EPCs. (a) Proliferation level of cells in each group determined by the CCK-8 assay. (b) Cytotoxicity of hydrogel scaffolds in each group evaluated by the LDH assay. (c-f) Angiogenesis ability of cells in each group determined using tube formation. * $P < 0.05$.

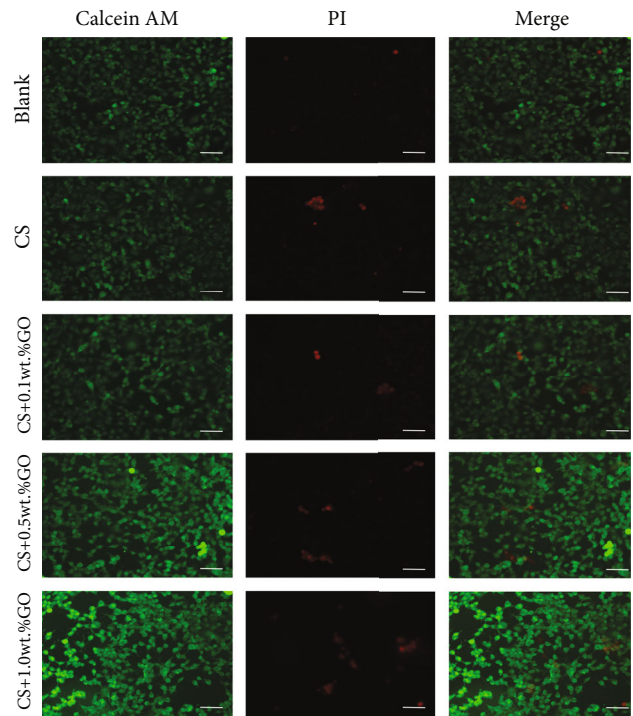
Hence, we predict that the cells can expand and grow better in hydrogel scaffold materials, which would facilitate the exchange of substances between the implanted body and the outside environment for providing more energy to promote the formation of blood vessels and tissues. All these results suggest that the CS/GO hydrogel scaffold may become a potential scaffold for tissue engineering.

This implied that the presence of GO enhanced the swelling rate of the CS hydrogel scaffold possibly owing to physical crosslinking between $-\text{COOH}$ and $-\text{OH}$ of GO and $-\text{NH}_2$ of CS, which may even chemically crosslink upon the addition of GNP; however, this requires further confirmation. Thus, it can be speculated that crosslinking inhibits the swelling of the CS hydrogel scaffold and thereby reduces the SR.

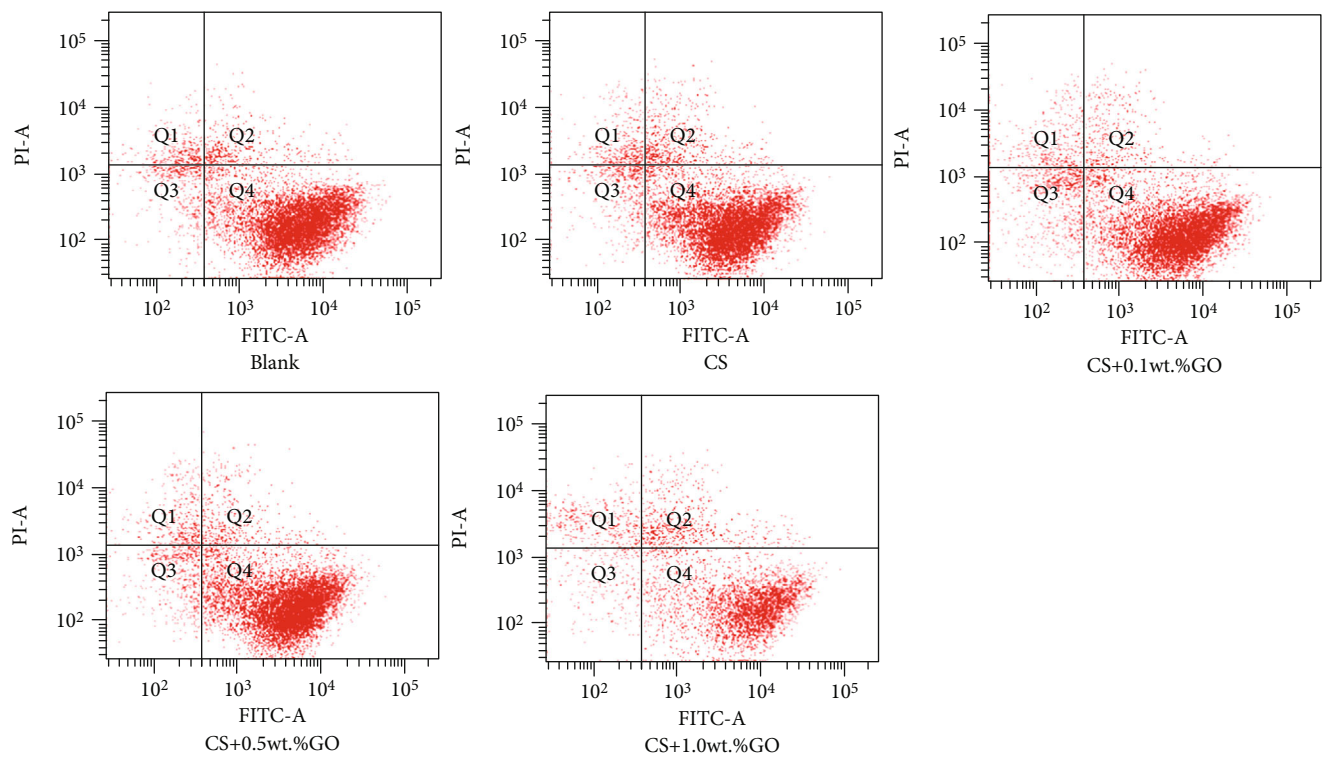
Therefore, the addition of GO significantly improved the tensile properties of the CS hydrogel scaffold. This is consistent with the previously reported results of CS/GO hydrogel films with different GO concentrations [49, 50]. In summary, we found that the addition of GO changed the structure of the chitosan hydrogel, which affected the physical and chemical properties of the material.

To further explore the biocompatibility and angiogenic effect of chitosan/graphene oxide hydrogel scaffolds, the EPCs were chosen. ECs (endothelial cells) cannot be widely used for the vascularization of bone tissue because of their low proliferation and low utilization [51]. Therefore, we used EPCs as the seed cells. The CCK-8 and cytotoxicity assay results showed that when the concentration of GO was higher than 0.5 wt.%, it inhibited the proliferation of EPCs and caused significant cytotoxicity to the cells. This is consistent with the results reported by Wang et al.; that is, GO has no considerable cytotoxicity at a suitable concentration, whereas it exhibits substantial cytotoxicity at doses higher than $50 \mu\text{g}/\text{mL}$ [52]. Therefore, as a new biomaterial, GO at an appropriate concentration can be used to prepare tissue engineering scaffold materials.

During the tube formation experiment, the CS hydrogel scaffold did not significantly promote angiogenesis, whereas after the addition of GO, it stimulated tube formation. However, when the concentration of GO was up to 1.0 wt.%, tube formation was inhibited. This proves that high concentrations of GO may inhibit angiogenesis of the EPCs. To further explore the molecular mechanism of blood vessel formation



(a)



(b)

FIGURE 6: Continued.

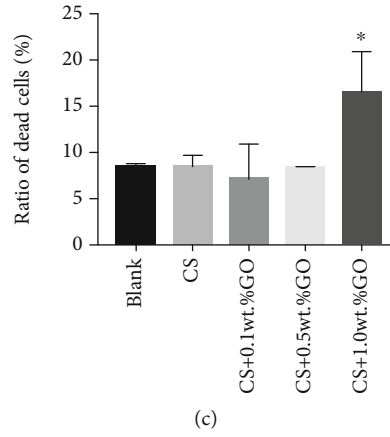


FIGURE 6: Dead and live cell staining of the EPCs in each coculture group: (a) staining images obtained using the fluorescence microscope; (b) dead and live cell staining results acquired by FCM; (c) ratio of dead cells in each group. * $P < 0.05$.

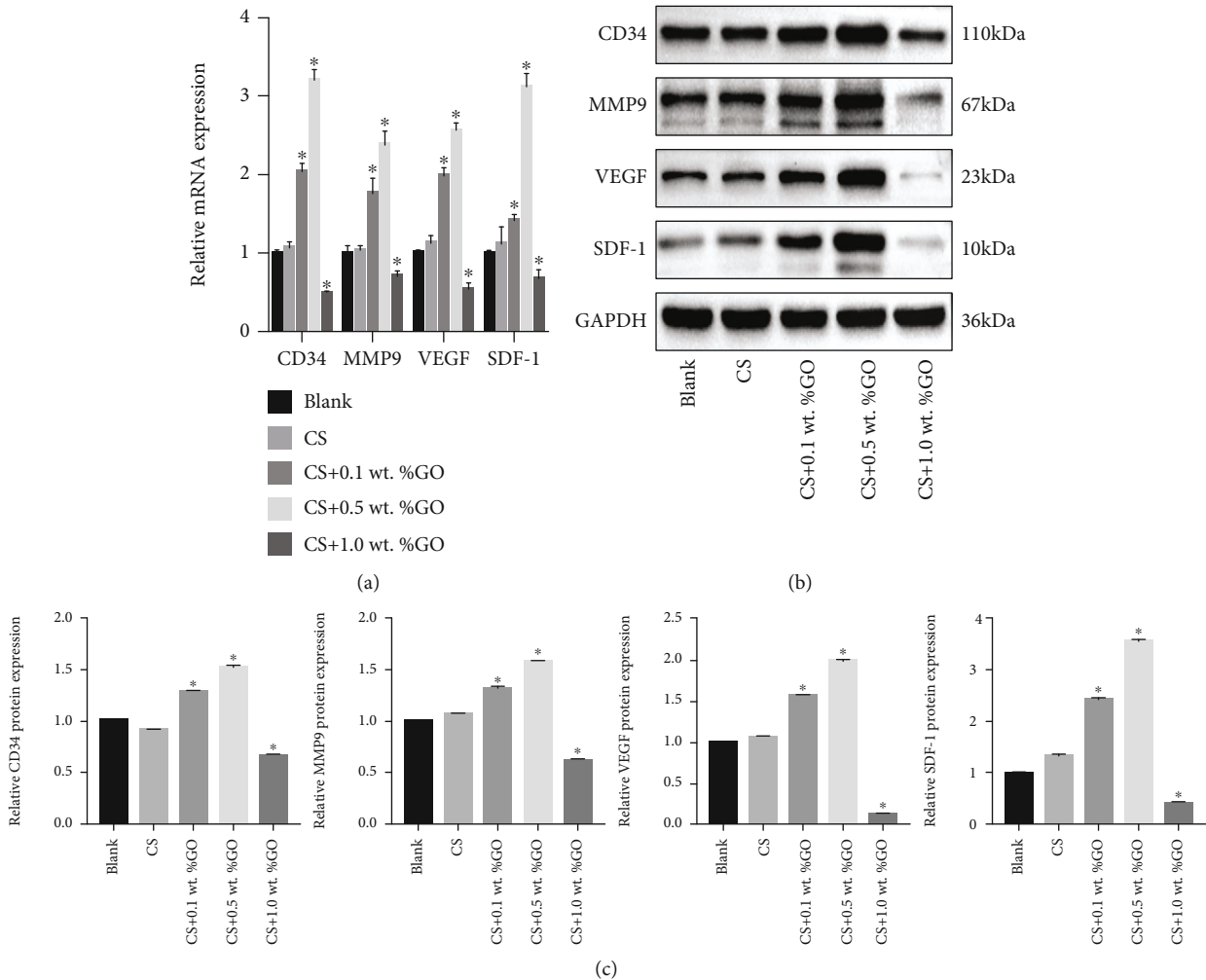


FIGURE 7: (a) qRT-PCR analysis of the CD34, VEGF, MMP9, and SDF-1 expressions in each group. (b) Western blot analysis results of CD34, VEGF, MMP9, and SDF-1 protein expressions in each group. * $P < 0.05$ compared with the blank group.

by the CS/GO hydrogel scaffolds, we conducted more experiments. CD34, VEGF, MMP9, and SDF-1 were chosen to explore the mechanism.

CD34 is a transmembrane glycoprotein that is selectively expressed on the surface of EPCs. SDF-1 and VEGF play a key role in EPC function. Studies have shown that SDF-1

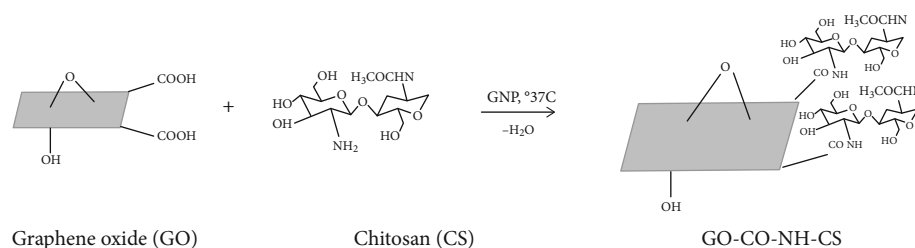


FIGURE 8

promotes the expression of VEGF in ECs and is an important cytokine to mobilize EPC [53]. Wang et al. confirmed that metallothionein (MT) promotes the angiogenesis of EPCs mediated by the HIF-1 α /SDF-1/VEGF pathway [54]. Several studies proved that the SDF-1/VEGF pathway is vital to the angiogenesis of EPCs [55, 56]. In our research, the expressions of the angiogenesis-related genes CD34, VEGF, MMP9, and SDF-1 were examined and found to be upregulated at an appropriate concentration of GO. Western blot analysis results also confirmed this phenomenon. Thus, we concluded that GO may regulate the angiogenic ability of EPC through the SDF-1/VEGF signaling pathway. We found few studies about the angiogenic mechanism of GO on EPCs, while different from ECs. Mukherjee et al. [26] found that the activation of phospho-eNOS and phospho-Akt might be the plausible mechanisms for GO- and rGO-induced angiogenesis of HUVECs. From the research, we concluded that the immune microenvironment induced by GO at an appropriate concentration promotes the angiogenesis of HUVEC through the VEGF pathway [57]. However, further investigation is required to understand the corresponding specific signaling molecular mechanism.

We predict that the suitable concentration of CS/GO hydrogel scaffolds can promote the proliferation and tube formation of EPCs and further stimulate the formation of blood vessels. The long-term prospect of this research is providing little evidence for the role of CS/GO hydrogel scaffolds combined with EPCs in promoting angiogenesis and the repair of tissue defects. We hope that these findings can provide a new theoretical basis for the application of the combination of CS/GO hydrogel scaffolds and EPCs in promoting tissue engineering repair and in tissue regenerative medicine. However, our research has several limitations. First, we did not comprehensively study the specific mechanism of CS and GO crosslinking by GNP. Second, only a few detailed studies were conducted on the molecular mechanism of EPC regulation by the CS/GO hydrogel scaffold. Third, as in vivo experiments were not performed, we cannot verify the role of this scaffold material in repairing bone defects in vivo.

5. Conclusion

In this study, we successfully prepared a series of CS/GO hydrogel scaffolds with different concentrations of GO. The addition of GO improved the structure of the CS hydrogel scaffold, facilitated the formation of the spatial network structure, and improved the physical, chemical, and mechan-

ical properties of the scaffold. At an appropriate concentration, GO had no significant cytotoxicity and promoted the extension and proliferation of EPCs, thereby stimulating the formation of blood vessels. However, research on the role of GO in basic and clinical medical fields is still in its infancy, and the molecular mechanism involved in angiogenesis needs further investigation. In conclusion, our study not only opens a new path for the future research of CS/GO hydrogel scaffolds but also provides new ideas for the application of these scaffolds in promoting the formation of new blood vessels.

Data Availability

Dr. Zhang, e-mail: summere0615@163.com, will provide the research data.

Conflicts of Interest

The authors declare that they have no conflicts of interest with the contents of this article.

Authors' Contributions

L.F.Z. contributed to the conception of the study, generated the data, and wrote the manuscript. X.P.L., G.Y.R., and Y.T.P. contributed significantly to the analysis and manuscript preparation. C.Y.S. provided the EPCs for this study. Y.H. provided comments and suggestions for submission. S.G.Z. revised it critically for important intellectual content and approved the final version. Lifang Zhang and Xiping Li are co-first authors of this work.

Acknowledgments

The authors acknowledge support from the Guangzhou Municipal Science and Technology Project (Grant No. 201707010193) and the Intra-hospital Fund of Southern Medical University of Stomatological Hospital (PY2020022).

References

- [1] B. Bakhshandeh, P. Zarrintaj, M. O. Oftadeh et al., "Tissue engineering: strategies, tissues, and biomaterials," *Biotechnology & Genetic Engineering Reviews*, vol. 33, no. 2, pp. 144–172, 2017.
- [2] M. Lovett, K. Lee, A. Edwards, and D. L. Kaplan, "Vascularization strategies for tissue engineering," *Tissue Engineering. Part B, Reviews*, vol. 15, no. 3, pp. 353–370, 2009.

- [3] E. B. Peters, "Endothelial progenitor cells for the vascularization of engineered tissues," *Tissue Engineering. Part B, Reviews*, vol. 24, no. 1, pp. 1–24, 2018.
- [4] K. E. Johnson and T. A. Wilgus, "Vascular endothelial growth factor and angiogenesis in the regulation of cutaneous wound repair," *Advances in Wound Care*, vol. 3, no. 10, pp. 647–661, 2014.
- [5] S. N. Sethu, S. Namashivayam, S. Devendran et al., "Nanoceramics on osteoblast proliferation and differentiation in bone tissue engineering," *International Journal of Biological Macromolecules*, vol. 98, pp. 67–74, 2017.
- [6] H. D. Kim, S. Amirthalingam, S. L. Kim, S. S. Lee, J. Rangasamy, and N. S. Hwang, "Biomimetic materials and fabrication approaches for bone tissue engineering," *Advanced healthcare materials*, vol. 6, no. 23, 2017.
- [7] S. Yin, W. Zhang, Z. Zhang, and X. Jiang, "Recent advances in scaffold design and material for vascularized tissue-engineered bone regeneration," *Advanced healthcare materials*, vol. 8, no. 10, article e1801433, 2019.
- [8] L. Reddy, D. Murugan, M. Mullick, E. T. Begum Moghal, and D. Sen, "Recent approaches for angiogenesis in search of successful tissue engineering and regeneration," *Current Stem Cell Research & Therapy*, vol. 15, no. 2, pp. 111–134, 2020.
- [9] Y. C. Chiu, M. H. Cheng, H. Engel et al., "The role of pore size on vascularization and tissue remodeling in PEG hydrogels," *Biomaterials*, vol. 32, no. 26, pp. 6045–6051, 2011.
- [10] M. Schleicher, H. P. Wendel, O. Fritze, and U. A. Stock, "In vivo tissue engineering of heart valves: evolution of a novel concept," *Regenerative Medicine*, vol. 4, no. 4, pp. 613–619, 2009.
- [11] Y. Wu, L. Wang, B. Guo, and P. X. Ma, "Injectable biodegradable hydrogels and microgels based on methacrylated poly(ethylene glycol)-co-poly(glycerol sebacate) multi-block copolymers: synthesis, characterization, and cell encapsulation," *Journal of materials chemistry. B*, vol. 2, no. 23, pp. 3674–3685, 2014.
- [12] M. Liu, X. Zeng, C. Ma et al., "Injectable hydrogels for cartilage and bone tissue engineering," *Bone research*, vol. 5, no. 1, p. 17014, 2017.
- [13] J. Ng, K. Spiller, J. Bernhard, and G. Vunjak-Novakovic, "Biomimetic approaches for bone tissue engineering," *Tissue Engineering. Part B, Reviews*, vol. 23, no. 5, pp. 480–493, 2017.
- [14] Z. Shariatnia and A. M. Jalali, "Chitosan-based hydrogels: preparation, properties and applications," *International Journal of Biological Macromolecules*, vol. 115, pp. 194–220, 2018.
- [15] L. J. Del Valle, A. Díaz, and J. Puiggalí, "Hydrogels for biomedical applications: cellulose, chitosan, and protein/peptide derivatives," *Gels*, vol. 3, no. 3, 2017.
- [16] S. Deepthi, J. Venkatesan, S. K. Kim, J. D. Bumgardner, and R. Jayakumar, "An overview of chitin or chitosan/nano ceramic composite scaffolds for bone tissue engineering," *International journal of biological macromolecules*, vol. 93, no. -Part B, pp. 1338–1353, 2016.
- [17] J. Venkatesan and S. K. Kim, "Chitosan composites for bone tissue engineering—an overview," *Marine Drugs*, vol. 8, no. 8, pp. 2252–2266, 2010.
- [18] M. L. Zhang, J. Cheng, Y. C. Xiao, R. F. Yin, and X. Feng, "Raloxifene microsphere-embedded collagen/chitosan/ β -tricalcium phosphate scaffold for effective bone tissue engineering," *International Journal of Pharmaceutics*, vol. 518, no. 1-2, pp. 80–85, 2017.
- [19] M. A. Nazeer, E. Yilgör, and I. Yilgör, "Intercalated chitosan/hydroxyapatite nanocomposites: promising materials for bone tissue engineering applications," *Carbohydrate Polymers*, vol. 175, pp. 38–46, 2017.
- [20] A. Topsakal, M. Uzun, G. Ugar et al., "Development of amoxicillin-loaded electrospun polyurethane/chitosan/ β -tricalcium phosphate scaffold for bone tissue regeneration," *IEEE Transactions on Nanobioscience*, vol. 17, no. 3, pp. 321–328, 2018.
- [21] G. R. Owen, M. Dard, and H. Larjava, "Hydroxyapatite/ β -tricalcium phosphate biphasic ceramics as regenerative material for the repair of complex bone defects," *Journal of Biomedical Materials Research. Part B, Applied Biomaterials*, vol. 106, no. 6, pp. 2493–2512, 2018.
- [22] S. F. Kiew, L. V. Kiew, H. B. Lee, T. Imae, and L. Y. Chung, "Assessing biocompatibility of graphene oxide-based nanocarriers: a review," *Journal of controlled release: official journal of the Controlled Release Society*, vol. 226, pp. 217–228, 2016.
- [23] M. Thangamuthu, K. Y. Hsieh, P. V. Kumar, and G. Y. Chen, "Graphene- and graphene oxide-based nanocomposite platforms for electrochemical biosensing applications," *International journal of molecular sciences*, vol. 20, no. 12, p. 2975, 2019.
- [24] J. Lee, J. Kim, S. Kim, and D. H. Min, "Biosensors based on graphene oxide and its biomedical application," *Advanced drug delivery reviews*, vol. 105, no. Part B, pp. 275–287, 2016.
- [25] L. Zhang, J. Xia, Q. Zhao, L. Liu, and Z. Zhang, "Functional graphene oxide as a nanocarrier for controlled loading and targeted delivery of mixed anticancer drugs," *Small*, vol. 6, no. 4, pp. 537–544, 2010.
- [26] S. Mukherjee, P. Sriram, A. K. Barui et al., "Graphene oxides show angiogenic properties," *Advanced Healthcare Materials*, vol. 4, no. 11, pp. 1722–1732, 2015.
- [27] Y. Chen, Z. Zheng, R. Zhou et al., "Developing a strontium-releasing graphene oxide-/collagen-based organic-inorganic nanobiocomposite for large bone defect regeneration via MAPK signaling pathway," *ACS Applied Materials & Interfaces*, vol. 11, no. 17, pp. 15986–15997, 2019.
- [28] S. Chakraborty, T. Ponrasu, S. Chandel, M. Dixit, and V. Muthuvijayan, "Reduced graphene oxide-loaded nanocomposite scaffolds for enhancing angiogenesis in tissue engineering applications," *Royal Society open science*, vol. 5, no. 5, article 172017, 2018.
- [29] E. López-Dolado, A. González-Mayorga, M. C. Gutiérrez, and M. C. Serrano, "Immunomodulatory and angiogenic responses induced by graphene oxide scaffolds in chronic spinal hemisectioned rats," *Biomaterials*, vol. 99, pp. 72–81, 2016.
- [30] T. Asahara, T. Murohara, A. Sullivan et al., "Isolation of putative progenitor endothelial cells for angiogenesis," *Science*, vol. 275, no. 5302, pp. 964–966, 1997.
- [31] R. Samuel, L. Daheron, S. Liao et al., "Generation of functionally competent and durable engineered blood vessels from human induced pluripotent stem cells," *Proceedings of the National Academy of Sciences of the United States of America*, vol. 110, no. 31, pp. 12774–12779, 2013.
- [32] R. A. Muzzarelli, M. El Mehtedi, C. Bottegoni, A. Aquili, and A. Gigante, "Genipin-crosslinked chitosan gels and scaffolds for tissue engineering and regeneration of cartilage and bone," *Marine Drugs*, vol. 13, no. 12, pp. 7314–7338, 2015.
- [33] F. L. Mi, "Synthesis and characterization of a novel chitosan-gelatin bioconjugate with fluorescence emission," *Biomacromolecules*, vol. 6, no. 2, pp. 975–987, 2005.

- [34] Y. H. Lin, K. Y. Lu, C. L. Tseng, J. Y. Wu, C. H. Chen, and F. L. Mi, "Development of genipin-crosslinked fucoidan/chitosan-N-arginine nanogels for preventing *Helicobacter* infection," *Nanomedicine*, vol. 12, no. 12, pp. 1491–1510, 2017.
- [35] M. E. Frohbergh, A. Katsman, G. P. Botta et al., "Electrospun hydroxyapatite-containing chitosan nanofibers crosslinked with genipin for bone tissue engineering," *Biomaterials*, vol. 33, no. 36, pp. 9167–9178, 2012.
- [36] K. Zafeiris, D. Brasinika, A. Karatza et al., "Additive manufacturing of hydroxyapatite-chitosan-genipin composite scaffolds for bone tissue engineering applications," *Materials science & engineering. C, Materials for biological applications*, vol. 119, article 111639, 2021.
- [37] A. Gilarska, J. Lewandowska-Lańcucka, K. Guzdek-Zajac et al., "Bioactive yet antimicrobial structurally stable collagen/chitosan/lysine functionalized hyaluronic acid - based injectable hydrogels for potential bone tissue engineering applications," *International Journal of Biological Macromolecules*, vol. 155, pp. 938–950, 2020.
- [38] S. Zeng, L. Liu, Y. Shi et al., "Characterization of silk fibroin/chitosan 3D porous scaffold and in vitro cytology," *PLoS one*, vol. 10, no. 6, article e0128658, 2015.
- [39] R. Langer and J. P. Vacanti, "Tissue engineering," *Science*, vol. 260, no. 5110, pp. 920–926, 1993.
- [40] P. Sharma, P. Kumar, R. Sharma, V. D. Bhatt, and P. S. Dhot, "Tissue engineering; current status & futuristic scope," *Journal of Medicine and Life*, vol. 12, no. 3, pp. 225–229, 2019.
- [41] L. Geris and I. Papantoniou, "The third era of tissue engineering: reversing the innovation drivers," *Tissue Engineering. Part A*, vol. 25, no. 11–12, pp. 821–826, 2019.
- [42] X. Wang, L. Gao, Y. Han et al., "Silicon-enhanced adipogenesis and angiogenesis for vascularized adipose tissue engineering," *Advanced science*, vol. 5, no. 11, article 1800776, 2018.
- [43] X. Jing, H. Y. Mi, M. R. Salick, T. M. Cordie, X. F. Peng, and L. S. Turng, "Electrospinning thermoplastic polyurethane/graphene oxide scaffolds for small diameter vascular graft applications," *Materials for biological applications*, vol. 49, pp. 40–50, 2015.
- [44] B. D. Holt, Z. M. Wright, A. M. Arnold, and S. A. Sydlik, "Graphene oxide as a scaffold for bone regeneration," *Wiley interdisciplinary reviews: Nanomedicine and nanobiotechnology*, vol. 9, no. 3, 2017.
- [45] H. Zhou, Z. Wang, H. Cao et al., "Genipin-crosslinked polyvinyl alcohol/silk fibroin/nano-hydroxyapatite hydrogel for fabrication of artificial cornea scaffolds—a novel approach to corneal tissue engineering," *Journal of Biomaterials Science. Polymer Edition*, vol. 30, no. 17, pp. 1604–1619, 2019.
- [46] F. Campos, A. B. Bonhome-Espinosa, G. Vizcaino et al., "Generation of genipin cross-linked fibrin-agarose hydrogel tissue-like models for tissue engineering applications," *Biomedical materials*, vol. 13, no. 2, article 025021, 2018.
- [47] Y. Gong, Y. Yu, H. Kang et al., "Synthesis and characterization of graphene oxide/chitosan composite aerogels with high mechanical performance," *Polymers*, vol. 11, no. 5, 2019.
- [48] S. Azizkhani, E. Mahmoudi, N. Abdullah, M. Ismail, A. W. Mohammad, and S. A. Hussain, "Synthesis and characterisation of graphene oxide-silica-chitosan for eliminating the Pb(II) from aqueous solution," *Polymers*, vol. 12, no. 9, p. 1922, 2020.
- [49] Y. Zhang, M. Zhang, H. Jiang et al., "Bio-inspired layered chitosan/graphene oxide nanocomposite hydrogels with high strength and pH-driven shape memory effect," *Carbohydrate Polymers*, vol. 177, pp. 116–125, 2017.
- [50] T. Agarwal, R. Narayan, S. Maji et al., "Gelatin/carboxymethyl chitosan based scaffolds for dermal tissue engineering applications," *International journal of biological macromolecules*, vol. 93, no. Part B, pp. 1499–1506, 2016.
- [51] Z. Gong and L. E. Niklason, "Blood vessels engineered from human cells," *Trends in Cardiovascular Medicine*, vol. 16, no. 5, pp. 153–156, 2006.
- [52] E. Paz, Y. Ballesteros, J. Abenojar, J. C. Del Real, and N. J. Dunne, "Graphene oxide and graphene reinforced PMMA bone cements: evaluation of thermal properties and biocompatibility," *Materials*, vol. 12, no. 19n, 2019.
- [53] M. Masyuk, A. Abduelmula, G. Morosan-Puopolo et al., "Retrograde migration of pectoral girdle muscle precursors depends on CXCR4/SDF-1 signaling," *Histochemistry and Cell Biology*, vol. 142, no. 5, pp. 473–488, 2014.
- [54] K. Wang, X. Dai, J. He et al., "Endothelial overexpression of metallothionein prevents diabetes-induced impairment in ischemia angiogenesis through preservation of HIF-1 α /SDF-1/VEGF signaling in endothelial progenitor cells," *Diabetes*, vol. 69, no. 8, pp. 1779–1792, 2020.
- [55] G. Yu, P. Liu, Y. Shi, S. Li, Y. Liu, and W. Zhu, "Sitagliptin stimulates endothelial progenitor cells to induce endothelialization in aneurysm necks through the SDF-1/CXCR4/NRF2 signaling pathway," *Frontiers in Endocrinology*, vol. 10, p. 823, 2019.
- [56] G. Odent Grigorescu, A. M. Rosca, M. B. Preda, R. Tutuianu, M. Simionescu, and A. Burlacu, "Synergic effects of VEGF-A and SDF-1 on the angiogenic properties of endothelial progenitor cells," *Journal of Tissue Engineering and Regenerative Medicine*, vol. 11, no. 11, pp. 3241–3252, 2017.
- [57] D. Xue, E. Chen, H. Zhong et al., "Immunomodulatory properties of graphene oxide for osteogenesis and angiogenesis," *International Journal of Nanomedicine*, vol. Volume 13, pp. 5799–5810, 2018.

Review Article

Mesenchymal Stem Cells: An Overview of Their Potential in Cell-Based Therapy for Diabetic Nephropathy

Yan Wu,¹ Chunlei Zhang,¹ Ran Guo,² Dan Wu,¹ Jiayi Shi,¹ Luxin Li,¹ Yanhui Chu,¹ Xiaohuan Yuan ¹ and Jie Gao ³

¹Heilongjiang Key Laboratory of Antifibrosis Biotherapy, Mudanjiang Medical University, Mudanjiang, China

²Department of Physiology, Mudanjiang Medical University, Mudanjiang, China

³Institute of Translational Medicine, Shanghai University, Shanghai, China

Correspondence should be addressed to Xiaohuan Yuan; yuanxiaohuan@mdjmu.edu.cn and Jie Gao; jmsx2021@shu.edu.cn

Received 20 November 2020; Revised 11 February 2021; Accepted 18 February 2021; Published 17 March 2021

Academic Editor: Adam Ye

Copyright © 2021 Yan Wu et al. This is an open access article distributed under the Creative Commons Attribution License, which permits unrestricted use, distribution, and reproduction in any medium, provided the original work is properly cited.

Diabetic nephropathy (DN) is a devastating complication associated with diabetes mellitus, and it is the leading cause of end-stage renal diseases (ESRD). Over the last few decades, numerous studies have reported the beneficial effects of stem cell administration, specifically mesenchymal stem or stromal cells (MSCs), on tissue repair and regeneration. MSC therapy has been considered a promising strategy for ameliorating the progression of DN largely based on results obtained from several preclinical studies and recent Phase I/II clinical trials. This paper will review the recent literature on MSC treatment in DN. In addition, the roles and potential mechanisms involved in MSC treatment of DN will be summarized, which may present much needed new drug targets for this disease. Moreover, the potential benefits and related risks associated with the therapeutic action of MSCs are elucidated and may help in achieving a better understanding of MSCs.

1. Introduction

Diabetes mellitus (DM) is a global epidemic disease affecting millions of people. According to the International Diabetes Federation (IDF), the morbidity rate of DM among adults aged between 20 and 79 years was estimated to be 9.3% in 2019, and the proportion is expected to rise to 10.9% by 2045. Moreover, the number of people with diabetes (20-79 years) will rise from 463 million in 2019 to 700 million by 2045 [1]. DM characterized with hyperglycemia may lead to the dysfunction of several major organs. Among them, diabetic nephropathy (DN) is one of the most significant microvascular complications for both type 1 and type 2 diabetic population. Previous studies have estimated that approximately 25% to 40% of those individuals living with both types of diabetes develop DN [2, 3], even when glucose control is nearly optimal, and it is the leading cause of end-stage renal disease (ESRD) [4]. In the absence of DN, the mortality rate among diabetic patients is roughly in line with that of the general population [5]. Currently, there are three

possibilities for the pharmacological prevention or alleviation of chronic kidney failure: control cardiovascular risk factors (often not optimal), avoid potential renal toxins (usually unfeasible), or use causal treatment for the disease whenever possible (with unstable curative effect and frequent complications). Therefore, DN still poses a significant clinical burden despite the tremendous advances made in its diagnosis and treatment [6]. Therefore, there is an urgent need to develop safe and effective therapeutic strategies against the disease. Fortunately, regenerative medicine provides a potential strategy against DN.

Several studies have reported the potent effects of mesenchymal stem or stromal cells (MSCs) for treating kidney diseases. This has led many scientists to pursue treatment of DN using MSCs. A study conducted in 2006 reported that human bone marrow MSCs could increase pancreatic islets and beta cells that produce insulin, and decrease mesangial thickening and macrophage infiltration in diabetic mice. The study was the first to provide evidence on the potential of using restorative therapy as a cure for DN [7]. Since then, a growing

number of research advances have made MSCs a viable option for DN. Specifically, research has shown that MSCs may be used to recapitulate several mechanisms that are sufficient for alleviating the progression of DN. This review will offer an overview of recent research into DN with an emphasis on the concrete mechanisms through which MSCs may enhance the functional regeneration of kidney tissues.

2. Diabetic Nephropathy

Diabetic complications involve the dysfunction of several organs including the heart, brain, kidney, blood vessels, peripheral nerves, eyes, and feet leading to serious health problems such as cardiomyopathy, nephropathy, peripheral neuropathy, retinopathy, and diabetic foot, respectively [8]. Such health problems are in turn associated with high morbidity rates and can result in a heavy social and financial burden. DN is a long-term major microvascular complication of type 1 diabetes and type 2 diabetes [9]. Microalbuminuria is the initial clinical hallmark of established DN followed by glomerular hypertrophy, moderate expansion of the mesangial matrix, and thickening of the glomerular capillary walls. Glomerulosclerosis is the primary structural characteristic of DN which is caused by progressive albuminuria, glomerular basement membrane (GBM) thickening, mesangial cell expansion, destabilization of podocyte foot processes, renal fibrosis, extracellular matrix accumulation, fluid retention, and blood pressure elevation [10, 11]. As the disease continues to advance, glomerulosclerosis eventually develops into irreversible end-stage renal disease over a period of years or even decades. However, the exact molecular mechanisms underlying DN progression have not yet been clearly elucidated. This has led to a lack of effective medications for DN treatment. Presently, the core of DN treatment depends on optimal control of the renin-angiotensin-aldosterone (RAAS) system using angiotensin-converting enzyme inhibitors (ACEI), angiotensin receptor blockers (ARB), or aldosterone blockers (spironolactone or finerenone) [12]. Combining ACE and ARB into a dual blockade approach decreases proteinuria, but the blockade strategies cannot reduce the risk of ESRD and also increase the risk of side effects [13]. In addition, effective control of hyperglycemia and hypertension can delay development of DN in the early stages. Newly developed hypoglycemic agents, such as dipeptidyl peptidase-4 inhibitors, glucagon-like peptide-1 receptor agonist, and sodium-glucose cotransporter 2 inhibitors (SGLT2), have been proven to have cardiovascular and renal safety and efficacy [14]. Combination therapy is also a novel choice with a previous study reporting that using RAAS blockade with SGLT2 inhibitors can protect the kidney and the heart of DN patients [15]. However, the high-risk of hypoglycemia and alterations in the pharmacokinetics of antihyperglycemic drugs should be taken into account [16]. Renal dialysis can also help in treating kidney failure, but it cannot retard the gradual deterioration of DN. Kidney transplant is also an effective method for treating ESRD. However, the immune systems of recipients may reject the transplanted organ even in instances where the patients are placed on immunosuppressive therapy. It is worth noting that only a

few of the abovementioned pharmacological treatment options can mitigate the symptoms of DN. Regenerative medicine is a promising treatment option because it offers possible opportunities for restoring functionality to renal disease.

3. MSCs

Current research in the regenerative medical field has focused on MSCs which have been the subject of extensive investigations. Most researchers believe that MSCs are optimal candidates for cell-based treatment strategies [17]. The existence of MSCs was discovered in the late 1960s, where they were reported as occurring in the human body in mesodermal tissues. Over the years, the nomenclature of MSCs has been controversial. Currently, mesenchymal stem cells or mesenchymal stromal cells are the most commonly used terminologies for MSCs. However, some scholars have recently made a proposal to change the terminology to “medicinal signaling cells” [18, 19]. MSCs, which appear to be a native constituent of injured tissues, have emerged as a viable alternative to the standard pharmaceutical treatment modalities [20]. The following six aspects sum up the advantages of using MSCs as potential alternatives for disease treatment: [21–24] (1) MSCs are easily accessible from a variety of autologous or allogeneic adult tissues including bone marrow, adipose tissue, umbilical cord blood, skeletal muscle, synovium, spleen, thymus, lung, and amniotic fluid, and they can also be supplied by commercial providers; (2) the process of isolating MSCs is simple and rapid, and the cells can be quickly multiplied using *in vitro* systems; (3) MSCs can differentiate into a wide variety of mesodermal lineage cells and endodermal or ectodermal cells; (4) MSCs can selectively migrate to sites of injured tissues; (5) MSCs have low immunogenicity and have shown no adverse reactions whether by allogeneic or autologous engraftment; and (6) the use of MSCs does not pose any ethical controversy. The functional features of MSCs have been well exhibited in several studies, especially in studies with the aim of promoting tissue repair by means of cell-to-cell interactions [25–27]. It is worth noting that MSCs have a high metabolic activity, and their secretome processes involve the same mechanisms that are commonly described for other cell types [25]. Previous studies have shown that MSCs can secrete chemokines, cytokines, growth factors, and paracrine factors [26, 27]. In addition, the produced paracrine molecules consist of extracellular vesicles, such as exosomes [27]. Therefore, the secreted biomaterials rebuild a protective environment that enhances host cell recovery, thereby preserving or even rescuing the injured tissue from destruction. Several preclinical studies have revealed that MSCs may have a huge potential for treating a number of clinical diseases, including Alzheimer’s disease, myocardial infarction, lung ischemia-reperfusion injury, and hepatic failure [28–31]. Furthermore, the versatility of MSCs has also made them an attractive candidate for clinical translation in all sorts of therapeutic applications. The most representative MSC product has gained approval to treat pediatric graft-versus-host disease (GVHD) in New Zealand, Canada, and Japan (Prochymal®; Osiris

Therapeutics) [32, 33]. Additionally, recent years have seen several cell products associated with the clinical trials of other diseases [34]. Accordingly, these major developments suggest that MSC therapy will have a promising future.

4. MSC-Based Therapy for DN

4.1. Molecular Mechanisms of MSC-Based Therapy for DN. Experimental studies have demonstrated that MSCs can be used for relieving DN (Table 1). However, the exact mechanisms of DN have not been fully elucidated, and the molecular mechanisms for MSC-based therapy for DN is still under investigation. Regenerative applications for MSCs were initially heralded by their plastic ability since they are multipotent cells that have the ectopic capability of homing and differentiating into several cell types according to specific stimuli, including glomerular endothelial cells [7]. Although MSCs' homing processes are still largely unknown, studies have reported that they involve several molecules, such as chemokine receptors (CCR2, CCR4, CCR7, CCR10, CXCR5, CXCR6, and CXCR4) [35, 36], adhesion proteins, and the matrix metalloproteinase (MMP) family [37]. Among them, stromal cell-derived factor-1 (SDF-1) and its receptor CXCR4 are of great importance to MSCs and renal progenitor cell migration to a damaged kidney [38, 39]. An *in vitro* study reported that MSCs exhibited nonapoptotic membrane blebbing activity, similar to metastatic tumor cells, migrating through the endothelium and overcoming the basal barrier through the action of MMPs [40], especially MMP2 and MT1-MMP, which are essential for the migration of MSCs [41]. The expectation is that MSC infusion can have a long-term survival in the body, like hematopoietic stem cells, and accompany the individual throughout a lifetime. However, most of the studies have shown that only a small fraction of systemically administered cells can migrate to the injured tissue, and only a small percentage of the transplanted cells can differentiate into functional replacement tissue. In addition, the administered cells are almost undetectable in other organs within 24 hours. A previous study reported that some human cells were found in the glomeruli of human bone marrow MSC-treated NOD/SCID mice, but only a few of the cells differentiated into glomerular endothelial cells [7].

Currently, it is common knowledge that the MSCs can recognize and maintain the mechanical microenvironment they are exposed to by modifying their phenotype and secretome. When MSCs migrate to the injured tissue, they face a sophisticated microenvironment that features several chemical and physical stimuli that influences their biological behavior. In addition, MSCs strongly affect the organ microenvironment and local cellular dynamics, and further modulate the behavior of relevant cells [42]. The effect of MSCs is mainly mediated by secreting biologically active molecules for the reconstruction of the damaged tissues, such as transformed growth factor- β (TGF- β), vascular endothelial growth factor (VEGF), epithelial growth factor (EGF), hepatocyte growth factor (HGF), platelet-derived growth factor (PDGF), and interleukin-6 (IL-6) [25, 43]. Chang et al. reported that MSCs' conditioned medium (CM) obtained

from hypoxic cultures promoted neurogenesis and restored the neurological function of rat models having traumatic brain injury using VEGF and HGF [44]. The biological relevance of these released growth factors was also justified in our previous study in which bone marrow-derived MSC (BM-MSC) conditioned medium (CM) decreased both the proliferation and extracellular matrix production of human keloid fibroblasts and attenuated skin fibrosis of a mice model [45]. The results obtained indicated that the paracrine effects induced by the MSCs played a rival role in the progress of skin repair. Several investigations have also shown that the paracrine action of MSCs decreased the deposition of fibronectin and collagen I, and cell proliferation in DN models [46, 47]. At the same time, it was also demonstrated that the cooperation among the PI3K/Akt, MAPK, and TGF- β signaling pathways could mediate the attenuation of DN symptoms. Among the excreted agents, exosomes derived from MSC-CM exerted an antiapoptotic effect and elevated the tight junction structure in tubular epithelial cells of damaged kidney tissue [46].

Exosomes, one of the extracellular vesicles (EVs), is an emerging approach of MSC-based therapies in tissue regeneration. Investigations have indicated that these trophic factors are released from MSCs in a free state or contained within exosomes that are naturally occurring in secreted membrane vesicles (30–40 to 100–120 nm diameter). These extracellular vesicles are believed to be important mediators of cell-to-cell communication not only through the transfer of receptors and proteins but also through the transfer of genetic information (mRNA and microRNAs) [48, 49]. Recent studies have explored the therapeutic use of exosome-derived MSCs in renal disease. Microvesicles obtained from MSC supernatants improved renal tissue injury by inhibiting TGF- β -mediated epithelial-mesenchymal transition (EMT) in renal proximal tubular epithelial cells (PTECs) [50]. As an important secreted agent, exosomes derived from MSCs were reported to prevent apoptosis and degeneration of tubular epithelial cells (TECs) by repressing the caspase-3 overexpression in diabetic rats. The therapeutic effect of these microvesicles in acute injury kidney models seems to be more beneficial when compared with that of conditioned medium [51], although some contradictory studies illustrated an opposite effect in chronic kidney disease in rats [52]. The autophagy induction by MSC-derived exosomes could also markedly improve renal function in a rat model of streptozotocin-induced diabetes mellitus, with a dramatic increase of light chain-3 and Beclin-1 and a significant reduction of mTOR and fibrotic marker expression [53]. In any event, these trials indicated a potential mechanism by which MSC-derived microvesicles ameliorate DN.

Taking a step forward, MSCs may provide a means for recapitulating several mechanisms in terms of preventing or treating DN, including immune-modulatory, antioxidant, and fibrosis-inhibiting mechanisms.

Inflammation, a common characteristic of an injured site, is capable of affecting the action of MSCs, and it has been recognized as a key pathogenic factor in the development and progression of DN where there is a contribution due to the

TABLE 1: Representative research on DN treated with MSC-based therapy in preclinical studies.

Study	Model	Cell type	Route	Efficacy results
Li et al., 2020 [47]	Mice	UC-MSCs	IV	Albuminuria, glomerulus injury, and fibrosis were alleviated in DN mouse models after repeated injection with mUC-MSCs
Lang and Dai, 2016 [62]	Rats	BM-MSCs	IV	BM-MSCs significantly suppressed renal fibrosis by reducing PAI-1 protein and decreasing ECM accumulation in rats with DN
Liu et al., 2020 [81]	Rats	BM-MSCs	IV	MSCs modified with ACE2 can inhibit renal RAS activation and reduce glomerular fibrosis
Zhang et al., 2020 [57]	Rats	BM-MSCs	IV	MSCs possessed the protective effect on the kidney of DN rats, which may be related to CD8(+) T cell immunosuppression mediated by CD103(+) DCs
Yuan et al., 2020 [55]	Mice	BM-MSCs	IV	MSCs suppressed inflammatory response and ameliorated renal injuries in DN mice via TFFB-dependent MI/M2 macrophage (M ϕ) switch
Chen et al., 2020 [71]	Rats	UC-MSCs	IV	UC-MSCs inhibited 24-hour urinary total protein, urinary albumin to creatinine ratio, serum creatinine, and blood urea nitrogen, attenuated pathological abnormalities and reduced the apoptosis of renal cells in DN rats
Takemura et al., 2020 [73]	Rats	AD-MSCs	Under renal capsule	AD-MSC sheet engraftment directly into the kidney improved transplantation efficiency and inhibited renal injury progression
Lee et al., 2019 [58]	Mice	UC-MSCs	IV	MSCs prevented the progression of DN by reversing mitochondrial dysfunction in TECs via the induction of arginase-1 in macrophages
Konari et al., 2019 [59]	Rats	BM-MSCs	IV	BM-MSCs transferred their mitochondria to damaged proximal tubular epithelial cells and also have shown a potentially therapeutic effect on DN
Ebrahim et al., 2018 [53]	Rats	BM-MSCs	IV	MSC-derived exosomes could exhibit the potential nephroprotective effects of a DN model by upregulating autophagy associated with suppression of mTOR pathway
Ly et al., 2014 [90]	Rats	BM-MSCs	IV	MSC injection attenuated glomerular injury in streptozotocin-induced DN model via inhibiting oxidative stress
Rashed et al., 2018 [78]	Rats	BM-MSCs	IV	BM-MSCs pretreated with melatonin enhanced its proliferation and efficiency, and ameliorated kidney functions in a rat model with DN
Wu et al., 2014 [75]	Rats	BM-MSCs	IV	Destruction of ultrasound-targeted SDF-1-loaded microbubbles could promote MSCs homing to early DN kidneys
An et al., 2019 [69]	Rhesus macaque	BM-MSCs	IV	MSCs could ameliorate a rhesus macaque model of DN by influencing SGLT2 expression, glycemic control, and anti-inflammation
Pan et al., 2014 [68]	Tree shrews	BM-MSCs	IV	MSC transplantation could home to injured kidneys and pancreas, and reduced 24 h proteinuria and improved insulin resistance of a tree shrew model with DN
Rao et al., 2019 [61]	Rats	SHED	IV	SHED attenuated DN by inhibiting advanced glycation end product-activated EMT
Ni et al., 2015 [72]	Rats	AD-MSCs	IV	AD-MSC engraftment might alleviate renal injury in DN by activating klotho and inhibiting Wnt/ β -catenin pathway
Wang et al., 2013 [65]	Rats	BM-MSCs	Intra-arterial injection	MSCs attenuated podocyte injury and albuminuria in a type 1 DN rat model by mediating in part the increase of BMP-7 secretion

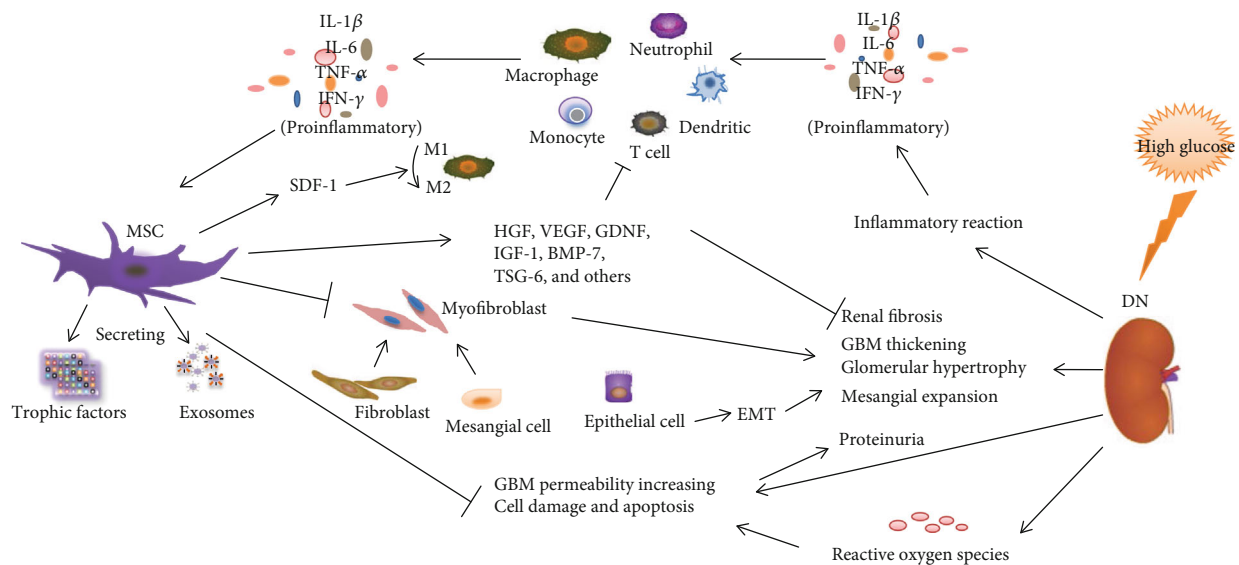


FIGURE 1: MSCs attenuate the pathological changes and clinical manifestations of DN by regulating inflammatory reaction, fibrotic response, and immune cells.

imbalance of M1/M2 macrophages. In the context of sepsis, *in vivo* studies have been performed to show that MSCs can elicit macrophages to change into a M2 anti-inflammatory phenotype by secreting prostaglandin E2 (PGE2) and promoting IL-10 secretion in response to PGE2 [54]. MSCs reverted macrophages to adopt an anti-inflammatory phenotype and prevented renal injury in DN mice, which was attributed to the activation of transcription factor EB, and subsequent restoration of lysosomal function and the autophagy activity of macrophages [55]. Meanwhile, MSCs have been demonstrated to significantly decrease proinflammatory M1 macrophage-associated changes such as in IL-1 β , IL-6, TNF- α , and IFN- γ [56]. Furthermore, MSCs are capable of suppressing and altering the function of mature dendritic cells (DCs) by reducing the development of CD103+ DC-associated transcription factors including basic leucine zipper transcriptional factor ATF-like 3, Batf3, DNA-binding protein inhibitor (ID-2, Id2), and FMS-like tyrosine kinase-3 (Flt3) [57]. This finding indicates that the immunomodulatory effect of MSCs is crucial for the success of tissue repair in the inflammatory environment of a DN setting.

Mitochondrial dysfunction is also a major pathogenic factor in diabetes-induced kidney injury. It was reported that MSC injection can suppress albuminuria and injury to TECs by improving mitochondrial function [58]. Konari et al. also demonstrated mitochondria transfer from MSCs that prevented apoptosis of impaired renal PTECs [59]. The difference between the two studies is that the mitochondria in the latter study originated from systemically administered MSCs. MSCs transferred their mitochondria to injured PTECs when cocultured *in vitro*, which rescued impaired renal cells [59]. Generally, the occurrence of an inflammatory disease is also accompanied by the release of reactive oxygen species (ROS) and the depletion of endogenous antioxidants, but antioxidant enzymes such as superoxide dismutase (SOD) are widely known to be very effective scavengers of

ROS [60]. MSC-derived isolated mitochondria promoted the expression of mitochondrial SOD and Bcl-2, and at the same time inhibited ROS production *in vitro* [59]. The efficacy of mitochondria transfer from MSCs is probably a result of their ability to improve the expression of SOD followed by SOD acting to disproportionate the superoxide radical to oxygen and hydrogen peroxide, thereby protecting damaged cells against ROS generated during DN. The abovementioned study was the first study to show mitochondria transfer to rescue injured cells, which is a novel action of MSCs in DN.

The accumulation of extracellular matrix proteins, such as the synthesis and increase of collagen type I or IV, fibronectin, and laminin, is a common feature of DN. It has been suggested that EMT contributes to the fibrotic process in DN [61]. Several studies have demonstrated that MSC delivery improves renal fibrosis in various types of kidney diseases. For example, Li et al. showed that mouse UC-MSC paracrine alleviated renal fibrosis by decreasing the deposition of fibronectin and collagen I, and elevated the levels of MMP2 and MMP9, and the mechanism may be related to TGF- β 1-triggered myofibroblast transdifferentiation, and PI3K/Akt and MAPK signaling pathways [47]. Another study conducted on DN of a type 2 diabetes rat model reported that bone marrow-derived MSCs induced a significant inhibition of renal fibrosis, which was involved in inhibiting the TGF- β 1/Smad3 pathway and decreasing plasminogen activator inhibitor-1 [62]. MSC administration therapy also operates through other several mechanisms, including antiapoptotic [63] and autophagy-regulating mechanisms [53]. However, it is worth noting that the mechanisms underlying these interactions are often involved at one or more levels within the complex molecular processes of DN, rather than being viewed separately (Figure 1). Arguably, cell therapy has been shown to have the most promising clinical therapeutic effects directly through tissue regeneration as well as through indirect action to enhance the natural regenerative processes on

damaged and diseased tissues. Further studies on MSC action will contribute to shed light on the clinical impact of the cell-based therapy in DN. Currently, researchers are conducting preclinical and clinical studies to explore the application of MSCs to prevent the progression of DN.

4.2. Preclinical Studies of MSC-Based Therapy for DN. The published literature provides evidence that MSC engraftment can significantly ameliorate proteinuria serum creatinine/urea and improve renal pathological changes, including GBM thickening, glomerular sclerosis, tubule dilatation, mesangial proliferation, podocyte foot process effacement, and interstitial fibrosis. However, it is worth noting that not all the studies demonstrated a reduction in blood glucose after MSC systemic administration [64, 65], which can be probably attributed to the blood glucose control of MSC infusion delaying the progression of DN independent of direct renoprotective effects. Some studies reported that islet cell regeneration could be found in the pancreas after MSCs were engrafted. A variety of explanations, such as the animal model used, the origin of the MSC tissue, the cell dose factor, and the administration route, have been proposed to account for the phenomenon of inconsistencies in the reduction of blood glucose [66]. Moreover, these factors also have an enormous influence on other clinically relevant indicators of DN. Clarifying these factors will be critical for maximizing the efficacy of MSC therapy during application to human DN.

Rodents have always served as the primary animal model for DN experiments due to their widespread availability, definite genotypes, abundant associated experimental reagents, cost advantages, and amenability to genetic modification [67]. Almost all *in vivo* studies investigating MSCs for DN using animal models have been carried out in mice or rats. However, other animals can also be used as DN models. Pan et al. used a new DN model in tree shrews to evaluate the effect of BM-MSCs [68]. After BM-MSC transplantation, levels of glucose, triglycerides, and total cholesterol were decreased, and the levels of creatinine and urea nitrogen and 24h proteinuria were also reduced. The study demonstrated that a tree shrew model of DN can be induced successfully with a high-sugar and high-fat diet combined with STZ injection, and BM-MSCs can alleviate the symptom of DN. Taking a step forward, An et al. developed another animal model—a rhesus macaque model of DN—and the MSCs administered in the study ameliorated the early stage of DN potentially by adjusting sodium-glucose cotransporter 2 (SGLT2) expression and resulted in improved glycemic control and anti-inflammation [69]. The two species mentioned above have greater genome homology with *Homo sapiens* when compared to rodents. Therefore, they can be used to develop an improved animal model for the study of human DN.

The different sources of MSCs may also have an effect on their action. MSCs used for research purposes are mostly obtained from bone marrow, umbilical cord, or subcutaneous adipose tissue owing to their greater accessibility. There are more studies reporting the use of BM-MSCs than those that have used umbilical cord-derived MSCs (UC-MSCs) and adipose tissue-derived MSCs (AD-MSCs). However, the clinical use of BM-MSCs faces several challenges includ-

ing morbidity, pain, and low cell number during harvest. On the other hand, UC-MSCs and AD-MSCs have several advantages including higher stability in culture, higher replicative potential, lower immunogenicity, and a noninvasive harvest procedure when compared with those of other stem cells [70]. Therefore, some researchers have shifted their focus on the effect of UC-MSCs and AD-MSCs on DN. Chen et al. proved that UC-MSCs have definite therapeutic effects on DN [71]. The obtained results indicated that nephrocyte injury and albuminuria were ameliorated through their antiapoptotic property in rat models with DN when the animals received UC-MSCs. Ni et al. found that AD-MSCs could relieve renal injury in DN via activating *klotho* and inhibiting the Wnt/-catenin pathway [72]. In addition, Takemura et al. directly transplanted AD-MSC sheets into the kidneys of a DN rat model in order to avoid low engraftment of AD-MSCs in target organs after intravascular administration [73]. The results indicated that the method improved the engraftation efficiency and suppressed the progression of renal injury. Interestingly, another study reported that stem cells from human exfoliated deciduous teeth (SHED) significantly alleviated the pathological changes and clinical manifestations of DN in Goto-Kakizaki rats [61]. Moreover, the serum levels of inflammatory factors including IL-1 and TNF- α were dramatically downregulated. Additionally, the *in vitro* coculture of SHED with AGE-induced HK-2 cells also inhibited EMT of the epithelial cells. Therefore, SHED provides a novel potential effective therapeutic approach for attenuating DN.

MSC-based therapy has broad application prospects for the treatment of DN. However, researchers remain unsatisfied with the curative effect of the cells. For instance, the cell dose factor is a crucial aspect of cell therapy. In addition, most homing and transplantation studies only reported the observation of a small amount of MSCs upon systemic administration for long-term engraftment (>1 week) [74]. Representative studies described that the majority of transplanted MSCs (>80%) immediately accumulate in the lung tissue and then are cleared with a half-life of 24 hours [74]. Another major barrier to the effective application of MSC therapy is that insufficient MSCs are retained in injured kidneys. Therefore, Wu et al. developed SDF-1 loaded microbubbles (MBSDF-1) via covalent conjugation [75]. MSCs were intravenously transplanted after MBSDF-1 was released in the targeted kidneys in combination with diagnostic ultrasound. The obtained results indicated that the homing efficacy of MSCs to DN kidneys following the target release of SDF-1 was significantly improved at 24 hours. Zhang et al. adopted a noninvasive ultrasound-targeted microbubble destruction (UTMD) technique to enhance the homing of MSCs to kidneys, thereby improving renal repair in DN rats [76]. It is worth noting that higher doses of MSCs (4×10^6 cells) may give rise to treatment-related adverse events, such as vomiting and increased respiratory rate, during transplantation of the cells [77].

In addition, some researchers have begun to attempt to promote the function of MSCs aside from considering the cell dose. Rashed et al. used new methods to increase the effect of MSCs for DN as well [78]. MSCs were pretreated with melatonin before the cells were infused into the DN model, which showed that pretreatment of MSCs with

TABLE 2: Ongoing or completed clinical trials with MSC-based therapy in DN.

ClinicalTrials.gov identifier	Cell type	Subject number	Cell dosage	Route	Trial status
NCT01843387	BM-MPC	30	1 dose: 150, 300 × 10 ⁶ cells	IV	Completed
NCT02585622	BM-MSCs	48	1 dose: 80, 160, 240 × 10 ⁶ cells	IV	
NCT04216849	UC-MSCs	54	5 doses: 1.5 × 10 ⁶ cells/kg	IV	Phase 2
NCT03288571	UC-MSCs	20	3 doses: 1 ml cell suspension	Renal parenchyma	Phase 2
NCT03840343	AD-MSCs	30	2 doses: 2.5, 5 × 10 ⁶ cells/kg	Intra-arterial delivery	Phase 1
NCT04125329	UC-MSCs	15	3 doses: 1 × 10 ⁶ cells/kg	IV	Early phase 1

melatonin improved kidney functions compared with MSC administration alone. All the abovementioned studies provided new insights into DN therapy, which may be used as a new therapy for underlying diabetic nephropathy (DN) pathogenesis.

The MSC administration route is also a key point that should not be overlooked. The majority of studies delivered MSCs through the tail vein because the operation of the method is simple. Wang et al. demonstrated by meta-analysis that MSC therapy could induce significant effects including a greater reduction in serum creatinine and a better preserved renal function using arterial delivery than when using the intrarenal delivery and intravenous treatment [79]. This can be attributed to the fact that the MSCs delivered by intrarenal injection were just located near the site of injection, while the infused MSCs by arterial injection would enter the damaged kidney more quickly owing to the fact that the artery is rich in blood flow and blood velocity. This meta-analysis aiming at the delivery route may provide significant clues for animal experiments even for human clinical applications.

4.3. Clinical Research on MSC-Based Therapy for DN. MSCs are being clinically explored as a new therapeutic for treating a variety of diseases. According to the official database of the U.S. National Institutes of Health (<https://ClinicalTrials.gov>), the majority of clinical studies currently focus on nervous system disorders and bone and cartilage diseases for MSCs registered as a potential therapy. In contrast, although a growing number of animal and in vitro studies have indicated good prospects for an MSC-based therapy in DN, only a handful of clinical studies are evaluating the regenerative and therapeutic role of MSCs in this condition now. The findings of these clinical trials serve as essential information, and the research bases for the later clinical studies are listed in Table 2 (completed and ongoing trials).

A multicenter, randomized, double-blind, dose-escalating, sequential, and placebo-controlled trial registered in ClinicalTrials.gov (NCT01843387) evaluated the safety, tolerability, and efficacy of adult allogeneic bone marrow-derived mesenchymal precursor cells (MPCs) in 30 volunteers with moderate-to-severe DN at three Australian centers. The patients received single intravenous (IV) infusion (150 × 10⁶ or 300 × 10⁶ allogeneic MPCs), and the trial duration was 60 weeks. This clinical study demonstrated that MPC infusion in patients with DN may be considered safe since there were no acute adverse events (AEs) associated with administration and no patients developed persistent

donor-specific anti-HLA antibodies. In addition, a more stabilizing or improving eGFR and mGFR was observed at week 12 in the MPC-treated group, thereby providing a potential mechanistic clue to stem cell actions in this disease [80]. Most of the clinical trials are in phase I or II studies and they are aimed at assessing safety and tolerability and exploring the therapeutic effects of cell-based therapy, thus indicating that the stem cells and related therapy in clinical application are still a long way off.

5. The Future Directions for MSCs and MSC Alternatives in DN

MSC-based therapy is a promising alternative for the treatment of diabetic kidney disease. Despite this review presenting an overview of MSC therapy for DN, many questions have not yet been answered. The key point to consider should be how to maximize the therapeutic impact of MSCs, which may potentiate the effects by enhancing their proliferation, survival, engraftment, and paracrine properties. Several strategies have been tested to heighten the benefits, principally physical, physiological, and pharmaceutical preconditioning of stem cells, such as biological cytokine, MSC cell sheet, specific drug hypoxia, or medical equipment induction, which have created new chances that should be further explored.

In addition to promoting the therapeutic effect of MSCs indirectly, some investigations have indicated that MSCs have typically involved genetic manipulations to alleviate DN. MSCs modified with the angiotensin-converting enzyme (ACE) 2 gene could significantly inhibit renin-angiotensin system (RAS) activation and reduce glomerular fibrosis [81], yet research literature on treating DN is still limited. Notably, previous studies have reported that there is a possibility that MSCs can be modified to express some peptides or proteins with antitumor properties [82, 83]. MSCs infected with herpes simplex virus thymidine kinase (TK) gene by lentiviral transduction could exert a great anti-tumor effect in an animal model bearing a metastatic RIF-1 (fibrosarcoma) tumor. However, the cells did not transform their stem cell properties [82]. Moreover, nongenetic modification of MSCs by incorporating nanoparticles carrying chemotherapeutics also almost did not alter their viability, differentiation, and/or migration potential [84]. In the A549 orthotopic lung tumor model, nanoengineered MSCs loaded with the anticancer drug paclitaxel (PTX) could home in to tumors and form cellular drug depots that released the drug load over a prolonged period of time [85]. The nanoengineered MSCs exerted significant inhibition of tumor growth

and better survival, despite extremely low doses of PTX, indicating that MSCs are an efficient delivery vehicle for specific drugs to enhance the efficacy of standard chemotherapy.

One of the most important action mechanisms for MSCs is mediated by exosomes. Exosomes, nanosized membranous vesicles secreted by an array of cells, were recently introduced as a new kind of drug delivery system due to their unique and important performance pharmacologically. Exosomes are closely associated with the occurrence and progression of a variety of diseases by participating in physiological processes such as cell communication, cell migration, angiogenesis, and antitumor immunity *in vivo*. And they have a high ability of penetrating organ interstitium and are endowed with a natural targeting ability due to their nanosize. MSC-derived vesicles modulate several pathways involved in the pathophysiological process of DN, including podocyte apoptosis and proliferation, inflammation response, immune regulation oxidative stress, and ECM remodeling. However, the number of exosomes released by most mammalian cells is relatively low, and their purification is very tedious, thereby leading to a relatively low yield [86]. In addition, the potential risks associated with MSC transplantation should be taken into account. However, the risks may not be observed in a short time period following administration. The long-term risks may comprise potential maldifferentiation, immunosuppression, and instigation of malignant tumor growth. Therefore, exosome-mimetic nanovesicles are very compelling for the development of a nanodrug delivery system. Nanosized cellular vesicles formed by membrane fusion after cell mechanical fragmentation feature long circulation time *in vivo*, small particle size, high tumor permeability, many kinds of encapsulated drugs (hydrophobic drugs, peptides, and nucleic acids), and slow drug release, which can achieve the effective load of nucleic acid drugs [87, 88] and also achieve the payload of chemotherapeutic drugs [89]. Currently, most experimental studies are primarily focused on short-term effects of MSC therapy, while largely ignoring the evaluation of long-term effects. This review has shown that the novel cell-free therapy based on MSCs might become an attractive alternative for the treatment of DN in future clinical applications.

It is projected that, within the next few years, the challenge for future studies will be to significantly expand our understanding of the key molecular mechanisms involved in MSC action. Elucidation of the key molecular mechanisms of MSC action will enhance their effects when applied in clinical trials; in turn, the strategy will be very conducive to reducing the morbidity and mortality of diabetic kidney disease. It is our hope that conditioned media, extracellular vesicles, and nanosized cellular vesicles will be used as cell-free substitutes for MSCs. In addition, conducting large experimental studies, registered clinical trials, and individual-data meta-analysis will help us understand and determine optimal cellular and subcellular therapies to attenuate diabetes-induced kidney injury.

6. Conclusions

DN remains a major clinical complication of diabetes mellitus patients, as it reduces the quality of life and overall survival. Increased academic research has focused on the

effectiveness of MSCs in the treatment of DN due to the lack of clinical effective therapeutic strategies and the recent advances for MSC therapy in regeneration medicine field. However, the safety profile of MSC-based therapy needs further research, as standardized approaches for MSCs are not yet developed, along with the optimal dosage, time, and route of administration. Furthermore, the therapeutic effect of MSCs in preclinical studies has not yielded satisfying outcomes. These challenges have made it difficult to visualize the use of the MSC-based therapy in clinical implementation in the short run. However, cell-free therapy based on MSCs or therapeutic genes of modified MSCs may become a future trend of development. The safety and effectiveness MSC products have not been officially recognized despite the approval for marketing of several MSC products in some countries. However, listing does not mean that MSC research has been terminated. The use of MSCs is fascinating because it always gives us some surprises, and thus the mystery behind these surprises should be elucidated. In conclusion, MSC-based therapy has a high potential for managing DN. However, the challenges associated with the therapy must be addressed before its application can be incorporated in clinical settings. Therefore, there is still a long way to go before such cell therapy can be used in clinical practice.

Abbreviations

ACE:	Angiotensin-converting enzyme
ACE2:	Angiotensin-converting enzyme 2
ACEI:	System using angiotensin-converting enzyme inhibitors
AD-MSCs:	Adipose tissue-derived mesenchymal stem cells
AEs:	Adverse events
ARB:	Angiotensin receptor blockers
BM-MPC:	Bone marrow-derived mesenchymal precursor cell
BM-MSCs:	Bone marrow-derived mesenchymal stem cells
BMP-7:	Bone morphogenetic protein-7
CCR:	Chemokine receptors
CM:	Conditioned medium
DCs:	Dendritic cells
DM:	Diabetes mellitus
DN:	Diabetic nephropathy
ECM:	Extracellular matrix
EGF:	Epithelial growth factor
EMT:	Epithelial-mesenchymal transition
ESRD:	End-stage renal diseases
EVs:	Extracellular vesicles
Flt3:	FMS-like tyrosine kinase-3
GBM:	Glomerular basement membrane
GDNF:	Glial cell line-derived neurotrophic factor
GVHD:	Graft-versus-host disease
HGF:	Hepatocyte growth factor
IFN- γ :	Interferon- γ
IGF-1:	Insulin-like growth factor 1
IL-1 β :	Interleukin-1 β
IL-6:	Interleukin-6
IV:	Intravenous
MBSDF-1:	SDF-1-loaded microbubbles

MMPs:	Matrix metalloproteinases
MSCs:	Mesenchymal stem or stromal cells
PDGF:	Platelet-derived growth factor
PGE2:	Prostaglandin E2
PTEC:	Proximal tubular epithelial cells
PTX:	Paclitaxel
RAAS:	Renin-angiotensin-aldosterone system
RAS:	Renin-angiotensin system
ROS:	Reactive oxygen species
SDF-1:	Stroma cell-derived factor 1
SGLT2:	Sodium-glucose cotransporter 2 inhibitors
SHED:	Stem cells from human exfoliated deciduous teeth
SOD:	Superoxide dismutase
TEC:	Tubular epithelial cell
TFEB:	Transcription factor EB
TGF- β :	Transformed growth factor- β
TK:	Thymidine kinase
TNF- α :	Tumor necrosis factor- α
TSG-6:	Tumor necrosis factor α stimulated gene 6
UC-MSCs:	Umbilical cord-derived mesenchymal stem cells
UTMD:	Ultrasound-targeted microbubble destruction
VEGF:	Vascular endothelial growth factor.

Conflicts of Interest

The authors declare that they have no conflict of interest.

Authors' Contributions

JG and XHY contributed to the conception of this study. YW and CLZ performed the literature research and drafted the manuscript. All other authors participated in revising the paper and finalizing the paper. All authors read and approved the final manuscript. Yan Wu and Chunlei Zhang contributed equally to this work.

Acknowledgments

This work was supported by the National Natural Science Foundation of China (nos. 81771964 and 81472829), the Natural Science Foundation of Heilongjiang Province (nos. LH2019H061 and LH2020H076) and the Climbing Program in Biomedicine Group of Heilongjiang Province Educational Committee (no. 2019-KYYWF-0987).

References

- [1] IDF, *IDF Diabetes Atlas*, The International Diabetes Federation (IDF), Brussels, Belgium, 2019.
- [2] C. Byrne, F. Caskey, C. Castledine et al., "UK Renal Registry: 20th Annual Report of the Renal Association," *Nephron*, vol. 139, supplement 1, pp. 24–35, 2018.
- [3] W. W. Williams, R. M. Salem, A. J. McKnight et al., "Association testing of previously reported variants in a large case-control meta-analysis of diabetic nephropathy," *Diabetes*, vol. 61, no. 8, pp. 2187–2194, 2012.
- [4] A. C. Webster, E. V. Nagler, R. L. Morton, and P. Masson, "Chronic kidney disease," *Lancet*, vol. 389, no. 10075, pp. 1238–1252, 2017.
- [5] M. Afkarian, M. C. Sachs, B. Kestenbaum et al., "Kidney disease and increased mortality risk in type 2 diabetes," *J Am Soc Nephrol*, vol. 24, no. 2, pp. 302–308, 2013.
- [6] B. Bochon, M. Kozubska, G. Surygała et al., "Mesenchymal stem cells—potential applications in kidney diseases," *International Journal of Molecular Science*, vol. 20, no. 10, p. 2462, 2019.
- [7] R. H. Lee, M. J. Seo, R. L. Reger et al., "Multipotent stromal cells from human marrow home to and promote repair of pancreatic islets and renal glomeruli in diabetic NOD/scid mice," *Proceedings of the National Academy of Sciences of the United States of America*, vol. 103, no. 46, pp. 17438–17443, 2006.
- [8] F. Hajiaghaalipour, M. Khalilpourfarshbafi, and A. Arya, "Modulation of glucose transporter protein by dietary flavonoids in type 2 diabetes mellitus," *International Journal of Biological Sciences*, vol. 11, no. 5, pp. 508–524, 2015.
- [9] F. E. Ezquer, M. E. Ezquer, D. B. Parrau, D. Carpio, A. J. Yañez, and P. A. Conget, "Systemic administration of multipotent mesenchymal stromal cells reverts hyperglycemia and prevents nephropathy in type 1 diabetic mice," *Biology of Blood and Marrow Transplantation*, vol. 14, no. 6, pp. 631–640, 2008.
- [10] I. Preguiça, A. Alves, S. Nunes et al., "Diet-induced rodent models of diabetic peripheral neuropathy, retinopathy and nephropathy," *Nutrients*, vol. 12, no. 1, p. 250, 2020.
- [11] M. K. Arora and U. K. Singh, "Molecular mechanisms in the pathogenesis of diabetic nephropathy: an update," *Vascular Pharmacology*, vol. 58, no. 4, pp. 259–271, 2013.
- [12] F National Kidney, "KDOQI clinical practice guideline for diabetes and CKD: 2012 update," *American Journal of Kidney Diseases*, vol. 60, no. 5, pp. 850–886, 2012.
- [13] L. F. Fried, N. Emanuele, J. H. Zhang et al., "Combined angiotensin inhibition for the treatment of diabetic nephropathy," *The New England Journal of Medicine*, vol. 369, no. 20, pp. 1892–1903, 2013.
- [14] J. J. Neumiller, R. Z. Alicic, and K. R. Tuttle, "Therapeutic considerations for antihyperglycemic agents in diabetic kidney disease," *J Am Soc Nephrol*, vol. 28, no. 8, pp. 2263–2274, 2017.
- [15] H. Zou, B. Zhou, and G. Xu, "Correction to: SGLT2 inhibitors: a novel choice for the combination therapy in diabetic kidney disease," *Cardiovascular Diabetology*, vol. 17, no. 1, p. 38, 2018.
- [16] Action to Control Cardiovascular Risk in Diabetes Study Group, H. C. Gerstein, M. E. Miller et al., "Effects of intensive glucose lowering in type 2 diabetes," *The New England Journal of Medicine*, vol. 358, no. 24, pp. 2545–2559, 2008.
- [17] D. C. Chambers, D. Enever, S. Lawrence et al., "Mesenchymal stromal cell therapy for chronic lung allograft dysfunction: results of a first-in-man study," *Stem Cells Translational Medicine*, vol. 6, no. 4, pp. 1152–1157, 2017.
- [18] A. I. Caplan, "Mesenchymal stem cells: time to change the name!," *Stem Cells Translational Medicine*, vol. 6, no. 6, pp. 1445–1451, 2017.
- [19] K. W. Witwer, B. W. M. van Balkom, S. Bruno et al., "Defining mesenchymal stromal cell (MSC)-derived small extracellular vesicles for therapeutic applications," *Journal of Extracellular Vesicles*, vol. 8, no. 1, article 1609206, 2019.
- [20] W. M. Jackson, L. J. Nesti, and R. S. Tuan, "Mesenchymal stem cell therapy for attenuation of scar formation during wound healing," *Stem Cell Research & Therapy*, vol. 3, no. 3, p. 20, 2012.

- [21] I. Sekiya, B. L. Larson, J. R. Smith, R. Pochampally, J.&. G. Cui, and D. J. Prockop, "Expansion of human adult stem cells from bone marrow stroma: conditions that maximize the yields of early progenitors and evaluate their quality," *Stem Cells*, vol. 20, no. 6, pp. 530–541, 2002.
- [22] K. Le Blanc and O. Ringden, "Immunobiology of human mesenchymal stem cells and future use in hematopoietic stem cell transplantation," *Biology of Blood and Marrow Transplantation*, vol. 11, no. 5, pp. 321–334, 2005.
- [23] D. J. Prockop, C. A. Gregory, and J. L. Spees, "One strategy for cell and gene therapy: harnessing the power of adult stem cells to repair tissues," *Proceedings of the National Academy of Sciences USA*, vol. 100, Supplement 1, pp. 11917–11923, 2003.
- [24] S. François, M. Bensidhoum, M. Mouseddine et al., "Local irradiation not only induces homing of human mesenchymal stem cells at exposed sites but promotes their widespread engraftment to multiple organs: a study of their quantitative distribution after irradiation damage," *Stem Cells*, vol. 24, no. 4, pp. 1020–1029, 2006.
- [25] M. Madrigal, K. S. Rao, and N. H. Riordan, "A review of therapeutic effects of mesenchymal stem cell secretions and induction of secretory modification by different culture methods," *Journal of Translational Medicine*, vol. 12, no. 1, p. 260, 2014.
- [26] D. Kyurkchiev, I. Bochev, E. Ivanova-Todorova et al., "Secretion of immunoregulatory cytokines by mesenchymal stem cells," *World J Stem Cells*, vol. 6, no. 5, pp. 552–570, 2014.
- [27] I. Linero and O. Chaparro, "Paracrine effect of mesenchymal stem cells derived from human adipose tissue in bone regeneration," *PLoS One*, vol. 9, no. 9, article e107001, 2014.
- [28] C. A. Elia, M. Tamborini, M. Rasile et al., "Intracerebral injection of extracellular vesicles from mesenchymal stem cells exerts reduced $\alpha\beta$ plaque burden in early stages of a preclinical model of Alzheimer's disease," *Cells*, vol. 8, no. 9, p. 1059, 2019.
- [29] Y. Peng, J. L. Zhao, Z. Y. Peng, W. F. Xu, and G. L. Yu, "Exosomal miR-25-3p from mesenchymal stem cells alleviates myocardial infarction by targeting pro-apoptotic proteins and EZH2," *Cell Death and Disease*, vol. 11, no. 5, p. 317, 2020.
- [30] C. Lonati, G. A. Bassani, D. Brambilla et al., "Mesenchymal stem cell-derived extracellular vesicles improve the molecular phenotype of isolated rat lungs during ischemia/reperfusion injury," *The Journal of Heart and Lung Transplantation*, vol. 38, no. 12, pp. 1306–1316, 2019.
- [31] H. Haga, I. K. Yan, K. Takahashi, A. Matsuda, and T. Patel, "Extracellular vesicles from bone marrow-derived mesenchymal stem cells improve survival from lethal hepatic failure in mice," *Stem Cells Translational Medicine*, vol. 6, no. 4, pp. 1262–1272, 2017.
- [32] B. Vaes, W. Van't Hof, R. Deans, and J. Pinxteren, "Application of MultiStem® allogeneic cells for immunomodulatory therapy: clinical progress and pre-clinical challenges in prophylaxis for graft versus host disease," *Frontiers in Immunology*, vol. 3, p. 345, 2012.
- [33] A. Konishi, K. Sakushima, S. Isobe, and D. Sato, "First approval of regenerative medical products under the PMD act in Japan," *Cell Stem Cell*, vol. 18, no. 4, pp. 434–435, 2016.
- [34] G. Rodas, R. Soler, R. Balius et al., "Autologous bone marrow expanded mesenchymal stem cells in patellar tendinopathy: protocol for a phase I/II, single-centre, randomized with active control PRP, double-blinded clinical trial," *Journal of Orthopaedic Surgery and Research*, vol. 14, no. 1, p. 441, 2019.
- [35] F. Nitzsche, C. Müller, B. Lukomska, J. Jolkkonen, A. Deten, and J. Boltze, "Concise review. MSC adhesion cascade—insights into homing and transendothelial migration," *Stem Cells*, vol. 35, no. 6, pp. 1446–1460, 2017.
- [36] K. Andreas, M. Sittlinger, and J. Ringe, "Toward in situ tissue engineering: chemokine-guided stem cell recruitment," *Trends in Biotechnology*, vol. 32, no. 9, pp. 483–492, 2014.
- [37] A. Monsel, Y. G. Zhu, S. Gennai, Q. Hao, J. Liu, and J. W. Lee, "Cell-based therapy for acute organ injury: preclinical evidence and ongoing clinical trials using mesenchymal stem cells," *Anesthesiology*, vol. 121, no. 5, pp. 1099–1121, 2014.
- [38] F. Togel, J. Isaac, Z. Hu, K. Weiss, and C. Westenfelder, "Renal SDF-1 signals mobilization and homing of CXCR4-positive cells to the kidney after ischemic injury," *Kidney International*, vol. 67, no. 5, pp. 1772–1784, 2005.
- [39] B. Mazzinghi, E. Ronconi, E. Lazzeri et al., "Essential but differential role for CXCR4 and CXCR7 in the therapeutic homing of human renal progenitor cells," *The Journal of Experimental Medicine*, vol. 205, no. 2, pp. 479–490, 2008.
- [40] G. S. Teo, J. A. Ankrum, R. Martinelli et al., "Mesenchymal stem cells transmigrate between and directly through tumor necrosis factor- α -activated endothelial cells via both leukocyte-like and novel mechanisms," *Stem Cells*, vol. 30, no. 11, pp. 2472–2486, 2012.
- [41] C. Ries, V. Egea, M. Karow, H. Kolb, M. Jochum, and P. Neth, "MMP-2, MT1-MMP, and TIMP-2 are essential for the invasive capacity of human mesenchymal stem cells: differential regulation by inflammatory cytokines," *Blood*, vol. 109, no. 9, pp. 4055–4063, 2007.
- [42] T. Squillaro, G. Peluso, and U. Galderisi, "Clinical trials with mesenchymal stem cells: an update," *Cell Transplantation*, vol. 25, no. 5, pp. 829–848, 2016.
- [43] M. B. Murphy, K. Moncivais, and A. I. Caplan, "Mesenchymal stem cells: environmentally responsive therapeutics for regenerative medicine," *Experimental & Molecular Medicine*, vol. 45, no. 11, p. e54, 2013.
- [44] C. P. Chang, C. C. Chio, C. U. Cheong, C. M. Chao, B. C. Cheng, and M. T. Lin, "Hypoxic preconditioning enhances the therapeutic potential of the secretome from cultured human mesenchymal stem cells in experimental traumatic brain injury," *Clinical Science (London, England)*, vol. 124, no. 3, pp. 165–176, 2013.
- [45] Y. Wu, Y. Peng, D. Gao et al., "Mesenchymal stem cells suppress fibroblast proliferation and reduce skin fibrosis through a TGF- β 3-dependent activation," *The International Journal of Lower Extremity Wounds*, vol. 14, no. 1, pp. 50–62, 2015.
- [46] K. Nagaishi, Y. Mizue, T. Chikenji et al., "Mesenchymal stem cell therapy ameliorates diabetic nephropathy via the paracrine effect of renal trophic factors including exosomes," *Scientific Reports*, vol. 6, no. 1, article 34842, 2016.
- [47] H. Li, P. Rong, X. Ma et al., "Mouse umbilical cord mesenchymal stem cell paracrine alleviates renal fibrosis in diabetic nephropathy by reducing myofibroblast transdifferentiation and cell proliferation and upregulating MMPs in mesangial cells," *Journal of Diabetes Research*, vol. 2020, Article ID 3847171, 14 pages, 2020.
- [48] S. Bruno, S. Porta, and B. Bussolati, "Extracellular vesicles in renal tissue damage and regeneration," *European Journal of Pharmacology*, vol. 790, pp. 83–91, 2016.
- [49] V. B. Konala, M. K. Mamidi, R. Bhonde, A. K. Das, R. Pochampally, and R. Pal, "The current landscape of the

- mesenchymal stromal cell secretome: a new paradigm for cell-free regeneration,” *Cytotherapy*, vol. 18, no. 1, pp. 13–24, 2016.
- [50] Y. Wang, B. Fu, X. Sun et al., “Differentially expressed micro-RNAs in bone marrow mesenchymal stem cell-derived microvesicles in young and older rats and their effect on tumor growth factor- β 1-mediated epithelial-mesenchymal transition in HK2 cells,” *Stem Cell Research & Therapy*, vol. 6, no. 1, p. 185, 2015.
- [51] G. ZHANG, D. WANG, S. MIAO, X. ZOU, G. LIU, and Y. ZHU, “Extracellular vesicles derived from mesenchymal stromal cells may possess increased therapeutic potential for acute kidney injury compared with conditioned medium in rodent models: a meta-analysis,” *Experimental and Therapeutic Medicine*, vol. 11, no. 4, pp. 1519–1525, 2016.
- [52] A. van Koppen, J. A. Joles, B. W. van Balkom et al., “Human embryonic mesenchymal stem cell-derived conditioned medium rescues kidney function in rats with established chronic kidney disease,” *PLoS One*, vol. 7, no. 6, p. e38746, 2012.
- [53] N. Ebrahim, I. A. Ahmed, N. I. Hussien et al., “Mesenchymal stem cell-derived exosomes ameliorated diabetic nephropathy by autophagy induction through the mTOR signaling pathway,” *Cells*, vol. 7, no. 12, p. 226, 2018.
- [54] K. Németh, A. Leelahavanichkul, P. S. Yuen et al., “Bone marrow stromal cells attenuate sepsis via prostaglandin E₂-dependent reprogramming of host macrophages to increase their interleukin-10 production,” *Nature Medicine*, vol. 15, no. 1, pp. 42–49, 2009.
- [55] Y. Yuan, L. Li, L. Zhu et al., “Mesenchymal stem cells elicit macrophages into M2 phenotype via improving transcription factor EB-mediated autophagy to alleviate diabetic nephropathy,” *Stem Cells*, vol. 38, no. 5, pp. 639–652, 2020.
- [56] J. S. Henao Agudelo, T. T. Braga, M. T. Amano et al., “Mesenchymal stromal cell-derived microvesicles regulate an internal pro-inflammatory program in activated macrophages,” *Frontiers in Immunology*, vol. 8, p. 881, 2017.
- [57] F. Zhang, C. Wang, X. Wen et al., “Mesenchymal stem cells alleviate rat diabetic nephropathy by suppressing CD103(+) DCs-mediated CD8(+) T cell responses,” *Journal of Cellular and Molecular Medicine*, vol. 24, no. 10, pp. 5817–5831, 2020.
- [58] S. E. Lee, J. E. Jang, H. S. Kim et al., “Mesenchymal stem cells prevent the progression of diabetic nephropathy by improving mitochondrial function in tubular epithelial cells,” *Experimental & Molecular Medicine*, vol. 51, no. 7, p. 77, 2019.
- [59] N. Konari, K. Nagaishi, S. Kikuchi, and M. Fujimiya, “Mitochondria transfer from mesenchymal stem cells structurally and functionally repairs renal proximal tubular epithelial cells in diabetic nephropathy _in vivo_,” *Scientific Reports*, vol. 9, no. 1, p. 5184, 2019.
- [60] O. A. Kost, O. V. Beznos, N. G. Davydova et al., “Superoxide dismutase 1 nanozyme for treatment of eye inflammation,” *Oxidative Medicine and Cellular Longevity*, vol. 2016, Article ID 5194239, 13 pages, 2016.
- [61] N. Rao, X. Wang, J. Xie et al., “Stem Cells from Human Exfoliated Deciduous Teeth Ameliorate Diabetic Nephropathy In Vivo and In Vitro by Inhibiting Advanced Glycation End Product- Activated Epithelial-Mesenchymal Transition,” *Stem Cells International*, vol. 2019, Article ID 2751475, 15 pages, 2019.
- [62] H. Lang and C. Dai, “Effects of bone marrow mesenchymal stem cells on plasminogen activator inhibitor-1 and renal fibrosis in rats with diabetic nephropathy,” *Archives of Medical Research*, vol. 47, no. 2, pp. 71–77, 2016.
- [63] F. Ezquer, M. Giraud-Billoud, D. Carpio, F. Cabezas, P. Conget, and M. Ezquer, “Proregenerative microenvironment triggered by donor mesenchymal stem cells preserves renal function and structure in mice with severe diabetes mellitus,” *BioMed Research International*, vol. 2015, Article ID 164703, 23 pages, 2015.
- [64] L. Zhang, K. Li, X. Liu et al., “Repeated systemic administration of human adipose-derived stem cells attenuates overt diabetic nephropathy in rats,” *Stem Cells and Development*, vol. 22, no. 23, pp. 3074–3086, 2013.
- [65] S. Wang, Y. Li, J. Zhao, J. Zhang, and Y. Huang, “Mesenchymal stem cells ameliorate podocyte injury and proteinuria in a type 1 diabetic nephropathy rat model,” *Biology of Blood and Marrow Transplantation*, vol. 19, no. 4, pp. 538–546, 2013.
- [66] G. C. Davey, S. B. Patil, A. O’Loughlin, and T. O’Brien, “Mesenchymal stem cell-based treatment for microvascular and secondary complications of diabetes mellitus,” *Frontiers in Endocrinology (Lausanne)*, vol. 5, p. 86, 2014.
- [67] K. Azushima, S. B. Gurley, and T. M. Coffman, “Modelling diabetic nephropathy in mice,” *Nature Reviews. Nephrology*, vol. 14, no. 1, pp. 48–56, 2018.
- [68] X. H. Pan, X. Y. Yang, X. Yao et al., “Bone-marrow mesenchymal stem cell transplantation to treat diabetic nephropathy in tree shrews,” *Cell Biochemistry and Function*, vol. 32, no. 5, pp. 453–463, 2014.
- [69] X. An, G. Liao, Y. Chen et al., “Intervention for early diabetic nephropathy by mesenchymal stem cells in a preclinical non-human primate model,” *Stem Cell Research & Therapy*, vol. 10, no. 1, p. 363, 2019.
- [70] T. Li, M. Xia, Y. Gao, Y. Chen, and Y. Xu, “Human umbilical cord mesenchymal stem cells: an overview of their potential in cell-based therapy,” *Expert Opinion on Biological Therapy*, vol. 15, no. 9, pp. 1293–1306, 2015.
- [71] Z. Wang, J. Cheng, X. Zhang, L. Chen, and J. Liu, “Umbilical cord-derived mesenchymal stem cells ameliorate nephrocyte injury and proteinuria in a diabetic nephropathy rat model,” *Journal of Diabetes Research*, vol. 2020, Article ID 8035853, 9 pages, 2020.
- [72] W. Ni, Y. Fang, L. Xie et al., “Adipose-derived mesenchymal stem cells transplantation alleviates renal injury in streptozotocin-induced diabetic nephropathy,” *The Journal of Histochemistry and Cytochemistry*, vol. 63, no. 11, pp. 842–853, 2015.
- [73] S. Takemura, T. Shimizu, M. Oka, S. Sekiya, and T. Babazono, “Transplantation of adipose-derived mesenchymal stem cell sheets directly into the kidney suppresses the progression of renal injury in a diabetic nephropathy rat model,” *J Diabetes Investig*, vol. 11, no. 3, pp. 545–553, 2020.
- [74] R. H. Lee, A. A. Pulin, M. J. Seo et al., “Intravenous hMSCs improve myocardial infarction in mice because cells embolized in lung are activated to secrete the anti-inflammatory protein TSG-6,” *Cell Stem Cell*, vol. 5, no. 1, pp. 54–63, 2009.
- [75] S. Wu, L. Li, G. Wang et al., “Ultrasound-targeted stromal cell-derived factor-1-loaded microbubble destruction promotes mesenchymal stem cell homing to kidneys in diabetic nephropathy rats,” *International Journal of Nanomedicine*, vol. 9, pp. 5639–5651, 2014.
- [76] Y. Zhang, C. Ye, G. Wang et al., “Kidney-Targeted Transplantation of Mesenchymal Stem Cells by Ultrasound- Targeted

- Microbubble Destruction Promotes Kidney Repair in Diabetic Nephropathy Rats,” *BioMed Research International*, vol. 2013, Article ID 526367, 13 pages, 2013.
- [77] J. M. Quimby, T. L. Webb, L. M. Habenicht, and S. W. Dow, “Safety and efficacy of intravenous infusion of allogeneic cryopreserved mesenchymal stem cells for treatment of chronic kidney disease in cats: results of three sequential pilot studies,” *Stem Cell Research & Therapy*, vol. 4, no. 2, p. 48, 2013.
- [78] L. A. Rashed, S. Elattar, N. Eltablawy, H. Ashour, L. M. Mahmoud, and Y. el-Esawy, “Mesenchymal stem cells pretreated with melatonin ameliorate kidney functions in a rat model of diabetic nephropathy,” *Biochemistry and Cell Biology*, vol. 96, no. 5, pp. 564–571, 2018.
- [79] Y. Wang, J. He, X. Pei, and W. Zhao, “Systematic review and meta-analysis of mesenchymal stem/stromal cells therapy for impaired renal function in small animal models,” *Nephrology (Carlton)*, vol. 18, no. 3, pp. 201–208, 2013.
- [80] D. K. Packham, I. R. Fraser, P. G. Kerr, and K. R. Segal, “Allogeneic mesenchymal precursor cells (MPC) in diabetic nephropathy: a randomized, placebo-controlled, dose escalation study,” *EBioMedicine*, vol. 12, pp. 263–269, 2016.
- [81] Q. Liu, S. Lv, J. Liu, S. Liu, Y. Wang, and G. Liu, “Mesenchymal stem cells modified with angiotensin-converting enzyme 2 are superior for amelioration of glomerular fibrosis in diabetic nephropathy,” *Diabetes Research and Clinical Practice*, vol. 162, article 108093, 2020.
- [82] C. Song, J. Xiang, J. Tang et al., “Thymidine kinase gene modified bone marrow mesenchymal stem cells as vehicles for anti-tumor therapy,” *Human Gene Therapy*, vol. 22, no. 4, pp. 439–449, 2011.
- [83] J. Yin, J. K. Kim, J. H. Moon et al., “hMSC-mediated concurrent delivery of endostatin and carboxylesterase to mouse xenografts suppresses glioma initiation and recurrence,” *Molecular Therapy*, vol. 19, no. 6, pp. 1161–1169, 2011.
- [84] T. Sadhukha, T. D. O’Brien, and S. Prabha, “Nano-engineered mesenchymal stem cells as targeted therapeutic carriers,” *Journal of Controlled Release*, vol. 196, pp. 243–251, 2014.
- [85] B. Layek, T. Sadhukha, J. Panyam, and S. Prabha, “Nano-engineered mesenchymal stem cells increase therapeutic efficacy of anticancer drug through true active tumor targeting,” *Molecular Cancer Therapeutics*, vol. 17, no. 6, pp. 1196–1206, 2018.
- [86] S. M. van Dommelen, P. Vader, S. Lakhali et al., “Microvesicles and exosomes: opportunities for cell-derived membrane vesicles in drug delivery,” *Journal of Controlled Release*, vol. 161, no. 2, pp. 635–644, 2012.
- [87] M. Wang, F. Xie, X. Wen et al., “Therapeutic PEG-ceramide nanomicelles synergize with salinomycin to target both liver cancer cells and cancer stem cells,” *Nanomedicine (Lond)*, vol. 12, no. 9, pp. 1025–1042, 2017.
- [88] T. R. Lunavat, S. C. Jang, L. Nilsson et al., “RNAi delivery by exosome-mimetic nanovesicles - Implications for targeting c-Myc in cancer,” *Biomaterials*, vol. 102, pp. 231–238, 2016.
- [89] S. C. Jang, O. Y. Kim, C. M. Yoon et al., “Bioinspired exosome-mimetic nanovesicles for targeted delivery of chemotherapeutics to malignant tumors,” *ACS Nano*, vol. 7, no. 9, pp. 7698–7710, 2013.
- [90] S. Lv, J. Cheng, A. Sun et al., “Mesenchymal stem cells transplantation ameliorates glomerular injury in streptozotocin-induced diabetic nephropathy in rats via inhibiting oxidative stress,” *Diabetes Research and Clinical Practice*, vol. 104, no. 1, pp. 143–154, 2014.

Research Article

Semaphorin3B Promotes Proliferation and Osteogenic Differentiation of Bone Marrow Mesenchymal Stem Cells in a High-Glucose Microenvironment

Quan Xing ^{1,2}, Jingyi Feng ^{2,3} and Xiaolei Zhang ^{2,3}

¹Department of Zhujiang New Town Clinic, Guanghua School and Hospital of Stomatology, Sun Yat-sen University, Guangzhou 510055, China

²Guangdong Provincial Key Laboratory of Stomatology, Sun Yat-sen University, Guangzhou, China

³Department of Operative Dentistry and Endodontics, Guanghua School and Hospital of Stomatology, Sun Yat-sen University, Guangzhou 510055, China

Correspondence should be addressed to Quan Xing; xingquan@mail.sysu.edu.cn and Xiaolei Zhang; zhangxl35@mail.sysu.edu.cn

Received 2 December 2020; Revised 22 January 2021; Accepted 8 February 2021; Published 26 February 2021

Academic Editor: Adam Ye

Copyright © 2021 Quan Xing et al. This is an open access article distributed under the Creative Commons Attribution License, which permits unrestricted use, distribution, and reproduction in any medium, provided the original work is properly cited.

Bone marrow mesenchymal stem cells (BMSCs) play an essential role in osteogenesis and bone metabolism and have already been recognized as one of the most popular seed cells for bone tissue engineering for bone diseases. However, high-glucose (HG) conditions in type 2 diabetes mellitus (T2DM) exert deleterious effects on BMSC proliferation and osteogenic differentiation. Semaphorin 3B (Sema3B) increases osteoblast differentiation in bone metabolism. Here, we determined the role of Sema3B in the proliferation and osteogenic differentiation of BMSCs in the HG microenvironment. The HG microenvironment decreased Sema3B expression in BMSCs. Moreover, HG inhibited BMSC proliferation. Furthermore, HG inhibited osteogenic differentiation in BMSCs by decreasing the expression of bone formation markers, alkaline phosphatase (ALP) activity, and mineralization. However, the administration of recombinant Sema3B reversed all of these effects. Moreover, our study found that Sema3B could activate the Akt pathway in BMSCs. Sema3B rescues defects in BMSC proliferation and osteogenic differentiation in the HG microenvironment by activating the Akt pathway. These effects were significantly reduced by treatment with an Akt inhibitor. Together, these findings demonstrate that Sema3B promotes the proliferation and osteogenic differentiation of BMSCs via the Akt pathway under HG conditions. Our study provides new insights into the potential ability of Sema3B to ameliorate BMSC proliferation and osteogenic differentiation in an HG microenvironment.

1. Introduction

Bone marrow mesenchymal stem cells (BMSCs) are characterized by differentiation into various types of cells, such as osteoblasts, chondrocytes, and other cell types [1–3]. BMSCs play a critical role in osteogenesis and bone metabolism [1–6]. Inhibition of the proliferation and osteogenic differentiation of BMSCs induces dysfunction of bone metabolism and gives rise to multiple bone loss diseases, including osteoporosis, periodontitis, and dental implantation failure [2, 7, 8]. Moreover, BMSCs have already

become an attractive option as seed cells for the treatment of osteoblastic diseases [6–8]. However, many pathogenic factors suppress the proliferation and osteogenic differentiation of BMSCs, which leads to increased bone loss [9–12]. For instance, high-glucose conditions in type 2 diabetes mellitus (T2DM) exert deleterious effects on BMSC proliferation and osteogenic differentiation [9, 13–15].

T2DM is a highly prevalent metabolic disease globally and is characterized by excessive blood glucose, insulin resistance, and relative insulin deficiency [16]. T2DM is associated with impaired bone remodeling, osteopenia,

osteoporosis, and other diabetes-related bone diseases [17–19]. Diabetes mellitus impairs bone metabolism, suppresses bone formation, and impedes fracture healing [20, 21]. Increasing evidence suggests that a high-glucose environment inhibits BMSC proliferation and osteogenic differentiation, inducing diabetic bone disease [9, 13, 15, 22–24]. Agents that could promote the osteogenic differentiation and proliferation of BMSCs may represent promising candidates to ameliorate the disorder of BMSCs in diabetic osteopathy.

As secreted glycoproteins on the cell surface, semaphorins are capable of regulating cell growth, cell differentiation, and cell migration in various tissues [25, 26]. A few studies showed that some semaphorin family proteins are crucial regulators of skeletal homeostasis [25–27]. Former studies have shown that semaphorin 3B (Sema3B) is associated with the bone metabolism process [28–30]. $1,25(\text{OH})_2\text{D}_3$ was suggested to increase transcription of Sema3B in osteoblasts [28]. Osteoblasts derived from transgenic mice expressing overexpression of Sema3B could promote osteogenic differentiation of BMSCs in vitro, whereas depletion of Sema3B impaired BMSC osteoblastic differentiation [29, 30]. Moreover, $\text{TNF-}\alpha$ decreased Sema3B expression by inhibiting Wnt signaling, but Sema3B overexpression reversed the osteogenic defects of BMSCs treated with $\text{TNF-}\alpha$ [29]. Wnt signaling is involved in this process [29]. However, the role of Sema3B in BMSC proliferation and osteogenic differentiation in a high-glucose microenvironment has still not been elucidated. Thus, the present study is aimed at investigating the effect of high glucose on the proliferation and osteogenic differentiation of BMSCs and clarifying the role of Sema3B in this process.

2. Materials and Methods

2.1. Cell Culture. Mouse BMSCs were isolated from six-week-old male C57BL/6 mice. Briefly, the femur and tibia bones were aseptically removed. The bone marrow was rinsed with culture medium consisting of α -MEM (Invitrogen, USA) supplement with 20% FBS (HyClone, Rockford) and 1% penicillin/streptomycin. Then, the cells were allowed to grow at 37°C with 5% CO_2 . BMSCs were separated by differential adhesion to culture plastic. The attached cells were grown in culture medium and used for further experiments. All procedures involving mice were approved by the Animal Ethical and Welfare Committee of Sun Yat-sen University, China.

In the high-glucose treatment (HG) group, BMSCs were subject to high glucose by incubation in a medium with 25 mM glucose. The normal-glucose treatment (NG) group was treated with 5.5 mM glucose. For inhibition of the Akt signaling pathway, cells were pretreated with an Akt inhibitor (MK2206) at a concentration of $10\ \mu\text{M}$ (Selleck, China).

2.2. Flow Cytometry. Marker expression on the BMSC surface was assessed using FACSCalibur (BD Biosciences, USA). Briefly, BMSCs at passage 3 were trypsinized, washed, and resuspended in PBS. Then, 2×10^5 cells were incubated with PE- or FITC-labeled mouse cell surface

TABLE 1: Primer sequence used for real-time PCR analysis.

Gene	forward primer sequence (5'-3')	reverse primer sequence (5'-3')
Sema3B [29]	CTTCGGCTCTCCTTCAAGA	CAAGGCTTCATAACAGCAGGT
OCN [43]	CTGCGCTCTGTCTCTCTGAC	TTAAGCTCACACTGCTCCCG
ALP [43]	CCGGCTGGAGATGGACAAAT	CTCATTGCCCTGAGTGGTG
Runx2 [43]	AAATGCCTCCGCTGTTATGAA	GCTCCGGCCCCACAAATCT
COL1A1 [44]	GCAACAGTCGCTTACCTACA	CAATGTCCAAGGGAGCCACAT
β -Actin [42]	TGACAGGATGCAGAAGGAGA	CGTCAGGAGGAGCAATG

marker antibodies against CD29, CD44, CD34, and CD45 (BD Biosciences), as well as isotype control antibodies at 4°C for 30 min. Then, the samples were analyzed using FACSCalibur.

2.3. Real-Time PCR. Total RNA was isolated, and reverse transcription was performed using an Omniscript Reverse Transcription Kit (Qiagen, Germany). The primers used for the target sequence are listed in Table 1. Real-time PCR was performed by the QuantiTect SYBR[®] Green PCR Kit (Qiagen). The relative mRNA expression levels of the target genes were quantified in comparison to the expression of β -actin using the $2^{-\Delta\Delta\text{CT}}$ method. Real-time PCR results are presented as the mean \pm SEM.

2.4. Western Blotting. Total protein was prepared with M-PER Protein Extraction Reagent (Thermo Scientific). Protein concentrations were measured using a BCA protein assay reagent (Pierce). Briefly, 30 mg of sample was subjected to 10% SDS-PAGE and electrotransferred onto a PVDF membrane. The following primary antibodies were used for western blotting: Sema3B (1:1000, Abcam, Cambridge, UK), phospho-Akt (Ser473) (p-Akt) (1:1000, Cell Signaling Technology, USA), Akt (1:1000, Cell Signaling Technology), and β -actin (1:4000) (Santa Cruz Biotechnology, USA). PVDF membranes were then incubated with an appropriate horseradish peroxidase-conjugated antibody (Santa Cruz Biotechnology). The signal was visualized using a chemiluminescent reagent kit (Pierce). Relative band densities were calculated (Image J 1.8.0, NIH).

2.5. ALP Activity. BMSCs (1×10^4 cells/cm²) were treated with 100 ng/ml Sema3B (R&D Systems, USA) in NG or HG medium for up to 14 days. Total protein was extracted from cells on ice at days 7 and 14 using M-PER Protein Extraction Reagent (Thermo Scientific). Protein concentrations were assessed using a BCA protein assay reagent (Pierce). ALP activity was detected using an ALP activity detection kit (Sigma-Aldrich).

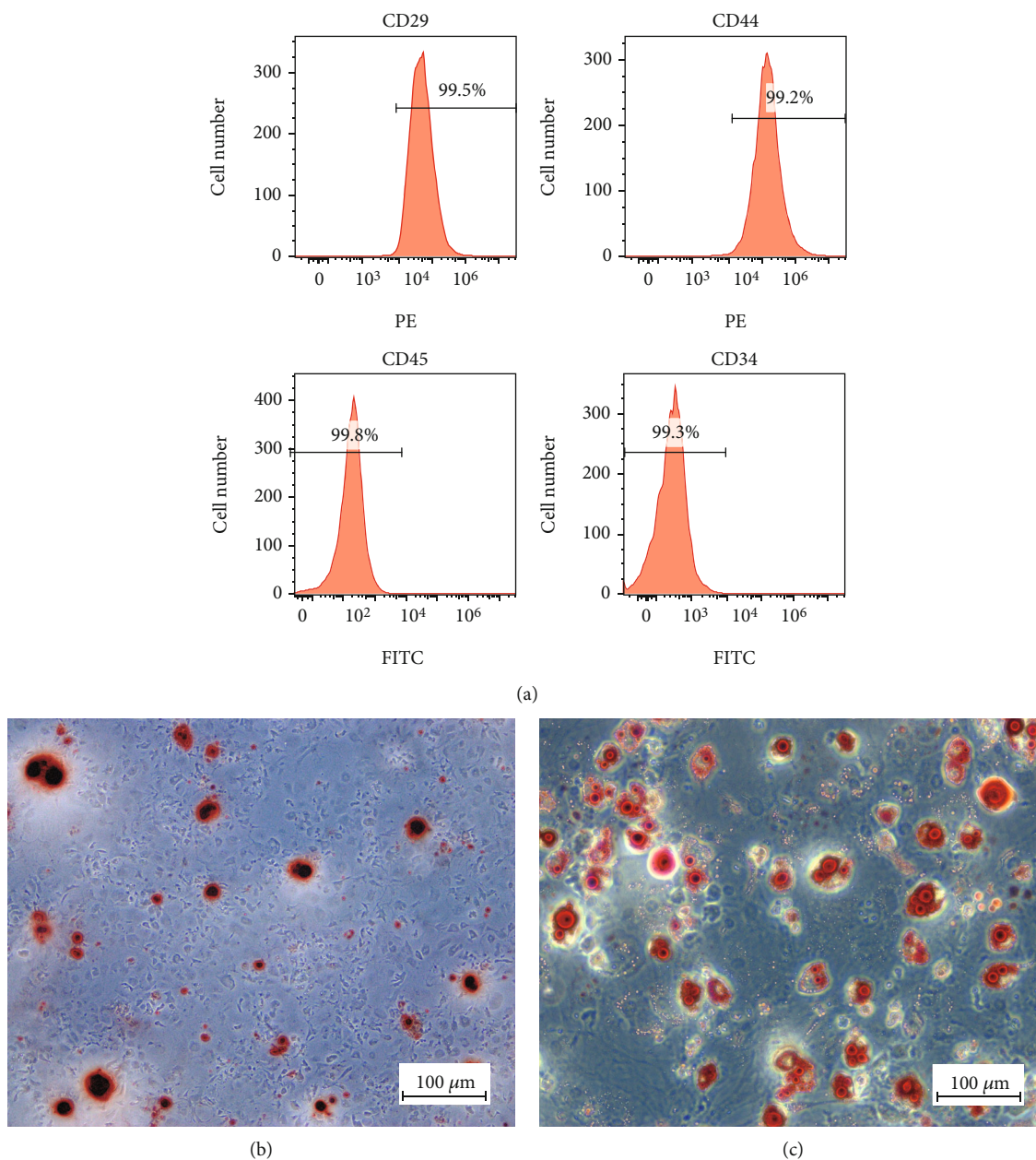


FIGURE 1: Identification of BMSCs. Cells were evaluated by surface markers and their multipotency to differentiate. (a) Cells were stained with FITC- or PE-conjugated antibodies. The differentiation of BMSCs using an induction medium induces cell differentiation into osteocytes and adipocytes. The multipotency of BMSCs was confirmed as positive by alizarin red (b) and oil red O staining (c), indicating the differentiation of BMSCs into osteocytes and adipocytes, respectively.

2.6. Mineralization Assay. BMSCs were treated with recombinant 100 ng/ml Sema3B in osteogenic differentiation media with NG or HG for 14 days. The culture medium was renewed every three days. Mineralization was identified by alizarin red staining on the 14th day as previously described [31]. Then, the cells were treated with ethylpyridium chloride and quantified at 550 nm.

2.7. Osteogenic and Adipogenic Differentiation of BMSCs. For adipogenesis, BMSCs (1×10^4 cells/cm²) were cultured in adipogenic differentiation medium containing with 0.1 μM

dexamethasone, 1 μM insulin, 200 μM dexamethasone, and 250 μM Misobutylmethylxanthine (Sigma-Aldrich). The medium was replaced every 3 days. Twenty-one days later, the cells were fixed with formalin and subjected to 0.5% (w/v) oil red O staining (Sigma-Aldrich).

For osteogenic differentiation, BMSCs (1×10^4 cells/cm²) were cultured in osteogenic differentiation medium containing α -MEM containing 10% FBS, 10 mM β -glycerophosphate, and 50 mg/ml ascorbic acid (Sigma-Aldrich). Twenty-one days later, the cells were fixed and stained with alizarin red (Sigma-Aldrich).

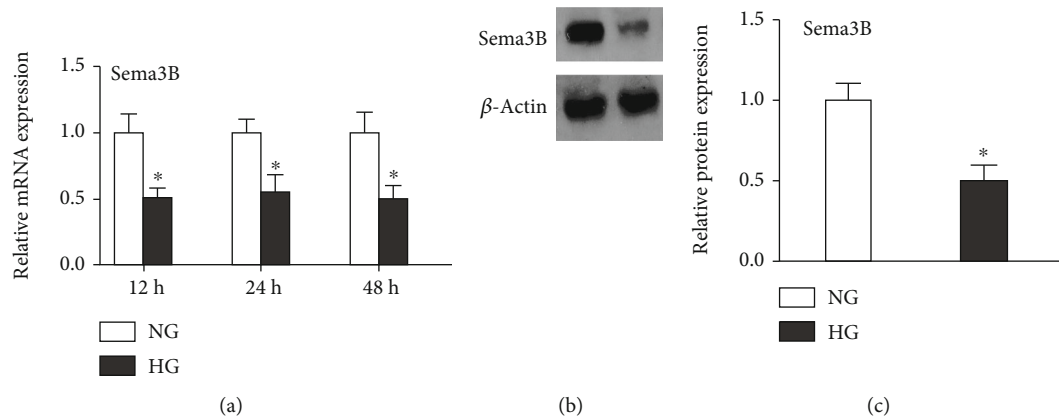


FIGURE 2: Effects of HG on Sema3B expression. Sema3B expression levels were measured by real-time PCR and western blotting. (a) HG treatment suppressed Sema3B mRNA expression in BMSCs at 24, 48, and 72 h. (b) Representative western blots. (c) HG decreased Sema3B protein expression in BMSCs. Data are expressed as the mean \pm SEM ($n = 3$). * $P < 0.05$ compared to the control sample.

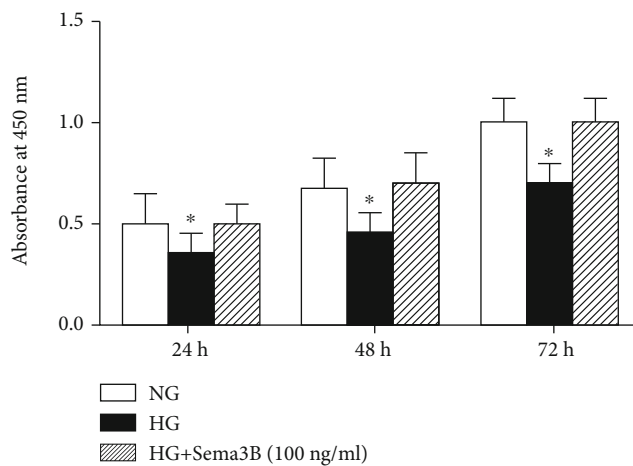


FIGURE 3: Effects of Sema3B on BMSC proliferation under HG treatment. The proliferation of BMSCs cultured under HG conditions was analyzed by CCK-8 assays at 24, 48, and 72 h. The results are represented the mean \pm SEM ($n = 3$). * $P < 0.05$ compared to the other sample.

2.8. Cell Proliferation Assay. Briefly, BMSCs were seeded in and incubated with experimental compounds for 24, 48, and 72 h. Then, 10 μ l of CCK-8 solution (Dojindo Molecular Technologies, Japan) was added to each well at the end of the experiment. The absorbance was measured at 450 nm 2 h later.

2.9. Statistical Analysis. All data are shown as the mean \pm SEM. Statistical comparisons were made by one-way ANOVA or two-way ANOVA as appropriate. A value of $P < 0.05$ was considered statistically significant.

3. Results

3.1. Characterization of Mouse BMSCs. The phenotypic characteristics of BMSCs were analyzed by flow cytometry, dem-

onstrating that the cells were CD29+, CD44+, CD45-, and CD34-. The results are shown in Figure 1(a).

As pluripotent stem cells, BMSCs were assessed for their ability to differentiate into osteoblasts using alizarin red and adipocytes using oil red O staining. The results showed positive staining, as demonstrated in Figures 1(b) and 1(c).

3.2. HG Suppressed Sema3B Expression in BMSCs. To assess the effects of HG on Sema3B expression, the mRNA and protein levels of Sema3B in BMSCs were measured by real-time PCR and western blotting. Real-time PCR demonstrated that HG significantly decreased Sema3B mRNA levels in BMSCs ($P < 0.05$) (Figure 2(a)). Western blotting revealed that HG significantly reduced Sema3B protein expression ($P < 0.05$) (Figures 2(b) and 2(c)).

3.3. The Effect of Sema3B on BMSC Proliferation under HG Conditions. To detect the effects of Sema3B on BMSC proliferation, we measured BMSC proliferation under HG conditions using CCK-8 assays. HG significantly decreased BMSC proliferation compared with that of any of the other groups at each indicated time point. Moreover, recombinant Sema3B reversed the reduction in cell proliferation ($P < 0.05$) (Figure 3(a)).

3.4. Sema3B Alleviates the Inhibition of Osteogenic Differentiation Markers. To investigate the effects of Sema3B on BMSCs in the HG microenvironment, we assessed the expression of specific osteogenesis markers by real-time PCR. The results showed that osteocalcin (OCN), Runx2, type I collagen α 1 (COL1A1), and ALP mRNA levels in BMSCs were markedly decreased upon treatment with HG. Furthermore, Sema3B markedly rescued the decrease in OCN, Runx2, COL1A1, and ALP mRNA expression levels in the HG groups (Figures 4(a)–4(d)).

3.5. Sema3B Ameliorates HG-Induced Inhibition of Osteogenic Differentiation. To investigate the role of Sema3B in osteogenic differentiation, we measured ALP activity and

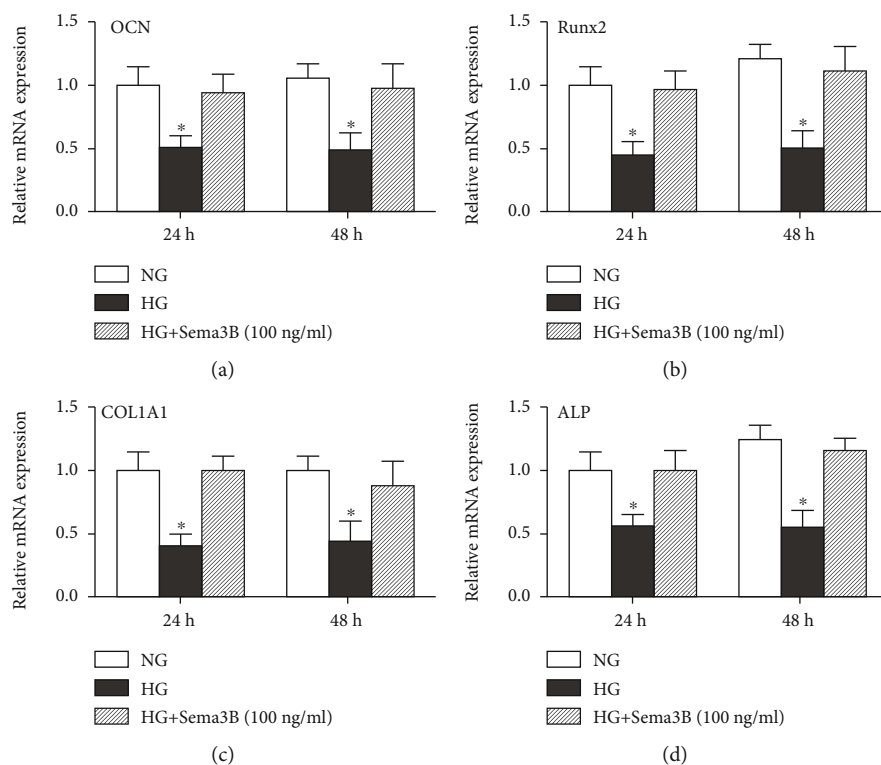


FIGURE 4: Effects of Sema3B on osteogenic markers under HG treatment. OCN (a), Runx2 (b), COL1A1 (c), and ALP (d) mRNA expression levels in BMSCs were measured by real-time PCR at each time point. Real-time PCR results are expressed as the mean \pm SEM ($n = 3$). * $P < 0.05$ compared to the other samples.

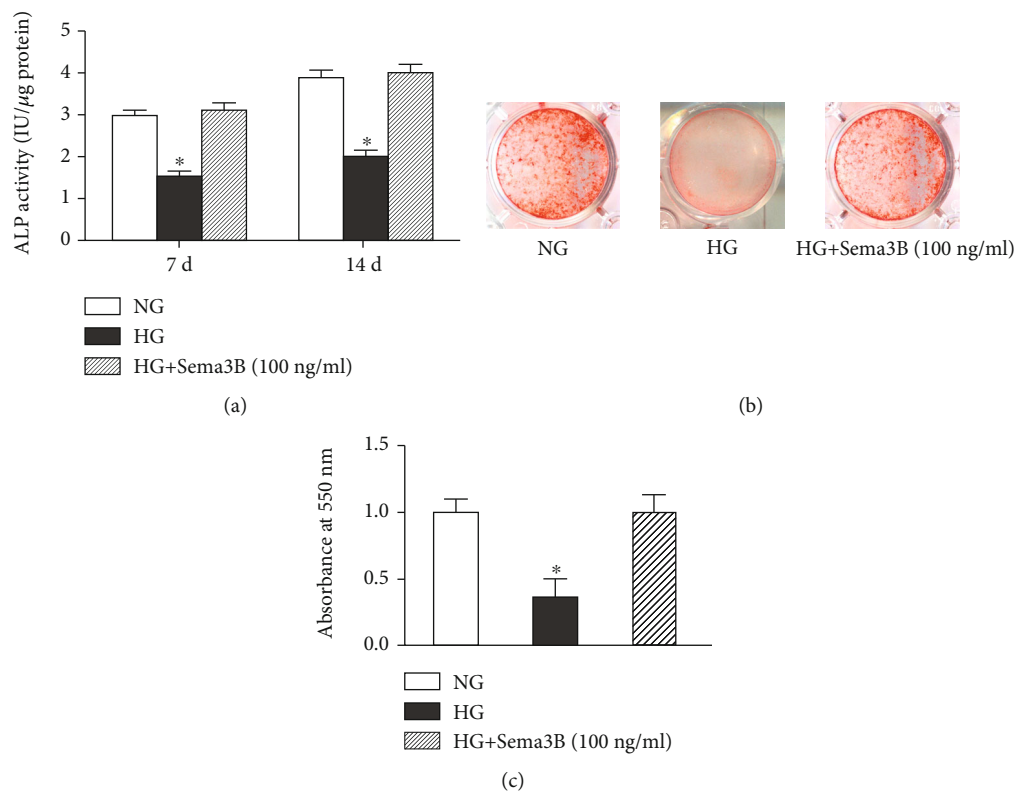


FIGURE 5: Effects of Sema3B on osteogenic differentiation under HG treatment. (a) ALP activity is presented as the mean \pm SEM ($n = 3$). (b) Alizarin red S staining. (c) Quantification of alizarin red staining. The results of alizarin red staining are presented as the mean \pm SEM ($n = 3$). * $P < 0.05$ compared to the other samples.

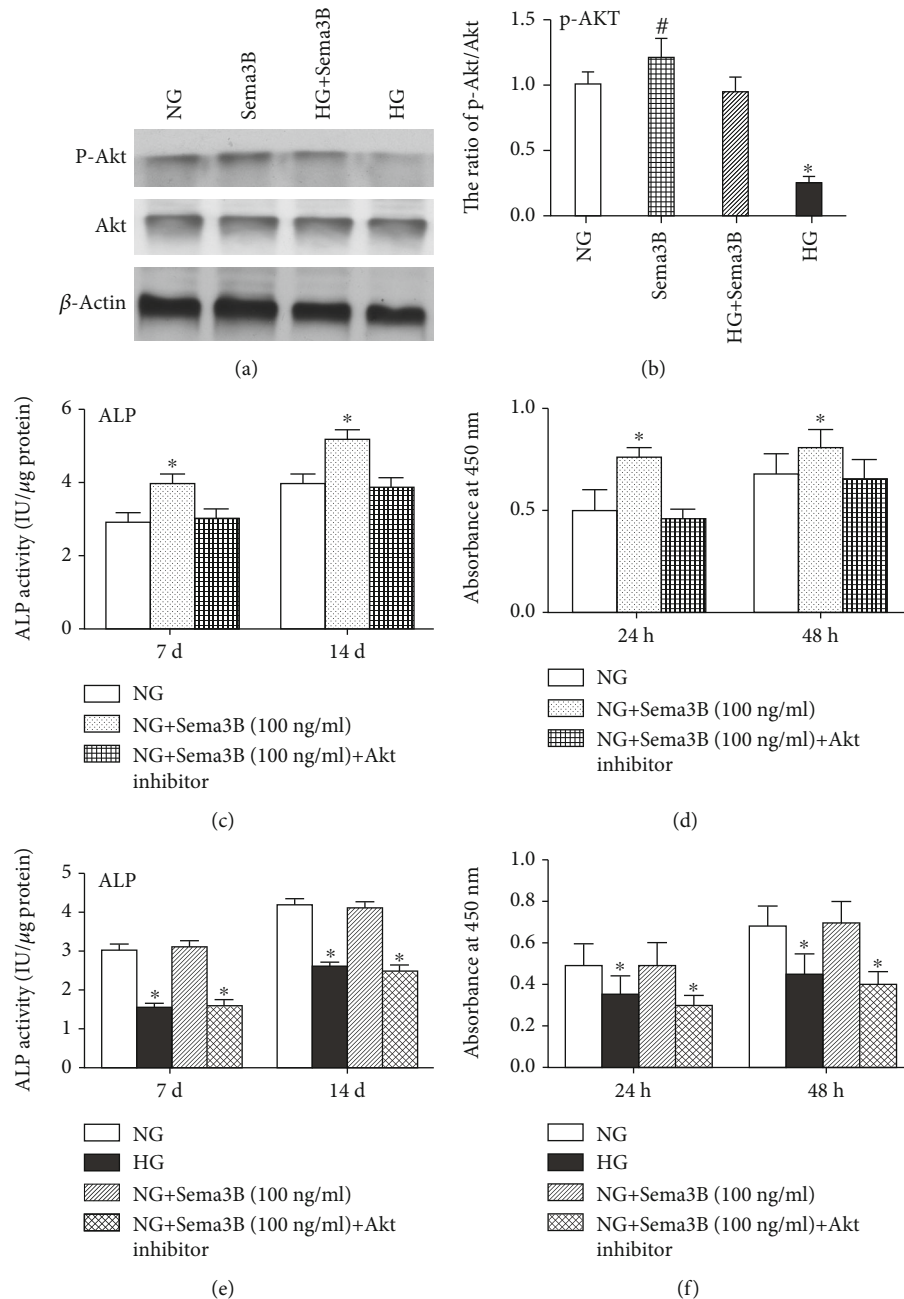


FIGURE 6: Effects of Sema3B on BMSCs by the Akt pathway under HG treatment. (a) Representative western blots are shown. (b) The expression levels of phospho-Akt and Akt were evaluated by western blotting. (c) ALP activity of BMSCs was detected using an ALP activity detection kit. (d) BMSC proliferation was assessed by CCK-8 assay. Cells were pretreated with an Akt inhibitor (MK2206) (10 μ M) for 2 h followed by stimulation with HG or HG + Sema3B. Then, (e) ALP activity of BMSCs and (f) the proliferation of BMSCs were assessed. Data are expressed as the mean \pm SEM ($n = 3$). * $P < 0.05$ compared to the other samples, # $P < 0.05$ compared to the control sample.

mineralization in BMSCs with and without Sema3B (100 ng/ml) treatment.

HG significantly reduced ALP activity in BMSCs at 7 days (1.50 IU/ μ g) and 14 days (2.01 IU/ μ g) ($P < 0.05$). Sema3B administration significantly reversed the decrease in ALP activity at the indicated time points (3.10 IU/ μ g at 7 days and 4.05 IU/ μ g at 14 days) ($P < 0.05$) (Figure 5(a)).

Mineralization was significantly decreased by HG treatment. The administration of Sema3B significantly rescued

the HG-induced inhibition of mineralization in BMSCs ($P < 0.05$) (Figures 5(b) and 5(c)).

3.6. Sema3B Rescues HG-Induced Inhibition of the Akt Pathway. In this experiment, we investigated the relationship between Akt signaling and Sema3B in BMSCs proliferation and osteogenic differentiation under an HG microenvironment. HG significantly decreased Akt phosphorylation compared with the NG group. However, treatment of cells

with Sema3B recovered the reduced levels of Akt phosphorylation observed under HG conditions ($P < 0.05$) (Figures 6(a) and 6(b)).

Moreover, Sema3B elevated ALP activity and proliferation in BMSCs. Inhibition of the Akt pathway abolished the Sema3B-mediated induction of ALP activity and proliferation in BMSCs ($P < 0.05$) (Figures 6(c) and 6(d)).

Furthermore, BMSCs are incubated with MK2206 prior to Sema3B administration. The results demonstrated that Sema3B restored HG-mediated suppression of ALP activity and proliferation. However, the protective effect of Sema3B was inhibited by pretreatment with an Akt inhibitor ($P < 0.05$) (Figures 6(e) and 6(f)). The results indicated that Sema3B ameliorates the suppression of BMSC proliferation and osteogenesis under an HG microenvironment via the Akt pathway.

4. Discussion

BMSCs derived from bone marrow stroma or connective tissue are easy to isolate and undergo pluripotent differentiation; thus, these cells are considered useful for applications in a variety of clinical therapies [8, 32–35]. In recent years, accumulating studies have demonstrated that BMSCs can be used in bone defect repair due to their capacity for osteogenic differentiation [3, 4, 6, 8]. However, many pathologic factors decrease proliferation and osteogenic differentiation, such as inflammation, a high-glucose environment, and other factors [9, 11–13]. Hyperglycemia is a major cause of a series of diabetic complications, including diabetic osteopathy [15, 20]. High glucose has been reported to inhibit the proliferation and osteogenic differentiation of BMSCs through the BMP signaling pathway [36]. Moreover, optimal glycemic control has been recognized to associate with successfully osseointegrated dental implantation in diabetic patients [37]. In our study, HG decreased BMSC proliferation. Moreover, HG reduced the expression of osteogenesis markers and osteogenic differentiation in BMSCs. The results were consistent with previous studies. However, the osteogenic differentiation of BMSCs under HG conditions is not completely understood. Identifying factors that could promote BMSC proliferation and osteogenic differentiation in the HG microenvironment may reveal promising candidates that can ameliorate the function of BMSCs in hyperglycemia-induced bone diseases.

The involvement of Sema3B in bone metabolism has been reported in previous studies [28–30]. Sema3B was confirmed to enhance osteogenic differentiation of BMSCs [29, 30]. Moreover, Sema3B was found to be involved in estrogen deficiency-induced osteoporosis [29]. The effect of HG on BMSC proliferation was analyzed by CCK-8 assay. Based on these results, HG caused significant inhibition of BMSC proliferation compared with that of the NG group. In addition, Sema3B treatment markedly reversed HG-induced inhibition of BMSC proliferation.

Our data also demonstrated that Sema3B reversed the HG-induced decrease in OCN, Runx2, ALP, and COL1A1 mRNA expression in BMSCs. Furthermore, Sema3B attenuated HG-induced reduction of ALP activity and mineraliza-

tion in BMSCs. Therefore, these observations may suggest that Sema3B is a promising candidate for promoting osteogenesis of BMSCs in an HG microenvironment.

The Akt pathway plays an essential role in bone development and skeletal remodeling [38, 39]. Recently, numerous studies have shown that high glucose suppresses proliferation and osteogenic differentiation by inactivating the PI3K/Akt signaling pathway in osteoblasts [22, 40, 41]. In this present experiment, we observed that Sema3B significantly increased Akt phosphorylation. However, pretreatment with an Akt inhibitor eliminated the increased proliferation and ALP activity of BMSCs in the HG microenvironment, suggesting that Sema3B promotes osteogenic differentiation of BMSCs under HG conditions by modulating the Akt pathway.

Thus, we found that HG impaired the proliferation and osteogenic differentiation of BMSCs. Furthermore, our study demonstrated that Sema3B could prevent HG-mediated BMSC dysfunction through modulation of the Akt pathway. Sema3B might represent a promising agent to ameliorate the proliferation and osteogenic differentiation of BMSCs in an HG microenvironment. Therefore, our study may lead to new insights into more effective clinical interventions for hyperglycemia-related bone diseases.

Data Availability

The data used to support the findings of this study are available from the corresponding author upon reasonable request.

Conflicts of Interest

No conflicts of interest exist regarding the submission of this manuscript, and all authors approved the manuscript for publication.

Authors' Contributions

Quan Xing and Jingyi Feng contributed equally to this study. Quan Xing and Jingyi Feng are co-first authors.

Acknowledgments

This study is supported by the National Nature of Science Foundation of China (Grant No. 81300874).

References

- [1] Y. J. Lv, Y. Yang, B. D. Sui et al., "Resveratrol counteracts bone loss via mitofilin-mediated osteogenic improvement of mesenchymal stem cells in senescence-accelerated mice," *Theranostics*, vol. 8, no. 9, pp. 2387–2406, 2018.
- [2] S. C. Huo and B. Yue, "Approaches to promoting bone marrow mesenchymal stem cell osteogenesis on orthopedic implant surface," *World Journal of Stem Cells*, vol. 12, no. 7, pp. 545–561, 2020.
- [3] M. N. Knight and K. D. Hankenson, "Mesenchymal stem cells in bone regeneration," *Advances in Wound Care*, vol. 2, no. 6, pp. 306–316, 2013.
- [4] P. Garg, M. M. Mazur, A. C. Buck, M. E. Wandtke, J. Liu, and N. A. Ebraheim, "Prospective review of mesenchymal stem

- cells differentiation into osteoblasts," *Orthopaedic Surgery*, vol. 9, no. 1, pp. 13–19, 2017.
- [5] J. O. Nehlin, A. Jafari, M. Tencerova, and M. Kassem, "Aging and lineage allocation changes of bone marrow skeletal (stromal) stem cells," *Bone*, vol. 123, pp. 265–273, 2019.
 - [6] Y. Z. Jin and J. H. Lee, "Mesenchymal stem cell therapy for bone regeneration," *Clinics in Orthopedic Surgery*, vol. 10, no. 3, pp. 271–278, 2018.
 - [7] Y. Feng, P. Wan, L. Yin, and X. Lou, "The inhibition of microRNA-139-5p promoted osteoporosis of bone marrow-derived mesenchymal stem cells by targeting Wnt/beta-catenin signaling pathway by NOTCH1," *Journal of Microbiology and Biotechnology*, vol. 30, no. 3, pp. 448–458, 2020.
 - [8] T. Ouchi and T. Nakagawa, "Mesenchymal stem cell-based tissue regeneration therapies for periodontitis," *Regenerative Therapy*, vol. 14, pp. 72–78, 2020.
 - [9] W. Hankamolsiri, S. Manochantr, C. Tantrawatpan, D. Tantikanlayaporn, P. Tapanadechopone, and P. Kheolamai, "The effects of high glucose on adipogenic and osteogenic differentiation of gestational tissue-derived MSCs," *Stem Cells International*, vol. 2016, Article ID 9674614, 15 pages, 2016.
 - [10] H. Kang, H. Chen, P. Huang et al., "Glucocorticoids impair bone formation of bone marrow stromal stem cells by reciprocally regulating microRNA-34a-5p," *Osteoporosis International*, vol. 27, no. 4, pp. 1493–1505, 2016.
 - [11] L. Wu, G. Zhang, C. Guo, X. Zhao, D. Shen, and N. Yang, "MiR-128-3p mediates TNF- α -induced inflammatory responses by regulating Sirt1 expression in bone marrow mesenchymal stem cells," *Biochemical and Biophysical Research Communications*, vol. 521, no. 1, pp. 98–105, 2020.
 - [12] J. Tang, T. Wu, J. Xiong et al., "Porphyromonas gingivalis lipopolysaccharides regulate functions of bone marrow mesenchymal stem cells," *Cell Proliferation*, vol. 48, no. 2, pp. 239–248, 2015.
 - [13] Z. Zhai, W. Chen, Q. Hu, X. Wang, Q. Zhao, and M. Tuerxunyming, "High glucose inhibits osteogenic differentiation of bone marrow mesenchymal stem cells via regulating miR-493-5p/ZEB2 signalling," *Journal of Biochemistry*, vol. 167, no. 6, pp. 613–621, 2020.
 - [14] Y. Tang, L. Zheng, J. Zhou et al., "miR-203-3p participates in the suppression of diabetes-associated osteogenesis in the jaw bone through targeting Smad1," *International Journal of Molecular Medicine*, vol. 41, no. 3, pp. 1595–1607, 2018.
 - [15] K. C. Huang, P. Y. Chuang, T. Y. Yang, T. W. Huang, and S. F. Chang, "Hyperglycemia inhibits osteoblastogenesis of rat bone marrow stromal cells via activation of the Notch2 signaling pathway," *International Journal of Medical Sciences*, vol. 16, no. 5, pp. 696–703, 2019.
 - [16] D. R. Whiting, L. Guariguata, C. Weil, and J. Shaw, "IDF diabetes atlas: global estimates of the prevalence of diabetes for 2011 and 2030," *Diabetes Research and Clinical Practice*, vol. 94, no. 3, pp. 311–321, 2011.
 - [17] C. Guja, L. Guja, and R. D. Miulescu, "Effect of type 2 diabetes medications on fracture risk," *Annals of Translational Medicine*, vol. 7, no. 20, p. 580, 2019.
 - [18] P. Vestergaard, L. Rejnmark, and L. Mosekilde, "Diabetes and its complications and their relationship with risk of fractures in type 1 and 2 diabetes," *Calcified Tissue International*, vol. 84, no. 1, pp. 45–55, 2009.
 - [19] C. Hamann, S. Kirschner, K. P. Günther, and L. C. Hofbauer, "Bone, sweet bone—osteoporotic fractures in diabetes mellitus," *Nature Reviews. Endocrinology*, vol. 8, no. 5, pp. 297–305, 2012.
 - [20] J. M. Forslund and M. T. Archdeacon, "The pathobiology of diabetes mellitus in bone metabolism, fracture healing, and complications," *American journal of orthopedics (Belle Mead, N.J.)*, vol. 44, pp. 453–457, 2015.
 - [21] M. Al-Hariri, "Sweet bones: the pathogenesis of bone alteration in diabetes," *Journal of Diabetes Research*, vol. 2016, Article ID 6969040, 5 pages, 2016.
 - [22] X. Ying, X. Chen, H. Liu et al., "Silibinin alleviates high glucose-suppressed osteogenic differentiation of human bone marrow stromal cells via antioxidant effect and PI3K/Akt signaling," *European Journal of Pharmacology*, vol. 765, pp. 394–401, 2015.
 - [23] X. Dong, X. Wang, M. Xing et al., "Inhibition of the negative effect of high glucose on osteogenic differentiation of bone marrow stromal cells by silicon ions from calcium silicate bioceramics," *Regenerative Biomaterials*, vol. 7, pp. 9–17, 2019.
 - [24] B. Cao, N. Liu, and W. Wang, "High glucose prevents osteogenic differentiation of mesenchymal stem cells via lncRNA AK028326/CXCL13 pathway," *Biomedicine & pharmacotherapy = Biomedecine & pharmacotherapie*, vol. 84, pp. 544–551, 2016.
 - [25] P. Giacobini and V. Prevot, "Semaphorins in the development, homeostasis and disease of hormone systems," *Seminars in Cell & Developmental Biology*, vol. 24, no. 3, pp. 190–198, 2013.
 - [26] L. Verlinden, D. Vanderschueren, and A. Verstuyf, "Semaphorin signaling in bone," *Molecular and Cellular Endocrinology*, vol. 432, pp. 66–74, 2016.
 - [27] M. Hayashi, T. Nakashima, M. Taniguchi, T. Kodama, A. Kumanogoh, and H. Takayanagi, "Osteoprotection by semaphorin 3A," *Nature*, vol. 485, no. 7396, pp. 69–74, 2012.
 - [28] J. Ryyänen, C. Kriebitzsch, M. B. Meyer et al., "Class 3 semaphorins are transcriptionally regulated by 1,25(OH) 2 D 3 in osteoblasts," *The Journal of Steroid Biochemistry and Molecular Biology*, vol. 173, pp. 185–193, 2017.
 - [29] C. Sang, Y. Zhang, F. Chen et al., "Tumor necrosis factor alpha suppresses osteogenic differentiation of MSCs by inhibiting semaphorin 3B via Wnt/ β -catenin signaling in estrogen-deficiency induced osteoporosis," *Bone*, vol. 84, pp. 78–87, 2016.
 - [30] A. L. Sutton, X. Zhang, D. R. Dowd, Y. P. Kharode, B. S. Komm, and P. N. Macdonald, "Semaphorin 3B is a 1,25-dihydroxyvitamin D3-induced gene in osteoblasts that promotes osteoclastogenesis and induces osteopenia in mice," *Molecular endocrinology (Baltimore, Md.)*, vol. 22, no. 6, pp. 1370–1381, 2008.
 - [31] Q. Xing, Q. Ye, M. Fan, Y. Zhou, Q. Xu, and A. Sandham, "Porphyromonas gingivalis lipopolysaccharide inhibits the osteoblastic differentiation of preosteoblasts by activating Notch1 signaling," *Journal of Cellular Physiology*, vol. 225, no. 1, pp. 106–114, 2010.
 - [32] F. A. Alzahrani, I. M. Saadeldin, A. Ahmad et al., "The potential use of mesenchymal stem cells and their derived exosomes as immunomodulatory agents for COVID-19 patients," *Stem Cells International*, vol. 2020, Article ID 8835986, 11 pages, 2020.
 - [33] M. Jafarzadeh Bejargafshe, M. Hedayati, S. Zahabiasli, E. Tahmasbpour, S. Rahmanzadeh, and A. Nejad-Moghadam, "Safety and efficacy of stem cell therapy for treatment

- of neural damage in patients with multiple sclerosis,” *Stem Cell Investigation*, vol. 6, p. 44, 2019.
- [34] A. Karamini, A. Bakopoulou, D. Andreadis, K. Gkiouras, and A. Kritis, “Therapeutic potential of mesenchymal stromal stem cells in rheumatoid arthritis: a systematic review of in vivo studies,” *Stem Cell Reviews and Reports*, vol. 16, no. 2, pp. 276–287, 2020.
- [35] D. T. Chu, T. N. T. Phuong, N. L. B. Tien et al., “An update on the progress of isolation, culture, storage, and clinical application of human bone marrow mesenchymal stem/stromal cells,” *International Journal of Molecular Sciences*, vol. 21, no. 3, p. 708, 2020.
- [36] J. Wang, B. Wang, Y. Li et al., “High glucose inhibits osteogenic differentiation through the BMP signaling pathway in bone mesenchymal stem cells in mice,” *EXCLI Journal*, vol. 12, pp. 584–597, 2013.
- [37] F. Javed and G. E. Romanos, “Impact of diabetes mellitus and glycemic control on the osseointegration of dental implants: a systematic literature review,” *Journal of Periodontology*, vol. 80, no. 11, pp. 1719–1730, 2009.
- [38] X. D. Peng, P. Z. Xu, M. L. Chen et al., “Dwarfism, impaired skin development, skeletal muscle atrophy, delayed bone development, and impeded adipogenesis in mice lacking Akt1 and Akt2,” *Genes & Development*, vol. 17, no. >11, pp. 1352–1365, 2003.
- [39] V. Ulici, K. D. Hoenselaar, H. Agoston et al., “The role of Akt1 in terminal stages of endochondral bone formation: angiogenesis and ossification,” *Bone*, vol. 45, no. 6, pp. 1133–1145, 2009.
- [40] P. Ma, B. Gu, W. Xiong et al., “Glimepiride promotes osteogenic differentiation in rat osteoblasts via the PI3K/Akt/eNOS pathway in a high glucose microenvironment,” *PLoS One*, vol. 9, no. 11, p. e112243, 2014.
- [41] Y. Chen, Y. Hu, L. Yang et al., “Runx2 alleviates high glucose-suppressed osteogenic differentiation via PI3K/AKT/GSK3 β / β -catenin pathway,” *Cell Biology International*, vol. 41, no. 8, pp. 822–832, 2017.
- [42] W. Yu, C. Zhu, W. Xu, L. Jiang, and S. Jiang, “Neuropeptide Y1 receptor regulates glucocorticoid-induced inhibition of osteoblast differentiation in murine MC3T3-E1 cells via ERK signaling,” *International Journal of Molecular Sciences*, vol. 17, no. 12, p. 2150, 2016.
- [43] L. Zhang, L. Zheng, C. Li, Z. Wang, S. Li, and L. Xu, “Sema3a as a novel therapeutic option for high glucose-suppressed osteogenic differentiation in diabetic osteopathy,” *Frontiers in Endocrinology*, vol. 10, p. 562, 2019.
- [44] S. P. Canelón and J. M. Wallace, “Substrate strain mitigates effects of β -aminopropionitrile-induced reduction in enzymatic crosslinking,” *Calcified Tissue International*, vol. 105, no. 6, pp. 660–669, 2019.